

Assessment of Soil Cover System Performance at the Antamina Mine, Peru

by

Juan Perez-Licera

A thesis submitted in partial fulfillment of the requirements for the degree of

Master of Science

in

GeoEnvironmental Engineering

Department of Civil and Environmental Engineering

University of Alberta

© Juan Perez-Licera, 2015

ABSTRACT

A study was implemented to evaluate different alternatives of soil cover systems for the closure of approximately 1539 Mt of waste rock at the Antamina Mine (Peru). The soil covers were designed to limit water percolation to the underlying waste rock, by combining a store/release and low permeability barrier layers. A total of four cover systems were built and installed on lysimeters where net percolation and runoff were measured continuously. Initial results showed net percolations of up to 63% of the total precipitation received by the covered lysimeters. No runoff was observed. The same net percolation and runoff trends were maintained during the four years that the experiment has been monitored.

This thesis presents the different activities developed to monitor and assess the covers' performance. A field investigation program was conducted to measure the hydraulic, geotechnical, and unsaturated properties of the installed cover materials. The program included density and in-situ permeability tests, soil matric suction and moisture content measurements, the recording of oxygen levels in the underlying waste rock, and the installation of complementary instrumentation. The in-situ material properties were used to create and update a series of numerical models in SoilCover, with the objective of evaluating alternatives to improve the observed performance.

The field tests showed the material characteristics and the construction process affected the hydraulic properties of the barrier layers. The in-situ saturated hydraulic conductivity values were one to four orders of magnitude greater than those measured in the laboratory. Field-testing and records from the recently installed instrumentation showed that the soil water characteristic curves of the materials also differed from the values measured in the laboratory. Oxygen levels measured in the waste rock revealed that one cover (topsoil and compacted clayey gravel till) has the potential to hinder oxygen diffusion from the atmosphere.

The results of the SoilCover models proved to be effective, with predicted net percolation and runoff values matching those measured in the field-scale experiment. The sensitivity analyses based on these models indicated that the saturated hydraulic conductivity is the primary soil property that limits percolation. The simulations showed that decreasing the saturated hydraulic conductivity by one order of

magnitude would reduce the net percolation up to 40%. The simulations also confirmed the potential for one of the cover profiles to provide a barrier to oxygen diffusion.

ACKNOWLEDGEMENTS

I would like to express my deepest gratitude to my supervisor Dr. G. Ward Wilson. I am grateful for the guidance, energy, and trust he has given me during the key moments of this project, and for his encouragement, patience, and motivation when I felt lost. I feel fortunate and proud not only for all the technical expertise I have learned from him, but for the kindness he has always showed towards me throughout these years; the same kindness that is also present in all his actions. I also would like to thank my former classmate, former coworker, and friend Pablo Urrutia for introducing me to the cover systems study, and for his suggestions and support at the different stages of this thesis.

This thesis would not have been completed without the help of the environmental department staff at the Antamina Mine. Special thanks to Bevin Harrison for facilitating the project whenever needed, and to Celedonio Aranda and Edsael Sanchez for their on-site assistance during my stay at Antamina. I owe a great deal to Bartolome Vargas and Haydee Aguirre, who have always given me unconditional help during my fieldwork, despite their multiple obligations. I also want to acknowledge the Natural Science and Engineering Research Council of Canada (NSERC), Teck, and Antamina for funding this project.

I would like to show my deepest appreciation to the members of the Antamina - University of British Columbia (UBC) Research Group. Many thanks to Dr. Roger Beckie for his enthusiastic guidance and for his creation of a joyful academic environment. I would also like to thank Dr. Daniele Pedretti for his invaluable contributions regarding the missing rainfall data, and for his comments during the last stage of the project. My gratitude is extended to the UBC members of the group: Laura Laurenzi, Mehrnoush Javadi, María Eliana Lorca, and Mélanie St-Arnault. Thank you for your help, ideas, and for making me laugh when things were challenging on the field. I would also like to thank Larisa Barber from O'Kane Consultants Inc. for her guidance during the installation of the new set of instruments.

The many friends I have made at the University of Alberta completed my experience as a graduate student. I would particularly like to thank Dr. Renato Macciotta for making the bad times good, and the good ones unforgettable. Thanks to Jorge Rodriguez for sharing, talking, and studying. Thanks to my

L1-114 'inmates' Neeltje Slingerland, Chao Kahn, Ahlam Abdulnabi, and Ngoc Bao Vu. I would also like to show my appreciation to my friends Alireza Roghani and Marzieh Salami.

Since I cannot forget where I come from, I am immensely thankful to my friends in Lima. Thank you to Viviana Moreno, Alberto Juarez, Jorge Cardenas, Marco Rivadeneira, Danny Gibbons, Eliana Melendez, Ursula Quintana, and Gabriela Acosta for showing me that distance means so little between friends, and for warming my heart during the frigid winters of Edmonton. Thanks to Carla Romero for encouraging me to pursue this graduate degree, for sharing your family with me, and for all the 'exaggerated' adventures in Peru and Canada.

I extend an enormous thank you to my uncle Roberto Silva, who has always taught me the value of responsibility and encouraged me to study since I was a child. Finally, but most importantly, I thank my mother, Lupe. Life will be not long enough to thank you for all the things you did and still do for me. Thanks for being my greatest motivation, for your love, patience, and understanding. This is for you and to you.

TABLE OF CONTENTS

ABSTRACT	ii
ACKNOWLEDGEMENTS.....	iv
TABLE OF CONTENTS.....	vi
LIST OF TABLES.....	x
LIST OF FIGURES.....	xii
CHAPTER 1: INTRODUCTION	1
1.1 General	1
1.2 Background.....	1
1.3 Scope and Objectives	3
1.4 Thesis Outline	4
CHAPTER 2: LITERATURE REVIEW AND BACKGROUND INFORMATION	5
2.1 Soil Covers.....	5
2.2 Documented Experiences with Engineered Soil Covers.....	7
2.2.1 Effects of Inclination in Oxygen Barriers	7
2.2.2 Use of Silty Materials as Oxygen Barrier	9
2.2.3 Covers with Capillary Barrier Effects (CCBE) and Water Diversion.....	10
2.2.4 Effects of Construction in Cover Barriers Performance	12
2.2.5 Use of Tailings as Soil Cover.....	14
2.2.6 Effects of Compaction on Saturated Hydraulic Conductivity and Soil Water Characteristic Curve in Soil Covers	16
2.3 Summary	19

CHAPTER 3: SOIL COVER EXPERIMENT AT ANTAMINA MINE, PERU	21
3.1 Field Lysimeters Constructed to Evaluate Different Cover Systems - Phase I (Previous Study)	21
3.2 First Year Performance Assessment Results - Phase I	28
3.2.1 Limitations of the Initial Assessment	30
3.3 Field Lysimeters Cover Experiment for Present Study - Phase II (2013-2014)	31
3.3.1 Field Investigation Program	31
3.3.3.1 Background and Scope of Work	32
3.3.3.2 Proposed Activities for Present Study - Phase II (2013-2014)	34
3.3.2 Field Tests Conducted	35
3.3.3.1 Saturated Hydraulic Conductivity by Guelph Permeameter Test	37
3.3.3.2 Measurement of Soil Suction by Jet Fill Tensiometers	42
3.3.3.3 Density by Nuclear Densometer	44
3.3.3.4 Oxygen Content in Waste Rock	46
3.3.3 Instrument Installation	48
3.3.3.1 Matric Water Potential Sensors and Water Content Reflectometers	49
3.3.3.1.1 Calibration	53
3.3.3.2 Thermal Conductivity Sensors	55
3.3.3.3 Tipping Buckets	56
3.3.3.3.1 Calibration	57
CHAPTER 4: FIELD AND MONITORING DATA	58
4.1 Field Testing Results	58
4.1.1 Saturated Hydraulic Conductivity	58
4.1.1.1 Topsoil	58
4.1.1.2 Compacted clayey gravel till	61

4.1.1.3	Non-compacted Clayey Gravel Till	64
4.1.1.4	Compacted Silty Till	66
4.1.2	Dry Density and Water Content.....	68
4.1.3	Soil Matric Suction.....	71
4.2	Instrumentation Data	75
4.2.1	Meteorological Data	76
4.2.1.1	Precipitation	77
4.1.1.1.1	Missing Precipitation Records	77
4.1.1.1.2	Precipitation Data for Cover Performance Assessment	82
4.2.1.2	Net Radiation	83
4.2.1.3	Air Temperature, Wind Speed and Relative Humidity	85
4.2.2	Percolation and Runoff.....	87
4.2.3	Matric Suction.....	93
4.2.4	Volumetric Water Content	96
4.2.5	Matric Suction and Volumetric Water Content Profiles.....	98
4.2.5.1	Degree of Saturation.....	99
4.2.6	Oxygen Content.....	101
4.2.7	Soil Water Characteristic Curve (SWCC)	103
CHAPTER 5:	PREDICTIVE NUMERICAL MODEL	110
5.1	Model Setup	110
5.1.1	Conceptual Model.....	111
5.1.2	Finite Element Mesh.....	112
5.1.3	Material Properties and Meteorological Data	114
5.1.4	Initial Conditions	117
5.2	Numerical Models First Run	118
5.3	Sensitivity Analysis	120

5.3.1	Thickness of the Topsoil Layer	120
5.3.2	Saturated Hydraulic Conductivity of the Barrier Layer.....	121
5.4	Results	122
5.4.1	Non-calibrated and Adjusted Base Cases	122
5.4.2	Sensitivity Analysis	127
5.4.2.1	Thickness of the Topsoil Layer	127
5.4.2.2	Saturated Hydraulic Conductivity of the Barrier Layer.....	130
5.4.3	Degree of Saturation and Oxygen Content.....	133
5.5	Water Balance	137
5.6	Field results and Numerical Modeling Predictions Comparison.....	140
5.7	Potential Cover Alternatives	143
	CHAPTER 6: SUMMARY AND CONCLUSIONS	148
6.1	Summary	148
6.2	Conclusions	152
6.3	Further Steps and Closing Remarks	155
	REFERENCES.....	157
	APPENDIX A: DRAWINGS	163
	APPENDIX B: PHOTOS.....	166
	APPENDIX C: FREDLUND THERMAL CONDUCTIVITY (FTC-100)	
	SENSORS READINGS	186
	APPENDIX D: CAMPBELL SCIENTIFIC CR1000 DATALOGGER	
	PROGRAM AND MONITORING STATION WIRING DIAGRAM	190

LIST OF TABLES

Table 3-1: Cover Systems Layout.....	22
Table 3-2: Summary of Laboratory Test Results conducted by Golder Associates (Urrutia, 2012) and Urrutia (2012).....	24
Table 3-3: Instrumentation Summary for the Soil Covers Experiment: Phase 1	27
Table 3-4: Summary of Guelph permeability tests conducted in compacted and non-compacted barrier layer materials (Lysimeters #1, #2, and #5)	40
Table 3-5: Summary of Guelph permeability tests conducted in topsoil (Lysimeters #1, #2, #4, and #5)...	41
Table 3-6: Results of the 2013 Density Tests Completed on Cover Materials.....	45
Table 3-7: CS229 matric suction sensors installed in Lysimeters #1 and #5	50
Table 3-8: CS616 water content probes installed in Lysimeters #1 and #5	50
Table 3-9: CS229 Calibration Equations and Coefficients Summary.....	54
Table 3-10: CS616 Calibration Coefficients Summary.....	55
Table 3-11: Tipping Buckets Information and Calibration Coefficients Summary	57
Table 4-1: Summary of Saturated Hydraulic Conductivity (k_{SAT}) tests results - Topsoil.....	58
Table 4-2: Laboratory and in-situ saturated hydraulic conductivity (k_{SAT}) test results for topsoil	61
Table 4-3: Laboratory and in-situ saturated hydraulic conductivity (k_{SAT}) test results for compacted clayey gravel till.....	63
Table 4-4: Laboratory and in-situ saturated hydraulic conductivity (k_{SAT}) test results for non-compacted clayey gravel till.....	65
Table 4-5: Laboratory and in-situ saturated hydraulic conductivity (k_{SAT}) test results for compacted silty till	67
Table 4-6: Dry densities and moisture content from nuclear densometer and corrected by oven-dried moisture content	69
Table 4-7: Net percolation for lysimeters #1, #2, #3, #4, and # 5.....	92
Table 5-1: Summary of parameters used in the SoilCover model for lysimeter #1	114
Table 5-2: Summary of parameters used in the SoilCover model for lysimeter #5	115

Table 5-3: Summary of parameters used in the SoilCover model for lysimeter #4	115
Table 5-4: SoilCover initial matric suction and temperature conditions for lysimeters #1 and #5	117
Table 5-5: SoilCover initial matric suction and temperature conditions for lysimeter #4	117
Table 5-6: Sensitivity analyses for topsoil layer thickness - Lysimeters #1 and #5	121
Table 5-7: Sensitivity analyses for saturated hydraulic conductivity (k_{SAT}) of the barrier layer - Lysimeters #1 and #5	121
Table 6-1: Summary of Cover Systems Performance (2011 - 2014)	149

LIST OF FIGURES

Figure 2-1: Covers and Climate Types (INAP, 2014).....	6
Figure 3-1: View of construction of the five lysimeters for the soil cover experiment at Antamina Mine (Urrutia, 2012).....	22
Figure 3-2: Soil Water Characteristic Curves for Topsoil. Clayey gravel till (compacted and non-compacted), and Silty till (compacted)	25
Figure 3-3: Schematic cross section for lysimeter #1: topsoil + compacted clayey gravel till (Urrutia, 2012)	26
Figure 3-4: Cumulative Precipitation and Lysimeters #1, #2, #3, #4, and #5 Net Percolation Records - Apr 20, 2011 to Feb 14, 2012 (After Urrutia, 2012)	28
Figure 3-5: Layout of the lysimeters constructed for the soil cover experiment (Urrutia, 2012)	33
Figure 3-6: Test pits location - Soil Cover Experiment Field Investigation 2013	36
Figure 3-7: Guelph permeameter test at Lysimeter #5	38
Figure 3-8: Guelph Permeability test in topsoil locations - Lysimeters #1, #2, #4, and #5	38
Figure 3-9: Tensiometers testing layout for Lysimeter #1	43
Figure 3-10: Tensiometers location for topsoil testing in Lysimeter #1 during 2014 field investigation	43
Figure 3-11: Oxygen content measurement in Lysimeter #1	47
Figure 3-12: Oxygen content (% in volume) measured during the 2013 and 2014 field investigations	48
Figure 3-13: Location of the excavated test for instruments installation - Lysimeters #1 and #5	52
Figure 3-14: Calibration Curve for CS229 sensor (SN3929).....	53
Figure 4-1: Saturated hydraulic conductivity (k_{SAT}) spatial distribution: a) Lysimeter #1, b) Lysimeter #2, c) Lysimeter #5, d) Lysimeter #4	60
Figure 4-2: Saturated hydraulic conductivity (k_{SAT}) distribution - Compacted clayey gravel till	62
Figure 4-3: Saturated hydraulic conductivity (k_{SAT}) distribution - Non-compacted clayey gravel till	64
Figure 4-4: Saturated hydraulic conductivity (k_{SAT}) distribution - Compacted silty till	66
Figure 4-5: Dry density and moisture content profiles for lysimeter #1	70
Figure 4-6: Dry density and moisture content profiles for lysimeter #5	70

Figure 4-7: Matric suction vs. Volumetric water content for topsoil - Laboratory and field measurements (2013 - 2014).....	72
Figure 4-8: Matric suction vs. Volumetric water content for compacted clayey gravel till - Laboratory and field measurements (2013 - 2014)	73
Figure 4-9: Matric suction vs. Volumetric water content for non-compacted clayey gravel till - Laboratory and field measurements (2013 - 2014)	73
Figure 4-10: Matric suction vs. Volumetric water content for compacted silty till - Laboratory and field measurements (2013 - 2014).....	74
Figure 4-11: View of the Experimental Waste Rock Piles built and monitored by the University of British Columbia (October 2013).....	78
Figure 4-12: Percolation rates comparison for a) Lysimeter #1, b) Lysimeter #3, c) Lysimeter #4, d) Lysimeter #5	79
Figure 4-13: Estimated and direct cumulative precipitation comparison for year 2014.....	81
Figure 4-14: Estimated and direct daily precipitation comparison for year 2014	81
Figure 4-15: Cumulative precipitation records for Punto B - Precipitations 1 and 2 (February 17, 2011 to December 31, 2014)	83
Figure 4-16: Daily net radiation records from Yanacancha and Punto B stations (February 17, 2011 to December 31, 2014)	84
Figure 4-17: Maximum and minimum air temperatures, and wind speed records from Yanacancha and Punto B stations (February 17, 2011 to December 31, 2014).....	86
Figure 4-18: Maximum and minimum relative humidity records from Yanacancha and Punto B stations (February 17, 2011 to December 31, 2014).....	86
Figure 4-19: Cumulative precipitation and lysimeter #1 net percolation records (February 15, 2011 to December 31, 2014)	87
Figure 4-20: Cumulative precipitation and lysimeters #1, #2, #4, and #5 net percolation records (March 24, 2011 to December 31, 2014)	88
Figure 4-21: Cumulative precipitation and lysimeters #1, #2, #3, #4, and #5 net percolation records (April 20, 2011 to December 31, 2014)	88

Figure 4-22: Daily precipitation and net percolation for lysimeter #1 (February 15, 2011 to December 31, 2014)	89
Figure 4-23: Daily precipitation and net percolation for lysimeter #2 (March 24, 2011 to December 31, 2014)	89
Figure 4-24: Daily precipitation and net percolation for lysimeter #3 (April 20, 2011 to December 31, 2014)	90
Figure 4-25: Daily precipitation and net percolation for lysimeter #4 (March 24, 2011 to December 31, 2014)	90
Figure 4-26: Daily precipitation and net percolation for lysimeter #5 (March 24, 2011 to December 31, 2014)	91
Figure 4-27: Soil matric suction readings comparison: Jet fill tensiometers, FTC-100 sensors, and CS229 - Lysimeter #1 (0.50 m)	94
Figure 4-28: Corrected soil matric suction readings for lysimeter #1 (November 20, 2013 to December 31, 2014)	94
Figure 4-29: Corrected soil matric suction readings for lysimeter #5 (November 20, 2013 to December 31, 2014)	95
Figure 4-30: Volumetric water content measurements for lysimeter #1 (November 20, 2013 to December 31, 2014)	96
Figure 4-31: Volumetric water content measurements for lysimeter #5 (November 20, 2013 to December 31, 2014)	97
Figure 4-32: a) Matric suction and b) volumetric water content profiles for lysimeter #1 (Topsoil+compacted clayey gravel till)	98
Figure 4-33: a) Matric suction and b) volumetric water content profiles for lysimeter #5 (Topsoil+compacted silty till)	99
Figure 4-34: Degree of saturation profiles for a) lysimeter #1, and b) lysimeter #5	100
Figure 4-35: Computed degree of saturation (S_r) for lysimeter #1 (November 20, 2013 to December 31, 2014)	102
Figure 4-36: Computed degree of saturation (S_r) for lysimeter #5 (November 20, 2013 to December 31, 2014)	102

Figure 4-37: In-situ soil water characteristic curves (SWCC) for topsoil in a) lysimeter #1 and b) lysimeter #5	104
Figure 4-38: In-situ soil water characteristic curves (SWCC) for compacted clayey gravel till (lysimeter #1) at a) 0.40 m, b) 0.50 m, c) 0.60 m, and d) 0.70 m of depth	104
Figure 4-39: In-situ soil water characteristic curves (SWCC) for compacted silty till (lysimeter #5) at a) 0.40 m, b) 0.50 m, c) 0.60 m, and d) 0.70 m of depth	105
Figure 4-40: In-situ soil water characteristic curve for topsoil - Lysimeters #1 and #5	108
Figure 4-41: In-situ soil water characteristic curve for compacted clayey gravel till (lysimeter#1)	108
Figure 4-42: In-situ soil water characteristic curve for compacted silty till (lysimeter #5)	109
Figure 5-1: Conceptual model for a) lysimeters #1 and #5, and b) lysimeter #4	112
Figure 5-2: Distribution of nodes for lysimeters #1 (topsoil + compacted clayey gravel till) and #5 (topsoil + compacted silty till)	113
Figure 5-3: Distribution of nodes for lysimeter #4 (topsoil)	114
Figure 5-4: Soil water characteristic curve for Waste Rock (SoilCover database)	116
Figure 5-5: SoilCover first run results for lysimeter #5	120
Figure 5-6: Non-calibrated base case cumulative water balance for lysimeter #1 - Precipitation 1	122
Figure 5-7: Non-calibrated base case cumulative water balance for lysimeter #1 - Precipitation 2	123
Figure 5-8: Non-calibrated base case cumulative water balance for lysimeter #4 - Precipitation 1	124
Figure 5-9: Non-calibrated base case cumulative water balance for lysimeter #4 - Precipitation 2	124
Figure 5-10: Adjusted base case cumulative water balance for lysimeter #5 - Precipitation 1	125
Figure 5-11: Adjusted base case cumulative water balance for lysimeter #5 - Precipitation 2	126
Figure 5-12: Net percolation sensitivity analysis results - Effect of topsoil layer thickness (Lysimeter #1, Precipitation 1)	127
Figure 5-13: Net percolation sensitivity analysis results - Effect of topsoil layer thickness (Lysimeter #1, Precipitation 2)	128
Figure 5-14: Net percolation sensitivity analysis results - Effect of topsoil layer thickness (Lysimeter #5, Precipitation 1)	129
Figure 5-15: Net percolation sensitivity analysis results - Effect of topsoil layer thickness (Lysimeter #5, Precipitation 2)	129

Figure 5-16: Net percolation sensitivity analysis results - Effect of barrier layer k_{SAT} (Lysimeter #1, Precipitation 1)	130
Figure 5-17: Net percolation sensitivity analysis results - Effect of barrier layer k_{SAT} (Lysimeter #1, Precipitation 2)	131
Figure 5-18: Net percolation sensitivity analysis results - Effect of barrier layer k_{SAT} (Lysimeter #5, Precipitation 1)	132
Figure 5-19: Net percolation sensitivity analysis results - Effect of barrier layer k_{SAT} (Lysimeter #5, Precipitation 2)	132
Figure 5-20: Predicted degree of saturation profiles from SoilCover models - a) Lysimeter #1, and b) lysimeter #5.....	134
Figure 5-21: Predicted oxygen levels for lysimeter #1 (November 21, 2013 to December 30, 2014)	135
Figure 5-22: Predicted oxygen levels for lysimeter #5 (November 21, 2013 to December 30, 2014)	136
Figure 5-23: Calculated and predicted cumulative actual evapotranspiration (AET) - Lysimeter# #1.....	138
Figure 5-24: Calculated and predicted cumulative actual evapotranspiration (AET) - Lysimeter# #5.....	139
Figure 5-25: Runoff and net infiltration field measurements and predictions comparison - Lysimeter #1	141
Figure 5-26: Runoff and net infiltration field measurements and predictions comparison - Lysimeter #5	141
Figure 5-27: Runoff and net infiltration field measurements and predictions comparison - Lysimeter #4	142
Figure 5-28: Cumulative water balance for modified cover system in lysimeter #1 - Precipitation 1.....	144
Figure 5-29: Cumulative water balance for modified cover system in lysimeter #1 - Precipitation 2.....	145
Figure 5-30: Predicted oxygen levels for the modified alternative cover in lysimeter #1 (November 21, 2013 to December 30, 2014)	146

CHAPTER 1: INTRODUCTION

1.1 General

The expansion of the mining business worldwide has provided not only the multiple benefits of this activity, but also some of the problems derived from it. Most of these problems are related to the environment, due to the perturbations generated during the ore extraction. Without appropriate care, ore extraction can lead to social conflicts, as well as to severe environmental impacts. One of the most common problems of the mining industry around the world is Acid Rock Drainage (ARD). ARD is formed by the natural oxidation of sulphide minerals that are exposed to air and water (INAP, 2009). The acid effluent dissolves and leaches other metals that have the potential of reducing water quality and thereby affect people, animals, and vegetation in the region.

Mining companies have been making many efforts to control the harmful effects of ARD; however, the commonly adopted strategies follow a reactive approach that does not prevent the problem. Due to the nature of the chemical reactions involved in ARD generation, acidic water will continue to occur for many years after ore extraction activities are finished. Thus, not only is ARD a problem during the operative period of a mine, but also becomes an ongoing environmental liability.

Engineered soil covers have generally become a realistic, effective, and sustainable alternative for ARD prevention and mitigation. The design of soil covers is based on fully coupled soil-atmosphere models, which have been studied by the scientific community for decades (Swanson et al., 2003). Cover systems, however, have been implemented with mixed results, as the performance can be affected by the meteorological conditions of the area, and the challenges induced by the construction process.

1.2 Background

Compañía Minera Antamina S.A. (Antamina) is one of the largest mining operations in the world. The company is a partnership between four of the leading companies in the mining business: BHP Billiton, Glencore, Teck, and Mitsubishi Corporation. The mine is located at approximately 270 km northeast of Lima, at an average altitude of 4300 meters above sea level, in the north part of the Peruvian central

Andes. Due to its location, the mean annual temperature is 6.0 °C, with maximum and minimum values of 23 °C and -4 °C, respectively. The average annual precipitation, which is 1200 mm, occurs mostly in one of the two distinctive seasons (wet and dry).

According to IntelligenceMine (2015), Antamina produces annually 331 and 176 kt of copper and zinc, respectively, and by the end of its 15 years of operative life, it would require to close and reclaim approximately 1539 Mt of waste rock (Golder, 2007 as cited in Urrutia et al., 2011). Recognizing the importance of ARD management measures at the early stages of the mine life, Antamina, Teck, and the University of British Columbia (UBC) started a research initiative in 2005 to develop and take the appropriate strategies required for the closure and reclamation of the different waste deposits. One of the components of this initiative was the development of a soil cover study. This study comprised the design, construction, and monitoring of four engineered soil covers, so that the results of this study would provide Antamina with valuable information regarding the best closure strategy.

The soil cover study was built between 2009 and 2011 by Urrutia (2012), and consisted of four soil covers designed to limit water percolation using a combination of a store and release layer, and a low permeability barrier. The four covers were installed over intrusive Class A waste rock that filled five lysimeters, one of them served as a control, built as part of the field scale experiment. Urrutia (2012) described the design, construction details, and the results of the performance assessment after one year of monitoring. Field measurements during the first year of the experiment reported high percolation volumes (53% to 70% of the total precipitation received), with total absence of runoff. These results, however, did not match the predictions obtained from a numerical model in SoilCover created by Urrutia (2012). Although the conclusions were drawn just after one year of monitoring, the high percolation levels suggested the hydraulic performance of the covers might have been compromised. Potential changes in the hydraulic properties of the cover materials also impacted the reliability of the predictions from the numerical models. An assessment of the in service properties of the cover materials was needed, not only to understand the reasons for the poor performance, but also to update and improve the numerical model predictions.

1.3 Scope and Objectives

The objective of the Antamina Soil Cover Study was to evaluate the performance of four different soil cover systems, and to provide Antamina with information that will help them choose the best alternative for the closure and reclamation of the waste rock deposits. Urrutia (2012) reported the activities and results of the first stage of the project, which included the materials' characterization, construction details, initial analysis, and conclusions after one year of monitoring.

The purpose of this thesis is to report the results of the second stage of the Antamina Soil Cover Study. These results include an updated performance assessment for all the different soil cover systems, soil properties measured in-situ, the calibration of three numerical models, and the performance predictions based in these calibrated models and the available meteorological data.

The objectives of this thesis is to achieve the following:

- Assess the hydraulic performance of the five lysimeters and four soil cover systems built as part of the Antamina Soil Cover Study. The assessment uses percolation, runoff, and meteorological data collected between February 2011 and December 2014.
- Plan and conduct a field investigation to assess the in-service hydraulic, geotechnical, and unsaturated properties of the different materials used to build the different soil cover systems. The investigation is aimed to identify the reasons for the reduced performance of the different covers.
- Install new instrumentation in the cover with a compacted barrier layer to evaluate the changes over time of soil matric suction and volumetric water content. The field measurements are used to characterize the in-situ soil water characteristic curve (SWCC) of the different materials, and to evaluate the changes during a hydrological year.
- Evaluate the effectiveness of the four cover systems as oxygen barriers to limit or prevent oxidation of the underlying waste rock.
- Update the existing computer numerical model in SoilCover for lysimeter #1 using the results of the field investigation, and propose a new conceptual model to account for the variability of the geotechnical, hydraulic, and unsaturated soil properties. The model results are compared to the runoff and percolations volumes reported during four years of field monitoring

- Create numerical models in SoilCover to predict the performance of the cover systems in two lysimeters (#4 and #5). The models' results are compared to the runoff and percolations volumes reported during four years of field monitoring.
- Analyze possible scenarios to improve the hydraulic performance of the soil covers in lysimeters #1, #4, and #5. Numerical models are used to predict water percolation, degree of saturation, and changes in oxygen levels inside the covers.
- Verify the reliability of the computer numerical model predictions by estimating actual evapotranspiration from a field water balance.

1.4 Thesis Outline

This thesis is comprised of six chapters. Chapter Two summarizes the literature review regarding soil covers, and some identified factors affecting their performance. A brief description of the soil cover experiment in Antamina, and a summary of the results after one year of monitoring are also included. Chapter Three describes in detail the methodology adopted for the different activities conducted as part of the proposed field investigation program. Chapter Four presents and discusses the results of the field tests, as well as the data collected by the geotechnical and meteorological instruments. Chapter Five describes the procedure followed to create and update the predictive numerical models in SoilCover, and presents a discussion of the results. Potential options to improve performance are also discussed. Finally, Chapter Six offers a summary of the findings and presents the conclusions of this thesis. Recommendations for further research activities are also included.

CHAPTER 2: LITERATURE REVIEW AND BACKGROUND INFORMATION

The following chapter summarizes the literature review conducted as part of this thesis. Although a brief description about soil covers is included, the literature review is mainly focused on some of the identified factors affecting the performance of different experimental cover systems. Reviewing previous experiments will lead to a better understanding of the potential factors that might affect the performance of the Antamina Soil Cover Experiment.

2.1 Soil Covers

Among the alternatives existing for decommissioning mine waste deposits, soil covers are commonly used at numerous sites around the world (Strunk et al., 2009). Their purpose is to encapsulate waste rock and tailings, and hence, to minimize oxygen and water flow into the underlying waste material (O'Kane et al., 1998); for this reason, soil covers are accepted as an effective method to minimize acid rock drainage (ARD) (Adu-Wusu and Yanful, 2006).

A soil cover is a profile conformed by a single soil layer or an arrangement of layers that are placed over waste. Depending on the material properties and the nature of the underlying waste, the cover can be designed to limit oxygen diffusion from the atmosphere or to limit water percolation. However, the meteorological characteristics of the region where the cover would be installed are important factors. The GARD Guide (INAP, 2014) provides a tri-linear plot that can be used as the starting point in the design process of a soil cover. This plot is shown in Figure 2-1 and relates precipitation, evaporation, temperature, and climate. Based on this information, the plot suggests the most suitable type of cover.

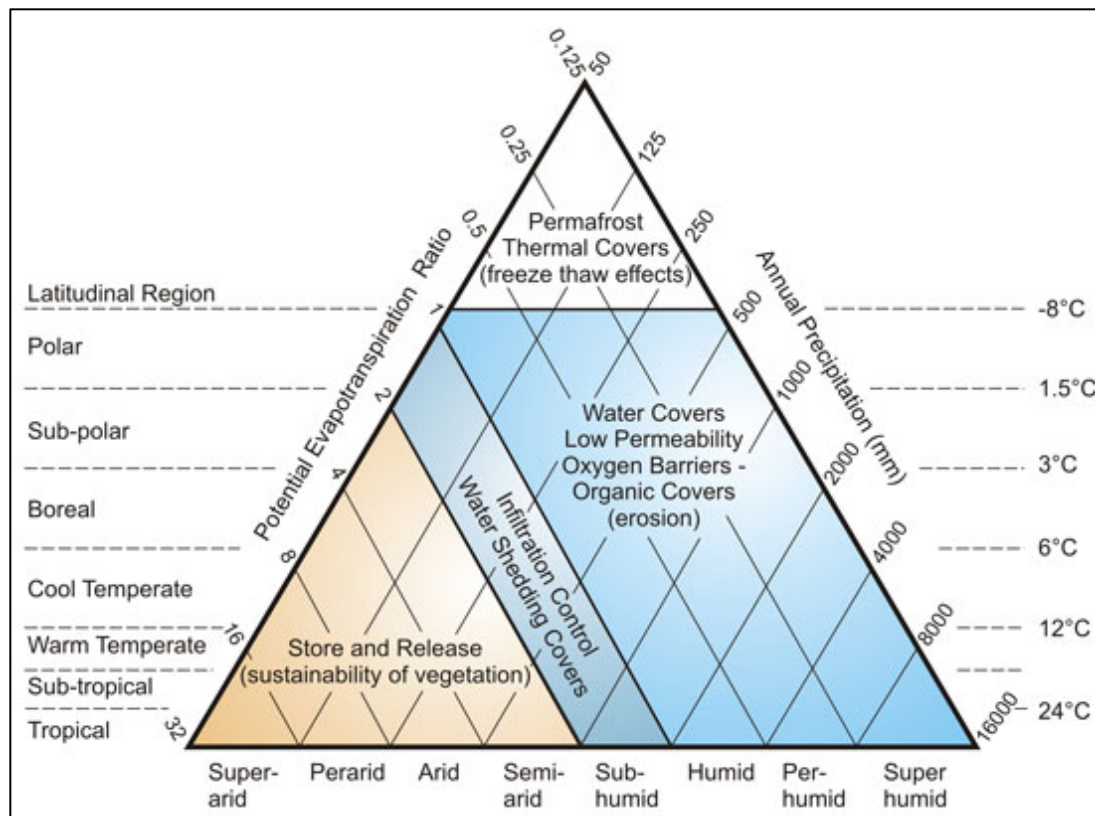


Figure 2-1: Covers and Climate Types (INAP, 2014)

There are two basic types of soil covers. The first one is called a store and release cover, which is designed to reduce infiltration if high levels of saturation cannot be sustained. This type of cover is common in regions where the climate regime results in evapotranspiration rates greater than precipitation. As the name indicates, water is collected and stored in the soil pores during the wet season, and then the stored water becomes available for evapotranspiration during the dry season. As the performance of the cover only depends on the storage capacity and the water retention properties of the material, store and release covers can be implemented as a single layer system. However, relying on a single protection layer may not always be as effective as expected, and thus leads to the development of the second basic type of soil covers. A multi-layered cover system usually consists of a surface layer used as growth medium (i.e. a fine-grained layer capable of sustaining a high degree of saturation) overlying a capillary break to prevent soluble salts migration from the underlying waste (INAP, 2014). The previous arrangement can be also modified depending on the region weather. An example is the use of clay rich

barriers in wet and temperate climates. The low hydraulic conductivity (k_{SAT}) of the clay barrier limits percolation and maintains high levels of saturation, such that the high degree of saturation reduces significantly oxygen diffusion (Aubertin, 2005 as cited in INAP, 2014). A capillary barrier, although described as part of a multi-layered system, can be designed as a single layer cover system. A capillary barrier takes advantage of the contrast between the hydraulic properties of two different soils (a fine-grained over a coarse-grained), and limits the amount of percolating water. The upper layer in a capillary barrier may function as an oxygen barrier, as it limits oxygen diffusion by sustaining high degrees of saturation. Although it can be used in wet/dry regions, the capillary break layer may not function as an oxygen barrier as the lack of precipitation during the dry season will lead to a reduction in the degree of saturation. Nevertheless, percolation would still be reduced.

2.2 Documented Experiences with Engineered Soil Covers

The performance of the soil cover system can be affected by several factors including the type of material used, the inclination of the slope, and the construction process. These factors can modify the hydraulic behavior of the cover system just after the construction or at some point during the cover life. Many laboratory and field investigations projects have been conducted in an attempt to identify and quantify the effect in performance of some of these factors. The following sections describe some experiences that were considered relevant for the assessment of the Antamina field experiment.

2.2.1 Effects of Inclination in Oxygen Barriers

Bussi re et al. (2003) studied the influence of geometry in the performance of covers with capillary barrier effect (CCBE). The objective of the study was to quantify the effect of the cover slope in the water retention potential of the cover material. The purpose of the CCBE is to sustain a highly saturated medium capable of limiting oxygen diffusion from the atmosphere towards the underlying mine waste. As a consequence, the amount of oxygen available for the initial sulfide mineral oxidation would be reduced, thus reducing the potential of ARD generation.

As part of the study, Bussi re et al. (2003) placed an arrangement of two layers with materials of water retention potentials very sensitive to changes in suction in an inclined box (2.5 m x 1 m). The bottom layer was made of gravel, compacted to reach a porosity (n) of 0.42, and had a thickness of 0.30 m. The gravel

was overlaid with a 0.50 m thick sand layer, which had an average n of 0.30. Both materials included time domain reflectometry (TDR) probes and tensiometers to measure water content and matric suction, respectively. Both materials were saturated by applying a constant precipitation rate, similar to the saturated hydraulic conductivity of the sand. The system then was allowed to drain. The experiment was conducted at three different β inclinations (0° , 9.5° , and 18.4°).

The laboratory experience showed that the inclination affected both suction and volumetric water content distributions through the barrier. At the upper part of the inclined cover, suction values were higher and lower volumetric water contents were induced depending on the locations along the slope. The changes in water volumetric content in a CCBE reduced the effectiveness of the system in terms of limiting oxygen migration from the atmosphere. The water content redistribution reduced the degree of saturation (S_r) by 30% at the upper part of the slope. A change of 10% in S_r can increase the effective diffusion coefficient of oxygen (D_e) in two orders of magnitude (INAP, 2014), representing a significant increase in oxygen flow towards the underlying waste.

Bussi re et al. (2003) compared the experimental results with predictions obtained from a finite element numerical model on SEEP/W (GEOSLOPE International, 1996 as cited in Bussi re et al., 2003). As the experimental values consistently matched the predictions, the numerical model was tested by predicting the behavior of an instrumented CCBE in a real mine site. The selected cover was constructed at Malartic, Quebec, Canada, and consisted of three layers of two different materials (sand, tailings, sand) and intended to prevent acid generation. The numerical model was also used to assess the effect of different inclinations (11.3° and 18.4°) and the length of the slopping cover (50 and 100 m). The results of a 60-day period of simulation showed good agreement with the measured values in terms of suction, and an acceptable one for volumetric water content. As in the case of the inclined box laboratory test, lower volumetric water contents were expected with an increase in distance from the bottom. Furthermore, volumetric water contents predicted by the numerical model were even lower when the inclination of the slope increased. In contrast, slope length did not seem to have an impact, as S_r values at the top of the slope were almost the same for both lengths considered.

2.2.2 Use of Silty Materials as Oxygen Barrier

Most of the experiences regarding the use of CCBE to limit oxygen migration were related to the use of clayey soils as moisture-retaining elements. For this reason, Bussière et al. (2007) conducted a study aimed to assess the efficiency of silty materials in CCBE. If properly designed, CCBE with silty soils can sustain high levels of saturation and hence limit oxygen diffusive flow. In addition, silty materials have good water retention capabilities, present low hydraulic conductivities, and can self-heal, all of which capacities represent a big advantage in comparison with clayey soils.

The study consisted in the construction of 4 field cells located on ITEC Mineral Inc.'s Norebec-Manitou site, near Val-d'Or, Quebec. Each CCBE consisted of a moisture-retaining layer underlying a 0.30 m thick layer of sand, and overlying another sand layer of 0.40 m of thickness. The moisture-retaining layer consisted of silt and non-acid generating tailings, and different thicknesses (0.30 m, 0.60 m, and 0.90 m) were also considered. Volumetric water content was measured constantly at each cell by TDR probes installed at different depths in the moisture-retaining layer, and in both top and bottom sand layers. Watermark sensors installed at the same depths and close to the TDR probes measured matric suction, while soil temperature was measured by underground thermistors at the same depths and locations.

The results of the field experiments showed that the efficiency of the moisture-retaining layer was variable depending on the selected material. The silty soil layer was the most effective material with the capacity to maintain a S_r greater than 90%. The non-reactive tailings were also very effective with a minimum S_r of 84% recorded during 1998. Furthermore, matric suction measurements recorded at the top sand layer showed that this element protected the underlying material (moisture-retaining) from the effects of evaporation. Matric suction and volumetric water content measured in the field were compared with the predictions obtained from a numerical model prepared in SoilCover (Unsaturated Soils Group, 1997 as cited in Bussière et al., 2007). The predictions were obtained considering a set of meteorological data typical of the same Quebec region.

After a four years period of monitoring, the field experiment was decommissioned and a field investigation was conducted in order to assess how much the cover capacity had changed over time. Samples were taken from both the CCBE materials and underlying reactive tailings. The observation of the average matric suction and volumetric water content showed that these values did not change significantly over

time; however, a reduction in capacity was noted at the bottom of one of the moisture-retaining layers, but the field investigation showed that this reduction was probably caused by a densification of the material at the base of the layer. Variability of the volumetric water content values was observed in the different layers of the covers, but it was more notable at the top sand layer as this layer was directly affected by the meteorological conditions. Both matric suction and volumetric water content measurements were also used to define the in-situ soil water characteristic curves (SWCC) for the different materials used in the CCBE. Field measurements for silt and non-reactive tailings did not differ from the laboratory SWCC, and all these values were less than the air entry value (AEV), which was reflected in the high degree of saturation measured in these layers. Some differences were observed, but they may be associated with local changes in porosity or with hysteresis. In contrast, measurements at both top and bottom sand layers were below the laboratory SWCC. This difference might have been caused by variations in grain-size distribution and porosity, and also by hysteresis effects. However, it is worth adding that the field SWCCs were wetting curves, while the laboratory ones were drying curves, and the former have lower volumetric water content values than the latter.

2.2.3 Covers with Capillary Barrier Effects (CCBE) and Water Diversion

As previously described, a cover system is a combination of layers of different materials designed to minimize the occurrence of ARD. The design and performance of a cover system depend on the interaction of the different materials used, and on the hydraulic and unsaturated properties of each of them. A CCBE is a system comprised of a coarse grained material layer and a moisture-retaining layer (fine grained soil), where the contrast of their unsaturated hydraulic properties prevents water from flowing out of the system and, in consequence, is capable of sustaining high levels of saturation. The retained water is then released by evapotranspiration mechanisms during the drying period. When compared to cover barriers, a CCBE represents a good alternative due its lower cost, durability, and easy construction; however, its design and performance are complex and affected by several factors. A CCBE is able to hinder oxygen flow when built in flat areas, but it is not very effective for this purpose when placed on tilted surfaces (Bussière et al., 2003). Aubertin et al. (2009) studied the effect of inclination on water diversion, as high slopes are common to waste rock and some tailings deposits.

The study consisted in a series of numerical simulations of a CCBE, with a silty moisture-retaining layer, in two different scenarios. These simulations were aimed to assess the different factors affecting the water diversion performance at different slopes. In a sloped CCBE, water tends to flow along the fine-grained material layer until it finally percolates towards the underlying coarse material if the precipitation rate is high enough or if it is sustained for a long period. The percolation takes place when the matric suction in the moisture-retaining layer equals the water penetration pressure, an equivalence that occurs when the water residual content is reached. The position along the slope where percolation finally occurs is called the down dip limit (DDL), and, as demonstrated by Bussi re et al. (2003), it is a zone rather than a specific point. The two considered scenarios for the numerical simulations were based on field experiences. The first case assessed the short-term performance of a CCBE over a waste rock deposit in a dry (semi-arid) environment in Nevada, US. The second case considered a CCBE over a steep slope and in a humid climate associated to a mine site in Abitibi, Quebec, Canada. All the simulations were modeled using SEEP/W (Geo-Slope International Ltd, 2002 as cited in Aubertin et al., 2009).

Results from the short-term case showed that the water diversion efficiency of the CCBE was controlled by the storage capacity of the moisture-retaining layer. In a dry climate, this layer is intended to keep water available to evapotranspire during the dry period of the year; however, if the precipitation events occurring during the wet season are high or long enough, then the storage capacity will be exceeded and water will percolate. For this reason, the performance assessment has to include the location of the DDL or diversion length (L_D). The simulations also showed that L_D values decreased with an increase in the precipitation, and this reduction also occurred when the precipitation rate increased during a single precipitation event. However, for this last scenario, the reduction would occur only if the precipitation rate exceeded a critical precipitation rate, which depends on the hydraulic properties of the moisture-retaining layer. The hydraulic properties can also affect L_D directly, but the extent of their impact depends on the saturated hydraulic conductivity (k_{SAT}) and the AEV of the moisture-retaining layer. As the storage capacity of the cover has to be exceeded for percolation to occur, thinner layers lead to smaller values of L_D , and L_D values will be even lower if there is also a simultaneous increase in the precipitation rate.

The long-term analysis did not focus on the intensity of precipitation events, but on the excess of water occurring in the system's annual balance, which is typical for a humid climate. The simulations showed a

similar trend as for the short-term, with L_D decreasing as water accumulates in the system over the year. These similar trends were evidence of the necessity of a transient analysis when assessing the water diversion performance of a CCBE. As in the short-term analysis, the thickness of the moisture-retaining layer had a direct impact on L_D , as this value is smaller for thinner layers (lower storage capacity). On the other hand, k_{SAT} did not have an impact on the diversion length as in the short-term analysis for dry regions. The complexity and dynamic behavior of a CCBE limit the system's effectiveness in terms of preventing percolation, but the cover system still represents a feasible alternative to significantly reducing the amount of infiltration.

2.2.4 Effects of Construction in Cover Barriers Performance

O'Kane Consultants Inc. designed and constructed a field test cover experiment for the Whistle Mine at Capreol, Ontario, Canada (Ayres et al., 2002 as cited in Adu-Wusu and Yanful, 2006). The experiment consisted of a barrier layer underlying a 0.90 m thick layer of non-compacted gravelly sand. Three different materials were considered for the barrier layer. The first option considered a 0.46 m thick layer consisting of 92% sand - 8% bentonite mixture, and with a dry density after construction of 1.95 Mg/m^3 , which represented 98-99% of the standard Proctor maximum dry density. The second option consisted of a 0.60 m thick sandy silt layer, which was placed at a dry density of 1.7 Mg/m^3 (98-99% of the standard Proctor maximum dry density). A 0.008 m thick geosynthetic clay liner (GCL) was considered for the third barrier type. The three covers were placed over a waste rock platform with a 20% slope, but some areas of this platform were not covered. For this reason, the experiment did not focus on the ability of the covers to limit oxygen diffusion, as the uncovered zones allowed oxygen flow towards the underlying waste rock. Adu-Wusu and Yanful (2006) assessed the performance in terms of limiting percolation of the cover systems after three years of monitoring, and the assessment showed that the GCL barrier was the most effective with 7% of percolation compared to 20% and 59.6% for the sandy silt and the sand-bentonite mixture barriers, respectively. After four years of monitoring, the cover system experiment was decommissioned and Adu-Wusu and Yanful (2007) conducted a post-monitoring investigation oriented to examining the possible causes of the unexpected high percolations observed at each of the covers.

The GCL used was a reinforced one consisting of sodium bentonite embedded between a woven and non-woven geotextiles needle punched together. The post-monitoring excavation revealed that the GCL

was in good condition, although some cracks were observed. An inadequate contact between the GCL and the underlying waste rock, however, caused the bentonite to be squeezed, and to accumulate in these areas. The variations in thickness caused by this inadequate contact created a preferential flow pattern, affecting the performance of the barrier. Furthermore, the GCL presented some wrinkles that could have been produced during the installation process or by some creeping due to the 20% slope of the waste rock platform. The self-healing ability of the GCL is a key factor for the performance of the barrier, but it was compromised by the freeze and thaw cycles, and by the presence of vegetation. The GCL core was made of sodium bentonite, and sodium is an easily exchangeable cation that was removed by root uptake, limiting hydration, and swelling. The reduced hydration also led to an increase in the hydraulic conductivity, as was demonstrated by comparing the field permeability test result against the laboratory tests conducted in a fully hydrated GCL.

The sand-bentonite mixture barrier layer was the least effective of the field experiment. The post-monitoring excavation showed that the downslope section of the cover had greater water content than the upslope one. This difference was a direct consequence of the 20% slope, which caused a redistribution of the water profile along the layer. Another consequence of this redistribution was the incomplete hydration of the drier areas, and the associated lower S_r . In addition, these wetter areas had a lower dry density and hence they were zones of greater percolation. Although no cracking was observed during the excavation, as bentonite self-healed any crack that might have occurred, the greatest problem observed was the accumulation of sand at the bottom of the barrier layer. As sand is heavier than bentonite, it segregated and settled down; furthermore, the segregation combined with the redistribution of the moisture content profile led to the formation of bentonite clumps, which are zones of low density and high percolation. In-situ hydraulic conductivity was also affected by the segregation, as some areas were highly permeable (sandy matrix), while other ones were below the detectable range for the Guelph permeameter.

The sandy silt barrier cover was an intermediate alternative in terms of performance, as the percolation measured was greater than the one recorded for the GCL, but lower than the sand-bentonite mixture's one. As for the sand-bentonite mixture, the surface slope caused a redistribution of the moisture content and wetter areas were observed downslope. The presence of sand pockets with a low dry density created

a highly permeable area ($k_{SAT} = 1 \times 10^{-4}$ m/s) producing a preferential flow pattern. This barrier was not exempt from the freeze and thaw effects, as vertical and horizontal cracks up to 2.5 cm wider were observed during the excavation. The areas around those cracks were wetter, indicating the occurrence of a preferential flow through these cracks. Although testing performed on an undisturbed sample determined that the water retention properties (SWCC) were not affected, the water retention performance of the whole system was affected by the segregation and cracking. From the experience with these three different covers, it is possible to conclude the performance can be drastically reduced by an inadequate installation process, and by a poor quality control of the materials used.

2.2.5 Use of Tailings as Soil Cover

Bussi re et al. (2003) used non-reactive tailings as the moisture-retaining layer for a CCBE. One of the purposes of a CCBE is, under the right meteorological conditions, to sustain high levels of saturation and hence to limit oxygen diffusion from the atmosphere towards the underlying reactive waste. An additional ARD prevention technique consists in the use of an oxygen-consuming material for the water-retaining layer. Desulphurised tailings, after several studies and testing (Bussi re et al., 2004 as cited in Cash et al., 2012), are considered a good alternative for this purpose. Due to their fine-grained nature, tailings are capable of sustaining high levels of saturation and of consuming oxygen at the same time, as they are not 100% desulphurised.

A desulphurised tailings cover was installed between 1998 and 1999 over the sulphidic tailings deposit at Detour Lake Mine, Ontario, Canada. The cover system, consisting of a 0.50 to 1.50 m thick single layer of tailings, was part of a combined closure strategy that also included a partial wet cover (Dobchuck, S. et al., 2003 as cited in Cash et al., 2012). The purpose of the cover was to limit oxygen diffusion by sustaining saturation levels greater than 85%. An initial investigation was conducted in 2000 (Dobchuck, S. et al., 2003 as cited in Cash et al., 2012) to evaluate geotechnical and geochemical characteristics of the cover. The test characterization allowed defining grain size distribution, SWCC, saturated hydraulic conductivity, water content, and pH levels. Acid Base Accounting (ABA) test was conducted in some samples to assess the neutralizing and acid generation potential of the cover materials. All the results of this initial investigation were used as input parameters for the predictive numerical model created in SoilCover (Unsaturated Soils Group, 1997 as cited in Cash et al., 2012).

Eleven years after the cover construction, Cash et al. (2012) conducted a new performance assessment before the existing tailings deposit was flooded by new waste. The new assessment consisted of a new field investigation that included water content and matric suction field measurements, pH, ABA tests, and metal analysis by aqua regia digestion and inductively coupled plasma mass spectrometry (ICP-MS).

The initial field investigation conducted by Dobchuck, S. et al. (2003 as cited in Cash et al., 2012) showed that desulphurised tailings were coarser than the reactive ones, and hence had a lower AEV. Furthermore, the saturated hydraulic conductivity of the tailings cover was between 2×10^{-6} and 1×10^{-7} m/s. As the desulphurization process did not remove all of the sulphidic minerals, the tailings cover still consumed oxygen, but at the same time it had enough neutralization potential to prevent acid drainage generation. There were some uncertainties regarding cover performance, as the water profiles evidenced that the cover was not able to keep a S_r greater than 85%. These uncertainties were even greater when geochemical testing showed an increase in sulphidic minerals with depth in the cover. Numerical modeling results confirmed the lower S_r values, but they also showed a low oxygen flow rate per year, as the oxygen content at the bottom of the cover was negligible.

Cash et al. (2012) conducted in 2011 a field investigation on a partially (naturally) vegetated cover, while the partial water cover was in the process of being drained. No extensive oxidation was observed at the surface of the tailings cover, and no oxidation front was spotted either at the different excavations. Due to the drainage of the water pond, the field matric suction values were in the range of the AEV. However, it was noted that the field water profiles were different from the ones measured in 2000, and this difference might have been caused by the high heterogeneity induced by the tailings deposition process. As the initial field measurements and numerical predictions indicated, S_r values were not above 85%, and the degree of saturation decreased with the distance from the pond. Neutral pH values obtained from the geochemical testing confirmed the low reactivity of the desulphurised material. Some samples were classified as uncertain regarding their acid generation potential, but some leaching of the alkaline components of the tailings might have caused this uncertainty. The water quality parameters complied with the Ontario province guidelines even though some of the samples were below neutrality in terms of pH, and above in terms of metal leaching. However, these exceptions were still below the discharge levels approved and allowed by the original discharge permit. The cover at Detour Lake proved desulphurised

tailings can be an effective replacement for water covers, as they represent both a geochemically and physically stable closure alternative despite not being able to maintain high levels of saturation.

2.2.6 Effects of Compaction on Saturated Hydraulic Conductivity and Soil Water Characteristic Curve in Soil Covers

Three of the different soil cover systems at Antamina include a barrier layer of glacial till. Glacial tills offer some advantages when compared to clayey or silty soils, as tills have high shear strengths, are less compressible, and have low saturated hydraulic conductivity (k_{SAT}). However, all these advantages can be lost or drastically affected by the compaction process that takes place during the cover installation. Watabe et al. (2000) conducted an investigation focused on the effect of compaction in pore-size distribution and k_{SAT} for glacial tills. Changes in pore-size distribution have an immediate effect in SWCC, and a direct impact on the cover system performance.

Watabe et al. (200) selected a glacial till from northern Quebec for the study, but only the fraction smaller than 5 mm was tested. The till, consisting of 7% of non-plastic clay, was classified as well-graded, and had a specific gravity (G_s) value of 2.7. Watabe et al. (2000) assessed changes in hydraulic conductivity by conducting 12 horizontal and 2 vertical tests using a radial flow permeameter. The samples were compacted close, above and below the optimum degree of saturation (S_{ropt}). As no anisotropy was observed, only the horizontal tests results were considered for the assessment. To assess the compaction impact on SWCC, five samples compacted at different S_r were tested. For both permeability and suction testing, the samples were mixed 24 hours in advance at the required water content. The samples for permeability test were saturated by applying a backpressure at different stages, while for suction testing the sample cells were filled with water, and then pressurized to obtain full saturation.

The permeability testing results showed that the samples' compressibility increased at lower initial dry densities. When compressing the samples (reducing void ratio e), k_{SAT} did not change if the samples were compacted at degrees of saturation greater than S_{ropt} ; however, samples compacted on the dry side of the compaction curve ($S_r < S_{ropt}$) reduced their permeability as e was reduced. These results evidenced the effect of compressibility on k_{SAT} depending on the compaction moisture content. In addition, samples compacted above the optimum degree of saturation did not change k_{SAT} when they were unloaded during

the test. This behavior might be an indicator of the development of macroporosity that was reduced with an increase in vertical stress. If compressibility is not considered, samples compacted on the dry side were up to two orders of magnitude more permeable than samples compacted close to or above S_{ropt} .

For the SWCC tests, Watabe et al. (2000) compacted three of the five samples considering S_r lower than S_{ropt} . The remaining two samples were compacted considering $S_r = 100\%$ and S_r above S_{ropt} . The laboratory results showed a set of different SWCCs for a single material with a given grain size distribution, and the difference between those curves depended on initial moisture and compaction. Watabe et al. (2000) transformed the different SWCCs into pore-size distribution curves using the expressions proposed by Marshall (1958, as cited in Watabe et al., 2000), and Garcia-Bengochea (1979, as cited in Watabe et al., 2000). Upon comparing the pore-size distribution curves for the SWCC samples, it was observed that drier than optimum samples had larger pores, which was evidence of macropores' presence. A change in pore size capable of modifying k_{SAT} in two orders of magnitude was induced by compacting the till with a degree of saturation between 60% and 95%. The Watabe et al. (2000) study concluded that the assumption of a single SWCC and a constant k_{SAT} is only feasible when fabric is not altered. Hydraulic and water retention properties can be significantly affected by the level of heterogeneity induced by the water content and level of compaction achieved during the cover construction.

The unsaturated behavior represented by the SWCC can be modified by different factors including soil structure, initial molding water content, void ratio, and method of compaction. Recognizing that these factors can lead to a variable engineering behavior, Vanapalli et al. (1999) studied the effect of initial water content on soil structure by comparing SWCC data with data from compacted samples. The soil used for the study was a sandy clay till consisting of 28% sand, 42% silt, and 30% clay. Vanapalli et al. (1999) compacted the samples at initial water contents above and below the optimum water content determined from the standard compaction tests.

The results of Vanapalli et al. (1999) study for the samples compacted on the wet side of the compaction curve showed that the material presented a greater resistance to desaturation. The soil samples were able to retain water at greater suctions when compared to the SWCC for the sample compacted at the optimum water content. On the other hand, the samples on the dry side desaturated easily and the SWCC presented a steeper curve. This different behavior was caused by the macro and microstructure

developed by fine-grained soils, as the macrostructure changed depending on the initial water content, as it affected the way both pores and aggregations were developed. Samples drier than optimum presented large pores and the soil behaved more as a coarse-grained material, while the wetter than the optimum ones had pores that were not generally interconnected.

Benson and Daniel (1990) studied the impact of clods on the hydraulic conductivity (k) of clays, as the difference in k between laboratory testing and field measurements is at least of one order of magnitude. Mitchell et al. (1965, as cited in Benson and Daniel, 1990) concluded that the most important variables affecting k were the initial molding water content, the method of compaction, the compaction effort, and the degree of saturation. For this study, samples with 2 different clod sizes (19 and 4.8 mm) were compacted at different water contents and with different levels of energy, and then tested in both rigid and flexible wall permeameters.

The results of the laboratory tests conducted by Benson and Daniel (1990) showed that clod size had an impact on the optimum moisture content, as the material with smaller clods achieved the maximum dry density at lower water content. The maximum dry density was almost the same for both types of materials; however, the sample with smaller clods was compacted more effectively at moisture contents lower than the optimum. Benson and Daniel confirmed the results obtained by Daniel (1984, as cited in Benson and Daniel, 1990) where it was suggested k was a function of clod size. In the Benson and Daniel study, the samples prepared with material with smaller clods were five orders of magnitude less permeable than the material when larger clods (for moisture contents from dry to optimum). At higher than optimum water contents, no difference in k was observed, as clods were easily compressible at high water contents. Benson and Daniel (1990) used a microscopic scan in some samples to get a better understanding of the behavior of the clods. This scan had the intention of observing if a flocculated (Lambe, 1958 as cited in Benson and Daniel, 1990) or a clod theory based (Olsen, 1962 as cited in Benson and Daniel, 1990) structure had been developed at different water contents. The microscope scan did not find evidence of any possible flocculation or dispersion of the clay particles. On the other hand, photographs of the samples indicated the presence of remnant clods after the compaction in drier than the optimum samples. Samples compacted above the optimum water content were free of evidence and showed a soft texture.

When more energy was applied during the laboratory compaction (modified compaction test), the samples compacted with water contents lower than the optimum presented lower values of k . An examination of the dry samples identified a more coarse-grained soil structure in samples with water contents lower than optimum, but compacted with standard effort. The energy applied was not enough to deform the clods and close the gaps existing between them. It is clear clods and initial water content control how interclod pores are generated during compaction, but water content and applied energy have to be adjusted to achieve the desired level of hydraulic conductivity. Prapaharan et al. (1991) assessed the difference in fabric between laboratory and field compacted soils. The study consisted in determining the pore size distribution of different samples by conducting mercury porosimetry tests. Samples were taken from ten different sections of a test embankment and had a 6% scatter in terms of water content. For the embankment compaction, two types of compaction equipment were used. For the laboratory samples, three different levels of compaction were considered (low energy, standard, and modified proctor). The porosimetry test results demonstrated that pore-size distribution curves had the same shape no matter what compaction method, compaction energy, or compaction water content were considered. However, the pore size frequencies were different, and hence laboratory and field compacted materials had different fabric, and as a result, they were different materials with different behavior.

2.3 Summary

Engineered soil covers represent a sustainable alternative to control erosion, ARD, and metal leaching. An efficient design has to consider not only the availability of materials but also the meteorological conditions. The type of material available for the construction plays a key role in the performance of the cover, as evaporative fluxes can be evaluated from the soil water characteristic curve (SWCC) and the water content (Wilson et al., 1997). The design of the soil cover depends on the type of soil available for construction, while the performance is controlled by the ability to replicate the unsaturated properties defined by laboratory testing (SWCC) on the field.

The laboratory and field experiences described in this chapter shown that a poor quality control of the construction materials, and the challenges of the construction process can reduce the performance of the designed cover system. The most important lesson is that the process of designing and implementing an engineered cover is unique, and it depends on several factors such as the scale of the project, the

meteorological conditions of the region, the type of materials available, and the quality control during the construction process.

CHAPTER 3: SOIL COVER EXPERIMENT AT ANTAMINA MINE, PERU

3.1 Field Lysimeters Constructed to Evaluate Different Cover Systems - Phase I (Previous Study)

Antamina is located at approximately 270 km northeast of Lima, at an average altitude of 4300 meters above sea level, in the north part of the Peruvian central Andes. Due to its location, the region has two clearly distinctive seasons. The wet season, characterized by high rainfall during the south summer period, goes from October to April, and has an average annual precipitation of 1200 mm. The dry season extends from May to September, and although some precipitation events may occur, the recorded volume can be classified as low or negligible. The mean annual temperature is 6.0 °C, with maximum and minimum values of 23 °C and -4 °C, respectively.

Urrutia (2012) detailed the design, material characterization, and construction process of the soil cover project, and conducted an evaluation of performance during the first year after construction. Five field scale lysimeters, as shown in Figure 3-1, were constructed in the zone named as Punto B. The four different cover systems were installed in four lysimeters with the fifth lysimeters providing a control (i.e. uncovered). The test covers were a combination of a store and release layer and a low permeability barrier, and they were designed to limit water percolation by triggering evapotranspiration (MEND, 2001). The four cover systems were designed to limit water percolation into the underlying waste material. Limiting water percolation will minimize waste rock weathering and metal leaching, and hence, the quality of the mine effluent would be improved and ARD occurrence could also be reduced. Based on the purpose of the cover systems, the performance of a cover can be defined as the percentage of the received precipitation measured as both percolation and runoff. Table 3-1 presents the layout of each cover system.



Figure 3-1: View of construction of the five lysimeters for the soil cover experiment at Antamina Mine (Urrutia, 2012)

Table 3-1: Cover Systems Layout

Lysimeter	Cover material (thickness in mm)
1	Compacted clayey gravel till (600 mm) + Topsoil (300 mm)
2	Non-compacted clayey gravel till (600 mm) + Topsoil (300 mm)
3	None (Control)
4	Topsoil (300 mm)
5	Compacted silty till (600 mm) + Topsoil (300 mm)

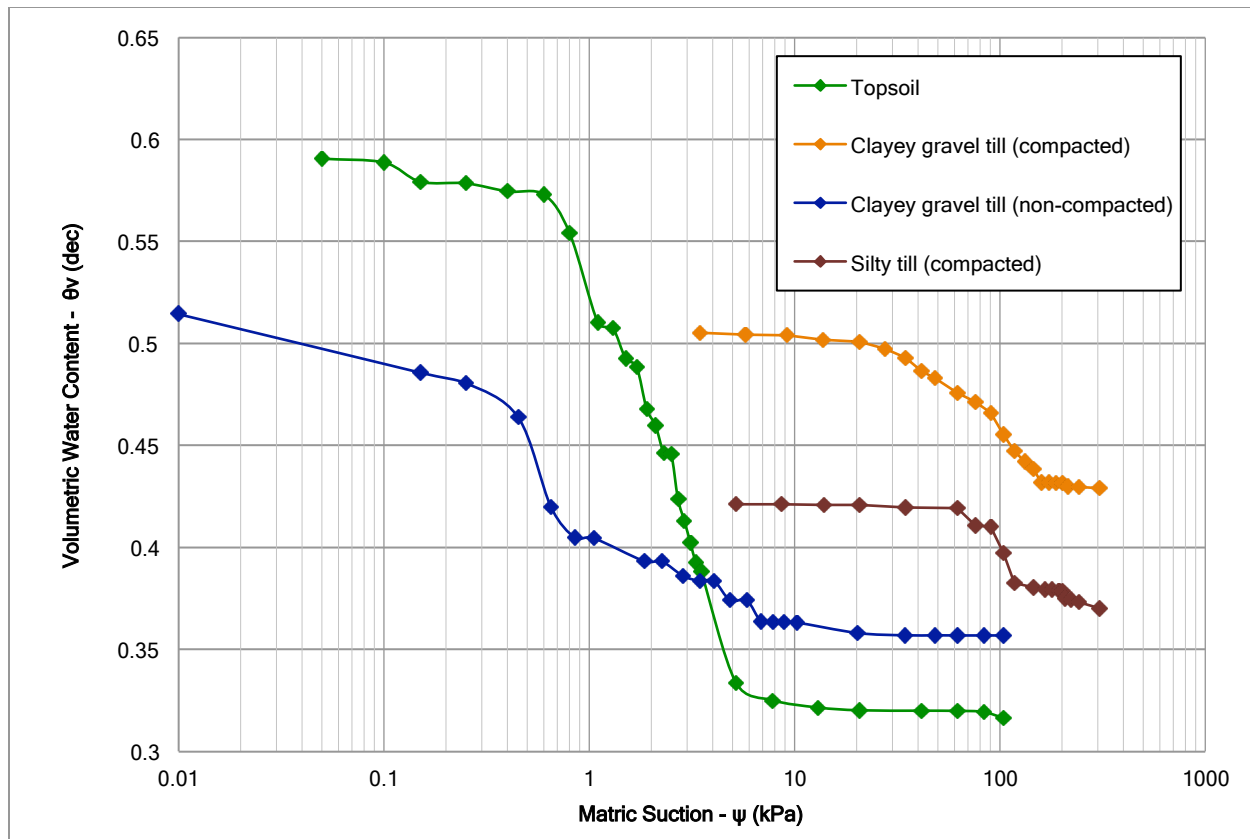
The different arrangements shown in Figure 3-1 and Table 3-1 were selected to compare covers of different levels of complexity. This complexity comprised the use of a single layer (topsoil) or a double layer system, the use of different materials (clayey gravel till and silty till), and the methodology to use during construction (compacted or non-compacted). All the materials used for the field experiment construction were native soils, and were characterized preliminarily by Golder Associates (Urrutia, 2012). The materials selected as low permeability barriers were classified as glacial tills based on the preliminary geotechnical assessment conducted for the waste dumps conducted by Piteau Associates Engineering Ltd. (1997, as cited by Urrutia, 2012). The glacial tills are described as a grey to brown, compact to dense, clayey, silty sand and gravel with cobbles and occasional boulders (up to about 400 mm in diameter), with

fine content varying between 4% to more than 50% (Piteau Associates Engineering Ltd., 1997 as cited by Urrutia, 2012). Due to the intrinsic heterogeneity created by the deposition process, the glacial tills at Antamina were divided in coarser (clayey gravel) and finer (silty) till. The laboratory tests conducted as part of the native material assessment and the construction quality control confirmed the heterogeneity described by Piteau (Piteau Associates Engineering Ltd., 1997 as cited by Urrutia, 2012). The coarse till can be described as clayey gravel to gravelly/sandy clay with sand and gravel, with a low plasticity fine fraction, and classified as GC to CL based on the Unified Soil Classification System (USCS). Alternatively, the finer till can be described as gravelly to sandy elastic silt, and classified using the USCS as MH.

During the construction, samples from the soils used for the different covers were taken and sent to Golder Associates laboratory to conduct a complete characterization. The characterization program included the determination of grain size distribution, Atterberg limits, specific gravities, and maximum dry densities and optimum water contents from Standard Proctor tests (Urrutia, 2012). Another group of samples were taken, mixed and quartered in order to get a representative sample that was sent to the University of Alberta for additional laboratory testing. The laboratory program at University of Alberta, conducted by Urrutia (2012), included Atterberg limits, saturated hydraulic conductivity, and Tempe pressure cell tests. A summary of the material properties determined by Golder Associates and Urrutia (2012) is presented in Table 3-2, and the SWCC obtained from the Tempe cell tests are shown in Figure 3-2. No additional laboratory testing was conducted as part of this research program, since the field investigation program was designed to avoid any disturbances that could impact the performance of the cover systems. Hence, the interpretation of the field experiment and numerical modeling results is based on the properties updated during the field investigation along with the initial characterization conducted by Golder Associates and Urrutia (2012).

Table 3-2: Summary of Laboratory Test Results conducted by Golder Associates (Urrutia, 2012) and Urrutia (2012)

Properties	Topsoil	Compacted clayey gravel till	Non-compacted clayey gravel till	Compacted silty till
Gravel	11	38.6 - 18.2	32.4 - 26.2	25.2 - 5.9
Sand	12.4	24.9 - 19.1	20.8 - 16.8	18.9 - 7.4
Fines	76.5	57.9 - 36.5	57.0 - 46.8	75.2 - 58.5
Liquid limit - <i>LL</i> (%)	78.3	34 - 38	36	50 - 54
Plasticity index - <i>PI</i> (%)	27.4	14 - 15	15-16	20 - 24
Specific gravity - <i>G_s</i>	-	2.38 - 2.76	2.54-2.62	2.69 - 2.74
Maximum dry density (kg/m^3)	-	1794 - 1903	1800 - 1857	1576 - 1603
Optimum water content (%)	-	14.0 - 16.6	15.1- 16.4	20.6 - 21.8
Laboratory saturated hydraulic conductivity (m/s)	10^{-6} - 10^{-5}	10^{-10} - 10^{-9}	10^{-8} - 10^{-7}	10^{-8} - 10^{-6}



Note: Adapted from Urrutia (2012)

Figure 3-2: Soil Water Characteristic Curves for Topsoil. Clayey gravel till (compacted and non-compacted), and Silty till (compacted)

The different covers were overlying intrusive Class A waste rock that partially filled four of the five lysimeters (Lysimeters #1, #2, #4, and #5). The lysimeters, as shown in Figure 3-3, are inverted truncated pyramids of 15 m x 15 m dimensions at the top, with 1.5:1 (H:V) sloped walls, 2.5 m of depth, and 7.5 m x 7.5 m dimensions at the bottom. Lysimeters #1, #2, #4, and #5 were covered by a 5.42 mm bituminous geomembrane (Coletanche NTP 4) to prevent any water from flowing out of the collection system, while two layers of a 2 mm HDPE geomembrane covered lysimeter #3. The base of the lysimeters has a 5 % slope oriented to the center where a sump with a pipe collects all the percolation water. The surface of each cover has a 3 % orientation to the east with the purpose of promoting runoff flow that would be collected by a 4" HDPE pipe. Both runoff and percolation flows are directed to separated 1 m³ tanks, where tipping buckets are located to record flow rate and volume.

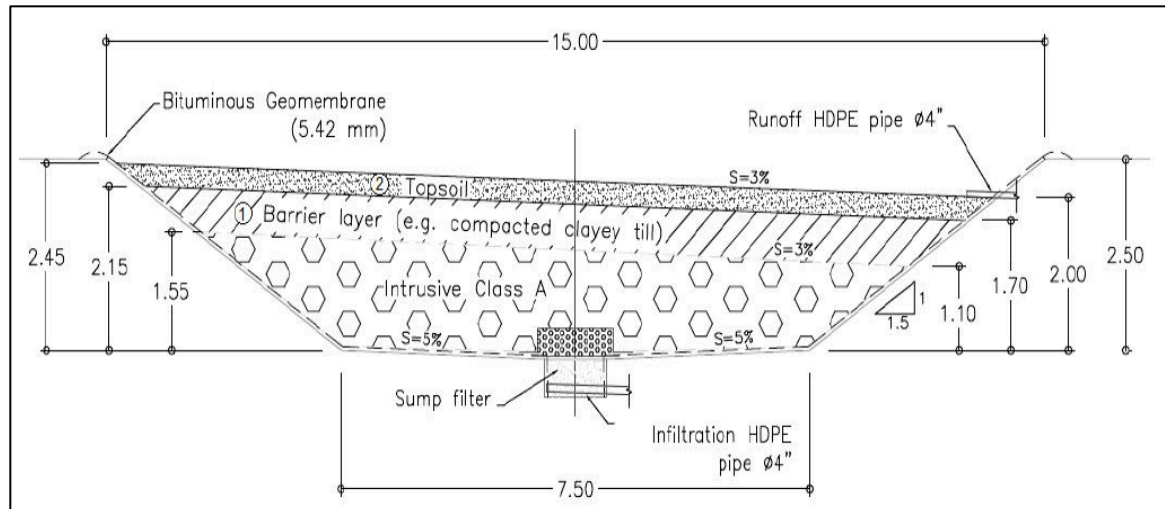


Figure 3-3: Schematic cross section for lysimeter #1: topsoil + compacted clayey gravel till (Urrutia, 2012)

The tipping buckets were connected to a Campbell Scientific Inc. CR-1000 datalogger (Campbell Scientific, Inc., 2011) that records the information every 30 min. All the cover systems were instrumented with Fredlund Thermal Conductivity Sensors (FTC-100) made by Geotechnical Consulting & Testing Systems (GCTS), which are used to measure matric suction indirectly (Urrutia, 2012). The changes in matric suction would allow evaluating the changes in volumetric water content, and hence changes in degree of saturation with time. A summary of the instruments installed at each lysimeter is presented in Table 3-3. Although the covers were not designed to prevent oxygen diffusion from the atmosphere towards the underlying reactive mine waste, oxygen diffusive flow can be hindered if the cover is able to maintain high levels of saturation. For this reason five 3.18 mm (1/8") inner diameter PVC sampling tubes were installed in the waste rock in lysimeters #1, #2, #4, and #5. These tubes were used in the second phase of the study to obtain oxygen measurements required to evaluate the efficiency of the cover as an oxygen diffusion barrier.

Table 3-3: Instrumentation Summary for the Soil Covers Experiment: Phase 1

Type of instrumentation by material	Installation depth (m below surface)				
	L#1	L#2	L#3 (control)	L#4	L#5
Topsoil					
Matric suction - Fredlund Thermal Conductivity Sensor FTC-100	0.15	0.15	N.A.	0.15	0.15
Compacted clayey gravel till					
Matric suction - Fredlund Thermal Conductivity Sensor FTC-100	0.48, 0.75	N.A.	N.A.	N.A.	N.A.
Non-compacted clayey gravel till					
Matric suction - Fredlund Thermal Conductivity Sensor FTC-100	N.A.	0.46, 0.75	N.A.	N.A.	N.A.
Compacted silty till					
Matric suction - Fredlund Thermal Conductivity Sensor FTC-100	N.A.	N.A.	N.A.	N.A.	0.45, 0.65

As the performance of the cover systems does not only depend on the hydrological and geotechnical properties of the soil materials, Urrutia (2012) installed a rain gauge and a NR-LITE net radiometer (Campbell Scientific, Inc., 2006) in the cover study zone at Punto B. Measurements of air temperature, wind velocity and direction, and relative humidity were initially recorded at the Yanacancha meteorological station. The information collected by the different sensors installed in each cover, the percolation and runoff measured by the tipping buckets, and the data collected by the weather station would be used to prepare a water balance for each cover system. In addition, both soil properties and weather data records were used as input parameters for a one-dimensional fully coupled soil-atmosphere numerical predictive model prepared in SoilCover (Unsaturated Soils Group, 2000). Urrutia (2012) created a model to predict the performance of the soil cover systems, and to compare these predictions with the field experiment results. This comparison will be used to make the necessary changes to improve or maintain the

performance of the different soil covers. As part of the first stage of the research project, Urrutia (2012) prepared only a predictive model for lysimeter #1 (topsoil and compacted clayey gravel till), and compared the predictions obtained by the numerical model in SoilCover against the percolation measurements recorded between February 2011 and February 2012.

3.2 First Year Performance Assessment Results - Phase I

Figure 3-4 shows the performance in terms of recorded percolation for the five different lysimeters and the respective four covers systems.

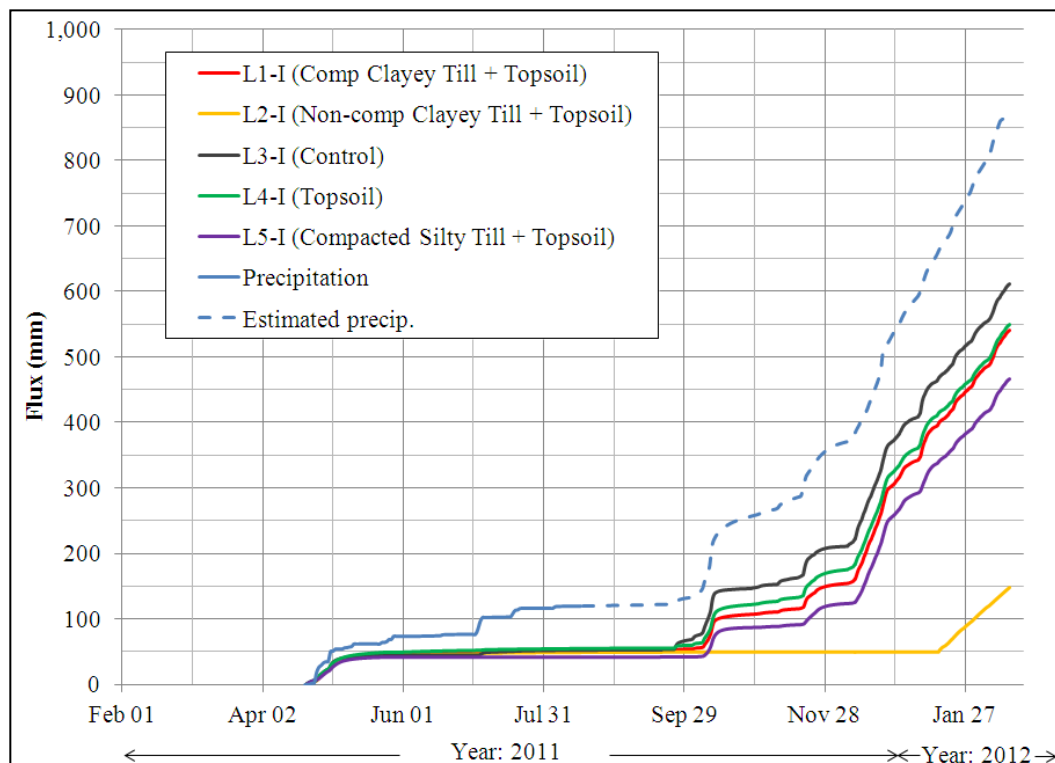


Figure 3-4: Cumulative Precipitation and Lysimeters #1, #2, #3, #4, and #5 Net Percolation Records - Apr 20, 2011 to Feb 14, 2012 (After Urrutia, 2012)

Urrutia (2012) reported 68% of the total precipitation received by lysimeter #1 as percolation between February 15, 2011 and February 14, 2012. Lysimeters #4 and #5 were monitored from March 24, 2011 to February 15, 2012 and registered 66% and 58% of percolation respectively during that period. The control lysimeter (lysimeter #3) started to be operative in April 20, 2011 and 70% of the total precipitation was registered as percolation until February 15, 2012. The performance assessment for lysimeter #2 was

compromised by some problems with the flow and volume measurement system, and reliable data is available from March 24, 2011 to September 19, 2011. During this period, 67% of the total precipitation was reported as net percolation. When the performance of the five lysimeters is compared during the same period, as shown in Figure 3-4, it is observed that all the lysimeters perform following the same trend, with percolation increasing as soon as the rainy season starts. Another point in common for all the different cover systems, including the control lysimeter, is the absence of runoff during the assessed period, which was confirmed by a visual inspection of the 1m^3 collection tanks.

The percolation predictions for lysimeter #1 from the one-dimensional numerical model in SoilCover were compared with the percolation records for the first year of monitoring. The uncalibrated model, which considered a k_{SAT} equal to 2×10^{-9} m/s (Urrutia, 2012), predicted 470 mm of runoff, and a lower percolation for the first year. As no runoff was observed on the field, it was suggested the barrier layer (compacted clayey gravel till) was more permeable than expected, allowing water to percolate instead of overwhelming the storage capacity of the topsoil layer.

Urrutia (2012) compared the precipitation rates with the percolation rates observed in the field for certain periods during the rainy season. After the comparison, Urrutia (2012) concluded that average rain intensities were greater than k_{SAT} defined by laboratory testing for the compacted clayey gravel till. Runoff would occur under these conditions, but its absence and the observed percolation levels suggested the field k_{SAT} is greater than the laboratory value. For purposes of the numerical modeling, Urrutia (2012) introduced a new k_{SAT} by averaging the precipitation rates defined during the rainy season, and by considering those rates infiltrated directly through the cover system. The resultant k_{SAT} (7×10^{-8} m/s) was one order of magnitude greater than the laboratory k_{SAT} , and the percolation predictions obtained from the numerical model, considering the new k_{SAT} , matched the field percolation records.

Urrutia (2012) also conducted different sensitivity analyses to evaluate how performance was impacted by variations in k_{SAT} , Leaf Area Index (LAI), and topsoil layer thickness. Urrutia (2012) concluded percolation would be reduced by 75%, from the initial base case, if k_{SAT} could be lowered one order of magnitude. A reduction in the topsoil layer thickness would generate some runoff, but not a significant volume as the element controlling the system percolation is k_{SAT} for the barrier layer. Regarding LAI, the development

and quality of vegetation would not have an impact on evapotranspiration, as both evaporation and actual transpiration consume almost all the energy of the system.

3.2.1 Limitations of the Initial Assessment

The first year performance assessment for the soil cover experiment and the numerical model predictions had some limitations. The first limiting factor was the unavailability of meteorological information for the field experiment zone (Punto B). As a result, the majority of this information required as input for the numerical model in SoilCover came from the Yanacancha weather station. Evaporation and evapotranspiration are not constant for a given site, as they change depending on various factors such as microclimates, topography, surface exposure, slope, orientation, and wind flow. As noted by Weeks (2006), net radiation changes dramatically depending on the direction of the slope exposure, and this change would lead to different levels of potential evaporation within the same zone. The use of net radiation records from a different weather station would have an impact on the numerical predictions for the soil cover experiment.

Urrutia (2012) reported percolation volumes as a percentage of the total precipitation recorded at the field experiment area. The rain gauge installed at Punto B collected information accurately until August 11, 2011, and stopped working after that date. Due to the difference in elevation and location between the Punto B area and the location of the Yanacancha weather station, the precipitation data collected at the latter could not be used directly for both percolation assessment and numerical modeling. Bay (2009) proposed a correlation to estimate precipitation at Punto B from Yanacancha records, but it was only effective in terms of weekly precipitation as the daily values presented a great variability. Blackmore (2012) proposed a correlation to estimate precipitation at Punto B from the outflow volumes measured by Lysimeters A and D at one of the experimental waste rock piles (Pile 4), located in the same area as the soil cover experiment. As the outflow was only measured during the rainy season, Urrutia (2012) followed the recommendations provided by Blackmore (2012) and used the lysimeters outflow volume to estimate daily precipitation during almost all the rainy season (October to March). Urrutia (2012) also used the equation proposed by Bay (2009) to estimate any missing precipitation record from the end until the beginning of the rainy season (April to September). Both methodologies were used to estimate precipitation between August 2011 and February 2012, and they proved to be satisfactory for the

Urrutia study (2012). The use of an estimation based on lysimeter outflow, however, has some limitations, as the methodology proposed by Blackmore (2012) is based on the development of preferential flow inside Pile 4. A change in the flow path would lead to an underestimation of the precipitation at Punto B, and in consequence to an overestimated percolation.

Urrutia (2012) acknowledged that a change in k_{SAT} for the compacted clayey gravel till might have been induced by the presence of coarse particles in the material during the construction, and by placing the barrier material on the dry side of the compaction curve. The studies conducted by Watabe et al. (2000), Vanapalli et al. (1999), Benson and Daniel (1990), and Mitchel et al. (1965 as cited in Benson and Daniel, 1990) provided evidence that initial water content at molding was one of the most important factors affecting k_{SAT} . In addition, both water content and method of compaction also have an impact on the barrier layer fabric. A change in soil fabric also means a change in the pore-size distribution, which is directly related to the water retention potential (SWCC) of the material. As documented by Urrutia (2012), the barrier layers for the different covers were placed and compacted in layers, and at different initial moisture conditions. The resultant heterogeneity might be greater than expected and also responsible for the high levels of percolation recorded, and for the difference with the predictive model results.

3.3 Field Lysimeters Cover Experiment for Present Study - Phase II (2013-2014)

The results of the first year performance assessment of the soil cover experiment at Antamina showed percolation levels higher than expected. In order to get more accurate predictions and to analyze possible changes to improve the performance, a field investigation program was executed in two stages. The following sections present a description of the different activities conducted between October and November 2013, and June and July 2014. These activities included measurement of saturated hydraulic conductivity in all the cover systems and at different depths, matric suction readings with jet fill tensiometers, measurement of oxygen content in the underlying waste rock, and the installation of new instrumentation to evaluate the changes in matric suction and volumetric water content in time.

3.3.1 Field Investigation Program

The field investigation program was developed following the recommendations provided by Urrutia (2012), and this program was presented in the Antamina Waste Rock Study - 2012 Lessons Learned Report

(Blackmore et al., 2013). The activities proposed in the investigation program were aimed at both improving the monitoring system and the performance of the covers and refining the rainfall-infiltration predictive model in SoilCover (Unsaturated Soils Group, 2000). The investigation was conducted in two stages. The first stage was carried out between October 1 and November 22, 2013 at the onset of the wet season. Dr. G. Ward Wilson was present on site from October 21 to 23, 2013 to provide guidance during the initial stages of the field-testing. As it was necessary to reconnect one of the instrumentation data collection systems removed during the first stage, a second field trip was scheduled between June 23 and July 17, 2014. Additional field-testing was planned and conducted to take advantage of this trip to the site, and calibration of the tipping buckets was also undertaken during this period.

3.3.3.1 Background and Scope of Work

The purpose of the soil cover study was to assess the performance of four cover systems. This evaluation consists in measuring the volume of water percolating through the covers and the waste rock material. A numerical model was prepared by Urrutia (2012) to predict the behavior of the four experimental configurations. Both the predictive model and the field experiment will provide Antamina with the required information to select the best closure and reclamation cover alternative for the waste rock deposits at the mine site.

The first phase of the soil cover experiment consisted of the design, material characterization, construction, and instrumentation of the four different soil cover configurations (Urrutia, 2012). Figure 3-5 shows the final layout of the five lysimeters constructed as part of the soil cover experiment. Based on the design elements and material properties defined by laboratory testing, a numerical model was prepared and some preliminary conclusions were obtained after one year of monitoring (February 2011-February 2012). It was observed that between 58% and 70% of the total precipitation received percolated through both the cover and waste rock. Furthermore, neither runoff nor ponding was observed in both the four soil covers and control lysimeter.

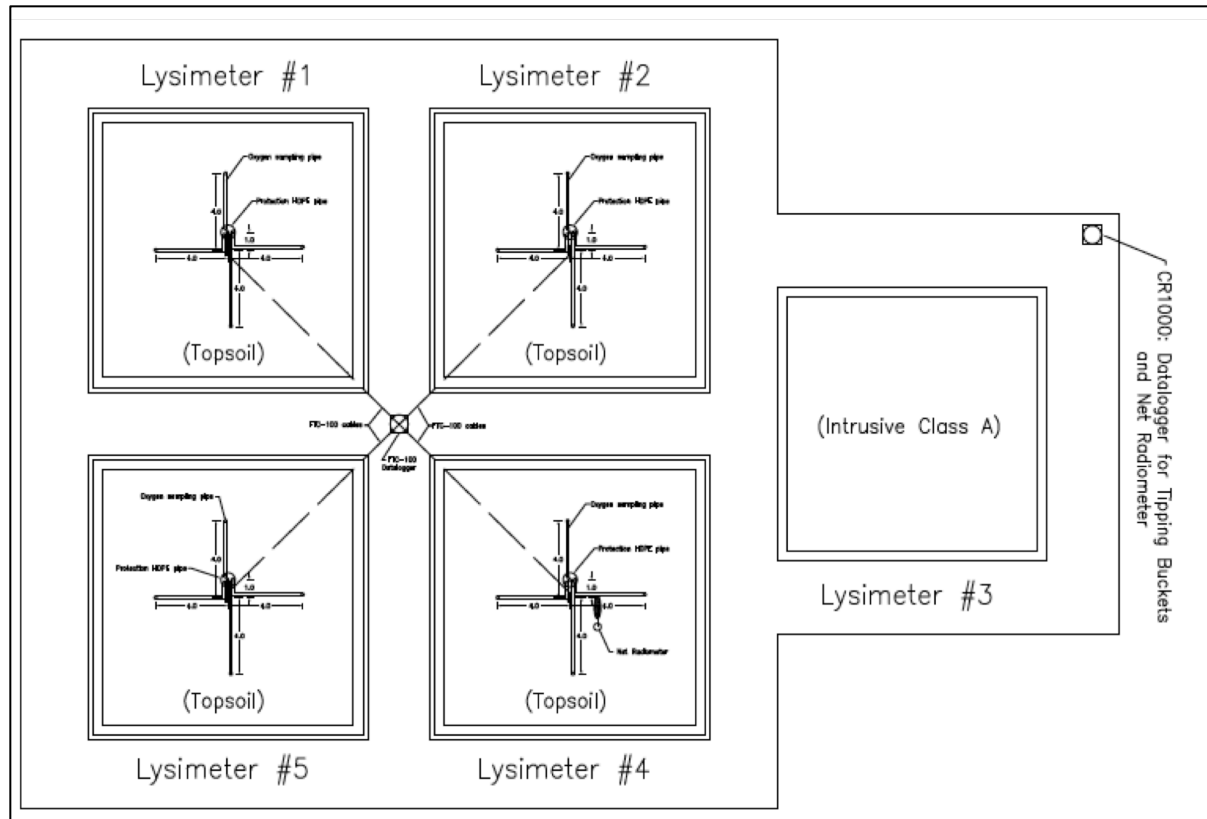


Figure 3-5: Layout of the lysimeters constructed for the soil cover experiment (Urrutia, 2012)

The most relevant conclusion from Phase 1 observations is the absence of runoff. Runoff is a key mechanism for the performance of a soil cover, and the understanding of its driving mechanisms is a crucial factor to improve the in-service conditions of a soil cover. As concluded by Wilson et al. (2006, as cited in Jubinville, 2013) and Miskolczi (2007, as cited in Jubinville, 2013), infiltration can be reduced in two orders of magnitude if surface runoff is increased. The occurrence of runoff is related to the dominant runoff mechanism, the hydraulic properties of the surface soil, and the rainfall intensity in the area. The initial results suggest that the rainfall intensities are not high enough to exceed the infiltration potential and to generate ponding on the soil's surface. As a result, an assessment of the in-service hydraulic properties of the soil covers was required to update the predictive numerical model, and at the same time to evaluate alternatives for improving the performance.

The four different soil covers were designed to perform as a barrier and store and release system, capable of working independently or integrated depending on the chosen configuration. Although the first

layer, designed as a store and release element, would allow some percolation, the volumes recorded by the tipping buckets were an indicator that the hydraulic properties of the barrier layer had been modified. The construction process might have contributed to the modification of the hydraulic properties of the till used as barrier. These changes might have been caused by variability in the composition of the till, segregation induced by placement (Adu-Wusu and Yanful, 2007), or the initial water content at compaction (Watabe et al., 2000). Another possibility was the fact that water could be flowing through a structure of connected macropores created during the construction of the barriers (Watabe et al., 2000). The determination of the in-service hydraulic properties was required to update the predictive model and at the same time, an evaluation of the conditions of the barrier layer would provide valuable information both to improve the performance of the system and to achieve the final design.

The evapotranspiration predictions were also limited by the lack of in-situ matric suction readings caused by the unreliability of the FTC-100 data collection system. Furthermore, the effectiveness of the cover system as an oxygen barrier had not been assessed, and limiting oxygen diffusion from the atmosphere could play a key role in the upcoming closure process if percolation could not be reduced.

3.3.3.2 Proposed Activities for Present Study - Phase II (2013-2014)

Based on the research purpose, the initial observations from the first stage of the project, and given the current in-situ conditions, the following activities were proposed as part of the field investigation:

- Maintenance and repair of the previously installed instrumentation (data loggers included).
- Assessment of the in-service conditions of the different materials used to build the different cover alternatives. This evaluation was aimed at identifying any change in the soil structure that could be affecting the performance of the soil cover system. The nuclear densometer was the equipment selected for the assessment, as this device allowed the obtaining of in-situ density profiles with minimal soil disturbance in both the topsoil and barrier (till) layers.
- In-service materials characterization meant to update the hydraulic properties of the soil cover materials. The Guelph permeameter tests were conducted to obtain in-situ infiltration data (saturated hydraulic conductivity) at different depths in the barrier layer. Furthermore, additional

Guelph permeameter tests were carried out at different locations of the topsoil layer to assess spatial variation of the saturated hydraulic conductivity (k_{SAT}).

- In-situ measurements to obtain information related to the degree of saturation in the topsoil and the till barrier. These measurements were directed at observing suction profiles in the cover system and were carried out using jet fill tensiometers.
- Determination of field soil-water characteristic curve (SWCC) based on in-situ characterization of density, moisture content, and matric suction measurements at a suitable resolution to minimize disturbance in the cover. The integration of the moisture, density and matric suction profiles would define the SWCC in service conditions.
- Quantification of the soil covers' effectiveness as an oxygen barrier to prevent waste rock oxidation. Sampling tubes were installed as part of the first stage of the soil cover experiment, and a portable gas analyzer was used to measure the oxygen content.
- Installation of new instrumentation in the most and least effective cover system with barriers in terms of percolation (lysimeters #5 and #1, respectively). The purpose of the new instrumentation was to obtain additional information regarding volumetric water content and matric suction. Furthermore, this new instrumentation will allow monitoring SWCC variations over time.

Although the in-situ matric suction measurements in the cover materials were considered as the first source of information regarding the degree of saturation, one of the priorities was to restore at operation of the matric suction monitoring system that had been previously installed in each lysimeter.

3.3.2 Field Tests Conducted

In order to minimize the disturbance of the different covers, most of the field tests were conducted on the topsoil surface. However, some test pits were excavated to conduct field tests on the different barrier layers. Two test pits of 1.0 m x 1.0 m dimensions and 0.30 m of depth were manually excavated in lysimeters #1, #2, and #5. Test pit excavation was not necessary at lysimeter #4, as the installed cover only consisted of a 0.30 m of depth single layer of topsoil. Figure 3-6 shows the location of the different test pits. The test pits location was defined considering the previously installed instrumentation. The turf

developed over the topsoil was carefully removed, piled in the vicinity of the excavation zone, and protected by a plastic tarp to minimize desiccation. Although the target excavation depth was 0.30 m, topsoil material was removed until the barrier layer material was visually observed. During periods when no field tests were being conducted in the test pits, they were covered with a plastic tarp to minimize material desiccation and to prevent material softening due to precipitation events. The test pits were backfilled once the 2013 field investigation program was completed, but were re-excavated for the 2014 campaign. The same excavation procedure was followed during the second field investigation, and the test pits were backfilled once all the field-testing had been completed.

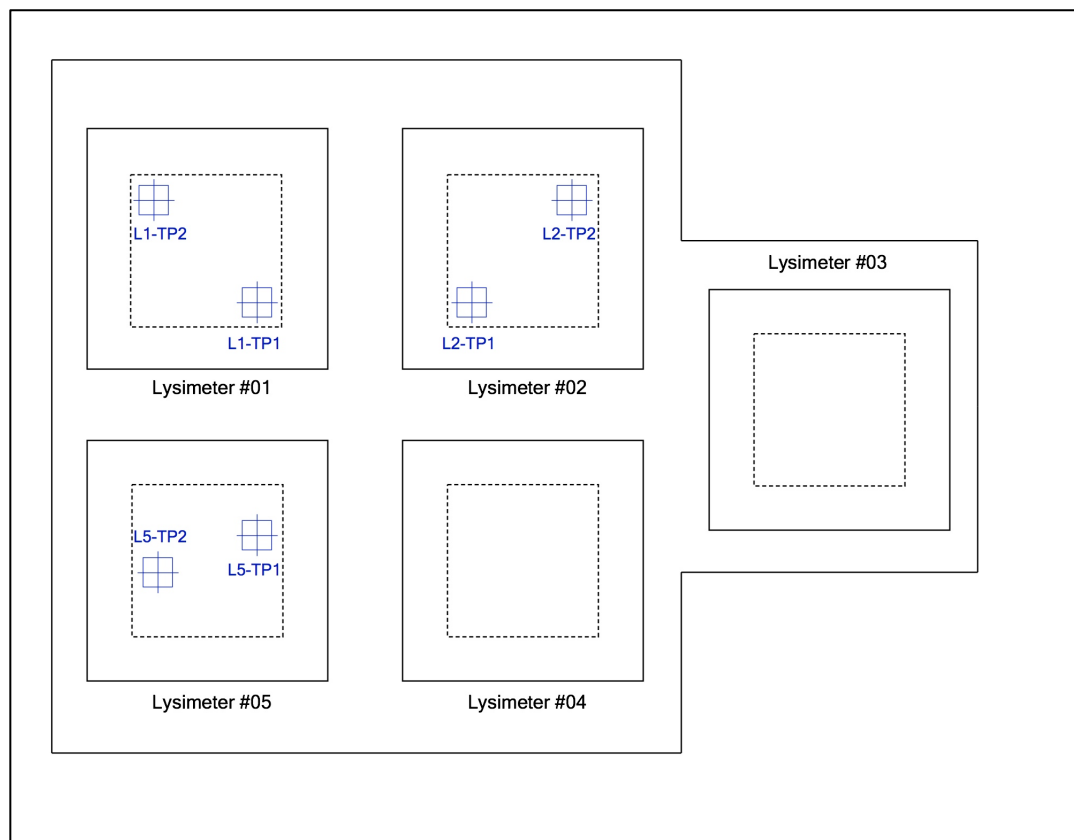


Figure 3-6: Test pits location - Soil Cover Experiment Field Investigation 2013

The following tests were conducted either on the topsoil surface or at the bottom of the excavated test pits during the 2013 field investigation program.

- Guelph permeameter test for saturated hydraulic conductivity (k_{SAT}) measurements at different depths,

- Density and moisture content measurements with a nuclear densometer at different depths,
- Soil suction measurements with jet fill tensiometers at different depths,
- Moisture content sampling at each soil suction measurement.

Oxygen content measurements were not conducted at the excavated test pits. The PVC sampling tubes installed in the waste rock during the construction were used for this purpose.

As one purpose of the 2014 field trip was to reconnect the data collection system for the FTC-100 sensors, only the soil suction testing with the respective moisture content sampling, as well as the oxygen content measurements were performed during the second stage of the field investigation. Since the second field investigation took place at the height of the dry season, the executed tests were valuable to assess the behavior of the cover during the drying period.

The following sections present a detailed description of the different tests performed as part of the two field investigation campaigns completed for the present study. In addition, details of the installation of the new instrumentation and a description of the required calibration process are also described. Chapter 4 outlines the results of the tests and the information collected by the existing and new instrumentation between 2012 and 2014.

3.3.3.1 Saturated Hydraulic Conductivity by Guelph Permeameter Test

The saturated hydraulic conductivity (k_{SAT}) of both topsoil and the compacted and non-compacted barrier layers at each cover system was determined by conducting in-situ permeability tests with the Guelph permeameter (Figure 3-7). The tests were conducted at different locations within the topsoil layer of each cover, and at different depths for the compacted and non-compacted barrier layers. For all the tests in the barrier layer, the Guelph permeameter was placed inside the two test pits excavated in each lysimeter. Although limited to two locations, the results of testing at different depths would be used to create a k_{SAT} profile, and to identify possible differences in k_{SAT} with depth and location. In the case of tests conducted in topsoil, the different locations were selected to evaluate k_{SAT} spatial distribution and to assess the possible existence of a preferential flow path. All the permeability tests in topsoil were conducted at 0.10 m of depth from the surface and the location of each test is shown in Figure 3-8.



Figure 3-7: Guelph permeameter test at Lysimeter #5

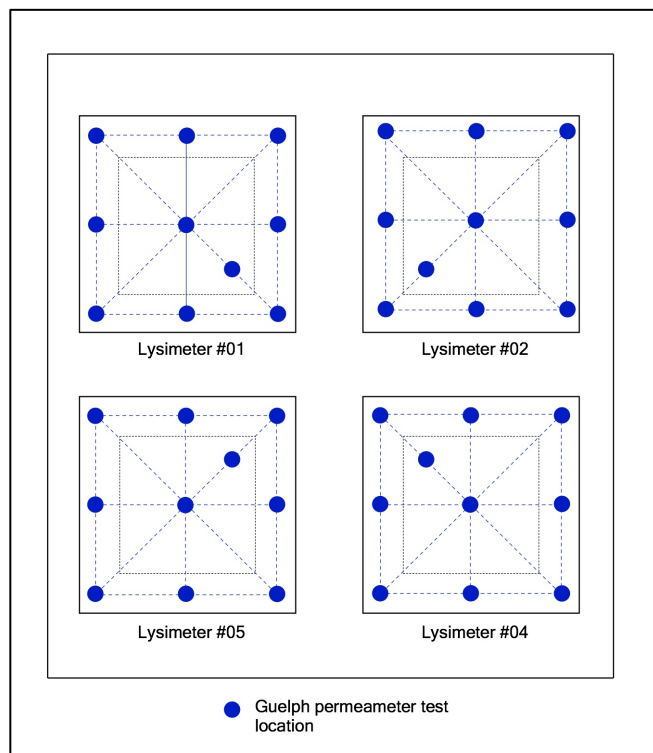


Figure 3-8: Guelph Permeability test in topsoil locations - Lysimeters #1, #2, #4, and #5

In order to evaluate k_{SAT} for the different compacted and non-compacted barrier layers, the Guelph permeameter was installed at the bottom of the two test pits excavated in lysimeters #1, #2, and #5. As the barrier layers were constructed with compacted and non-compacted clayey gravel till (lysimeter #1 and #2) or compacted silty till (lysimeter #5), several attempts were made to complete the test because, in some situations, the testing depth could not be reached due to the presence of rocks in the soil profile. The test followed the procedure indicated in the operation manual for the Guelph permeameter (Soil Moisture Equipment Corp., 2012).

The Guelph permeameter is a constant head permeameter that operates under the Mariott principle. Water flows from the permeameter reservoir into the unsaturated soil until a zone of full saturation is created (bulb), and at this point a steady-state flow rate is generated and can be measured. The measured rate flow is used along with the water head in the permeameter and the test hole dimensions to determine k_{SAT} . Depending on the level of accuracy required for k_{SAT} a single or double head can be used to run the test, and based on the expected permeability of the tested soil, the water supply for the test can come from a combined or a single reservoir. During the present field investigation, all the permeability tests were executed using only one head as the level of accuracy (factor of two) provided by this option was considered sufficient, and the reservoir selection depended on the observations made during the first minutes of the test. All the tests performed on topsoil used a combined reservoir, while the tests executed on the barrier layer materials used mostly a single reservoir. Summaries of the details for each conducted test are presented in Table 3-4 and Table 3-5.

Table 3-4: Summary of Guelph permeability tests conducted in compacted and non-compacted barrier layer materials (Lysimeters #1, #2, and #5)

Lysimeter	Test	Depth (cm)	Material	Method	Reservoir	
					Combined	Single
1	TP1-40-13	40	Compacted CGT ¹	One Head		X
	TP1-41-13	41	Compacted CGT	One Head	X	
	TP1-50-13	50	Compacted CGT	One Head	X	
	TP1-60-13A	60	Compacted CGT	One Head		X
	TP1-60-13B	60	Compacted CGT	One Head		X
	TP1-60-13B	60	Compacted CGT	One Head		X
	TP2-40-13	40	Compacted CGT	One Head	X	
	TP2-50-13	50	Compacted CGT	One Head		X
	TP2-60-13	60	Compacted CGT	One Head	X	
2	TP1-42-13	42	Non-compacted CGT	One Head		X
	TP1-45-13	45	Non-compacted CGT	One Head		X
	TP1-63-13	63	Non-compacted CGT	One Head		X
	TP2-45-13	45	Non-compacted CGT	One Head		X
	TP2-50-13	50	Non-compacted CGT	One Head	X	
	TP2-62-13	62	Non-compacted CGT	One Head		X
5	TP1-45-13	45	Compacted ST ²	One Head		X
	TP1-51-13	51	Compacted ST	One Head		X
	TP1-65-13	65	Compacted SG	One Head		X
	TP2-42-13	42	Compacted ST	One Head		X
	TP2-51-13	51	Compacted ST	One Head		X
	TP2-61-13	61	Compacted ST	One Head		X

Note:

¹: CGT = Clayey gravel till

²: SGT = Silty till

Table 3-5: Summary of Guelph permeability tests conducted in topsoil (Lysimeters #1, #2, #4, and #5)

Lysimeter	Test	Depth (cm)	Method	Reservoir	Lysimeter	Test	Depth (cm)	Method	Reservoir
				Combined					Combined
1	L1-01-13	10	One Head	X	4	L4-01-13	10	One Head	X
	L1-02-13	10	One Head	X		L4-02-13	10	One Head	X
	L1-03-13	10	One Head	X		L4-03-13	10	One Head	X
	L1-03B-13	10	One Head	X		L4-04-13	11	One Head	X
	L1-04-13	11	One Head	X		L4-05-13	11	One Head	X
	L1-05-13	10	One Head	X		L4-06-13	10	One Head	X
	L1-06-13	11	One Head	X		L4-07-13	10	One Head	X
	L1-07-13	11	One Head	X		L4-08-13	10	One Head	X
	L1-08-13	11	One Head	X		L4-08B-13	10	One Head	X
	L1-09-13	11	One Head	X		L4-09-13	10	One Head	X
	L1-10-13	11	One Head	X		L4-10-13	10	One Head	X
2	L2-01-13	10	One Head	X	5	L5-01-13	6	One Head	X
	L2-01B-13	11	One Head	X		L5-02-13	15	One Head	X
	L2-02-13	10	One Head	X		L5-03-13	8	One Head	X
	L2-03-13	11	One Head	X		L5-04-13	11	One Head	X
	L2-04-13	10	One Head	X		L5-05-13	10	One Head	X
	L2-05-13	11	One Head	X		L5-06-13	10	One Head	X
	L2-05B-13	11	One Head	X		L5-07-13	10	One Head	X
	L2-06-13	11	One Head	X		L5-08-13	11	One Head	X
	L2-07-13	12	One Head	X		L5-09-13	10	One Head	X
	L2-08-13	11	One Head	X		L5-10-13	10	One Head	X
	L2-08B-13	10	One Head	X		L5-11-13	10	One Head	X
	L2-09-13	10	One Head	X					
	L2-10-13	10	One Head	X					

3.3.3.2 Measurement of Soil Suction by Jet Fill Tensiometers

Measurements of matric suction at different depths were a key activity at this stage of the project since no matric suction data for the covers were available due to the unreliability of the FTC-100 sensors. For this reason, jet fill tensiometers were used to measure soil suction at different locations for the different topsoil layers, and at different depths for the compacted and non-compacted barrier layer materials. The tensiometers were placed in water while they were filled with distilled water, and entrapped air bubbles were removed with the help of vacuum hand pump. After all the tensiometers were filled with distilled water, they were placed in water for 24 hours to saturate the ceramic tip prior to conducting any measurement. The tensiometers were also placed in water when no testing was being conducted.

For the 2013 field investigation, suction measurements in topsoil were taken at 0.15 m of depth, next to the excavated test pits for lysimeters #1, #2, and #5. For lysimeter #4, tests were also conducted at 0.15 m of depth, but the selected locations were close to the center of the lysimeter. Measurements for the barrier layer materials were taken in each of the excavated test pits and at different depths. As in the case of the Guelph permeameter, the presence of rocks limited the installation process of the tensiometers. The tensiometers were pushed into the topsoil directly as the material was soft and free of gravel; however, for the compacted and non-compacted barrier layers, tensiometers could not be driven directly as gravel and rock could have damaged the ceramic tip. A ½" PVC pipe and a mallet were used to core a hole where the tensiometers would be inserted. Different locations were selected, and the testing depth had to be adjusted in order to minimize the cover disturbance. Once the tensiometers were placed, they were allowed to equilibrate before recording final soil suction readings. Figure 3-9 shows a typical tensiometers arrangement for soil suction measurements in lysimeter #1.



Figure 3-9: Tensiometers testing layout for Lysimeter #1

Measurements taken during the 2014 field investigation in the compacted and non-compacted barrier layers followed the same methodology used in 2013. The measurements in topsoil, however, were not taken next to the excavated test pits as in the previous investigation campaign, but at different locations as shown in Figure 3-10. This change was made in order to help evaluate how the topsoil lost water during the dry season.



Figure 3-10: Tensiometers location for topsoil testing in Lysimeter #1 during 2014 field investigation

After finishing with the matric suction measurement, a sample of the tested zone was taken for moisture content determination. Samples were stored in double Ziplock bags in order to prevent any loss of water. The moisture content was measured following the procedure outlined by the ASTM D2216 (2010). During the 2013 field investigation, samples were oven dried at the soil mechanics laboratory Antamina had on site. This laboratory was not available during the 2014 field investigation and, during this campaign, the samples had to be tested at the tailings laboratory at Antamina's Process Plant. In both cases, soil samples were dried for at least 16 hours at a temperature of 110°C.

3.3.3.3 Density by Nuclear Densometer

As described by Urrutia (2012), the construction of the cover was affected by several factors that caused an excessive drying of the materials used for the different compacted barrier layers. In addition, the thickness of the compacted layers had to be adjusted to satisfy the required compaction specifications (95% of the maximum dry density of the standard Proctor test). Density tests were conducted as part of the 2013 field investigation with the purpose of assessing the density levels at different zones and depths of the covers.

The density tests were performed following the procedure established by the ASTM D6938 (2010), and using a Troxler 3440 Surface Moisture - Density Gauge. Both topsoil and barrier materials densities were assessed next to the locations selected for matric suction measurements with jet fill tensiometers. The testing depths were 0.15 m for topsoil, and 0.40 m and 0.60 m for the barrier layers. Moisture content (gravimetric) was also measured along with density at every testing point. Table 3-6 summarizes the results of the density testing performed on the different cover materials. No density or moisture content measurements were conducted as part of the 2014 field investigation.

Table 3-6: Results of the 2013 Density Tests Completed on Cover Materials

Lysimeter	Test Pit	Point	Material	Depth (m)	Dry Density γ_d (g/cm ³)	Water Content ω (%)
1	L1-TP1	1	Compacted CGT ¹	0.40	1.63	23.5
		2	Compacted CGT	0.60	1.65	23.4
		3	Topsoil	0.15	0.98	45.2
		4	Topsoil	0.15	1.03	40.4
	L1-TP2	5	Compacted CGT	0.40	1.73	17.8
		6	Compacted CGT	0.60	1.74	17.8
		7	Topsoil	0.15	1.07	36.8
		8	Topsoil	0.15	1.05	35.2
2	L1-TP1	1	Non-compacted CGT	0.40	1.43	22.8
		2	Non-compacted CGT	0.60	1.45	23.2
		3	Topsoil	0.15	1.04	39
		4	Topsoil	0.15	1.07	34.6
	L1-TP2	5	Non-compacted CG	0.40	1.46	21.9
		6	Non-compacted CGT	0.60	1.47	22.2
		7	Topsoil	0.15	0.97	40.4
		8	Topsoil	0.15	1.05	31.1
5	L1-TP1	1	Compacted ST ²	0.40	1.38	29.8
		2	Compacted ST	0.60	1.28	32.4
		3	Topsoil	0.15	1.02	38.2
		4	Topsoil	0.15	1.05	36
	L1-TP2	5	Compacted ST	0.40	1.30	32.7
		6	Compacted ST	0.60	1.30	33.3
		7	Topsoil	0.15	1.02	38.2
		8	Topsoil	0.15	0.98	36.1
4	N.A.	1	Topsoil	0.15	1.09	29.8
		2	Topsoil	0.15	1.04	32.5
		3	Topsoil	0.15	1.33	21.7
		4	Topsoil	0.15	1.00	33

Note:

¹: CGT = Clayey gravel till

²: ST = Silty till

3.3.3.4 Oxygen Content in Waste Rock

During the construction of the soil cover experiment, five oxygen-sampling tubes were left buried in the waste rock placed in lysimeters #1, #2, #4, and #5. These oxygen tubes were close to the contact between the cover system materials and the waste rock (Urrutia, 2012). The tubes were made of PVC, and had a 3.18 mm (1/8") inner diameter. They were protected by PVC tubes and expandable foam along horizontal sections, and by HDPE tubes, sand, and bentonite at the vertical ones. Oxygen measurements were recorded with a VRAE PGM-7800 Multi Gas Monitor (RAE Systems Inc., 2001) as shown in Figure 3-11. The gas sampler has an internal pump capable of drawing air from the soil at 300 and 400 cm³/min in its low and high settings, respectively. These flow rates are low enough to avoid air deficits in the soil due to negative pressure from pumping. All measurements were conducted at the lowest pump flow rate, except when some plugging was observed and the highest setting was required to clear the tube. Measurements were taken from November 15 to 20, 2013 (wet season onset), and between June 25 and July 16, 2014 (dry season high). Oxygen readings were recorded twice a day, early in the morning and during the afternoon, with the objective of observing any possible change due to air temperature fluctuations during the day. During 2014, the readings were not recorded on a daily basis and they were taken mostly during afternoons. For all the measurements, a water trap filter made of PTFE (Teflon) membrane with a 0.2-micron pore size was used to prevent any water from being sucked into the gas sampler. Two tubes in lysimeter #5 were plugged at the time of the 2013 investigation, but one of them became available after increasing the gas sampler pump speed. The remaining tube was not available for any reading; however, a new sampling attempt was conducted in 2014 and oxygen contents were registered without problems. The tube might have been blocked by a combination of water and dust that could not be removed by the applied pump speed. As the 2014 readings were taken during the dry season, dust might have been removed easily.



Figure 3-11: Oxygen content measurement in Lysimeter #1

Before taking any measurement, the accuracy of the gas monitor was tested by connecting the device to a gas tank with a known oxygen concentration (oxygen 20.9%, and nitrogen 79% in volume). In addition, the sampler was re-calibrated every week. The calibration process consisted in exposing the sensor to two gases with different known oxygen concentrations. The same gas tank used for the daily testing was selected as the “fresh air” point, and a second tank with 100% nitrogen in volume was used to set the 0% oxygen point. Figure 3-12 shows the oxygen content (% in volume) registered for lysimeters #1, #2, #4, and #5 during both the 2013 and 2014 field investigations. Although the presented values are an average of the five readings, it is necessary to mention that the measurements of each tube are different. The difference is more notorious during the dry season. Chapter 4 examines the possible reasons for these differences.

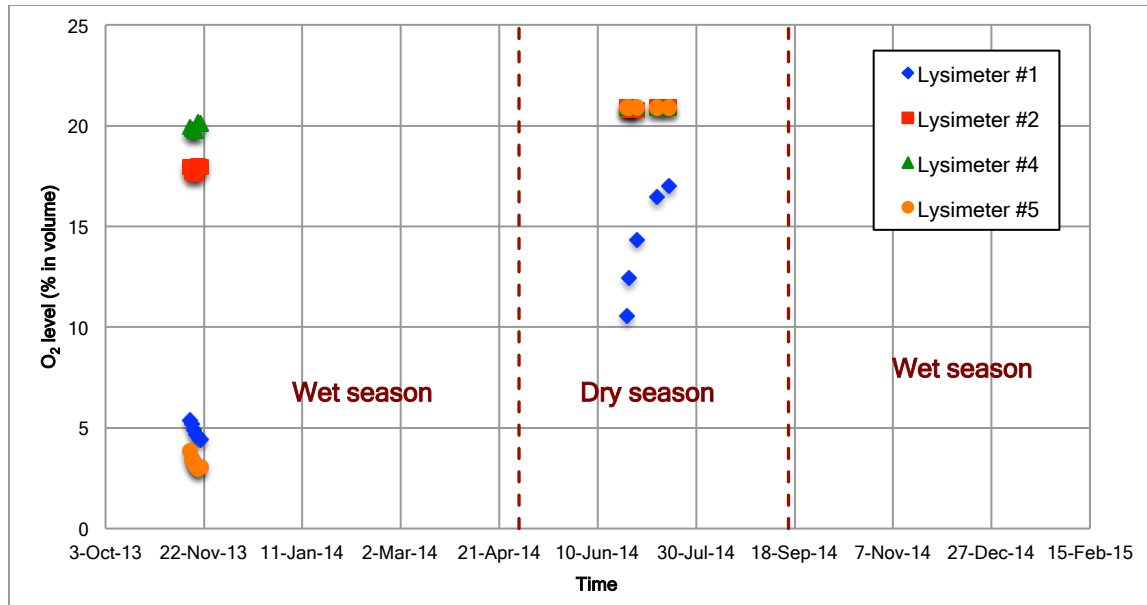


Figure 3-12: Oxygen content (% in volume) measured during the 2013 and 2014 field investigations

3.3.3 Instrument Installation

The soil cover lysimeter field experiments were instrumented with hydrological, geotechnical, and weather instruments (Urrutia, 2012). The performance of the existing instrumentation was variable between 2012 and 2013 due to intermittent data collection. Precipitation records at the experiment area were not available since August 17, 2012, and the net radiometer on site did not function effectively during the first stage of the experiment evaluated by Urrutia (2012). In addition, matric suction readings were not available during 2011 due to a problem with the FTC-100 sensors controller. The sensors collected information at the beginning of 2012, following reparation and maintenance conducted by the manufacturer (GCTS); however, a new problem arose shortly after it was put in service and data collection stopped in August 2012.

Based on the initial performance assessment, lysimeters #1 and #5 were classified as the least and most effective systems in terms of limiting percolation. With the purpose of getting a better understanding of the water retention properties of the cover materials, a new set of instrumentation was installed during the 2013 field investigation. In addition, the FTC-100 sensors controller was sent back one more time to the

manufacturer for a new technical check. During 2014, tipping buckets for both percolation and runoff flow measurements were calibrated, and a complete meteorological station was installed and put in service in May 2014 in the experiment zone (Punto B). All the systems are currently collecting information, and the collected data are the basis for the predictive numerical models and the water balance developed as part of this thesis.

3.3.3.1 Matric Water Potential Sensors and Water Content Reflectometers

Matric suction is a property associated with the water content of a soil. As described in Chapter 2, water content and the compaction method itself can modify the water retention properties of a till. In order to determine the field soil water characteristic curves (SWCC) for the covers' materials in lysimeters #1 and #5, matric suction and water content probes were installed at different depths.

Matric suction was indirectly measured by installing Campbell Scientific 229 (CS229) Heat Dissipation Matric Water Potential Sensors (2009). The suction measurement is indirect as heat dissipation is what the sensor records. The sensor consists of a cylindrical-shaped porous ceramic body with a heating element in the center, and this element also has a thermocouple in its middle section. Water in soil moves due to the existence of a gradient, and the movement leads to a change in soil suction that at the same time generates water flow inside the ceramic sensor. The changes in water content and suction inside the sensor modify its thermal conductivity, and this variation is reflected in how much the sensor temperature increases when some power is applied by the heating element. As the water content inside the sensor increases, the thermal conductivity also increase, and the increment in temperature generated is reduced when the sensor is heated. On the other hand, a drier sensor has a lower thermal conductivity and will experiment a higher temperature increment due to the low heat dissipation.

Volumetric water content is required to complement matric suction readings, and hence to determine the in-situ SWCC. Campbell Scientific 616 (CS616) Water Content Reflectometers (2012) were installed at the same depths as CS229 sensors. Volumetric water content in the soil is measured indirectly by the probe's sensitivity to the dielectric permittivity of the surrounding medium. The probe consists of two stainless steel rods connected to a printed circuit board, which generates an electromagnetic pulse that travels along each rod. The impulse propagation velocity depends on the dielectric permittivity of the surrounding soil, and this velocity is decreased under the presence of high water contents because there

are more water molecules to polarize. The pulse is reflected when it reaches the end of the rod and travels back to the probe head, where part of the circuit board detects the reflected impulse and generates a new one. The impulse frequency output is used empirically to determine the water content from a calibration equation. With both matric suction and volumetric water content readings, it is possible to determine the state of the soil at any time during a drying/wetting cycle. A total of five CS229 sensors and five CS616 probes were installed in each lysimeter #1 and #5, at the depths and within the materials shown in Table 3-7 and Table 3-8.

Table 3-7: CS229 matric suction sensors installed in Lysimeters #1 and #5

Location	Serial Number	Field Number	Depth (m)	Material
Lysimeter 1	3938	1	0.15	Topsoil
	3937	2	0.40	Compacted clayey gravel till
	3936	3	0.50	
	3935	4	0.60	
	3934	5	0.70	
Lysimeter 5	3929	10	0.15	Topsoil
	3930	9	0.40	Compacted silty till
	3931	8	0.50	
	3932	7	0.60	
	3933	6	0.70	

Table 3-8: CS616 water content probes installed in Lysimeters #1 and #5

Location	Field Number	Depth (m)	Material
Lysimeter 1	1	0.15	Topsoil
	2	0.40	Compacted clayey gravel till
	3	0.50	
	4	0.60	
	5	0.70	
Lysimeter 5	10	0.15	Topsoil
	9	0.40	Compacted silty till
	8	0.50	
	7	0.60	
	6	0.70	

Both the CS616 water content and CS229 matric suction sensors were connected to a Campbell Scientific CR1000 datalogger (2011). Since the CS229 sensors required a constant current source to operate, a

Campbell Scientific CE4 Current Excitation Module was required to provide energy to all the sensors during the reading periods. In addition, the number of available connection ports in the CR1000 data logger was not enough to connect all the required CS229, and a Campbell Scientific AM16/32B Multiplexer (2013) was included in the arrangement to increase and to improve the system wiring. The entire data collection system was placed inside a Campbell Scientific ENC16/18 Enclosure, which was mounted to the mast of a Campbell Scientific CM110 Tripod (2012). All the sensors and collection data devices were powered by a 12-V battery that is recharged by a solar panel (BP Solar, SX320J). The monitoring system was set to collect data and to transmit information via telemetry on a daily basis. The data transmission system consists of a Campbell Scientific RF416 2.45 to 2.46 GHz Spread Spectrum Radio connected to a Campbell Scientific L16755 2.4 GHz, 13 dBd Yagi Enclosed Directional Antenna. During the installation time, Antamina was in the process of migrating its entire telemetry network to a new radio frequency spectrum. For this reason, the data have been manually downloaded since the monitoring station was put in service (November 20, 2013). The monitoring station was set using LoggerNet 3.3.1 (2009), developed by Campbell Scientific, Inc., and this software was used to manually download the data for the evaluation period covered by this thesis. All the equipment was supplied by O’Kane Consultants Inc. in Saskatoon, Canada, and Enviroequip S.A.C. in Lima, Peru.

The installation of the CS229 and CS616 instruments was conducted following the guidelines provided by O’Kane Consultants Inc. (2013). Two test pits of 0.80 m of depth were excavated in lysimeters #1 and #5. One of test pits excavated in lysimeter #1 for the field investigation (0.30 m of depth) was deepened until reaching the required depth. The location of the test pit in lysimeter #5 was adjusted to match the available cable length for the CS229 sensors. The final location of the installation test pits is shown in Figure 3-13. Both test pits were excavated manually, and the sensors were installed at the depths and in the materials showed in Table 3-7 and Table 3-8. CS616 and CS229 sensors were installed in pairs in one of the sidewalls of the excavated test pit, but as the CS616 probes have a sphere influence of approximately 0.10 m of radius, all the CS616s were staggered to maintain adequate distance from any other sensor. CS229 sensors were installed in ½” holes drilled with a cordless drill, ensuring a proper contact between the ceramic part of the sensor and the surrounding soil. Due to the presence of rocks in the compacted barrier layer materials, the installation process for CS616 probes had to be adjusted.

When possible, the CS616 rods were inserted in the soil material avoiding any possible bending. When a high presence of gravel and rocks was encountered, the probes were installed by burying the rods in the cover material during the backfilling and compaction process of the test pits. There were some concerns regarding the performance of the sensors installed following this methodology, as the compaction energy could cause some damage. The probes were placed in a base layer of the barrier material with no coarse elements, and were covered with 0.15 - 0.20 m of the same material. Special care was taken when compacting over the area where the sensors were installed. The barrier materials were compacted in four layers using a vibrating plate, and no damage was induced, as all the CS616 sensors were fully operational after the compaction. All the sensor cables were tied up at surface and extended to the location of the monitoring station in a 0.20 m deep trench. The cables were placed slightly bent as a protective measure in case of any unexpected tension might occur. The cables sections leaving the ground for the connection to the monitoring station were protected with 4" HPDE pipes. Drawings of the final installation arrangement and photos of the installation process are included in Appendixes A and B, respectively.

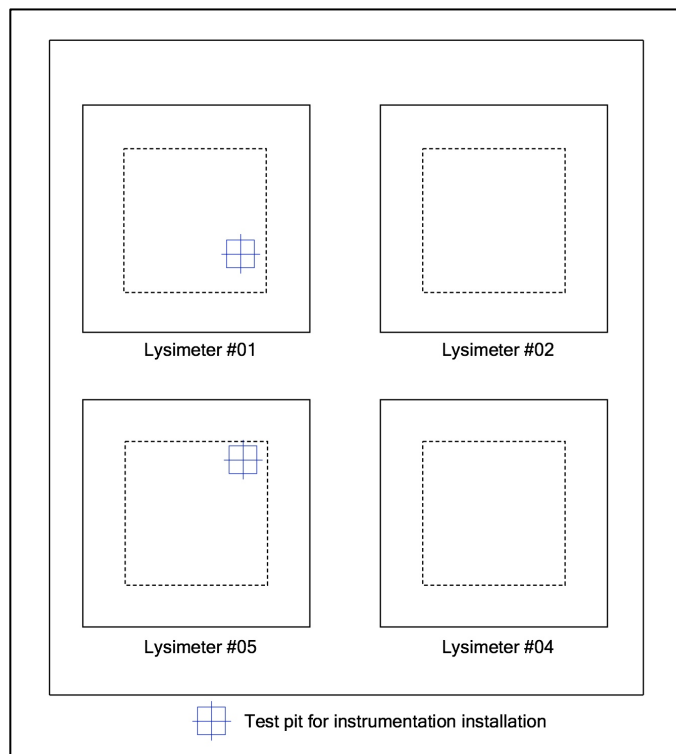


Figure 3-13: Location of the excavated test for instruments installation - Lysimeters #1 and #5

3.3.3.1.1 Calibration

The calibration of the CS229 sensors was conducted at O'Kane Consultants Inc. facilities in Saskatoon, Canada, and consisted in placing each sensor and soil in a pressure plate. Then, the entire system was saturated and different pressures (suction) were applied while the changes in temperature for the different suctions were recorded. The different readings resulted in a calibration curve, as that presented in Figure 3-14, for that typical sensor. For the estimation of matric suction, the calibration curves can be expressed in the form of power or linear equations (Campbell Scientific, Inc., 2009). Table 3-9 presents the ten calibration equations for the CS229 sensors installed in lysimeters #1 and #5.

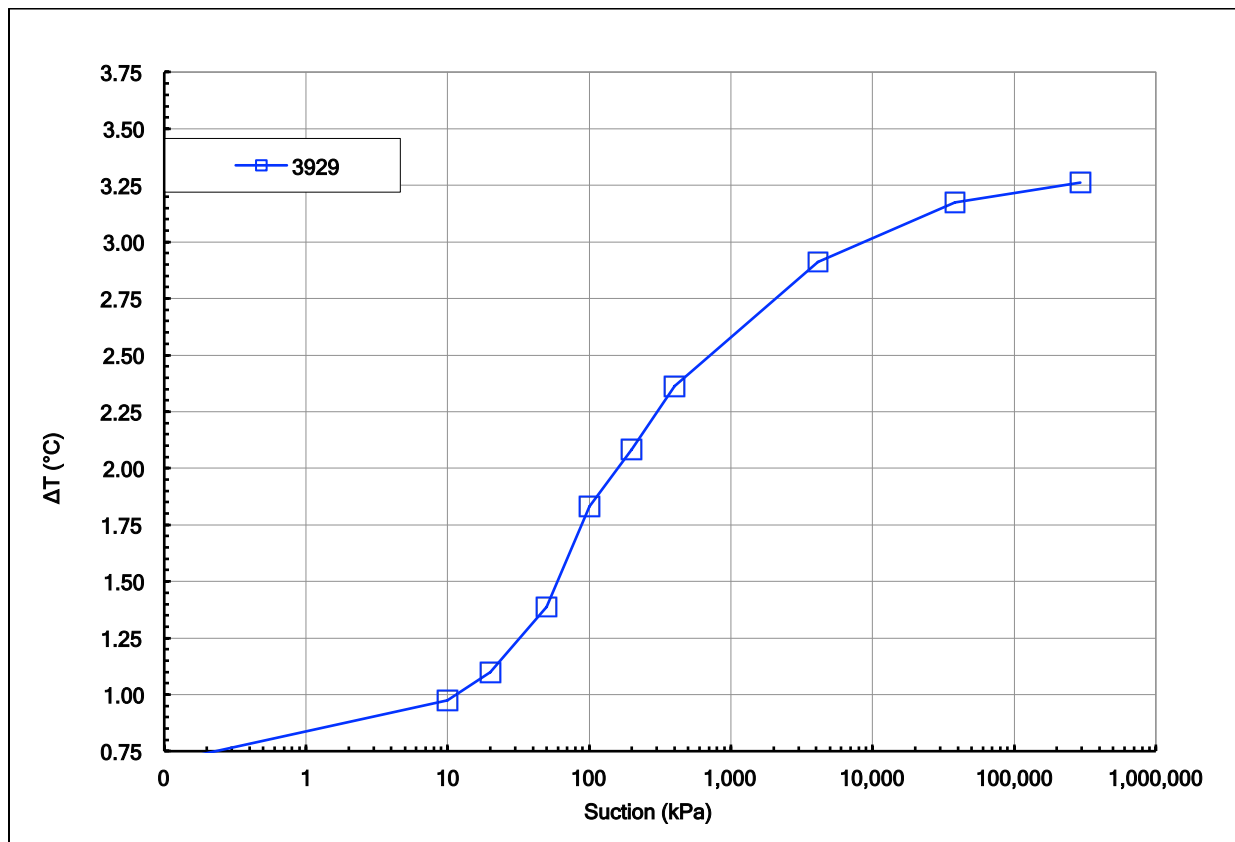


Figure 3-14: Calibration Curve for CS229 sensor (SN3929)

Table 3-9: CS229 Calibration Equations and Coefficients Summary

Field Number	Sensor Serial Number (SN)	Equation Type	A	B	R ²	ΔT_{dry}	ΔT_{wet}
1	3938	Linear ¹	2.68	0.16	0.99	3.37	0.7
2	3937	Power ²	2.90	0.95	0.98	3.15	0.7
3	3936	Linear	2.52	0.43	0.98	3.36	0.7
4	3935	Power	2.95	0.96	0.97	3.10	0.7
5	3934	Power	2.81	1.03	0.98	3.06	0.7
6	3933	Linear	3.12	-0.81	0.99	3.23	0.7
7	3932	Linear	3.16	-1.00	0.98	3.25	0.7
8	3931	Linear	3.03	-0.96	0.99	3.36	0.7
9	3930	Linear	3.02	-0.91	0.99	3.41	0.7
10	3929	Power	2.54	1.05	0.98	3.26	0.7

Note:

¹: Linear form, $\ln(\psi) = A \cdot \Delta T + B$

²: Power form, $\ln(\psi) = A \cdot \Delta T^B$

ψ : Matric suction (kPa)

The estimation of matric suction from heat dissipation is sensitive to soil temperature, and a correction is required to maintain accuracy (Campbell Scientific, Inc., 2009). The soil temperature at calibration was 20°C, hence readings obtained in the field at lower or higher temperatures need to be corrected. Flint et al. (2002) propose an iterative temperature correction to reduce sensor-to-sensor variability, which is based in normalized temperature. Flint et al. (2002) proposed the iterations continue until an error less than 10^{-3} is achieved. However, for the recorded readings, the number of iterations required to reach this level of accuracy led to constant values that did not reflect the changes in suction experienced during the year. As Flint et al. (2002) also state that other levels of accuracy can be set, the number of iterations required for the temperature correction was defined considering the suction readings from the FTC-100 sensors. The analysis of the FTC-100 sensors readings showed that these readings matched the CS229 corrected readings after one iteration cycle.

The CS616 probes also required calibration but, unlike the CS229 sensors, the calibration depends on the type of soil. As the probes measure the frequency of the impulse travelling along the probe rods, the presence of a conductive soil would create a path between the rods, causing an attenuated response. Before the installation, CS616 probes were calibrated on site using soil samples that were retained after

the soil cover experiment was constructed. The calibration procedure was provided by O’Kane Consultants Inc. (2013), and consisted in taking CS616 readings in the three different soils used and at different water contents. Some of the calibration points did not have the required level of confidence, and a re-calibration was needed. As all the CS616 probes were already installed by the time the re-calibration was needed, samples of the three different materials were sent to Saskatoon, Canada for a new calibration at O’Kane Consultants facilities. Table 3-10 presents the calibration coefficients for the topsoil, clayey gravel till, and silty till.

Table 3-10: CS616 Calibration Coefficients Summary

Material	Coefficient			
	A	B	C	D
Topsoil	0.0000134	-0.001704	0.0783	-0.895
CCGT ¹	0.00003	-0.003246	0.1252	-1.375
CST ²	-0.0000273	0.002529	-0.0579	0.388

Note:

¹: CCGT = Compacted clayey gravel till

²: CST = Compacted silty till

Equation type: $\Theta_v = A \cdot X^3 + B \cdot X^2 + C \cdot X + D$, where X is the output period in microseconds and Θ_v is volumetric water content

3.3.3.2 Thermal Conductivity Sensors

During the construction of the soil cover experiment, Urrutia (2012) installed ten Fredlund Thermal Conductivity Sensors (FTC-100) in lysimeters #1, #2, #4, and #5 at different depths. The purpose of these sensors was to indirectly measure soil matric suction, which is directly associated to the degree of saturation. Urrutia (2012) reported the operational principle of the sensors, and described the procedure followed for their installation. Urrutia (2012) also reported problems with the sensors controller that prevented data collection during the first year of the experiment. As the same problem continued during 2013, no soil matric suction data were available since the beginning of the project.

During the 2013 field investigation, the FTC-100 sensors controller was inspected on site. After unsuccessfully following the different trouble shooting procedures recommended by the manufacturer, the controller was disconnected and sent to GCTS facilities in Tempe, Arizona, for repair. Once repaired, the

controller was sent to the University of Alberta in Edmonton, Canada, where it was tested before being shipped back to Antamina in May 2014.

The FTC-100 sensors controller was reconnected in June 26, 2014 during the second field investigation. Although it worked without any problems during the first days, the measurement frequency and the connectivity between the controller and the project laptop seemed to be affected by air temperature in the project zone. The controller performance improved after the application of an artisanal protective cover made of an insulating mat, cardboard, plastic wrap, and appliance epoxy paint. The controller has been registering matric suction measurements during the period evaluated as part of this thesis. However, two sensors seem to be damaged, as matric suctions readings are equal to zero (0.15 m in lysimeter #5, 0.75 m in lysimeter #2). The matric suction measurements from FTC-100 sensors are presented in Chapter 4.

3.3.3.3 Tipping Buckets

Ten tipping buckets were installed downstream and north of the soil cover experiment in order to measure the volumes of runoff and percolation at the five different lysimeters (Urrutia, 2012). The tipping buckets installation process, and the details of the data collection system are described by Urrutia (2012). The tipping buckets have been collecting reliable information since February 2012, but those recording percolation volumes for lysimeters #1, #3, and #5 have some gaps at certain points in time. The percolation tipping bucket for lysimeter#3 was not operative from December 18, 2012 to June 22, 2013 due to a problem with the magnetic reed switch used by the system to record a tip. The same problem was reported by the percolation tipping buckets for lysimeters #1 and #5 and no data has been registered since July10, 2014. The magnetic reed switches were corroded and were replaced during 2014-2015 rainy season. Since March 2015, all the lysimeters have been fully operational with the exception of the one measuring percolation in lysimeter #2. This tipping bucket stopped working for the first time in August 2011 as reported by Urrutia (2012), but it was back in service in January 2012. Although the initial measurements showed a similar trend as the ones observed in the other lysimeters, the performance of lysimeter #2 between 2012 and 2014 evidences a constant problem with the tipping bucket.

3.3.3.3.1 Calibration

The tipping buckets installed as part of the soil cover experiment have two different sizes: 0.6 L and 1.0 L per tip. In addition, the required volume of water to tip the instrument depends on the flow rate. For these reasons, all the tipping buckets must be calibrated considering different flow rates. Urrutia (2012) proposed a calibration frequency of six months, but the tipping buckets have been calibrated only four times during the four years of monitoring. The first calibration was performed in January 2011 just before the lysimeters started collecting information. The three remaining calibrations were conducted before the start of the wet season in September 2011, June 2013, and July 2014 during the second field investigation.

For the initial assessment, a single calibration equation was defined to transform the tip rate (sec/tip) recorded into a flow rate (mL/sec). The flow rate was used to calculate the volume over the evaluated period. For this assessment, four different equations have been defined considering the different calibrations performed over time. The calibration coefficients for each evaluated period and some information for each tipping bucket are presented in Table 3-11.

Table 3-11: Tipping Buckets Information and Calibration Coefficients Summary

Tipping Bucket	Serial No.	Approx. mL/tip	Calibration Coefficients ¹							
			February 2011 - May 2011		June 2011 - July 2012		August 2012 - December 2013		January 2014 - December 2014	
			A	B	A	B	A	B	A	B
L1-I ²	09-27	0.6	715.2	-1.011	722.4	-1.011	816.1	-1.042	829.1	-1.037
L1-R ³	09-23	1.0	1095.9	-0.985	1207.3	-1.018	1207.3	-1.018	1239.3	-1.012
L2-I	09-28	0.6	776.5	-1.036	691.1	-0.992	681.7	-0.989	867.0	-1.045
L2-R	09-24	1.0	1102.7	-1.01	1133.4	-1.015	1270.2	-1.026	1128.6	-1.006
L3-I	09-29	0.6	960.3	-1.139	726.6	-1.006	859.1	-1.057	824.9	-1.039
L3-R	09-30	0.6	730.6	-1.026	792.5	-1.029	737.2	-0.978	771.8	-1.024
L4-I	09-31	0.6	694.5	-1.012	743.7	-1.021	811.2	-1.036	813.6	-1.034
L4-R	09-25	1.0	1212.7	-1.013	1287.3	-1.036	1212.3	-0.995	1255.3	-1.025
L5-I	09-32	0.6	706.5	-1.019	765.7	-1.045	844.7	-1.046	898.1	-1.044
L5-R	09-26	1.0	1149.1	-1.008	1005.1	-0.982	1198.5	-1.021	1212.0	-1.017

Note:

¹: Equation type: $y = A \cdot X^B$, where y = flow rate (mL/sec) and X = tip rate (sec/tip)

²: I = Infiltration

³: R = Runoff

CHAPTER 4: FIELD AND MONITORING DATA

This chapter presents and discusses the results of the tests conducted as part of two field investigation campaigns carried out in 2013 and 2014. The data collected by the different instruments installed between 2011 and 2014 is also included and reviewed in this chapter.

4.1 Field Testing Results

As Chapter 3 outlined, a number of field tests were conducted to characterize in-situ the hydrological and geotechnical properties of the soil cover material. The following sections summarize and evaluate the results of these tests.

4.1.1 Saturated Hydraulic Conductivity

4.1.1.1 Topsoil

A total of 46 Guelph permeameter tests were conducted in the topsoil layer on four of the five lysimeters. The testing distribution and depths are presented in Figure 3-3 and Table 3-2, respectively. The saturated hydraulic conductivity (k_{SAT}), considering the 46 tests, ranged from 1.7×10^{-6} to 2.1×10^{-5} m/s, with a geometric average equal to 7.8×10^{-6} m/s. Table 4-1 presents maximum, minimum, and geometric average values for topsoil at each lysimeter.

Table 4-1: Summary of Saturated Hydraulic Conductivity (k_{SAT}) tests results - Topsoil

Lysimeter	Number of tests	k_{SAT} (m/s)		
		Minimum	Maximum	Geometric Mean
1	11	3.5E-06	1.6E-05	7.0E-06
2	13	1.7E-06	2.0E-05	5.7E-06
4	11	2.6E-06	2.0E-05	8.5E-06
5	11	5.7E-06	2.1E-05	1.1E-05

The results presented in Table 4-1 show a relatively uniform k_{SAT} distribution for the four different topsoil layers. Maximum and minimum k_{SAT} values are in the same order of magnitude, and although the k_{SAT} geometric mean for lysimeter #5 is higher than for the other ones, it is possible to consider a uniform average trend for this material. The purpose of conducting a greater number of tests in each topsoil layer

was to evaluate the possible existence of preferential flow. Preferential flow is a phenomenon where water moves along certain pathways, bypassing other volume fractions of the porous soil matrix (Gerke, 2006). This process can be caused by differences in hydraulic conductivity or the presence of macropores. The k_{SAT} spatial distribution for the topsoil at each lysimeter is shown in Figure 4-1. Although slight differences in k_{SAT} were noted, all the values ranged from 10^{-6} (blue columns) to 10^{-5} m/s (red columns). Even though some peaks were observed in lysimeters #2 and #4, these peak values were not outside of the range observed in all the lysimeters, and hence they did not represent an area of high percolation. In addition, precipitation rates in the experiment zone are in the order of 10^{-7} m/s, which is an order of magnitude lower than the k_{SAT} geometric average (10^{-6} m/s) from the 46 field tests. The difference supports the initial conclusion that rainfall intensities are not high enough to generate runoff on the topsoil layer.

The in-situ values of k_{SAT} measured were compared with the laboratory values determined by both Golder Associates (Golder) and University of Alberta (U of A). Golder tested a single topsoil sample using an effective vertical stress of 7 kPa, while U of A samples were tested at vertical stresses of 0, 10, and 20 kPa. Both field and laboratory k_{SAT} values are summarized in Table 4-2. As in the spatial distribution charts presented previously, all the k_{SAT} in-situ values were in the same order of magnitude as the ones from laboratory testing.

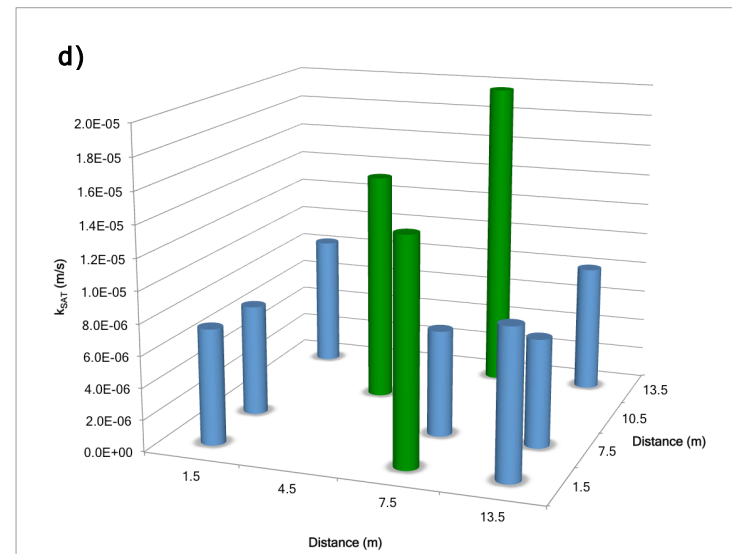
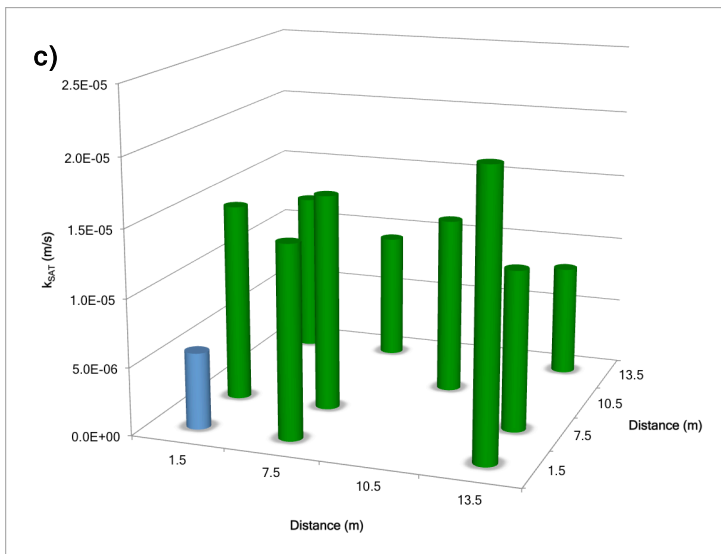
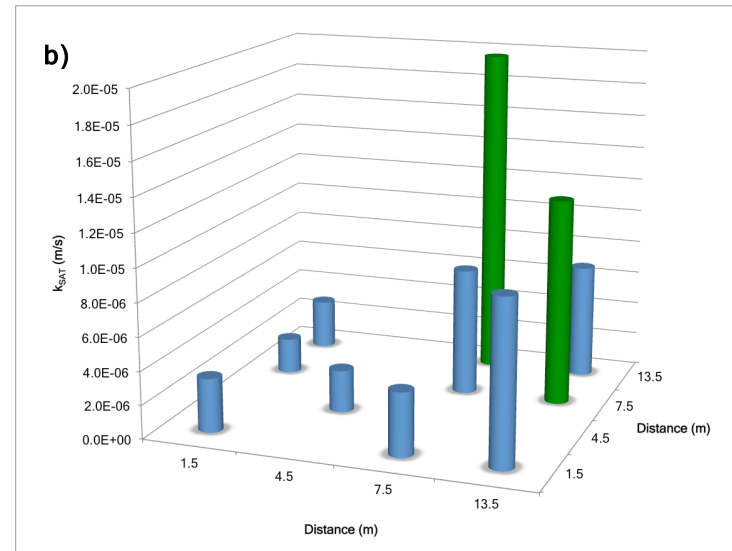
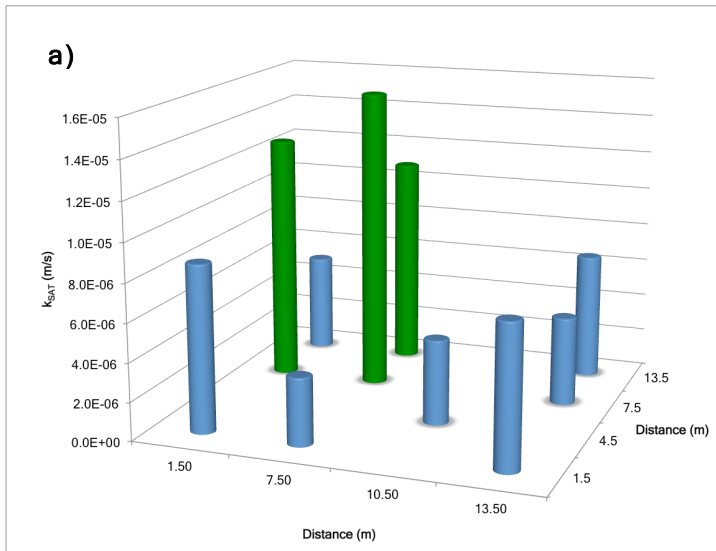


Figure 4-1: Saturated hydraulic conductivity (k_{SAT}) spatial distribution: a) Lysimeter #1, b) Lysimeter #2, c) Lysimeter #5, d) Lysimeter #4

Table 4-2: Laboratory and in-situ saturated hydraulic conductivity (k_{SAT}) test results for topsoil

Source	Depth (m)	Dry Density (g/cm ³)	Lab. Vertical Effective Stress (kPa)	In-situ Vertical Effective Stress (kPa)	k_{SAT} (m/s)
Golder	N.A.	N.A.	7	N.A.	4.6E-06
U of A	N.A.	N.A.	0	N.A.	1.1E-05
	N.A.	N.A.	10	N.A.	2.5E-06
	N.A.	N.A.	20	N.A.	7.8E-07
	N.A.	N.A.			
L#1	0.15	0.93	N.A.	0.64	7.8E-06
	0.15	0.93	N.A.	0.66	7.8E-06
	0.15	0.97	N.A.	0.69	7.8E-06
	0.15	0.94	N.A.	0.63	7.8E-06
L#2	0.15	0.96	N.A.	0.67	7.5E-06
	0.15	0.94	N.A.	0.66	7.5E-06
	0.15	0.92	N.A.	0.54	7.5E-06
	0.15	0.91	N.A.	0.57	7.5E-06
L#5	0.15	0.93	N.A.	0.62	1.2E-05
	0.15	0.93	N.A.	0.64	1.2E-05
	0.15	0.93	N.A.	0.62	1.2E-05
	0.15	0.88	N.A.	0.49	1.2E-05
L#4	0.15	1.00	N.A.	0.62	9.6E-06
	0.15	0.99	N.A.	0.56	9.6E-06
	0.15	1.13	N.A.	0.92	9.6E-06
	0.15	0.94	N.A.	0.50	9.6E-06

4.1.1.2 Compacted clayey gravel till

A total of 13 Guelph permeameter tests were carried out in the compacted clayey gravel till barrier in lysimeter #1 (Table 3-1). The tests were conducted in the two test pits excavated as part of the 2013 field investigation. The k_{SAT} geometric average was 1.7×10^{-6} m/s, and k_{SAT} at the tested depths ranged from 1.4×10^{-7} to 1×10^{-5} m/s. Figure 4-2 presents k_{SAT} values measured in the two excavated test pits along with the geometric average values at each depth and for all data.

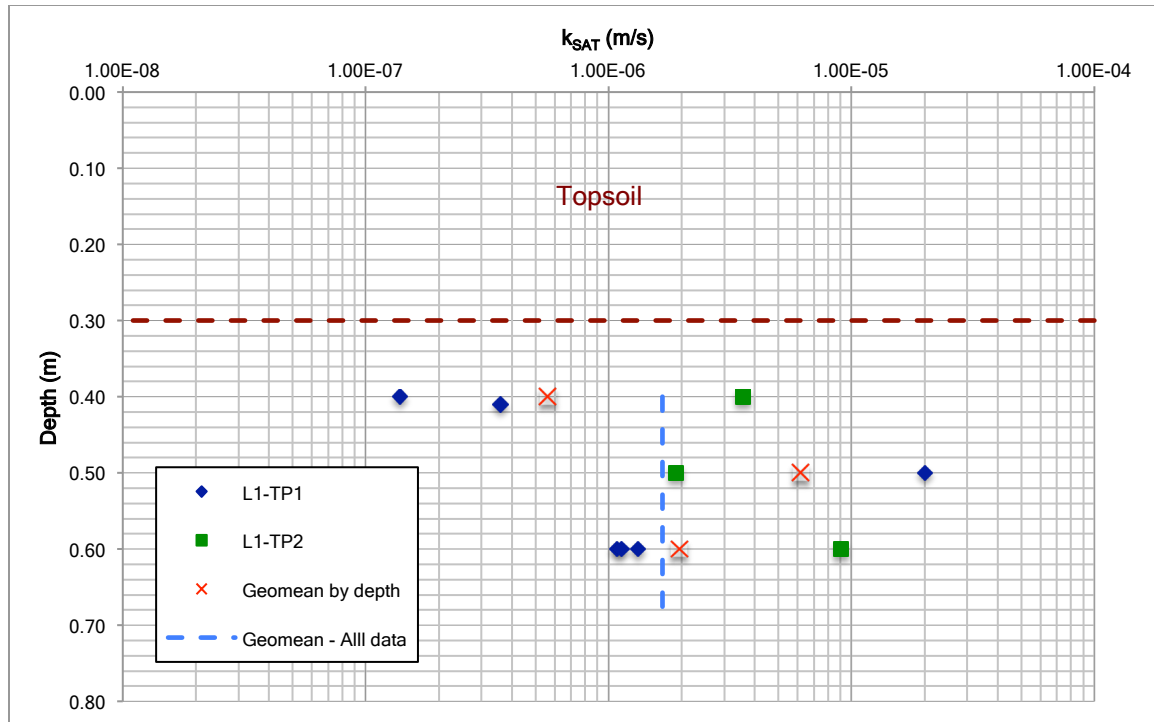


Figure 4-2: Saturated hydraulic conductivity (k_{SAT}) distribution - Compacted clayey gravel till

Figure 4-2 shows that although there are a couple of extreme values at the top and middle zones of L1-TP1, most of the k_{SAT} values are in the 10^{-6} m/s order of magnitude. This value is three orders of magnitude greater than the ones obtained by Golder at an effective vertical pressure of 8.85 kPa, and for a sample compacted at 95% of the maximum dry density from the standard Proctor test. The U of A tests were performed using the material fraction passing #4 sieve (4.75 mm opening), which was compacted based on the information from the compaction test. Unlike topsoil, the Guelph permeameter test was executed next to the location where density had been measured with the nuclear densometer. Table 4-3 presents the field, Golder, and U of A laboratory tests results.

Table 4-3: Laboratory and in-situ saturated hydraulic conductivity (k_{SAT}) test results for compacted clayey gravel till

Source	Depth (m)	Dry Density (g/cm ³)	Lab. Vertical Effective Stress (kPa)	In-situ Vertical Effective Stress (kPa)	k_{SAT} (m/s)
Golder	N.A.	N.A.	8.85	N.A.	2.1E-09
U of A	N.A.	N.A.	0	N.A.	1.5E-09
	N.A.	N.A.	10	N.A.	6.0E-10
	N.A.	N.A.	20	N.A.	9.2E-11
	N.A.	N.A.		N.A.	
L#1	0.40	1.64	N.A.	2.32	2.5E-07
	0.60	1.66	N.A.	4.36	1.2E-06
	0.40	1.64	N.A.	2.36	3.6E-06
	0.60	1.66	N.A.	4.44	9.0E-06
	0.50	1.64	N.A.	3.33	2.0E-05
	0.50	1.64	N.A.	3.39	1.9E-06

Table 4-3 shows the k_{SAT} field values are 2 to 4 orders of magnitude greater than the laboratory ones (U of A). Urrutia (2012) reported that the compacted clayey gravel till had been apparently over compacted during placement in the permeability test cell. The over compaction can also be associated with the absence of coarse material, as only the fraction finer than #4 sieve (4.75 mm opening) was used for testing purposes. Although particles greater than four inches were removed manually when found during construction (Urrutia, 2012), there is still a significant coarse fraction that was not removed (18.2% - 38.6%, Table 2-2). Hence, the characteristics and hydraulic properties of the field materials are different from the laboratory tested ones. In addition, the k_{SAT} reported by Golder is slightly greater than the one defined by U of A. The sample tested by Golder presented a higher dry density (1892 kg/m³) when compared with the maximum dry densities from the different standard Proctor tests conducted, but at the same time it was on the wet side of the compaction curve. Watabe et al. (2000) showed that glacial tills experienced a significant decrease in hydraulic conductivity when compacted at moisture contents lower than the optimum one. Dry density controls during the construction process showed that most of the layers at the different lysimeters were compacted on the dry side of the compaction curve. Although placement and compaction conditions can have an impact on the final k_{SAT} , the characteristics of the clayey gravel till played a key role in the measured permeability of the barrier. Clay is susceptible to cracking and the presence of coarse gravel promotes the development of a macropore structure. The

difference between the laboratory test and construction conditions is also an important factor. Daniel (1981, as cited in Urrutia, 2012) concluded hydraulic conductivities from laboratory tests might differ from field ones, as the laboratory result was obtained from a sample at a given density and under a particular stress condition. The combination of all the previously mentioned factors might have influenced the final k_{SAT} outcome for the compacted clayey gravel till barrier.

4.1.1.3 Non-compacted Clayey Gravel Till

The k_{SAT} field assessment for the non-compacted clayey gravel till (lysimeter #2) consisted of six Guelph permeameter tests (Table 3-1). As for the compacted clayey gravel till in lysimeter #1, the tests were conducted in the two 0.30 m deep test pits excavated during the 2013 field investigation. The in-situ k_{SAT} values ranged from 1.7×10^{-6} to 9.3×10^{-6} m/s, and had a geometric average of 3.6×10^{-6} m/s. Figure 4-3 presents a k_{SAT} distribution with depth for the two excavated test pits. Geometric average values at each tested depth and for the whole barrier are also included in Figure 4-3.

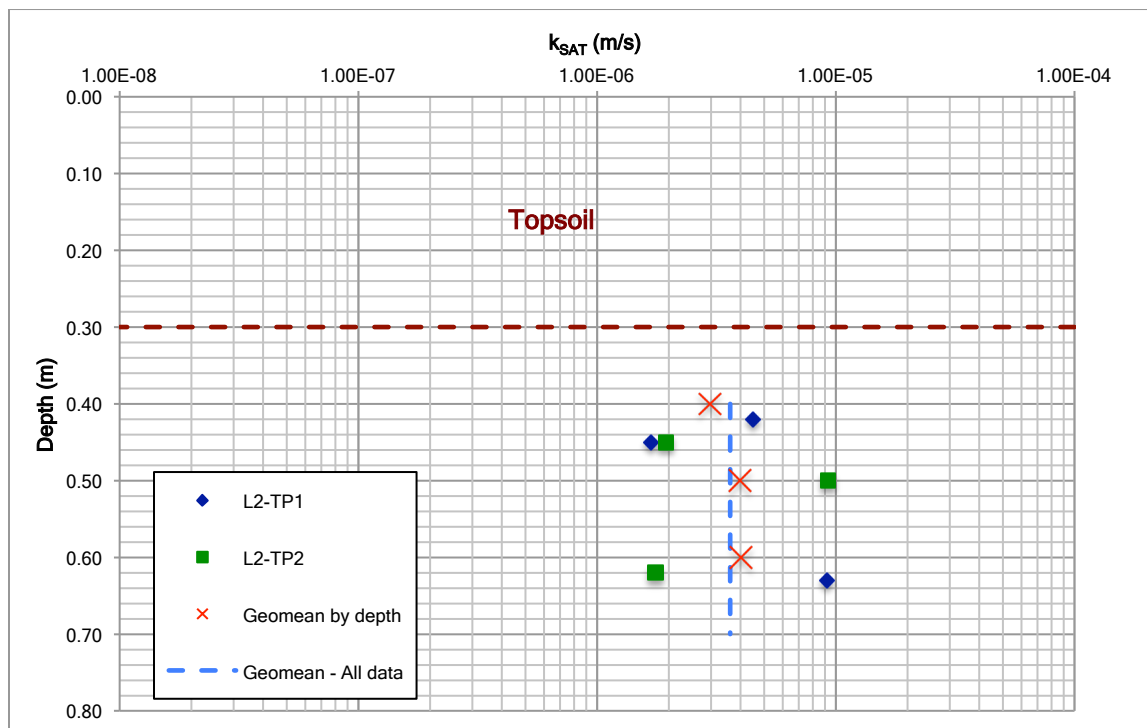


Figure 4-3: Saturated hydraulic conductivity (k_{SAT}) distribution - Non-compacted clayey gravel till

Results shown in Figure 4-3 confirmed the initial conclusions drawn by Urrutia (2012). The hydraulic performance of lysimeters #1 and #2 were very close during the initial assessment. The field k_{SAT} for the non-compacted clayey gravel till was in the 10^{-6} m/s order of magnitude, which is the same for the compacted clayey gravel till. Although there were some differences when evaluating k_{SAT} with depth for both test pits, the geometric average was uniform along the total thickness of the barrier. Furthermore, in-situ k_{SAT} values were 1 to 2 orders of magnitude greater than the ones measured at U of A (Table 4-4). The U of A laboratory tests were also conducted at vertical effective stresses of 0, 10, and 20 kPa, and using the material fraction passing #4 sieve (4.75 mm opening). Golder, as part of its testing program, did not conduct any permeability test in the non-compacted clayey gravel till. The U of A k_{SAT} laboratory test results and 2013 k_{SAT} field measurements at different vertical effective stresses are presented in Table 4-4.

Table 4-4: Laboratory and in-situ saturated hydraulic conductivity (k_{SAT}) test results for non-compacted clayey gravel till

Source	Depth (m)	Dry Density (g/cm ³)	Lab. Vertical Effective Stress (kPa)	In-situ Vertical Effective Stress (kPa)	k_{SAT} (m/s)
U of A	N.A.	N.A.	0	N.A.	3.7E-08
	N.A.	N.A.	10	N.A.	1.8E-08
	N.A.	N.A.	20	N.A.	7.1E-09
L#1	0.40	1.49	N.A.	2.09	4.5E-06
	0.60	1.44	N.A.	3.63	9.2E-06
	0.40	1.42	N.A.	1.89	1.9E-06
	0.60	1.42	N.A.	3.46	1.8E-06
	0.50	1.49	N.A.	2.85	1.7E-06
	0.50	1.42	N.A.	2.67	9.3E-06

The difference between field and laboratory k_{SAT} was between 1 to 2 orders of magnitude. As the material was not compacted during construction, the difference is a direct consequence of the presence of the coarser fraction (gravel). Table 3-2 shows that the placed material had a gravelly fraction of 26.2% to 32.4%. From these results it is possible to affirm that the coarse fraction of the clayey gravel till is one of the reasons for the high levels of percolation observed in lysimeter #1. The difference in gradation between both field and laboratory materials led to underestimated k_{SAT} values, and this the impact of the gravel presence was increased by the construction conditions and the material characteristics.

4.1.1.4 Compacted Silty Till

Six Guelph permeameter tests, as detailed in Table 3-1, were conducted in the two test pits excavated in lysimeter #5. The k_{SAT} field values ranged from 3.8×10^{-8} to 8.0×10^{-7} m/s, with a geometric average of 1.2×10^{-7} m/s. Figure 4-4 illustrates the distribution of k_{SAT} measured at different depths for the two excavated test pits. Geometric average values are also included in this figure.

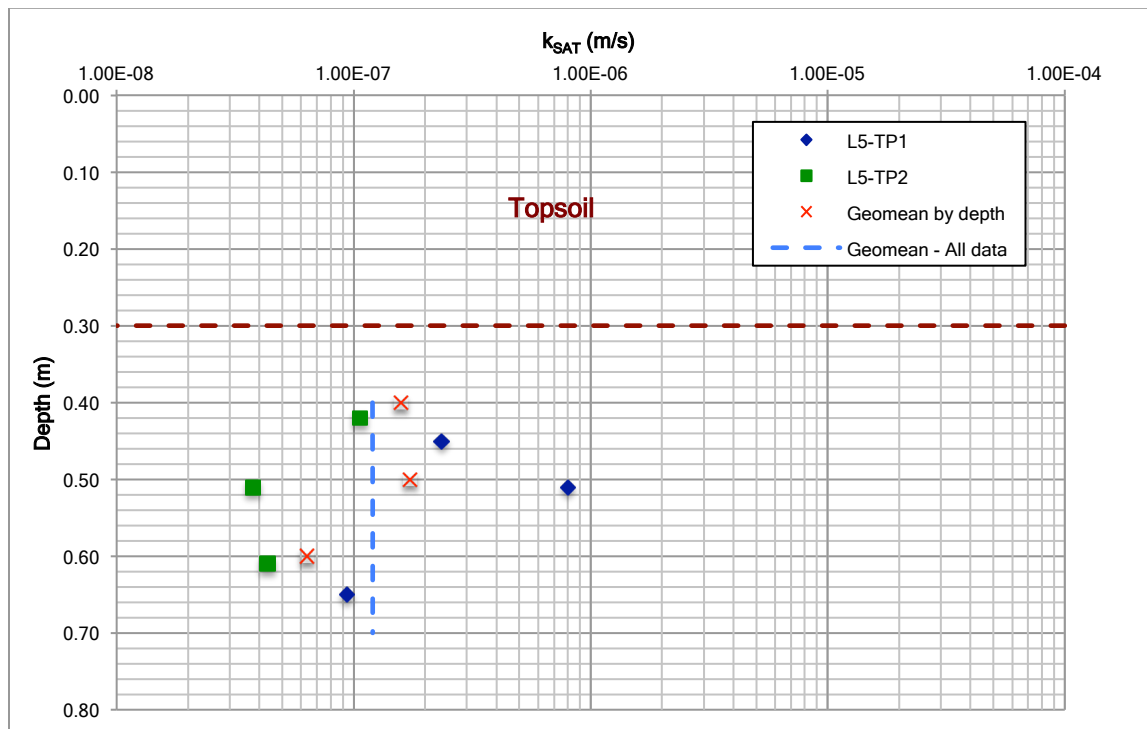


Figure 4-4: Saturated hydraulic conductivity (k_{SAT}) distribution - Compacted silty till

The in-situ k_{SAT} for the compacted silty till was 1 to 2 orders of magnitude lower than the one for the clayey gravel till. One of the reasons for the difference may be the grain size distribution of the silty till. The silty till presented a fine content as high as 75% in some cases (Table 2-2), and some samples tested as part of the QA/QC program during the construction were classified as elastic silts. As the laboratory k_{SAT} results were obtained from samples consisting in the fraction finer than #4 sieve, the impact of the presence of gravel is smaller. In addition, the density tests during construction showed dry density values close to the required specification, even though the material was placed drier than the optimum in some cases. The U of A permeability tests were performed at vertical effective stresses of 0, 10, and 20 kPa. The test carried out by Golder was performed at a vertical effective pressure of 7 kPa, and at a dry density

of 1359 kg/m^3 , which is lower than those obtained from the different standard Proctor tests. However, the sample initial moisture content was higher than the optimum one determined by the same compaction tests. Table 4-5 summarizes shows the laboratory (U of A and Golder) and field k_{SAT} results at different vertical effective stresses for the compacted silty till.

Table 4-5: Laboratory and in-situ saturated hydraulic conductivity (k_{SAT}) test results for compacted silty till

Source	Depth (m)	Dry Density (g/cm^3)	Lab. Vertical Effective Stress (kPa)	In-situ Vertical Effective Stress (kPa)	k_{SAT} (m/s)
Golder	N.A.	N.A.	7	N.A.	7.3E-08
U of A	N.A.	N.A.	0	N.A.	4.2E-06
	N.A.	N.A.	10	N.A.	3.3E-08
	N.A.	N.A.	20	N.A.	1.7E-08
L#1	0.40	1.50	N.A.	2.03	2.4E-07
	0.60	1.29	N.A.	3.49	9.3E-08
	0.40	1.43	N.A.	1.84	1.1E-07
	0.60	1.32	N.A.	3.30	4.3E-08
	0.50	1.50	N.A.	2.80	8.0E-07
	0.50	1.43	N.A.	2.57	3.8E-08

The field k_{SAT} values were up to 1 order of magnitude lower than the U of A laboratory results. A loss of compaction during the sample saturation prior to the initiation of the test was reported by Urrutia (2012), and for this reason the U of A laboratory results were not considered representative. As Daniel (1981, as cited in Urrutia, 2012) concluded, the resultant k_{SAT} depended on the sample characteristics during testing. The field results were close or slightly lower than the 'non-representative' laboratory outcomes, but this similarity was an indicator of the barrier field conditions. As previously mentioned, the dry densities measured during both the construction process and 2013 field investigation were lower than the construction specification set from the standard Proctor tests. This outcome is expected due to the high sensitivity of silty materials to changes in water content that may occur during compaction. As laboratory samples were compacted at 95% of the maximum dry density from the standard Proctor Test, the laboratory results are not representative, but instead due to the differences in density induced by the construction process.

4.1.2 Dry Density and Water Content

Dry density and water content were measured in all the cover materials at depths of 0.15, 0.40, and 0.60 m. The values were obtained by using a Troxler 3440 Surface Moisture - Density Gauge, and the results appear in Table 3-6. As part of the field investigation, soil samples were taken at the locations and depths where soil suction measurements had been recorded. These samples were oven dried to determine the gravimetric water content for volumetric water content estimation purposes. The dry density and water content measured by the nuclear densometer were recorded at the same depths, and at the adjacent location to where the soil suction test was conducted. The moisture contents measured by the nuclear densometer were compared to the ones determined by oven drying, and some differences were observed. Table 4-6 shows moisture contents by nuclear densometer and oven drying, and the difference between them.

The clayey gravel till in both lysimeters #1 and #2 was considered as a single group disregarding compaction, and there was a difference of -1% to 6% between densometer and oven dried water content. A negative value meant that the oven-dried sample had lower moisture content than the one from the densometer. The difference for the silty till ranges from -12% to 0%. The high negative values were measured at 0.40 m of depth, and they might be a consequence of their proximity to the test pit bottom, which might have led to some loss of water by evaporation. Moisture content measurements for topsoil had the highest differences, ranging from 7% to 21%. These differences might have been due to the presence of organic material (hydrogen) and clayey minerals, as the chemical composition of the soil influences the final densometer output (ASTM D6938, 2010). For consistency purposes, all the moisture contents from the nuclear densometer were replaced with oven dried values, and the dry densities were recalculated considering these values and the total density readings from the densometer. The modified dry density values are also shown in Table 4-6. Both moisture contents and recalculated dry densities by depth were compared with the 2010-2011 construction density control results. Figure 4-5 and Figure 4-6 present dry density and moisture content profiles for lysimeters #1 and #5, respectively.

Table 4-6: Dry densities and moisture content from nuclear densometer and corrected by oven-dried moisture content

Test Pit	Point	Material	Depth (m)	From Densometer		Water Content (Oven dried)- ω (%)	Difference in Water content (%)	Modified Dry Density - γ_d (g/cm ³)
				Dry Density - γ_d (g/cm ³)	Water Content - ω (%)			
L1-TP1	1	CCGT ¹	0.40	1.63	23.5	22.6	-0.9	1.64
	2	CCGT	0.60	1.65	23.4	22.6	-0.8	1.66
	3	Topsoil	0.15	0.98	45.2	53.9	8.7	0.93
	4	Topsoil	0.15	1.03	40.4	55.1	14.7	0.93
L1-TP2	5	CCGT	0.40	1.73	17.8	23.7	5.9	1.64
	6	CCGT	0.60	1.74	17.8	23.7	5.9	1.66
	7	Topsoil	0.15	1.07	36.8	50.0	13.2	0.97
	8	Topsoil	0.15	1.05	35.2	51.7	16.5	0.94
L2-TP1	1	NCCGT ²	0.40	1.43	22.8	17.6	-5.2	1.49
	2	NCCGT	0.60	1.45	23.2	24.2	1.0	1.44
	3	Topsoil	0.15	1.04	39	50.5	11.5	0.96
	4	Topsoil	0.15	1.07	34.6	53.6	19.0	0.94
L2-TP2	5	NCCGT	0.40	1.46	21.9	25.1	3.2	1.42
	6	NCCGT	0.60	1.47	22.2	26.3	4.1	1.42
	7	Topsoil	0.15	0.97	40.4	47.8	7.4	0.92
	8	Topsoil	0.15	1.05	31.1	51.0	19.9	0.91
L5-TP1	1	CST ³	0.40	1.38	29.8	17.8	-12.0	1.50
	2	CST	0.60	1.28	32.4	32.2	-0.2	1.29
	3	Topsoil	0.15	1.02	38.2	51.5	13.3	0.93
	4	Topsoil	0.15	1.05	36	54.2	18.2	0.93
L5-TP2	5	CST	0.40	1.30	32.7	21.0	-11.7	1.43
	6	CST	0.60	1.30	33.3	30.9	-2.4	1.32
	7	Topsoil	0.15	1.02	38.2	51.6	13.4	0.93
	8	Topsoil	0.15	0.98	36.1	51.8	15.7	0.88
N.A.	1	Topsoil	0.15	1.09	29.8	41.1	11.3	1.00
	2	Topsoil	0.15	1.04	32.5	39.5	7.0	0.99
	3	Topsoil	0.15	1.33	21.7	43.1	21.4	1.13
	4	Topsoil	0.15	1.00	33	42.3	9.3	0.94

Note:

¹: CCGT = Compacted clayey gravel till

²: NCCGT = Non-compacted clayey gravel till

³: CST = Compacted silty till

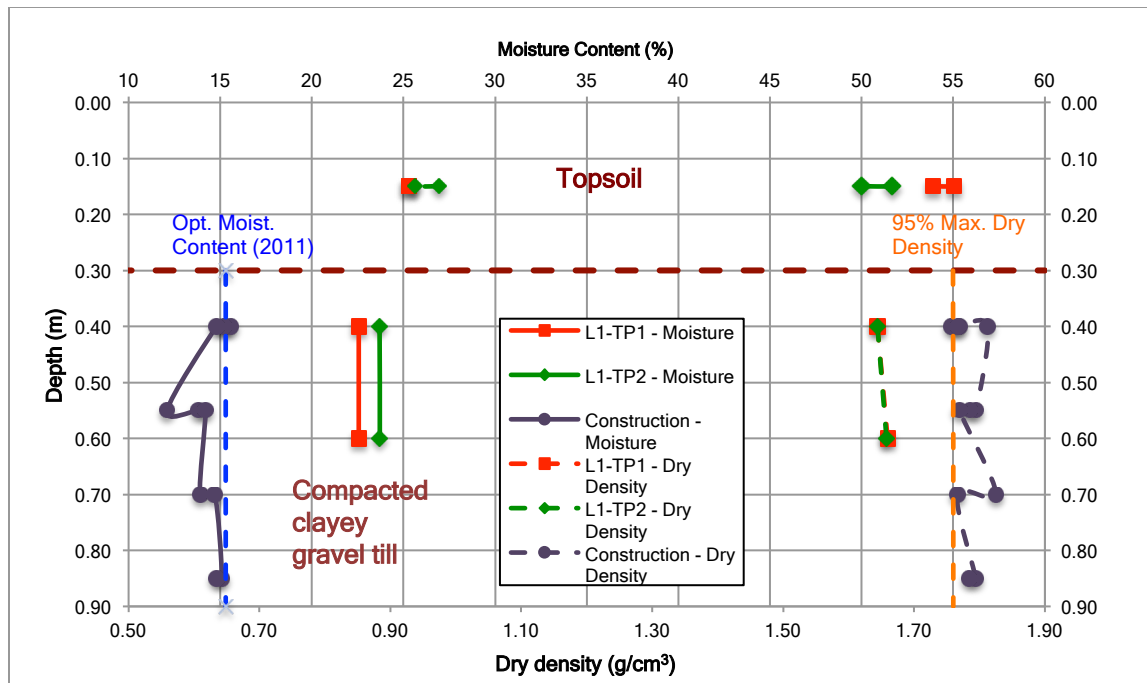


Figure 4-5: Dry density and moisture content profiles for lysimeter #1

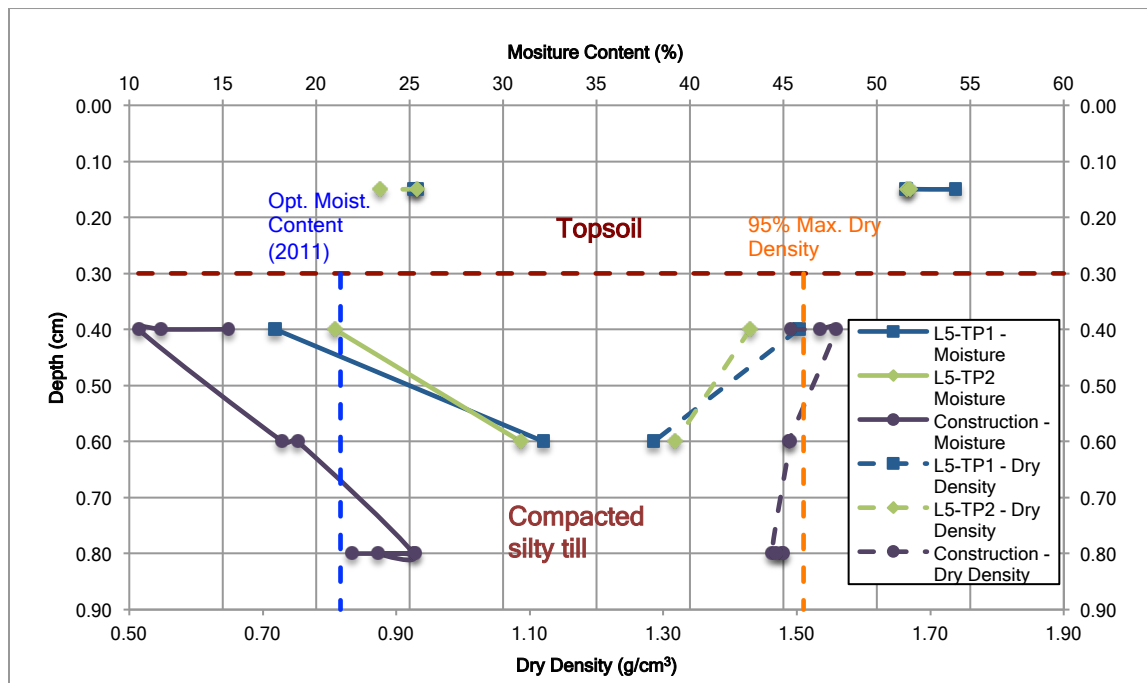


Figure 4-6: Dry density and moisture content profiles for lysimeter #5

Moisture contents for the compacted barrier layer materials at the time of construction are included in Figure 4-5 and Figure 4-6 to evaluate if those materials were placed drier or wetter than optimum. The moisture contents measured during the 2013 field investigation are not expected to be the same, and hence they cannot be compared with the optimum moisture content because infiltration has been occurring since 2011.

It is observed from Figure 4-5 and Figure 4-6 that topsoil had the same moisture content and dry density in both lysimeters #1 and #5. For lysimeter #1, as expected, moisture contents during the 2013 field investigation were higher than the ones measured during construction; however, the moisture content values during construction were lower than the optimum value defined by Proctor standard tests. High values of dry density were achieved by placing the material on the dry side of the compaction curve. Dry density measurements taken in 2013 were smaller than the minimum value set by construction specifications. Furthermore, dry density and moisture content measurements did not have a significant variation with depth and location of the test pit. The silty till in lysimeter #5 was placed in three 0.20 m thick layers. Figure 4-6 shows that two of the three layers were placed at moisture contents lower than the optimal, and that dry densities measured during construction were both slightly above and below the specification. The 2013 moisture contents were below the optimum value at the top of the barrier, but the samples might have lost some water during the testing. As the presented dry densities were recalculated using the oven-dried sample, the 2013 values were close to the construction specification. However, these values might be smaller as the moisture contents used for the re calculation seemed to be underestimated. The measurements at 0.60 m showed the same pattern observed at lysimeter #1. Moisture contents were above the optimum value, and the respective dry density values were below the specification at both test pits.

4.1.3 Soil Matric Suction

Soil matric suction was measured in all the materials at the different cover systems. As described in Chapter 3, measurements for topsoil were recorded at 0.15 m of depth, and at different depths (0.40, 0.50, and 0.60 m) for the barrier layers. Soil suction was measured with jet fill tensiometers, and soil samples were taken at the respective testing depths for gravimetric water content determination. As the purpose of recording soil matric suction was to assess the unsaturated properties of materials, the

gravimetric water content had to be transformed into volumetric water content. The conversion was achieved by using both soil dry density and the water density (Fredlund et al., 2012). For the topsoil volumetric water content calculation, the average dry density at each cover was used, and the average dry density at each depth was applied for the barrier layers. Figures 4-7 to 4-10 show the matric suction readings and volumetric water contents measured in 2013 (rainy season onset) and 2014 (dry season high) for the four different materials. The SWCCs determined by laboratory testing are also shown.

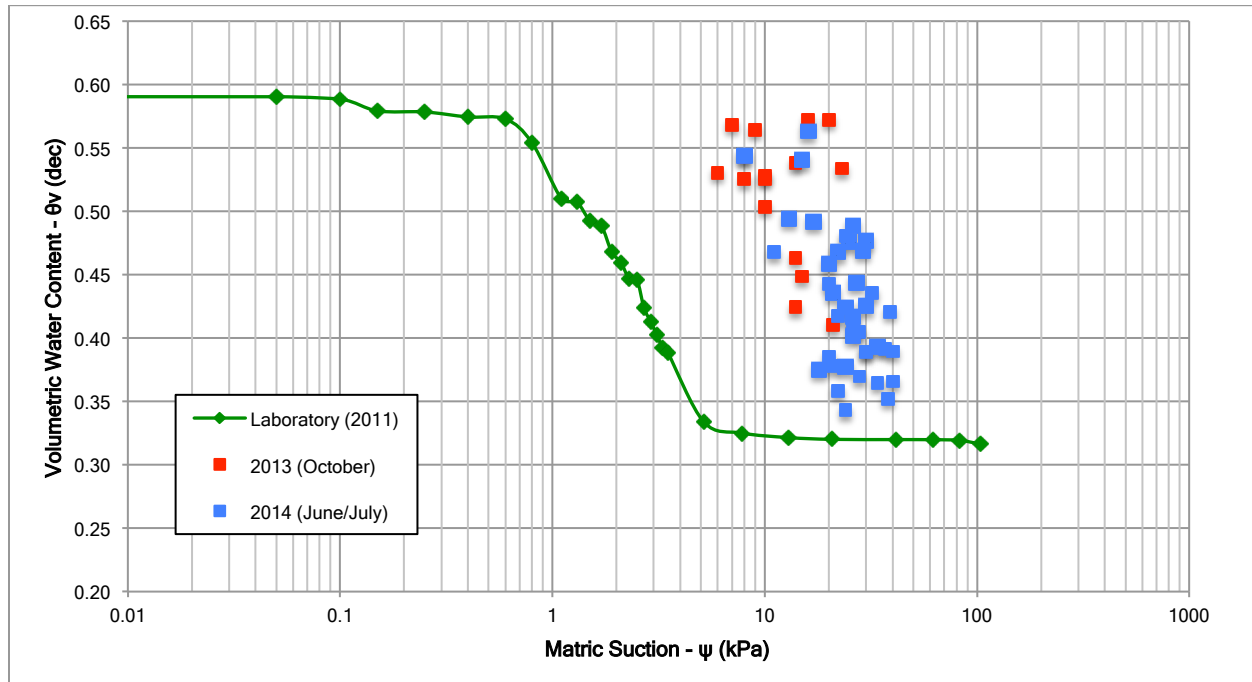


Figure 4-7: Matric suction vs. Volumetric water content for topsoil - Laboratory and field measurements (2013 - 2014)

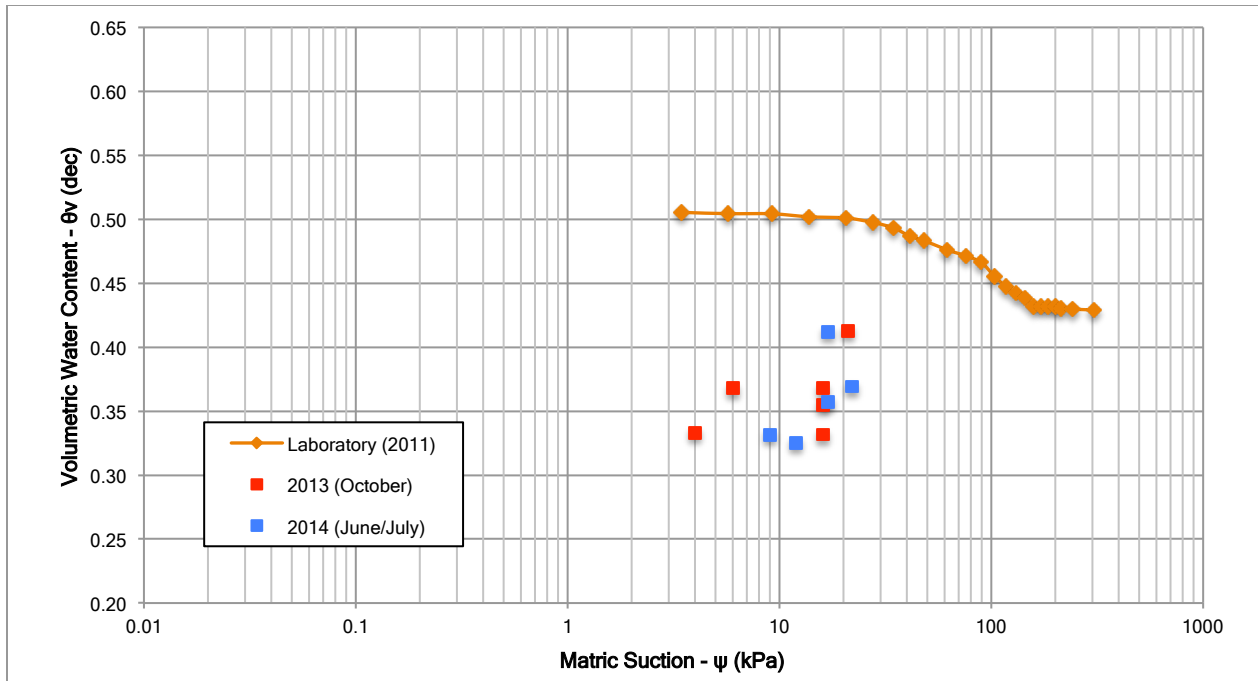


Figure 4-8: Matric suction vs. Volumetric water content for compacted clayey gravel till - Laboratory and field measurements (2013 - 2014)

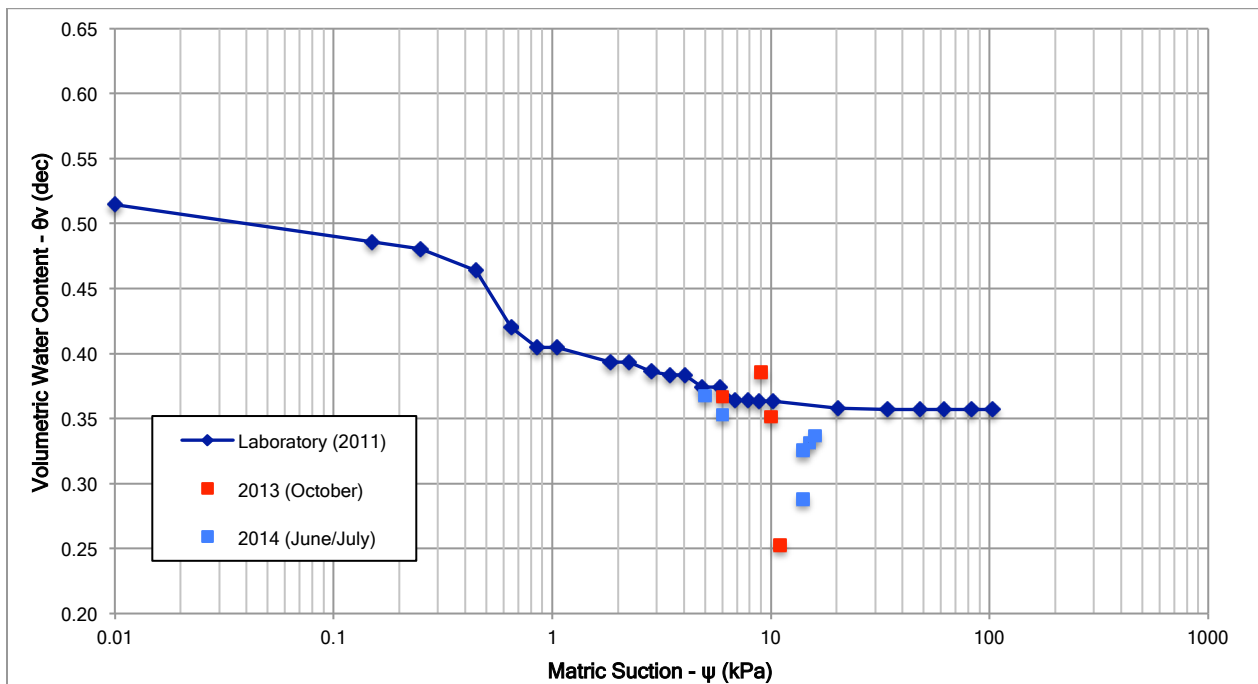


Figure 4-9: Matric suction vs. Volumetric water content for non-compacted clayey gravel till - Laboratory and field measurements (2013 - 2014)

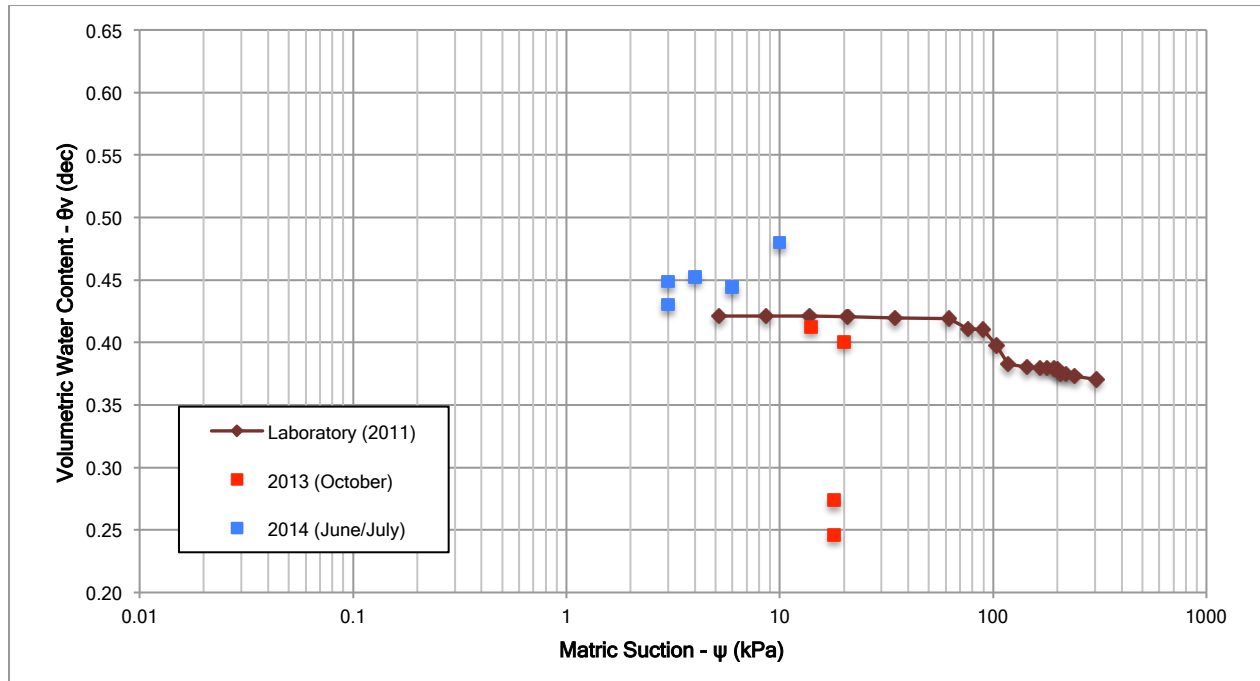


Figure 4-10: Matric suction vs. Volumetric water content for compacted silty till - Laboratory and field measurements (2013 - 2014)

The results shown in Figures 4-7 to 4-10 are mixed. Topsoil measurements for 2013 and 2014 (Figure 4-7) were shifted to the right of the laboratory SWCC. The data seems to define the slope of a new curve, with the red points (rainy season) placed at low matric suction and high volumetric water content, while the blue ones (dry season) are concentrated at slightly higher suctions and at lower water contents.

Results for the compacted clayey gravel till (Figure 4-8) are scattered, and only a few measurements were taken to minimize cover disturbance. However, all the computed volumetric water contents were below the ones defined by the laboratory SWCC. The reduced volumetric water content evidences a change in the unsaturated properties of the material, and this change might be associated to the coarse fraction presence, the material characteristics, and the initial water content during construction (Watabe et al., 2000). The results for the non-compacted clayey gravel till (Figure 4-9) were closer to the ones defined by the laboratory SWCC, and although the number of points were limited, they provided an indicator of the impact of compaction in the field unsaturated properties.

The different suction and volumetric water content readings for the silty till did not present a clear trend.

The 2013 readings showed two very low volumetric water contents, but these values belong to the

samples taken close to the bottom of the excavated test pit. As discussed in the previous section, the moisture contents measured by nuclear densometer at the same points were higher than the ones determined by oven drying. As these values might be higher, both points would be close to the measurements at 0.60 m (0.40 and 0.41 of volumetric water content). Particular attention should be given to the dry season results (blue points). Both matric suction and volumetric water content were in the same range as the ones presented by the laboratory SWCC. Although it is expected to be on the drying section of the SWCC at the high point of the dry season, readings from the installed instrumentation (discussed also in this chapter) showed that the silty till might be able to retain water for longer periods than the other materials. Based on this premise, the blue points in Figure 4-10 would not be out of the trend; however, they would not match the laboratory curve either due to the heterogeneity of the material, and the average dry density used for volumetric water content estimation purposes.

Although both field matric suction and volumetric water contents suggested the occurrence of changes in the unsaturated properties of the covers materials, the effect of hysteresis must be considered since the laboratory SWCC is a desorption (drying) curve. The wetting and drying cycles experimented by the cover profile due to the local precipitation are not captured by a single measurement at a certain point of time, since it cannot be determined whether the soil is on a drying path or a wetting path with just a field soil sample (Fredlund et al., 2012). The hysteretic behavior of the cover profile was captured by the CS229 matric suction sensor and CS616 water content probes, and their measurements are discussed in Section 4.2.7.

4.2 Instrumentation Data

Meteorological, percolation, and runoff data have been recorded since the beginning of the soil cover experiment in 2011. Therefore, the information collected and evaluated by Urrutia (2012) was also reported and examined as part of this assessment. Soil matric suction and volumetric water content values recorded by the new set of instrumentation installed in 2013 are presented and reviewed in the following sections. This information was also used to define in-situ SWCCs for three materials. Although already presented in Chapter 3, oxygen content measurements are analyzed in the following sections.

4.2.1 Meteorological Data

The meteorological data mainly came from the Yanacancha station, located at approximately 3.5 km from the soil cover experiment area (Punto B), and at an elevation of 4189 m.a.s.l. The station is approximately 190 m below Punto B, and both differences in elevation and location have an impact on the information collected.

Although a rain gauge was installed in Punto B to measure the precipitation in the experiment zone, it was only fully operative between February 17 and August 22, 2011. The initial assessment conducted by Urrutia (2012) covered a 365 day period between February 15, 2011 and February 14, 2012, and therefore there was a precipitation data gap between August 23, 2011 and February 14, 2012. Bay (2009) showed that precipitation records from Yanacancha and Punto B stations were different, and proposed a correlation to estimate precipitation at Punto B from Yanacancha data. As the correlation proposed by Bay (2009) was based on weekly records, Blackmore (2012) suggested a complimentary estimation method based on the percolation volumes measured at lysimeters A and D in Pile 4. Urrutia (2012) used both Blackmore (2012) and Bay (2009) methodologies to estimate missing precipitation at Punto B for the mentioned gap period.

The net radiometer installed in Punto B operated intermittently, and hence, data from the Yanacancha was used by Urrutia (2012) for the initial performance evaluation. As in the case of precipitation, net radiation records from the Yanacancha station were used to estimate evapotranspiration using a numerical model in SoilCover (Unsaturated Soils Group, 2000). As noted by Weeks (2006), using net radiation records from a different location had an impact on evapotranspiration predictions due to some factors like microclimates and topography. In addition, air temperature, wind speed, and relative humidity records from the Yanacancha station were also used for the initial model in SoilCover, as there were no direct measurements in the experiment zone. The Yanacancha station was also out of service a few times, and hence, there were some gaps in data. When a data gap was observed, Urrutia (2012) estimated the missing information by averaging two weeks of recorded data before and after the gap occurrence.

A complete meteorological station was installed in Punto B in May 2014, as direct measurements were required to improve the evapotranspiration predictions. The soil cover assessment period covered by this

thesis starts in February 15, 2012 and finishes in December 31, 2014, and data from Yanacancha and Punto B stations are reviewed in the following sections.

4.2.1.1 Precipitation

As described by Urrutia (2012), the rain gauge at Punto B was only operative between February and August 2011. The precipitation records between September 2011 and February 2012 were estimated following the methodology proposed by Bay (2009) and Blackmore (2012). Bay's correlation estimated weekly precipitation records from weekly values measured at the Yanacancha station. The Blackmore's methodology estimates daily precipitation values using the outflow volumes measured by lysimeters A and D at Pile 4. The Blackmore method is based on the assumption that preferential flow is developed inside Pile 4. The lysimeters outflow volumes were used to estimate precipitation during the rainy season, while Bay's correlation equation was used during the dry season. Although both methods proved to be satisfactory for the first part of the project, the percolation volumes measured at each lysimeter in the following years raised a few questions regarding the reliability of the estimation.

The new meteorological station was installed in Punto B during 2014, and hence direct precipitation records for the soil cover experiment area were available from February 17 to August 22, 2011 and April 30 to December 31, 2014. Some weather data were missing between September 9 and October 14, 2014, and it represented the only gap during the operative period of the new station. The details of the methodologies used to estimate the missing precipitation records at Punto B are discussed in the following section.

4.1.1.1.1 Missing Precipitation Records

In addition to the soil cover experiment, there are five experimental waste rock piles built and monitored by UBC. The piles are truncated pyramids of 36 m x 36 m x 10 m, as shown in Figure 4-11, and each of them is made of one of the different types of waste rock found in Antamina. Peterson (2014) studied the hydrological and geochemical processes controlling effluent water quality and quantity in waste rock deposits. The Peterson (2014) study focused on three of the five experimental waste rock piles in Antamina, and it was observed that the evaporation varied between 24% and 75% of the annual precipitation, and 28% to 59% of the precipitation in a multiyear scale. As in the five lysimeters for the soil

cover study, no runoff was observed in any of the piles. Urrutia (2012) reported percolation levels between 58% and 70% of the precipitation for the initial assessment, and as no runoff was observed, the difference, 30% to 42% of the precipitation, was attributed to evapotranspiration. As the soil covers were designed to enhance evapotranspiration, the measured values were considered low when compared to the ones from the uncovered waste rock piles. Peterson (2014) and Weeks (2006) recognized that evaporation was impacted by factors such as air circulation, topography, and microclimates, but the proximity between the piles and the soil cover experiment would suggest a smaller difference.



Figure 4-11: View of the Experimental Waste Rock Piles built and monitored by the University of British Columbia (October 2013)

In order to evaluate the nature of the observed differences, percolation volumes measured for the five lysimeters were compared with precipitation records estimated by the Blackmore (2012) and Bay (2009) methodologies. The comparison period was between February 2011 and April 2014, and the following scenarios were considered:

- Cumulative precipitation vs. cumulative infiltration: both records were compared at the end of each wet season.
- Yearly precipitation vs. yearly infiltration: precipitation and infiltration records for every hydrological year (wet and dry season - September 15 to September 14 next year) were compared.
- Wet season precipitation vs. wet season infiltration: wet season starts on September 15 and extends through April 30 of the following year.

The comparison was only conducted for lysimeters #1, #3, #4 and #5. Lysimeter #2 percolation

measurements were not evaluated due to the unreliability of the readings. Figure 4-12 shows the results of the comparison.

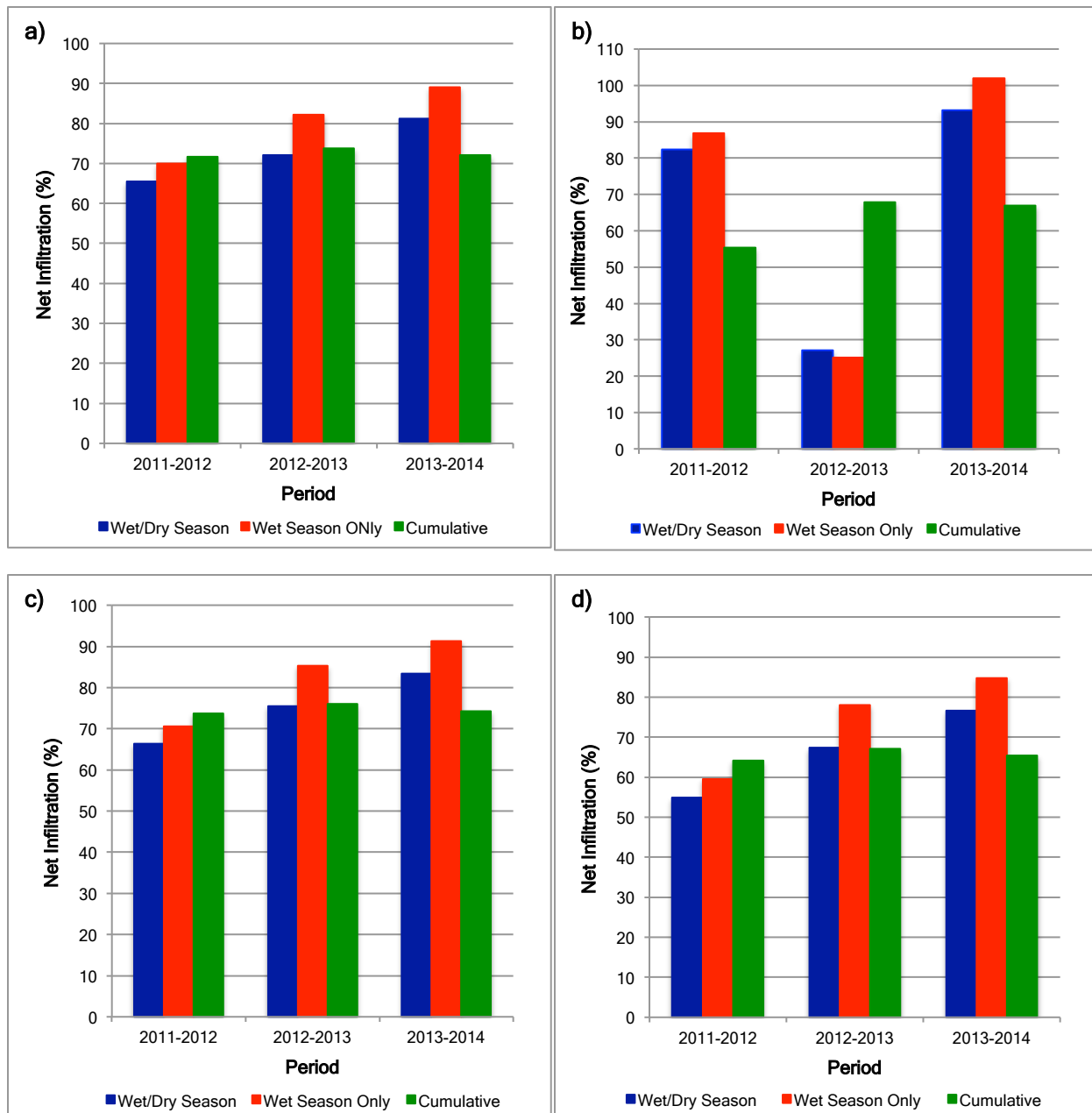


Figure 4-12: Percolation rates comparison for a) Lysimeter #1, b) Lysimeter #3, c) Lysimeter #4, d) Lysimeter #5

Figure 4-12 shows that percolation levels during the wet season were higher than the ones for a complete hydrological year (Wet/Dry) and cumulative values. As the precipitation during the dry season is low to negligible (Urrutia, 2012), the wet season infiltration should be the same or close to the infiltration for a complete hydrological year. The previous statement is only correct for the first year (2011-2012), with a maximum difference of 5%. For the following years, the infiltration for a hydrological year was smaller (10%) than the one occurring during the wet season. This change indicated a significant amount of rain was being estimated during the dry season, but low or nil percolation was observed. The comparison for lysimeter #3 (control) showed that the infiltration for the 2013-2014 wet season was greater than 100%. As percolation is expressed as a percentage of the precipitation, a value greater than 100% meant there was more water leaving than entering the system. This result and the lower percolation levels for a complete hydrological year suggested that precipitation was likely being overestimated during the dry season, and underestimated during the wet one.

As the estimation method used by Urrutia (2012) seemed to have a limited reliability for the years following the initial assessment, Pedretti and Beckie (2015) proposed a new approach. Pedretti and Beckie (2015) conducted a Montecarlo analysis to assess the level of error associated with the use of both chronological (linear and non-linear) and frequency pairing to estimate missing rainfall records. A chronological pairing (CP) consists on a regression-based estimation, where the data at a primary location is used to complete the missing records at a secondary location (e.g. Bay, 2009). On the other hand, a frequency pairing (FP) is based on the probability of non-exceedance (P_E) of an event at the primary location compared to P_E of another event at another location. It is concluded that CP is a better technique when the two locations have similar statistical distributions, and when the number of missing records is less than 100. If the source data is non-linearly correlated, FP outperforms any other technique in terms of the absolute errors and number of missing records.

Based on the aforementioned conclusions, a set of FP estimated rainfall records was prepared for 2014 (Pedretti, personal communication, March 26, 2015) and compared to the direct readings from the new weather station at Punto B. The period compared started in May 1, 2014 and finished in December 30, 2014. The data gap between September 9 and October 18, 2014 was completed using the weekly correlation proposed by Bay (2009). Figure 4-13 shows both estimated and direct cumulative

precipitation for the comparison period, and Figure 4-14 presents estimated and direct daily precipitation distributions for the same period.

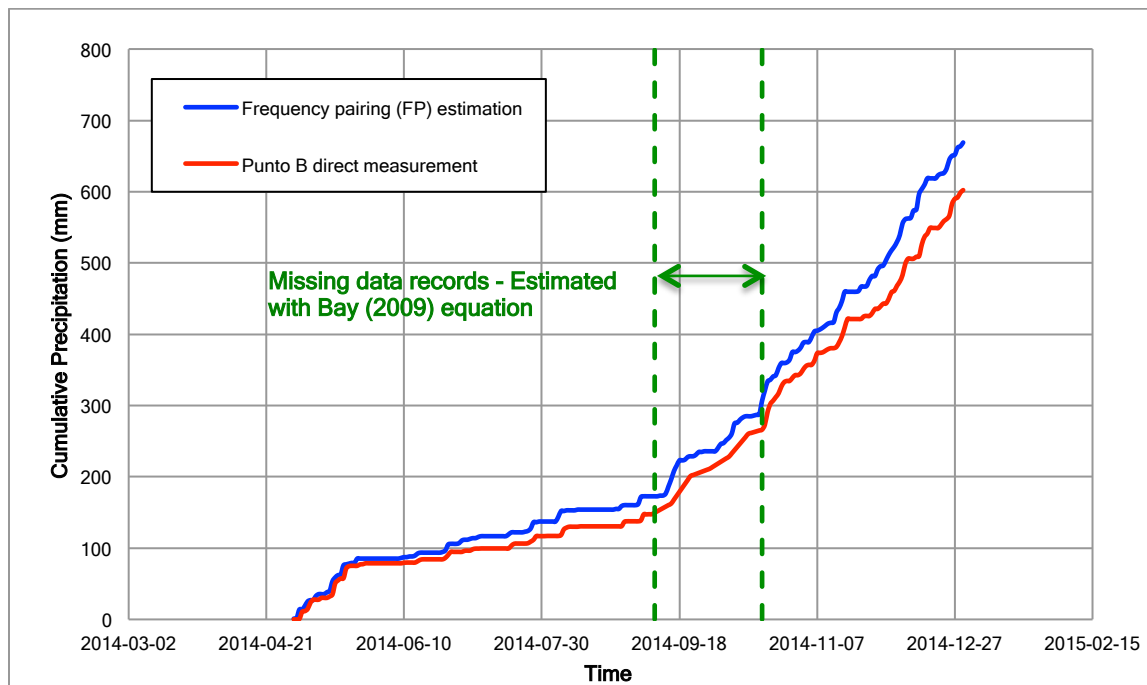


Figure 4-13: Estimated and direct cumulative precipitation comparison for year 2014

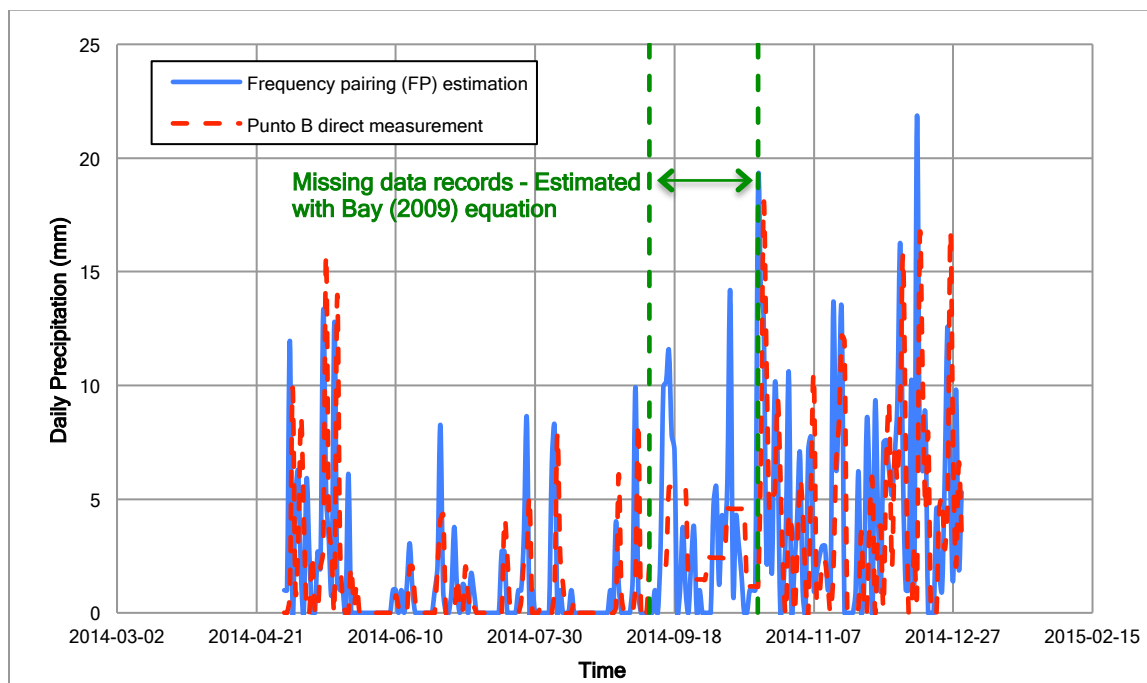


Figure 4-14: Estimated and direct daily precipitation comparison for year 2014

It is observed from Figure 4-13 that the estimated precipitation matched the direct measurements quite satisfactorily, and even the rainfall peaks in the daily precipitation distribution (Figure 4-14) matched. From this daily distribution it was also possible to observe that the chronologically pairing estimation (Bay, 2009) underestimated precipitation during the direct measurement gap period. However, the new estimation was not perfect as by the end of the comparison period there was 60 mm of difference (10%) between the estimated and direct measurements. This error could be reduced if more years were included in the analysis, as underestimated values could occur in some of them and they would compensate the overestimation in a cumulative assessment. The 10% error had to be taken into account when defining percolation rates, especially if calculated for individual years.

4.1.1.1.2 Precipitation Data for Cover Performance Assessment

Following the discussion in the previous section, a complete set of precipitation records from August 23, 2011 to April 29, 2014 was estimated following the methodology proposed by Pedretti and Beckie (2015). In addition, rainfall was estimated following the same methodology for the missing data period for Punto B in 2014 (September 9 to October 19, 2014). As the initial performance assessment conducted by Urrutia (2012) was based on the estimation method proposed by Blackmore (2012) and Bay (2009), a second set of precipitation records was estimated for the same periods, though using the methodology followed during the first part of the project. The purpose of the second precipitation data set was to maintain consistency with the initial assessment, since the Bay (2009) and Blackmore (2012) methods were used during the first phase of the study. Furthermore, as the performance of the covers is expressed in terms of a percentage of the precipitation received, the use of two sets of rainfall distribution would define a range of values of percolation. Expressing performance as an interval would account somewhat for the uncertainty created by the use of different rainfall estimation techniques caused by the lack of direct measurements.

Figure 4-15 shows the two sets of precipitations used for further percolation analysis and numerical modeling. Precipitation 1 considers the initial precipitation data used by Urrutia (2012), FP estimated rain records between 2012 and 2014, and Punto B direct measurements between May and December 2014. Precipitation 2 considers the direct measurements available for Punto B and all the gaps in data are estimated by the FP method proposed by Pedretti and Beckie (2015).

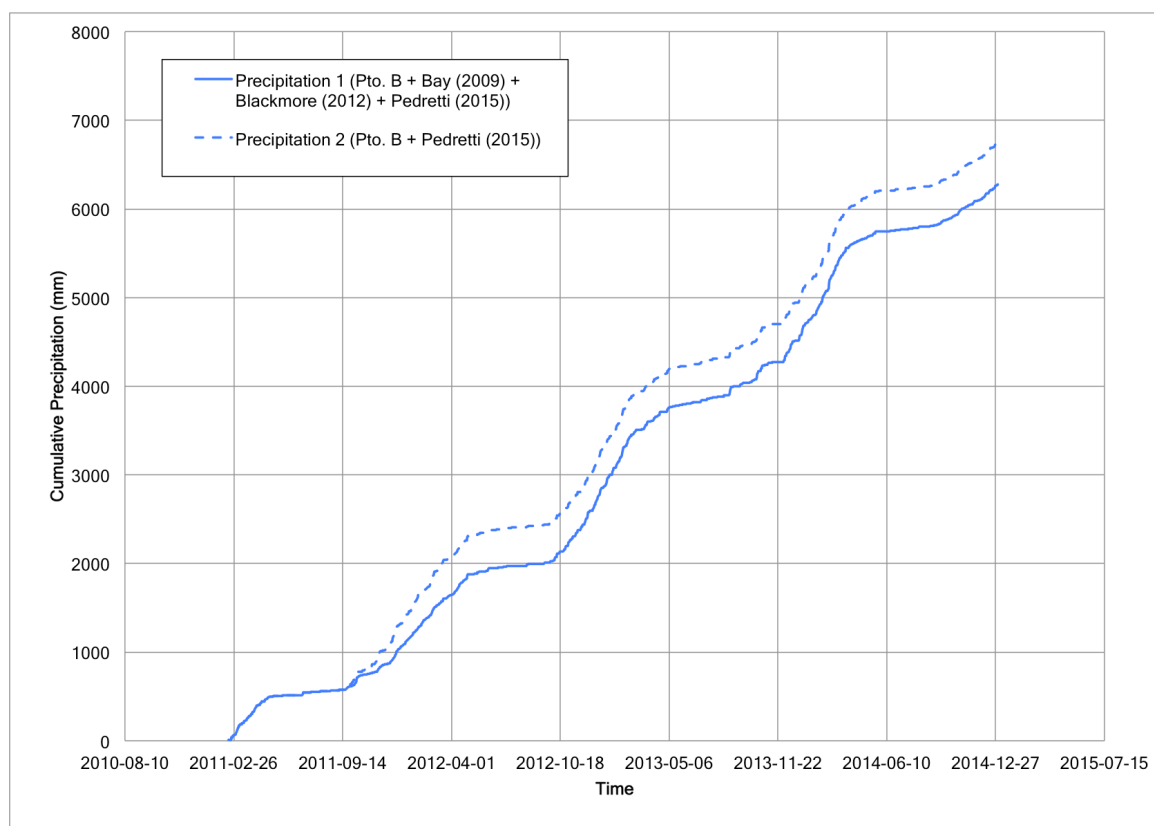


Figure 4-15: Cumulative precipitation records for Punto B - Precipitations 1 and 2 (February 17, 2011 to December 31, 2014)

4.2.1.2 Net Radiation

Net radiation is defined as the difference between the incoming short-wave radiation and the outgoing net long-wave radiation (Fredlund et al., 2012), and can be considered as a measurement of the available energy at the ground (Irmak et al., 2003 as cited in Fredlund et al., 2012). This available energy is a key element in the evapotranspiration process, and for this reason a direct net radiation measurement is required to calculate the levels of evapotranspiration in the different soil covers.

The net radiometer NR-Lite Net Radiometer installed in Punto B was not functioning effectively during the first year assessment of the experiment (Urrutia, 2012). Therefore, Yanacancha net radiation records were used for the numerical modeling predictions. The radiometer was not operative between 2012 and 2014, and it was reconnected in April 2014 as part of the setting of the new weather station at Punto B. For the current evaluation, Yanacancha net radiation records from February 17, 2011 to April 29, 2014

and Punto B records from April 30 to December 31, 2014 were considered. Both stations measured net radiation on an hourly basis, with the Yanacancha station recording average values, while the Punto B one recorded maximum and minimum values. Punto B maximum and minimum records were averaged in order to have set of data consistent with Yanacancha measurements. As the records for both stations had some gaps, the missing readings were estimated by averaging the two weeks of recorded data before and after the observed gap. This methodology was also applied by Urrutia (2012) during the first phase of the study. The gaps in net radiation measurements occurred in the following periods: February 17 to April 16, 2011; April 28 to May 5, 2011; August 17 to September 21, 2011; March 7 to March 18, 2013; and September 9 to October 18, 2014. Figure 4-16 shows the net radiation daily data, from both Yanacancha and Punto B stations, between February 17, 2011 and December 31, 2014. Despite being separated in both distance and elevation, the net radiation records for both stations were quite similar and no significant differences were observed.

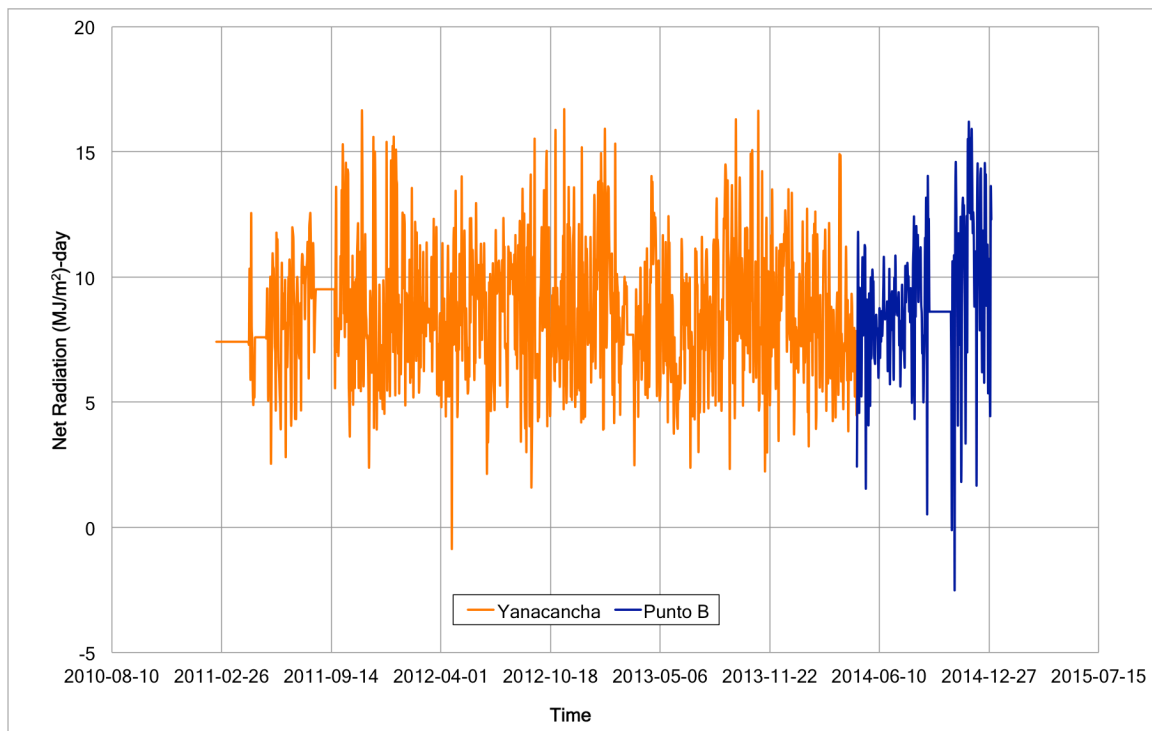


Figure 4-16: Daily net radiation records from Yanacancha and Punto B stations (February 17, 2011 to December 31, 2014)

4.2.1.3 Air Temperature, Wind Speed and Relative Humidity

Like net radiation, air temperature, wind speed, and relative humidity are needed to estimate evapotranspiration using the Penman-Wilson equation (Wilson, 1990 as cited in Wilson et al., 1994). As there was not a meteorological station set at Punto B until May 2014, information from Yanacancha station was used for the initial assessment carried out by Urrutia (2012), and for the present study between February 17 2012 and May 29, 2014. Direct measurements from the new weather station at Punto B were available from April 30 to December 31, 2014. Missing information for both stations was estimated by the same methodology used to fill gaps in data for net radiation. The missing records occurred in the following periods: February 17 to March 3, 2011; April 12 to April 16, 2011; April 28 to May 18, 2011; August 17 to September 20, 2011; March 8 to March 18 2013; and September 9 to October 18, 2014. Figure 4-17 shows the daily maximum and minimum air temperature, and wind speed records from Yanacancha and Punto B stations. Figure 4-18 summarizes both daily maximum and minimum relative humidity measurements for the same stations. Maximum air temperatures from Yanacancha were slightly higher (2 °C) than the ones recorded at Punto B, and no difference was observed in minimum air temperatures. On the other hand, wind speed measurements for Yanacancha had an average value around 9 km/h, while the Punto B records were on average close to 4 km/h. As noted by Peterson (2014) and Weeks (2006), air circulation and changes in climate have an impact on the evaporation rates estimated in the same region. These differences need to be considered when analyzing the results from the numerical modeling predictions.

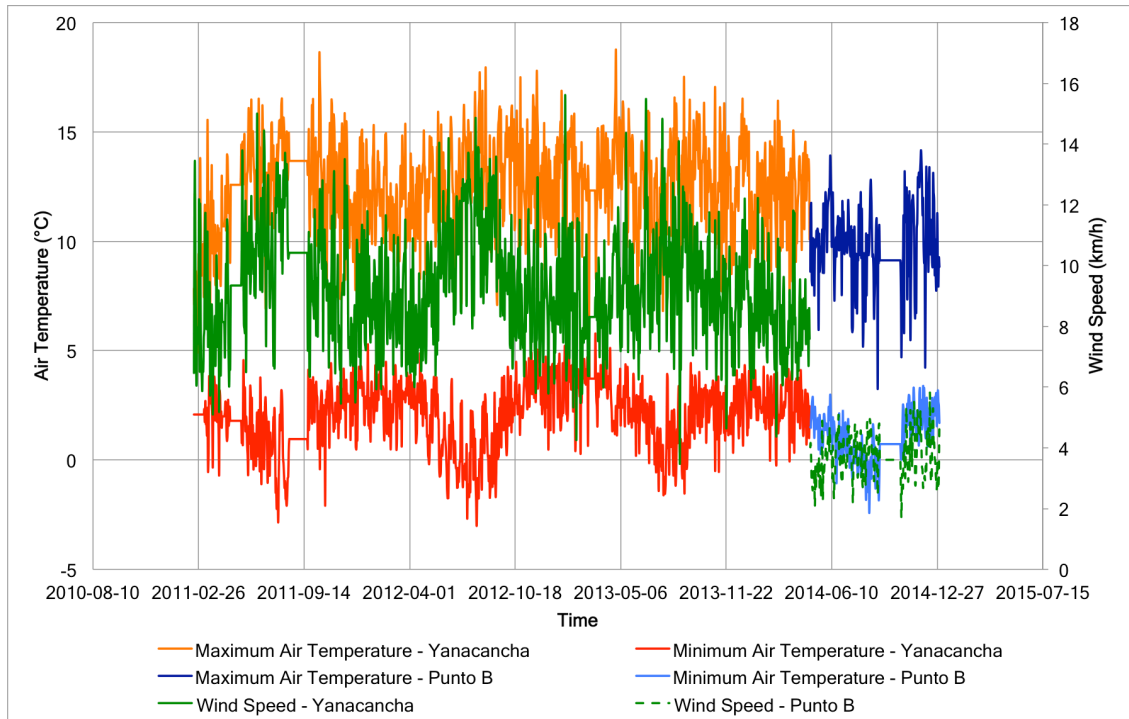


Figure 4-17: Maximum and minimum air temperatures, and wind speed records from Yanacancha and Punto B stations (February 17, 2011 to December 31, 2014)

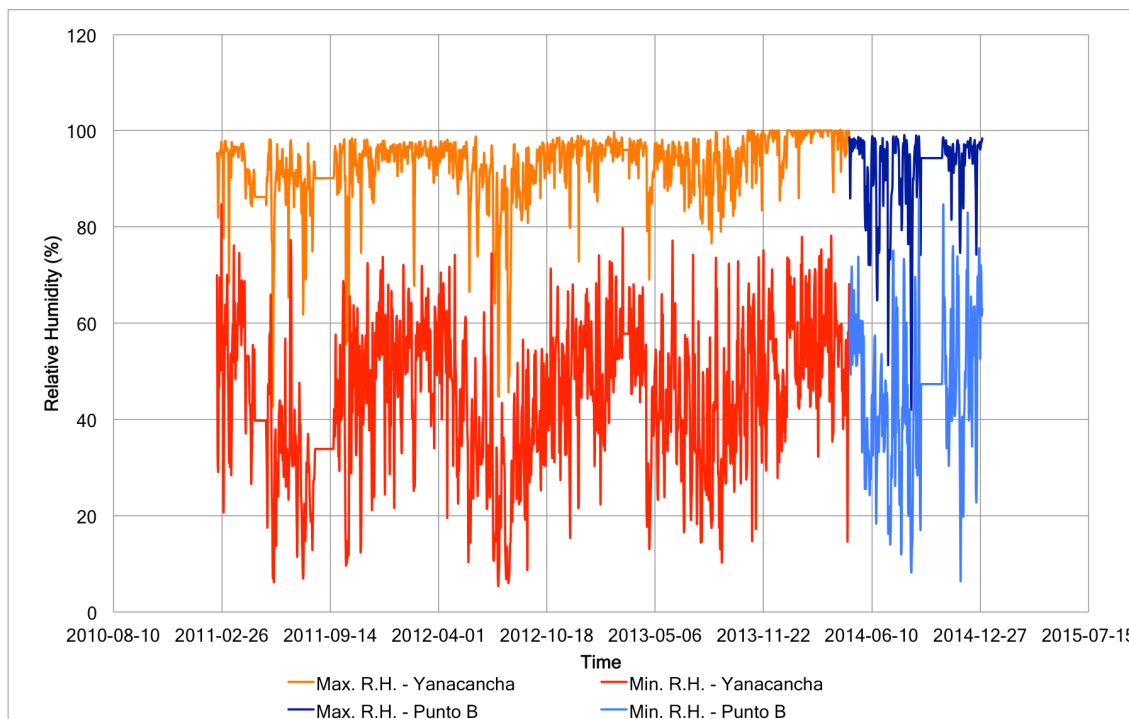


Figure 4-18: Maximum and minimum relative humidity records from Yanacancha and Punto B stations (February 17, 2011 to December 31, 2014)

4.2.2 Percolation and Runoff

Figure 4-19 shows the measured percolation records for lysimeter #1 for between February 15, 2011 and December 31, 2014. Due to a problem with the tipping bucket magnetic reed, there were no percolation readings from July 10 to December 31, 2014. For this reason, the performance assessment was conducted by comparing both cumulative percolation and precipitation records up to July 9, 2014. Figure 4-20 shows the performance assessment for lysimeters #1, #2, #4, and #5 from March 24, 2011 to December 31, 2014. A different start date was considered for this evaluation due to the availability of consistent records for lysimeters #2, #4, and #5 (Urrutia, 2012). The unreliability of readings for lysimeter #2 was previously discussed by Urrutia (2012), and mentioned in Chapter 3 of this thesis. A similar problem with the magnetic reed in the percolation-tipping bucket for lysimeter #5 prevented data collection from July 10, 2014. Figure 4-21 shows the percolation measurements for all lysimeters from April 20, 2011 to December 2014. Once again the assessment start date was modified to match the availability of reliable records for lysimeter #3. A corroded magnetic reed stopped data collection for lysimeter #3 between December 18, 2012 and June 22, 2013. During the period analyzed by this thesis, no runoff was either recorded or observed at any of the five lysimeters. Figures 4-22 to 4-26 show a comparison between daily precipitation and daily percolation records for lysimeters #1, #2, #3, #4, and #5, respectively.

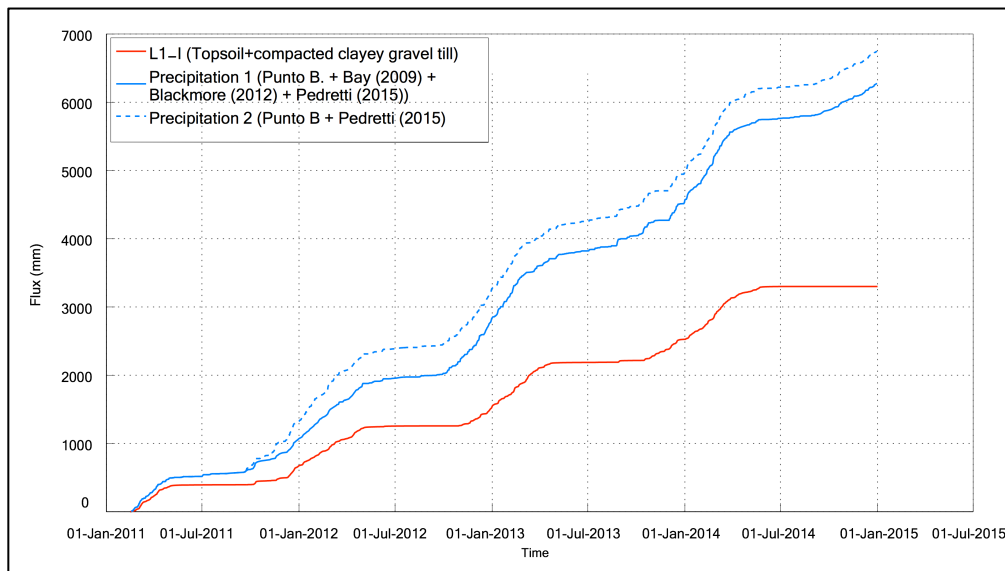


Figure 4-19: Cumulative precipitation and lysimeter #1 net percolation records (February 15, 2011 to December 31, 2014)

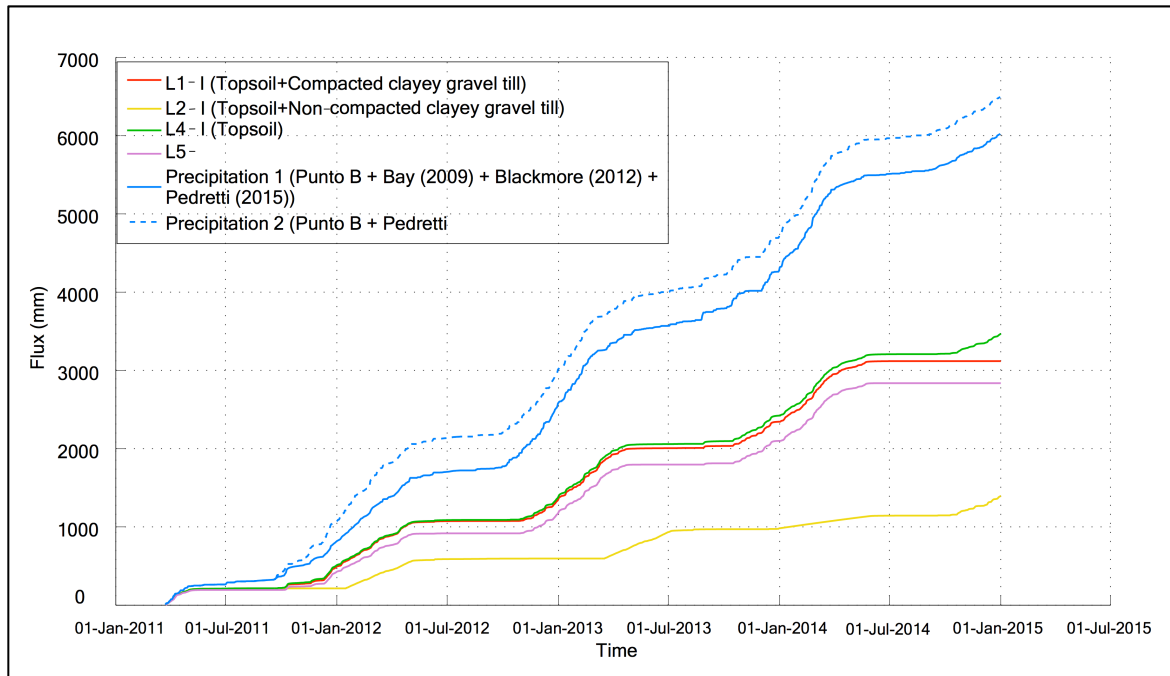


Figure 4-20: Cumulative precipitation and lysimeters #1, #2, #4, and #5 net percolation records (March 24, 2011 to December 31, 2014)

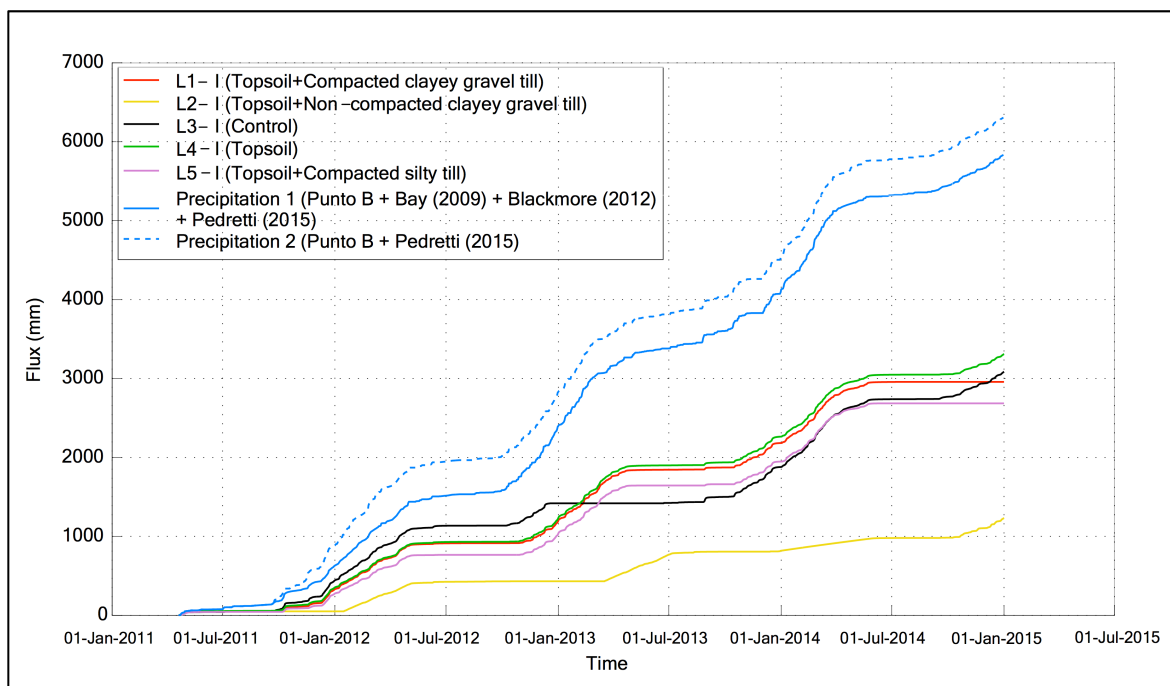


Figure 4-21: Cumulative precipitation and lysimeters #1, #2, #3, #4, and #5 net percolation records (April 20, 2011 to December 31, 2014)

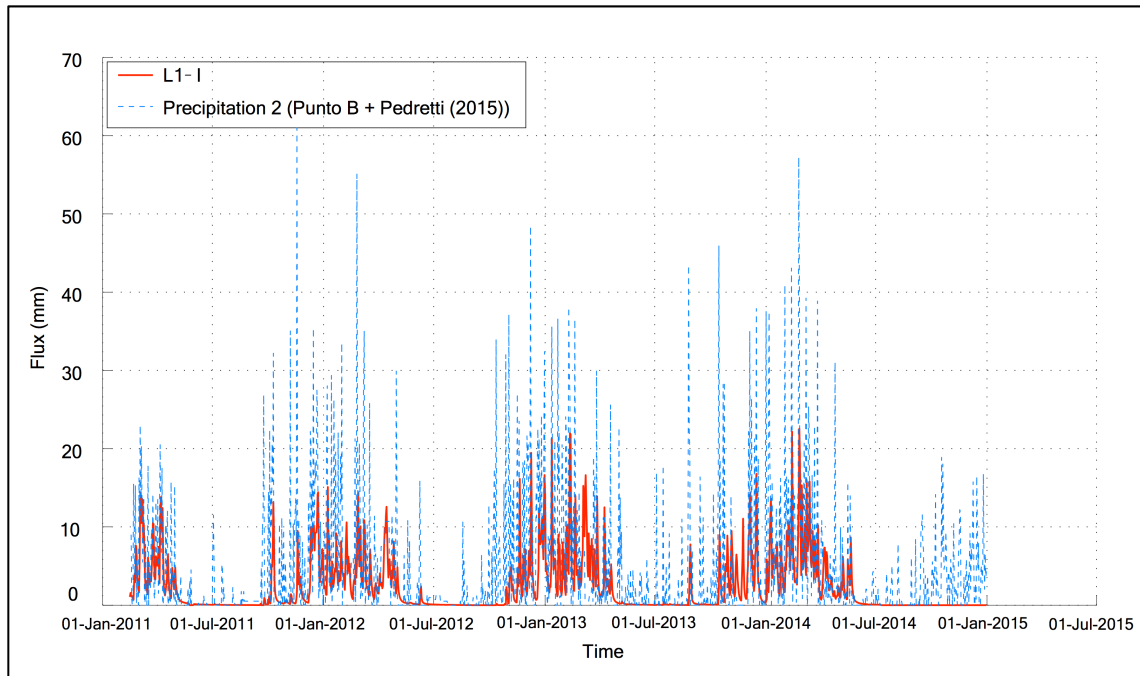


Figure 4-22: Daily precipitation and net percolation for lysimeter #1 (February 15, 2011 to December 31, 2014)

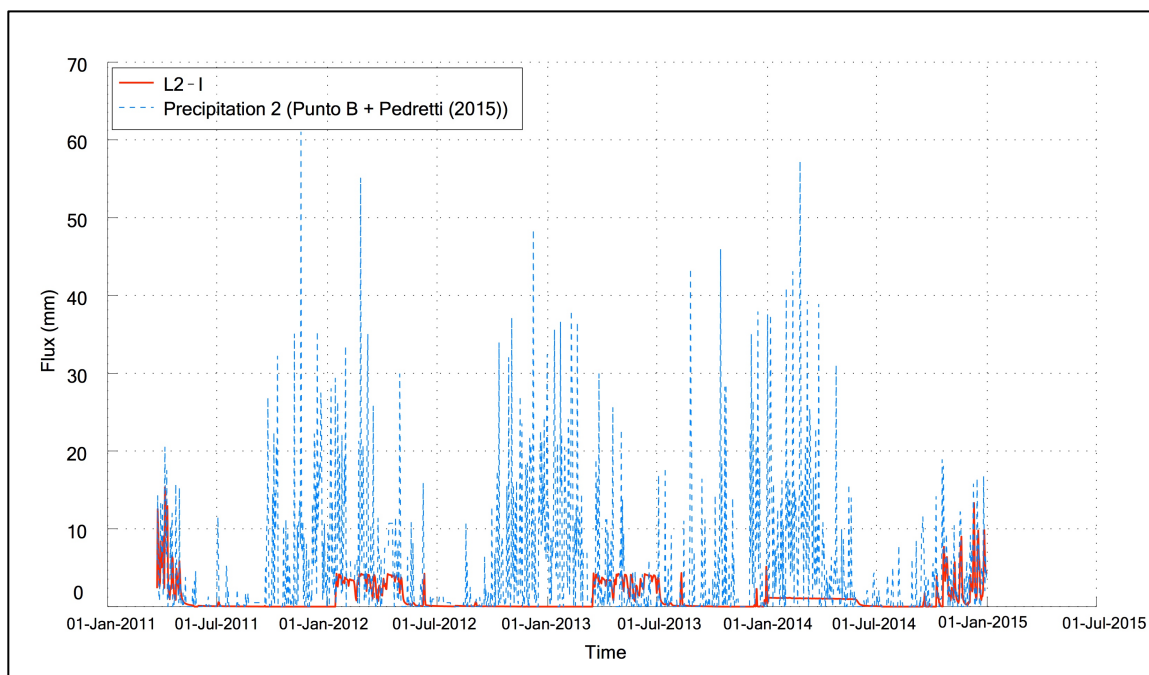


Figure 4-23: Daily precipitation and net percolation for lysimeter #2 (March 24, 2011 to December 31, 2014)

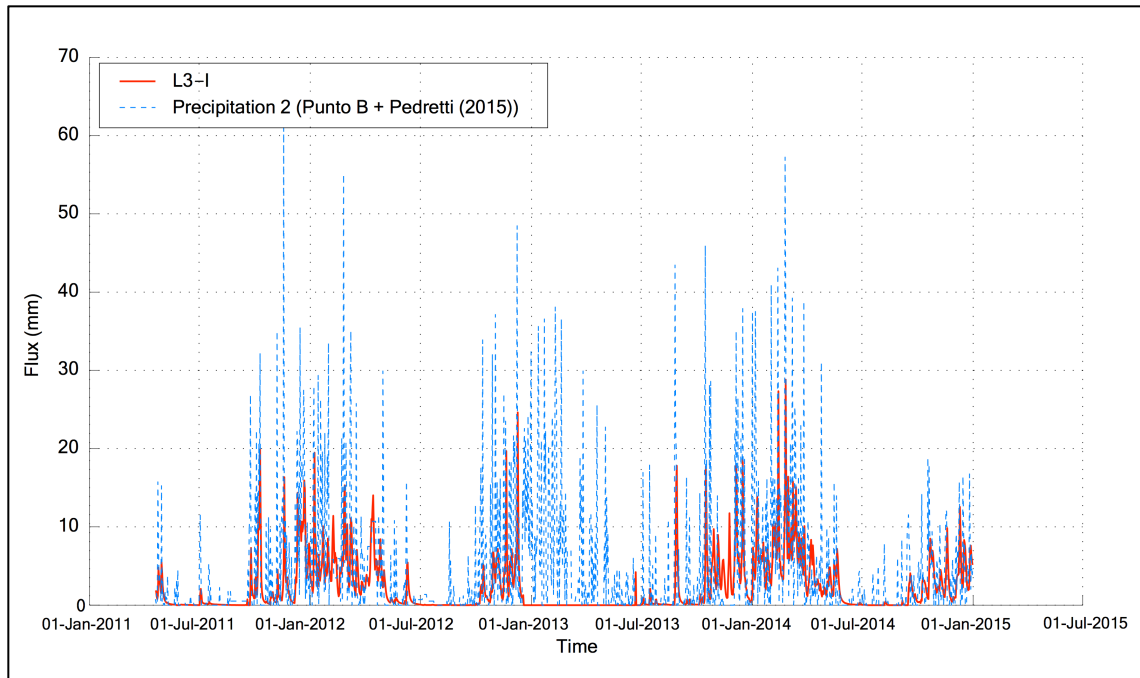


Figure 4-24: Daily precipitation and net percolation for lysimeter #3 (April 20, 2011 to December 31, 2014)

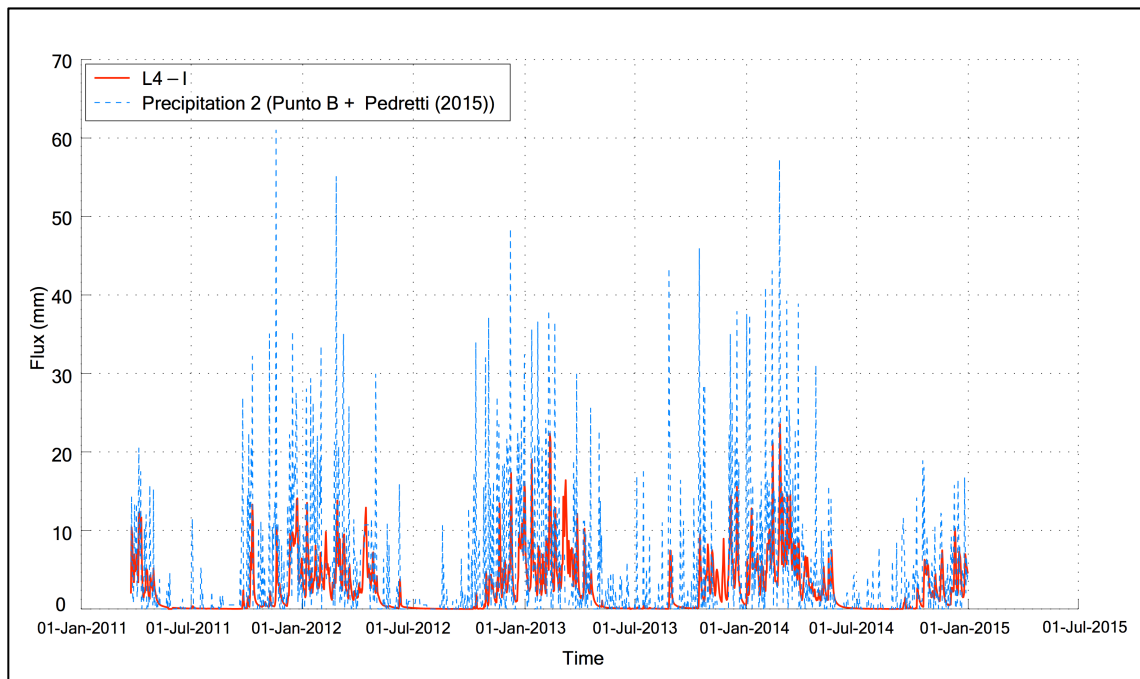


Figure 4-25: Daily precipitation and net percolation for lysimeter #4 (March 24, 2011 to December 31, 2014)

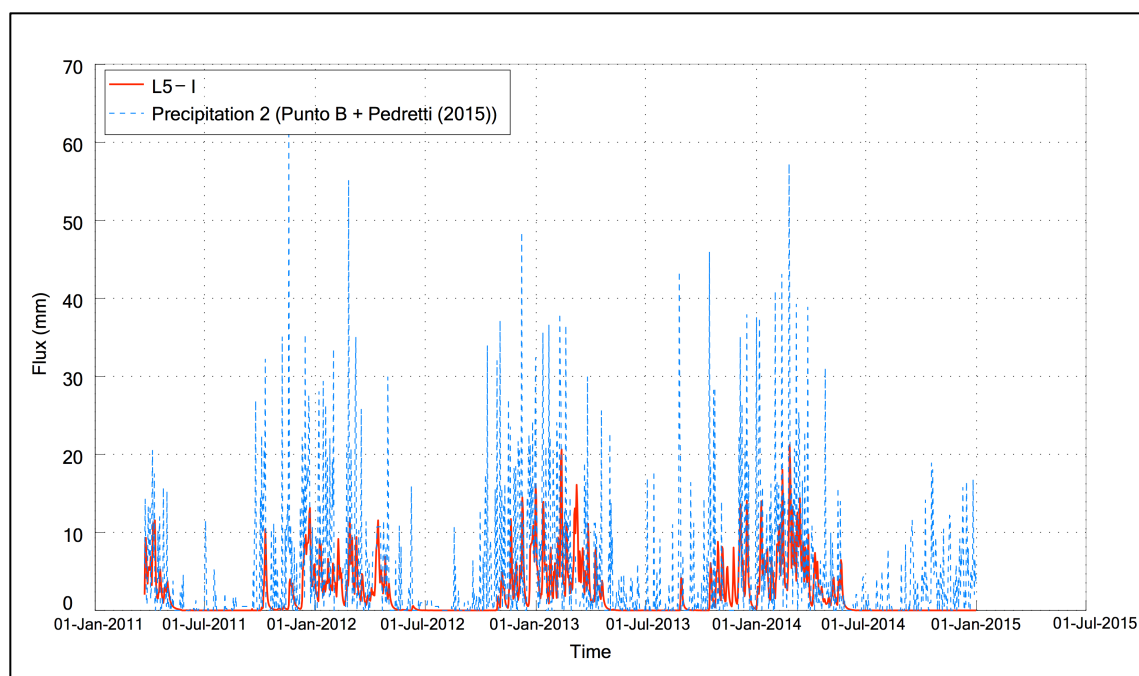


Figure 4-26: Daily precipitation and net percolation for lysimeter #5 (March 24, 2011 to December 31, 2014)

From Figures 4-19 to 4-21, it is possible to evaluate the different soil cover performances in terms of net percolation. The net percolation is presented as a percentage of the cumulative precipitation received by the lysimeter. Table 4-7 summarizes the net percolation for each lysimeter. As two different precipitation distributions were considered, two values of net percolation are also reported, and they define a range of possible outcomes. Furthermore, as the five lysimeters started to collect reliable information at three different dates, net percolation levels are also reported considering them.

When comparing the performance of all the lysimeters (April 20, 2011 to December 31, 2014), lysimeter #3 reported the highest net percolation, which is between 55% and 65% of the total precipitation received by the lysimeter area. As the infiltration records for lysimeter #3 were compromised between 2012 and 2013 due to malfunctioning in the data collection system, its accumulated infiltration records by December 31, 2014 were lower than the ones for the other lysimeters. For this reason, the net infiltration was calculated for the last date where the cumulative records were reliable and continuous (December 18, 2012). From the covered lysimeters, lysimeter #4 is the least effective in terms of limiting net percolation, as measured volumes range from 52% to 57% of the total precipitation. The most effective soil cover in terms of limiting net percolation is the one installed in lysimeter #5, with 46% to 50%

of the total precipitation received reported as percolation. Lysimeter #1 represents an intermediate condition with a net percolation between 51% and 56% of the total precipitation received.

Table 4-7: Net percolation for lysimeters #1, #2, #3, #4, and # 5

Period	Precipitation Distribution	Net Percolation (%)				
		Lysimeter				
		1 (Topsoil +CCGT ¹) ⁴	2 (Topsoil+ NCCGT ²)	3 (Control) ⁵	4 (Topsoil)	5 (Topsoil+ CST ³) ⁶
Feb 15, 2011 - Dec 31 2014	1	57	N.O. ⁷	N.O. ⁷	N.O. ⁷	N.O. ⁷
	2	53	N.O. ⁷	N.O. ⁷	N.O. ⁷	N.O. ⁷
Mar 24, 2011 - Dec 31 2014	1	57	23 ⁸	N.O. ⁷	58	51
	2	52	21 ⁸	N.O. ⁷	53	48
Apr 20, 2011 - Dec 31 2014	1	56	21 ⁸	65	57	50
	2	51	20 ⁸	55	52	46

Note

¹: CCGT = Compacted clayey gravel till

²: NCCGT= Non-compacted clayey gravel till

³: CST = Compacted silty till

⁴: Percolation up to June 10, 2014

⁵: Percolation up to December 18, 2012

⁶: Percolation up to July 10, 2014

⁷: N.O. = Not operative

⁸: Not reliable

The net percolations shown in Table 4-7 are lower than the ones reported by Urrutia (2012) as part of the initial evaluation, which were 68%, 70%, 66%, and 58% of the total precipitation for lysimeters #1, #3, #4, and #5, respectively. The difference is between 10% and 15%, and it resulted from the different methodologies used to estimate missing precipitation records. However, the same trend observed during the initial performance assessment is maintained. All the percolation occurred during the wet season (mid September to late April), and even though some rain was registered during the dry season, percolation was nil or negligible for that period. Daily precipitation and net percolations records in Figures 4-22 to 4-26 show that there are some differences between these values for certain points of time. The discrepancies, as noted by Urrutia (2012), are due to both the weather conditions in the area and the degree of saturation in the cover at those dates. Both of these aspects have an impact on the evapotranspiration and on the saturated/unsaturated flow developed in the cover. Therefore, in some cases the percolation might be hindered by evapotranspiration or delayed due to the changes in saturation.

4.2.3 Matric Suction

Matric suction was measured by FTC-100 and CS229 sensors. The FTC-100 sensors were installed in all the covers and at different depths as shown in Table 3-7, while CS229 probes were only installed in the covers in lysimeters #1 and #5. As described in Section 3.3.3.2, the FTC-100 performance was variable over time. Reliable readings during the first year of the project were only available for lysimeter #1 at 0.15, 0.48, and 0.76 m; lysimeter #2 at 0.46 m; and lysimeter #5 at 0.48 m. After the datalogger was reconnected in July 2014, the reliability of the readings changed and improved. FTC-100 sensors at lysimeter #1 were fully operative, and the ones installed at 0.15 and 0.46 m in lysimeter #2 were also working properly. A previously non-operative FTC-100 sensor at lysimeter #4 was operative, and sensors at 0.45 and 0.65 m in lysimeter #5 were also collecting information. Although the FTC-100 sensors were aimed to provide an estimation of the volumetric water content of the covers materials by using the laboratory SWCC, the changes in the SWCC discussed in Section 4.1.3 would lead to incorrect values. As it was necessary to define a certain level of precision to compute matric suction from CS229 readings, FTC-100 sensors and tensiometers measurements were compared to CS229 readings. This comparison was intended to set the number of iterations required for the temperature correction procedure proposed by Flint et al. (2002). The comparison was only conducted between sensors in lysimeters #1 and #5, and installed at similar depths. Figure 4-27 shows the comparison between FTC-100, tensiometers, and CS229 matric suctions calculated after one and three iterations. The compared values were at 0.50 m in the compacted clayey gravel till installed in lysimeter #1. Charts with the FTC-100 sensors readings for years 2012 and 2014 are included in Appendix C.

CS229 and FTC-100 soil matric suction readings had a good match when only a single iteration was considered for the temperature correction process (Flint et al., 2002). All the CS229 readings were corrected using a single iteration temperature correction. Figure 4-28 and Figure 4-29 show the corrected soil matric suction for lysimeters #1 and #5 at different depths. Daily precipitation records, direct and estimated, are also included in both figures to show the matric suction variations during the dry and wet seasons.

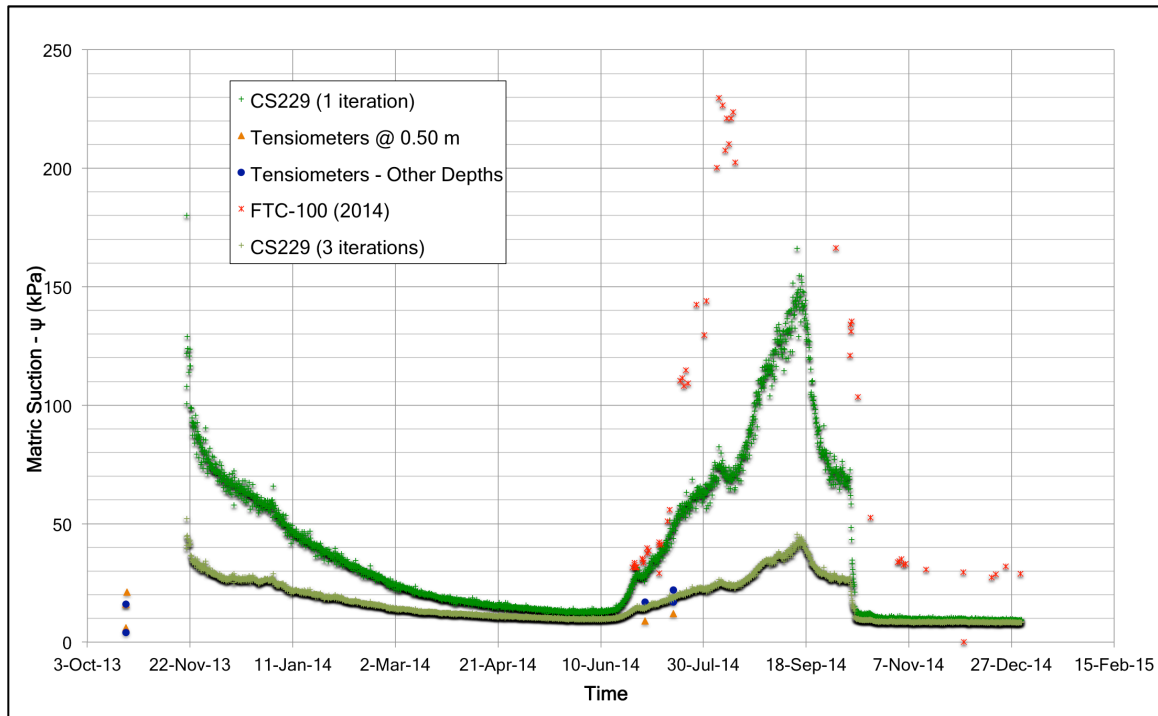


Figure 4-27: Soil matric suction readings comparison: Jet fill tensiometers, FTC-100 sensors, and CS229 - Lysimeter #1 (0.50 m)

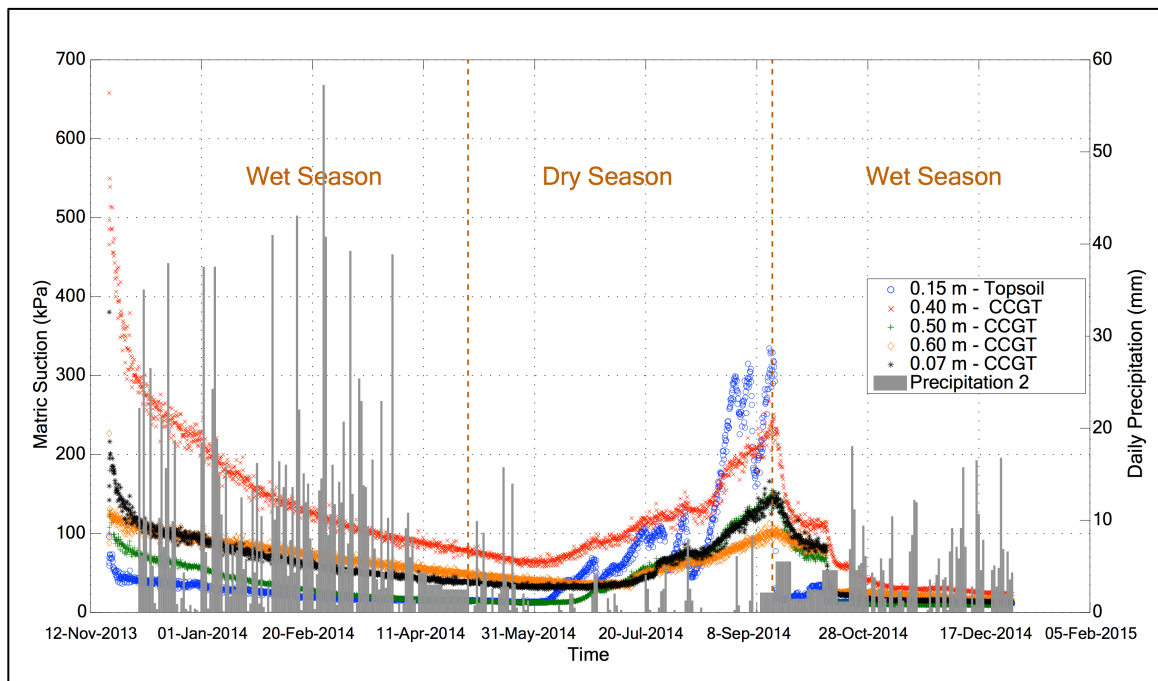


Figure 4-28: Corrected soil matric suction readings for lysimeter #1 (November 20, 2013 to December 31, 2014)

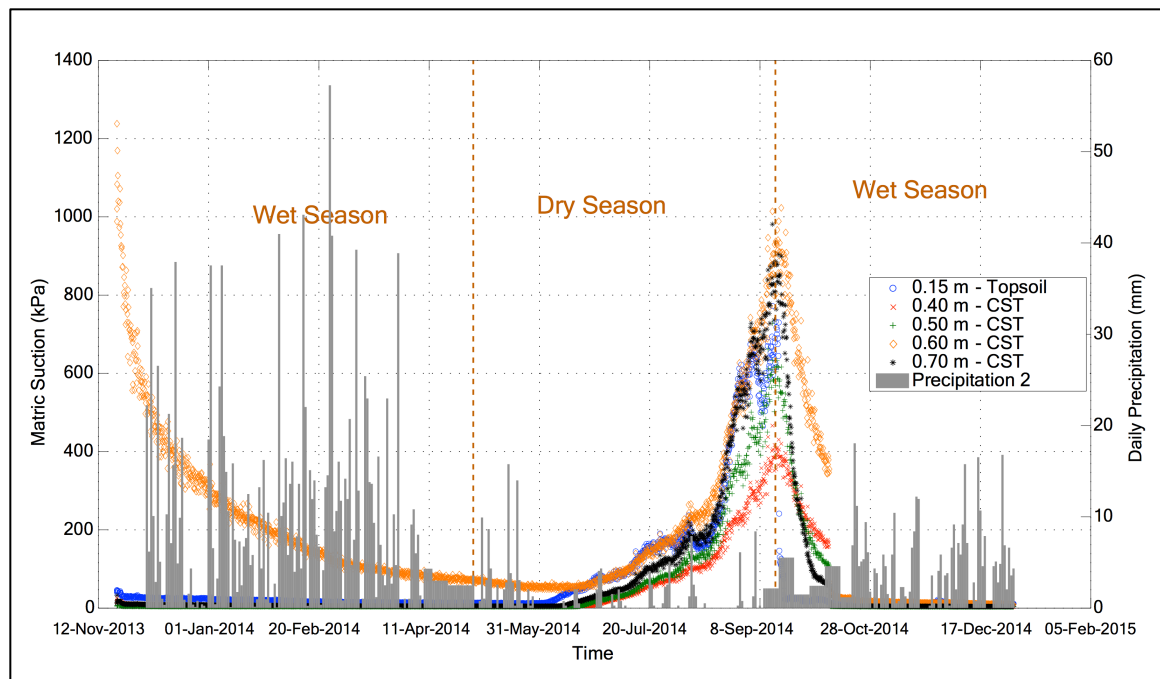


Figure 4-29: Corrected soil matric suction readings for lysimeter #5 (November 20, 2013 to December 31, 2014)

For lysimeter #1 (Figure 4-28), high matric suction readings were observed at 0.40 m (top of the compacted clayey gravel till layer) at the start of the monitoring period (November 2013). These high values might be associated with a long equilibration process between the CS229 probe and the surrounding material. In general, matric suction decreased with the progress of the wet season, and kept decreasing until mid-June (after the beginning of the dry season). Then matric suction started to increase as the cover dries due to the absence of precipitation. It was observed that the matric suction measured in the topsoil was easily affected by the scarce occurrence of precipitation, as it decreased when rainfall was reported. Topsoil matric suction dropped as soon as the wet season began, while the values for the deeper sensors in the cover slowly decreased until the rainfall became steady, and all of them converged to the same range as those for the topsoil. Matric suction in lysimeter #5 (Figure 4-29) shows a similar trend as in lysimeter #1. High matric suctions were also observed at 0.60 m (the middle of the compacted silty till), and these values might have also been caused by a long time to achieve equilibration between the probe and the material. The rest of the sensors presented low values of soil matric suction and, as in lysimeter #1, these values started to increase in early June. Unlike in lysimeter #1, all the readings were in the same range even during the drying process, and this similarity suggested a uniform profile in the zone

where the sensors were installed. With the start of the new wet season, soil matric suction decreased drastically to the same levels observed during the first wet season.

4.2.4 Volumetric Water Content

Figure 4-30 shows the volumetric water content recorded by the CS616 probes installed in lysimeter #1 at different depths. As in soil matric suction plots, daily precipitation records were also included to evaluate how rain occurrence affected volumetric water content.

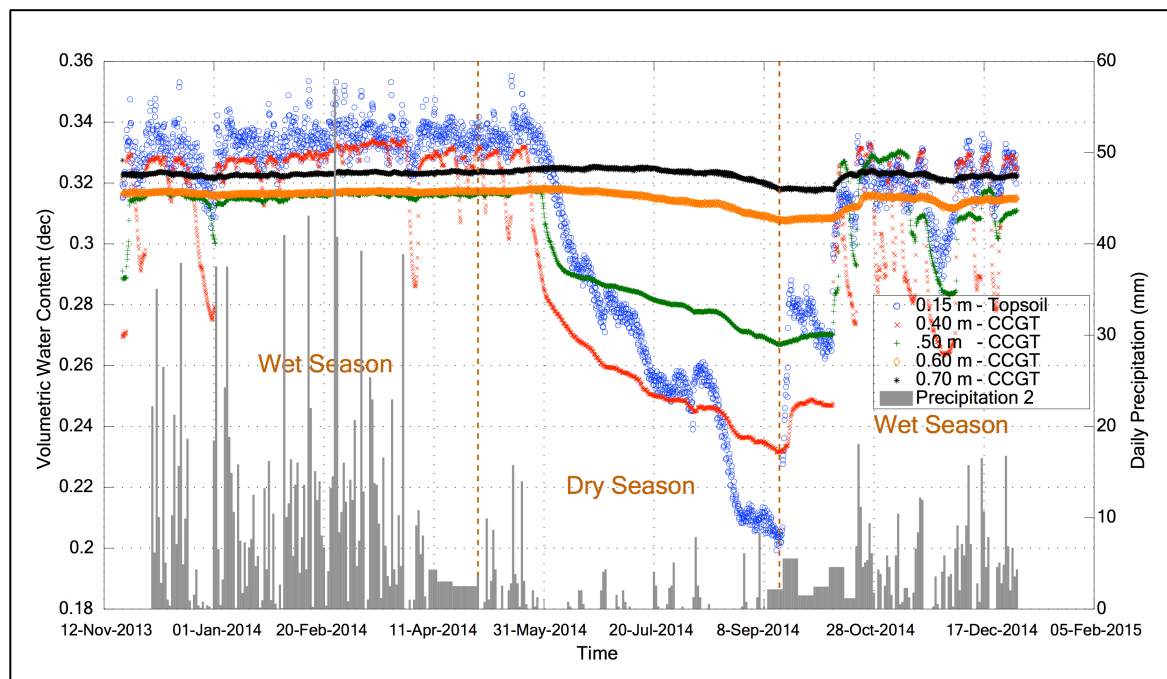


Figure 4-30: Volumetric water content measurements for lysimeter #1 (November 20, 2013 to December 31, 2014)

It is observed from Figure 4-30 that both topsoil layer and top of the compacted clayey gravel till barrier (0.40 m) were the most active zones in terms of water content change. The peaks observed in water content during the wet season evidence how sensitive topsoil was to precipitation occurrence. On the other hand, the upper compacted clayey gravel till (0.40 m) decreased in water content in the absence of or with a decrease in precipitation. There is a transition zone at 0.50 m, where no peaks were observed, and the loss of water was not as dramatic as in the overlying zones. Once the dry season started, the topsoil and the surficial clayey gravel till lost water faster than the transition zone (0.50 m). The bottom region of the barrier layer roughly maintained the same water content during the dry season. A slight

reduction in water content was observed at the base of the barrier towards the end of the dry season, and this reduction may have been due to the absence of precipitation and the advance of the drying front. The opposite effect was observed at the beginning of the 2014 wet season, where the topsoil and the top of the barrier were the first zones to increase their water content.

Figure 4-31 shows the volumetric water content recorded by the CS616 probes installed in lysimeters #5 at different depths. As in Figure 4-30, daily precipitation records were also included.

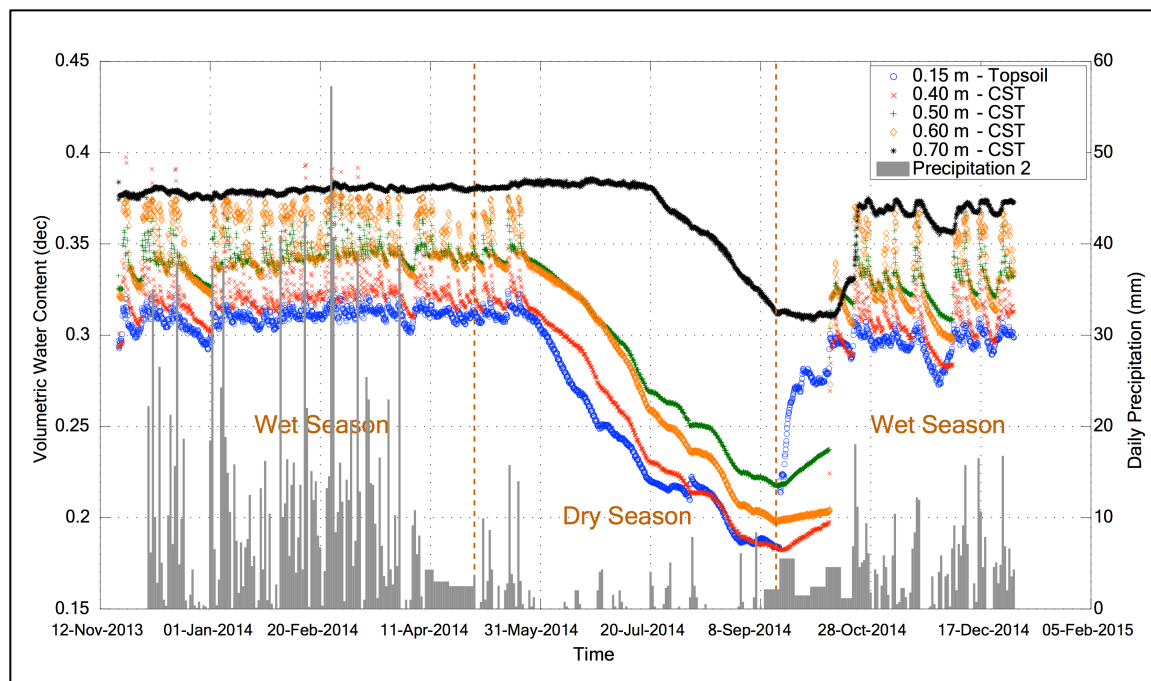


Figure 4-31: Volumetric water content measurements for lysimeter #5 (November 20, 2013 to December 31, 2014)

Figure 4-31 shows that both the topsoil and compacted silty till were very active in terms of variation in water content. The compacted clayey gravel till was not as sensitive to the precipitation occurrence, but to the reduction or absence of it. The volumetric water contents in the topsoil and compacted silty till increased with the occurrence of precipitation, and lost water during short drying periods. However, once the dry season commenced, both materials began to dry almost simultaneously, with the exception of the bottom part of the barrier layer (0.70 m). This section maintained constant water content until halfway through the dry season, when water content started decreasing at the same rate as that for the overlying zones. In general, the topsoil and silty till system showed dynamic behavior characterized by constant changes in volumetric water content due to meteorological conditions.

4.2.5 Matric Suction and Volumetric Water Content Profiles

Volumetric water content and matric suction should be assessed together for each soil cover. Figure 4-31 and Figure 4-33 present matric suction and volumetric water content profiles at different times for lysimeters #1 and #5.

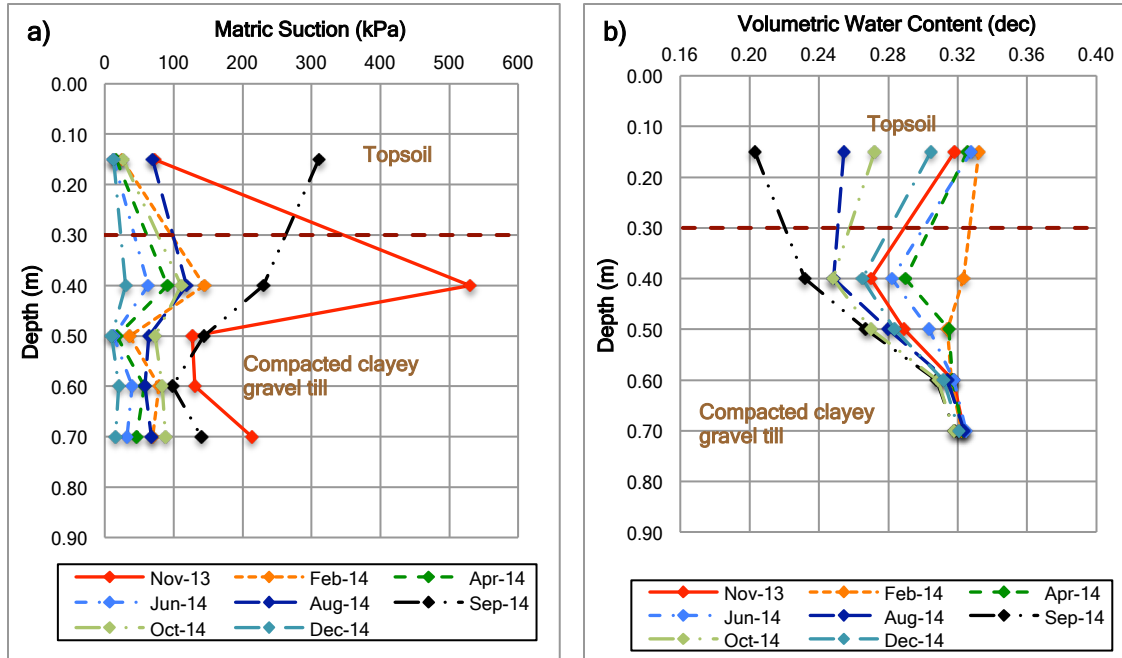


Figure 4-32: a) Matric suction and b) volumetric water content profiles for lysimeter #1 (Topsoil+compacted clayey gravel till)

Figure 4-32 a) shows soil matric suction profiles for lysimeter #1 at different points in time. The equilibration process of the probe at 0.40 m, which started with high levels of matric suction, was again obvious while the other sensors reduced their matric suction with the progress of the wet season. August and September 2014 profiles showed the expected increase in matric suction during the dry season, with the greatest changes occurring above 0.50 m. The water content profiles in Figure 4-32 b) illustrate the dynamic change in volumetric water content developed above 0.50 m, and the limited variation at the bottom of the clayey gravel till layer. The topsoil layer and the top zone of the compacted clayey gravel till (0.40 m) were the portions of the cover system with the greatest changes in water content.

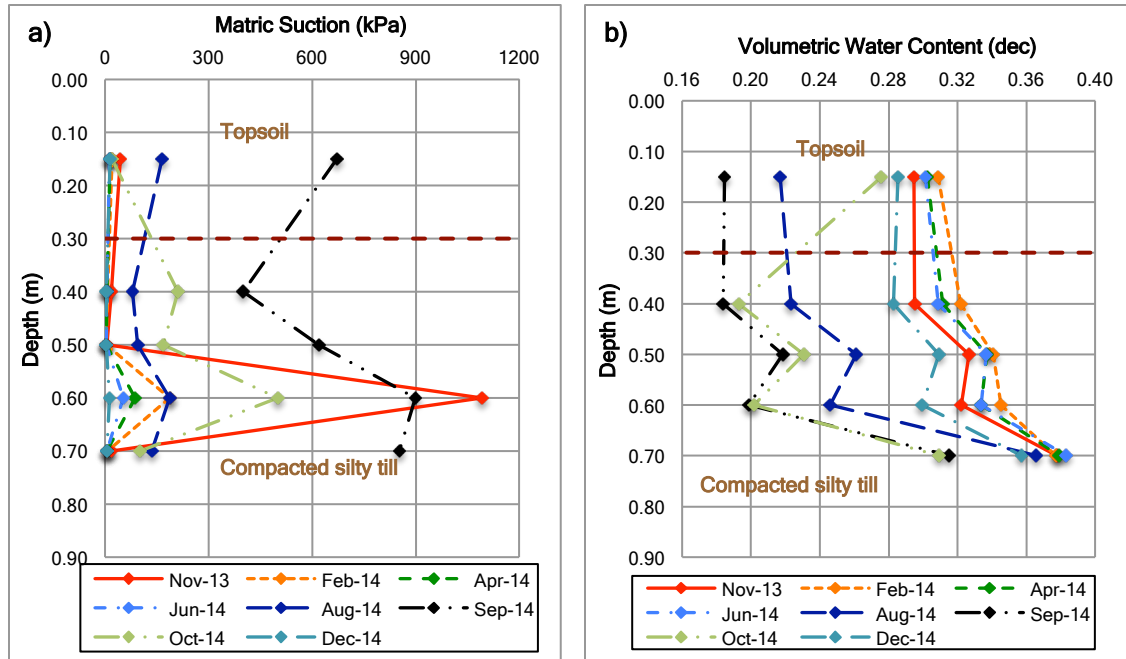


Figure 4-33: a) Matric suction and b) volumetric water content profiles for lysimeter #5 (Topsoil+compacted silty till)

Figure 4-33 a) presents the matric suction profiles for lysimeter #5. The probe installed at 0.60 m showed high matric suction values, probably associated with initially dry conditions during the installation, followed by a long equilibration process. Matric suction profiles were quite uniform, and the values changed at the same rate during both wet and dry season. The matric suction in the bottom region (0.70 m) of the silty till started to increase in the middle of the dry season, and kept increasing until right after the beginning of the wet season; this increase in matric suction is supported by the volumetric water content profiles shown in Figure 4-33 b), where the 0.70 m CS616 probe recorded little changes until August 2014.

4.2.5.1 Degree of Saturation

Given the volumetric water content profiles for lysimeters #1 and #5 (Figure 4-32 b) and Figure 4-33 b)), the degree of saturation (S_r) profiles could be computed. The purpose of calculating the degree of saturation was to evaluate the potential efficiency of the cover as an oxygen diffusion barrier (Aubertin, 2005 as cited in INAP, 2014). Volumetric water contents measured by CS616 sensors were transformed into S_r using dry density (ρ_d), and specific gravity (G_s) (Fredlund et al., 2012). These parameters were measured during the field investigation program in 2013 (ρ_d), or defined by Urrutia

(2012) as part of the initial laboratory-testing program (G_s). Figure 4-43 a) and b) present the degree of saturation profiles for lysimeters #1 and #5, respectively, at different points in time.

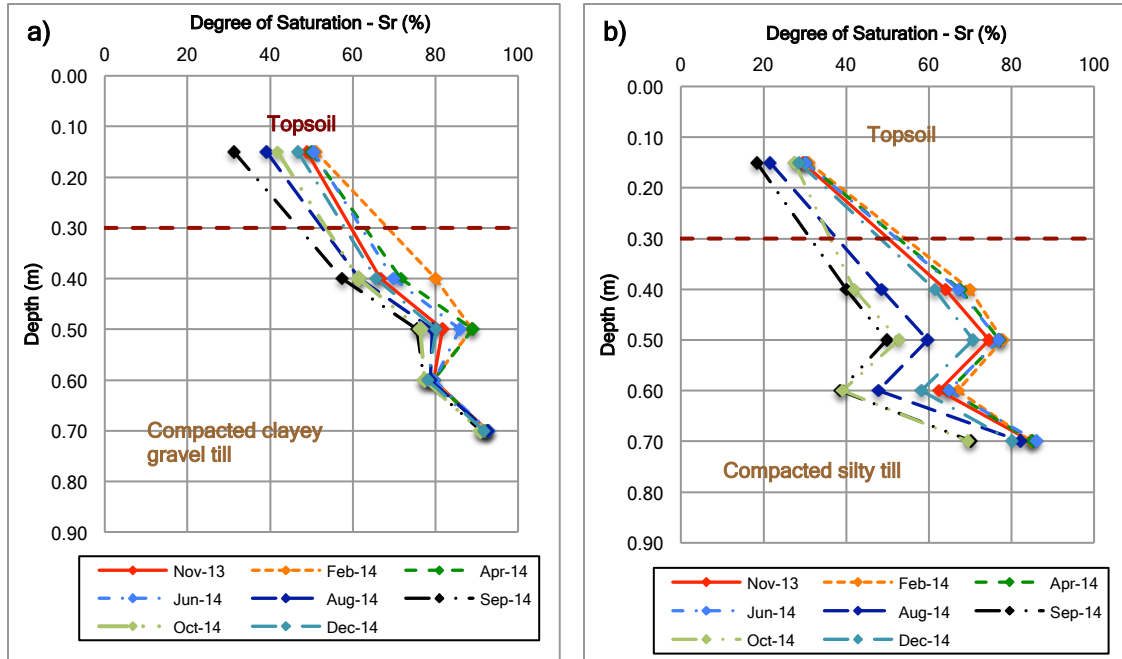


Figure 4-34: Degree of saturation profiles for a) lysimeter #1, and b) lysimeter #5

The degree of saturation profiles for lysimeter #1 (Figure 4-34 a)) show that the middle and bottom sections of the compacted clayey gravel till barrier had S_r above 80%. These values were maintained from November to June approximately, while S_r as low as 75% was observed for the remaining months. The topsoil layer and top section of the barrier had S_r values below 80% during the whole year, with S_r for topsoil ranging from 30% to 50%, and from 57% to 79% for the top section of the barrier layer. The fact that the middle and lower section of the barrier layer could sustain degrees of saturation above 80% has an impact on limiting oxygen diffusion. The effective diffusion coefficient (D_e) for a material with $S_r = 80\%$ is approximately $10^{-8} \text{ m}^2/\text{s}$ (Aubertin, 2005 as cited in INAP, 2014), and this value is three orders of magnitude smaller than the one for dry conditions ($S_r = 0\%$).

The dynamic change of volumetric water content shown in Figure 4-33 b) had an impact in S_r for lysimeter #5 (Figure 4-34 b)). The S_r values for topsoil during the year were between 20% and 30%, while S_r values

for the barrier layer, up to 0.60 m of depth, were between 45% and 75%. Although the bottom section of the barrier layer could maintain S_r close to 80% between November and August, it eventually lost water and S_r dropped to 70%. This 10% reduction in S_r represents an increase of one order of magnitude in D_e (Aubertin, 2005 as cited in INAP, 2014), making the silty till less effective than the clayey gravel till as an oxygen diffusion barrier.

4.2.6 Oxygen Content

As described in Section 3.3.3.4, the oxygen levels in the underlying waste rock was measured during both the 2013 and 2014 field investigations. During the 2013 field campaign, measurements were recorded early in the morning and late in the afternoon. The purpose was to observe any possible change due to air temperature fluctuations. As no difference was observed, oxygen levels were measured once a day, either in the morning or in the afternoon, during the 2014 field investigation.

Figure 3-12 shows the oxygen content (% in volume) registered for lysimeters #1, #2, #4, and #5. At the onset of the wet season (November 2013), waste rock in lysimeter #1, which is overlain by a compacted clayey gravel till barrier, presented average oxygen levels in volume of 5%. Furthermore, waste rock underlying the compacted silty till barrier in lysimeter #5 had an average oxygen level of 3.5%, while the waste material in lysimeters #2 (non-compacted clayey gravel till barrier) and #4 (topsoil) had oxygen levels of 18% and 20%, respectively.

Measurements taken during the 2014 dry season showed that the average oxygen level in the waste rock underlying lysimeters #2, #4, and #5 had increased up to 20.9%, which is the same value found in fresh air. The oxygen levels measured in waste rock at lysimeter #1 increased gradually from 10.6% to 17% in a 21-day period. Figure 4-35 and Figure 4-36 present the calculated S_r in time, and at different depths for lysimeters #1 and #5, respectively. In order to evaluate how the change in S_r affected the oxygen content in the underlying waste rock, the average oxygen measurements recorded in 2013 and 2014 are included in both figures.

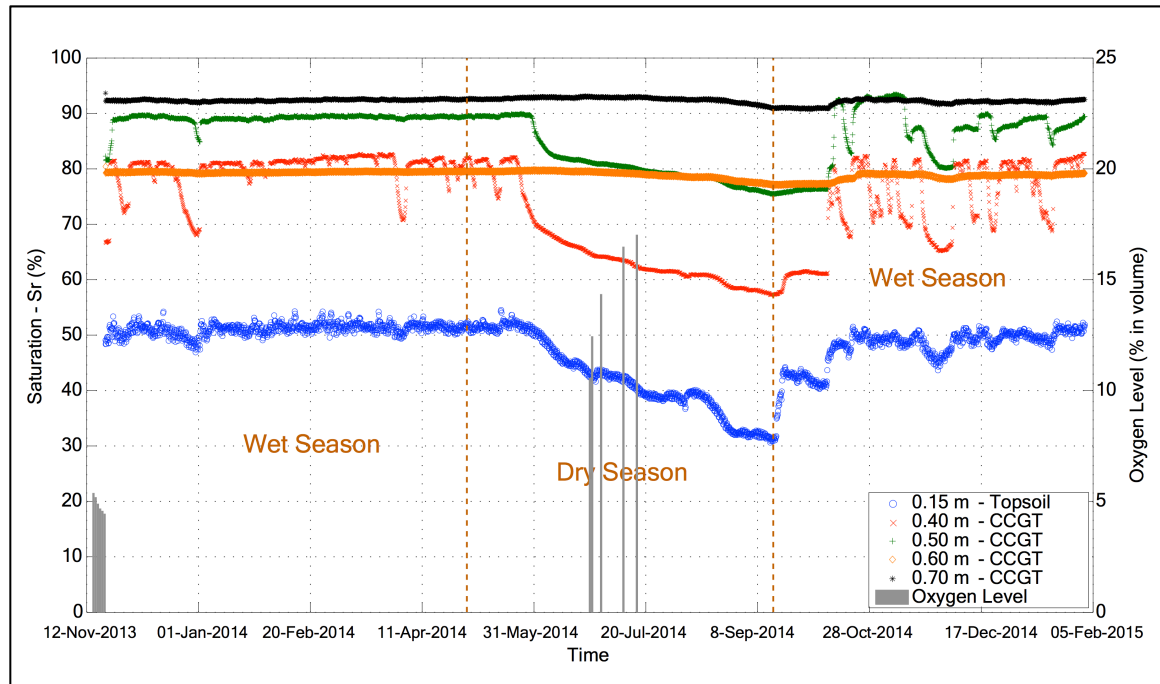


Figure 4-35: Computed degree of saturation (S_r) for lysimeter #1 (November 20, 2013 to December 31, 2014)

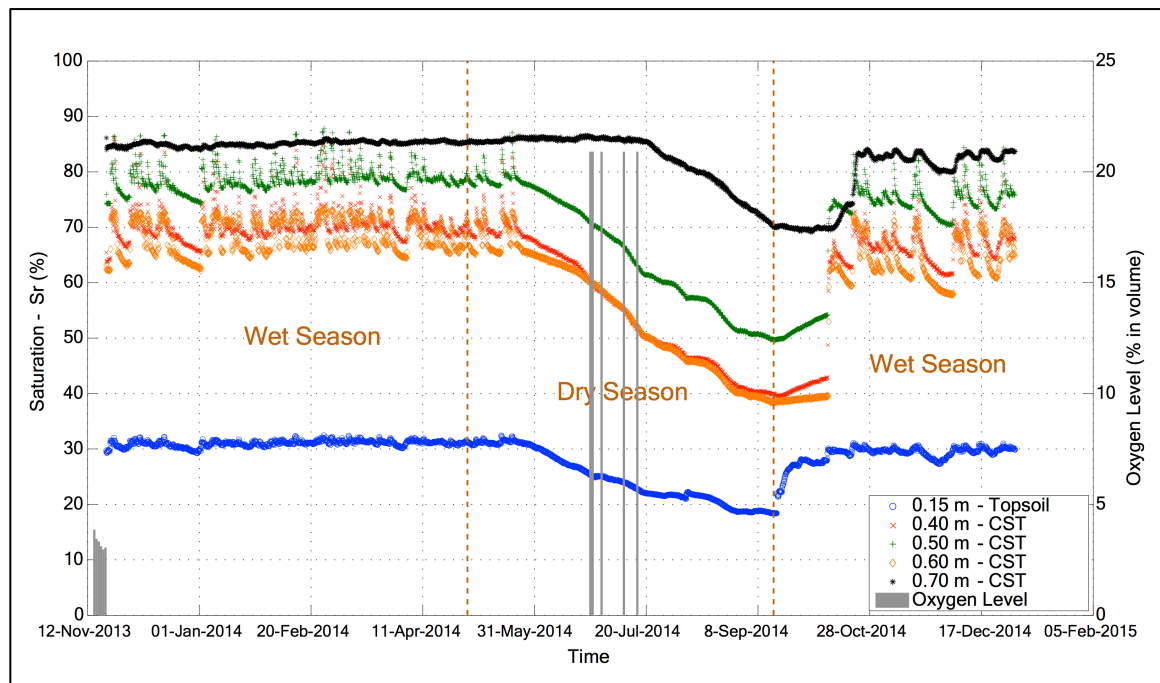


Figure 4-36: Computed degree of saturation (S_r) for lysimeter #5 (November 20, 2013 to December 31, 2014)

The volumetric water content and degree of saturation profiles show that the compacted silty till layer dries faster, and has lower values of S_r than the compacted clayey gravel till. The lower S_r values for the silty till allowed oxygen to diffuse readily from the atmosphere towards the underlying waste rock; therefore, the oxygen levels during 2014 were as high as the one found in fresh air. Although the average oxygen level for lysimeter #1 during the 2014 dry season increased from 10.6% to 17%, the measurements recorded for the different sampling tubes varied from 3% to 20.9% at different times. In addition, even though the volumetric water content profile for lysimeter #1 (Figure 4-32 b)) showed that S_r at the base of the clayey gravel till was above 80%, this S_r value was calculated from volumetric water content and dry density values measured at a particular location. Heterogeneity of the barrier material and differences in dry density might have created zones with lower values of S_r near the bottom of the barrier. As a result, this section of the layer was also drying but not uniformly and oxygen may have diffused through the areas with lower S_r values, and at a faster rate. However, the presence of regions capable of sustaining S_r values above 80% seemed to slow down the intake of oxygen.

4.2.7 Soil Water Characteristic Curve (SWCC)

One of the conclusions in the initial evaluation carried out by Urrutia (2012) was the absence of runoff. Runoff occurrence was expected, as it is one of the necessary mechanisms to reduce water percolation. One of the possible reasons for the lack of runoff was the underestimation of the hydraulic properties of the cover materials (Section 4.1.1.) However, a modification (due to the construction process) of the soils' water retention properties might be also a cause for high infiltration flows. The CS229 and CS616 sensors installed at the end of 2013 collected information for over a year, and they provided enough data to define an in-situ soil water characteristic curve (SWCC) for each material at different depths. Figures 4-37 to 4-39 show in-situ SWCCs for topsoil, compacted clayey gravel till, and compacted silty till, respectively.

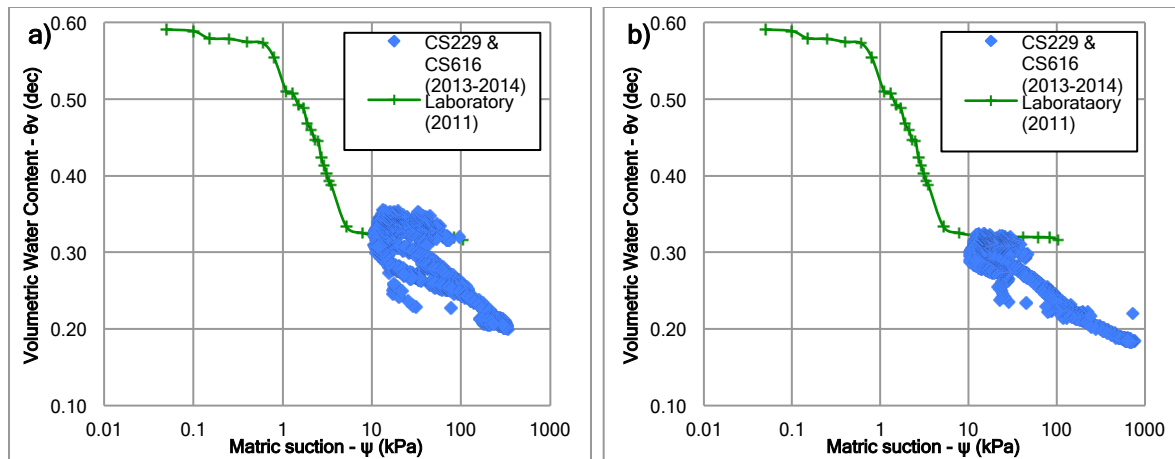


Figure 4-37: In-situ soil water characteristic curves (SWCC) for topsoil in a) lysimeter #1 and b) lysimeter #5

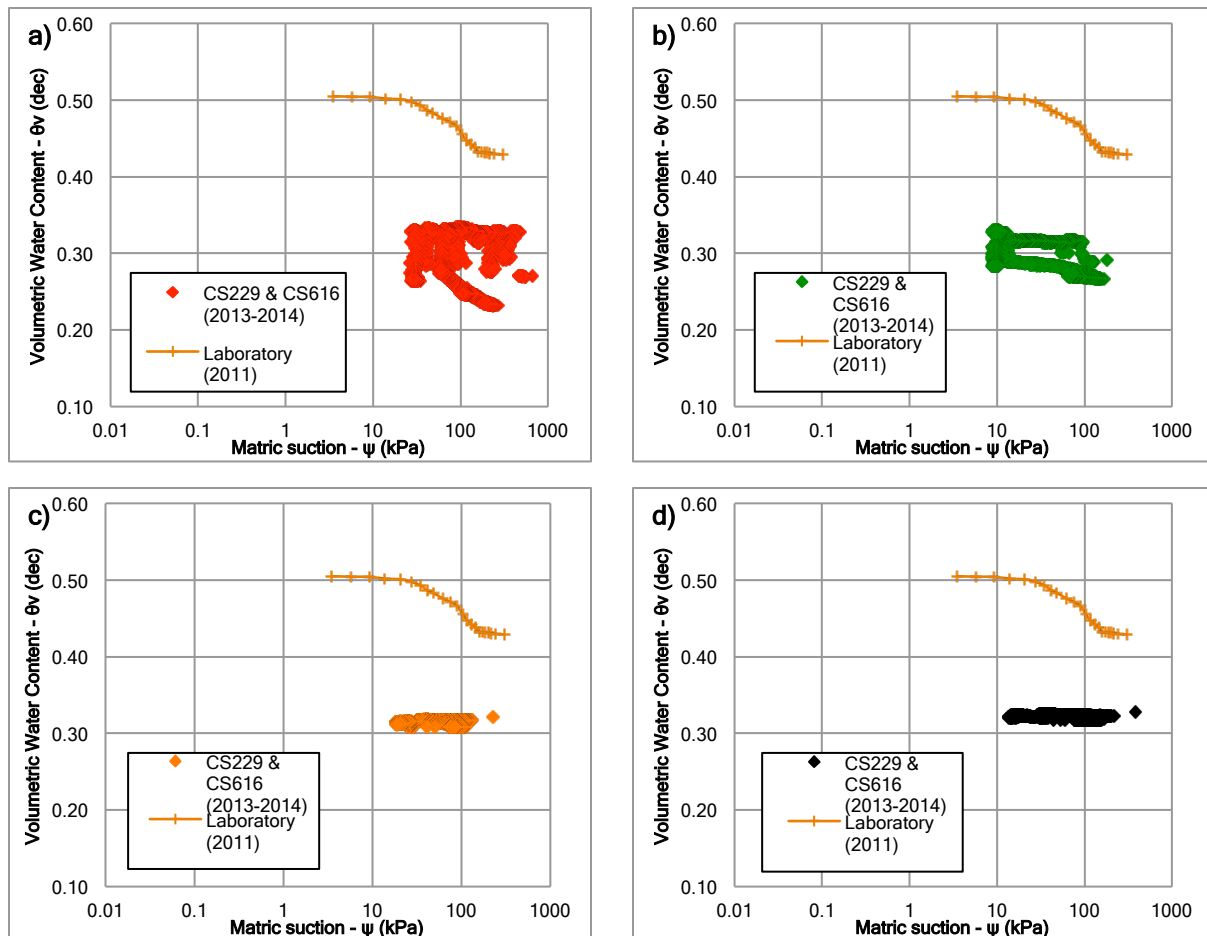


Figure 4-38: In-situ soil water characteristic curves (SWCC) for compacted clayey gravel till (lysimeter #1) at a) 0.40 m, b) 0.50 m, c) 0.60 m, and d) 0.70 m of depth

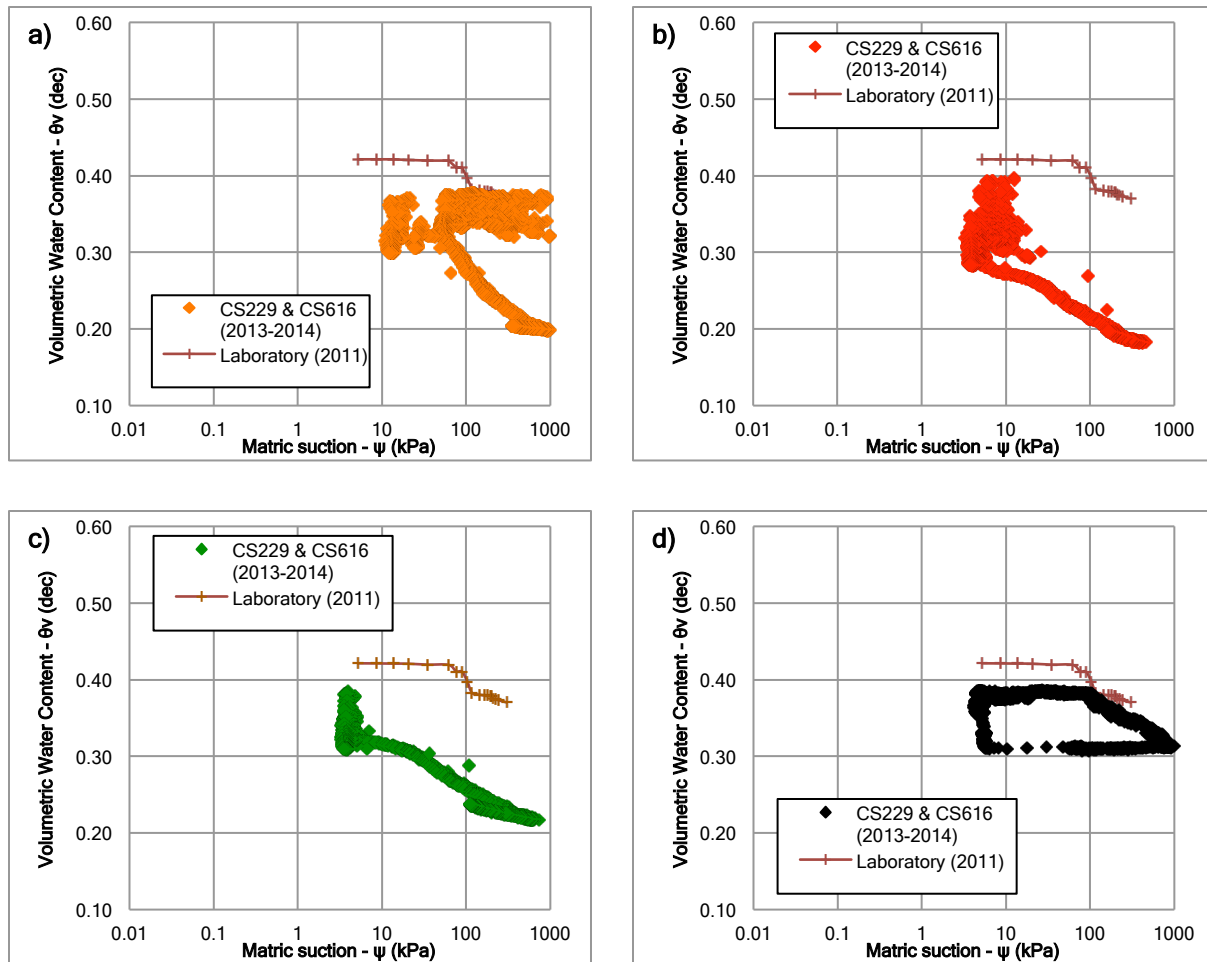


Figure 4-39: In-situ soil water characteristic curves (SWCC) for compacted silty till (lysimeter #5) at a) 0.40 m, b) 0.50 m, c) 0.60 m, and d) 0.70 m of depth

The previous charts show that all the materials have reduced their water retention potential. In-situ volumetric water contents are below those defined by laboratory testing, which means that less water can be retained in the soil voids, and thus less water is available for evaporation. Samples of both clayey gravel till and silty till used for laboratory testing did not include the coarse fraction that is actually placed in the barrier layers. The same conclusion can be drawn for the topsoil, where some coarse gravel was observed during the 2013 test pit excavation.

Another factor that could be related to these changes is the compaction energy applied during the construction stage. The clayey gravel till was placed and compacted in four 0.15 m layers, while for the

silty till only three 0.20 m layers were considered. More and thinner layers allow the application of greater compaction energy, and this increase in energy might have caused a change in the structure of the material particles, reducing the volume of the voids (from 0.50 to 0.30 for the clayey gravel till, and from 0.40 to 0.20 for the silty till). In addition to the decrease in the volumetric water content (i.e. volume of voids) for the in-situ SWCCC of the silty till, the AEV also appears to be reduced; however, it is important to note the accuracy of the CS229 matric suction sensors is limited to about 10 kPa.

The in-situ SWCCs for the compacted clayey gravel till have some common characteristics. The saturated volumetric water content (θ_s) is around 0.30 for all the curves (0.40 to 0.70 m of depth), and the transition zone for the 0.40 and 0.50 m curves has a steeper slope than the laboratory one. This change seems to be a consequence of the coarse fraction not considered during the laboratory test (Vanapalli et al., 1999). The AEV for all the curves increased and it is in between 40 and 70 kPa, while the AEV for the laboratory SWCC is approximately 30 kPa. The bottom section of the layer has the highest AEV, and this zone can keep high volumetric water contents during the dry season (Figure 4-32 b)). However, field measurements were not sufficient to define a complete SWCC at 0.60 and 0.70 m. Due to the high AEVs, the materials were just starting to lose water by the end of the dry season, and the initial rain recharged the layer moving the readings back to the full saturation zone.

The field SWCCs for the compacted silty till between 0.40 and 0.60 m of depth have are similar in shape and share some characteristics. In general, most of the curves have a similar AEV equal to 20 kPa with θ_s equal to approximately 0.30. Both field AEV and θ_s are lower than the laboratory ones, which are 20 kPa and 0.41, respectively. In addition, these curves have a lower slope in the transition zone than the one for the laboratory curve. The effect of the similarities in shape and elements was reflected in the volumetric water content changes over time, as shown in Figure 4-31. As θ_s and AEV are the same between 0.40 and 0.60 m of depth, the material lost water easily and started drying simultaneously as soon as the dry season began. Furthermore, as the field SWCCs have the same shape and slope for the transition zone, the change in water storage occurred at the same rate; however, the bottom of the compacted silty layer has a different SWCC, and therefore a different behavior. The SWCC at 0.70 m has similar characteristics to the laboratory one. It has an AEV of approximately 60 kPa, which explains why this zone was able to maintain high saturation until the middle of the dry season.

Materials placed on the dry side of the compaction curve require less suction to remove water from the pores, and hence their SWCCs have lower AEV (Vanapalli et al., 1999). In addition, the water content during compaction has an influence on the shape of the resultant SWCC (Zhou and Yu, 2005). The top and middle section of the silty till barrier (0.40 to 0.60 m of depth) were placed at moisture contents drier than the optimum, and at lower dry densities. These characteristics seem to explain the low AEVs, the similarity in shape between the SWCCs, and the fact that the field curves were below the laboratory curve (Miller et al., 2002). The bottom zone of the barrier was compacted on the wet side of the compaction curve, and the resultant dry density was close to specification value. These conditions, and the fact that the barrier material could have up to 70% of fines content in some cases, seem to explain the small differences between the laboratory SWCC and the in-situ SWCC at 0.70 m.

Figure 4-40 to 4-42 present the simplified in-situ SWCCs for topsoil, compacted clayey gravel till, and compacted silty till, respectively, based on the results and observations described above. As the CS229 sensors measure matric suction in the range of 10 to 2500 kPa (Campbell Scientific, Inc., 2009), the points in the field SWCCs with high volumetric contents were not reliable, since the associated matric suctions readings are out of the sensors range. Some effects of hysteresis were also observed, but as there were not enough measurements to define a sorption curve, they were not included in the analysis. In summary, the simplified SWCCs will be used in the numerical modeling described in the following chapter.

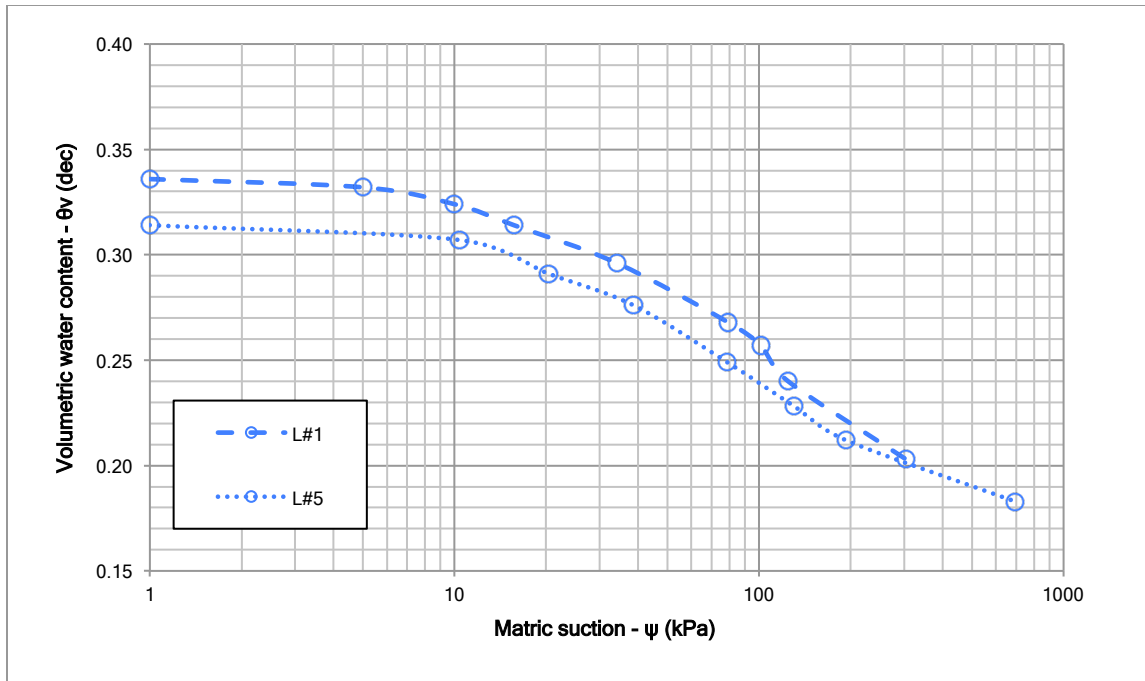


Figure 4-40: In-situ soil water characteristic curve for topsoil - Lysimeters #1 and #5

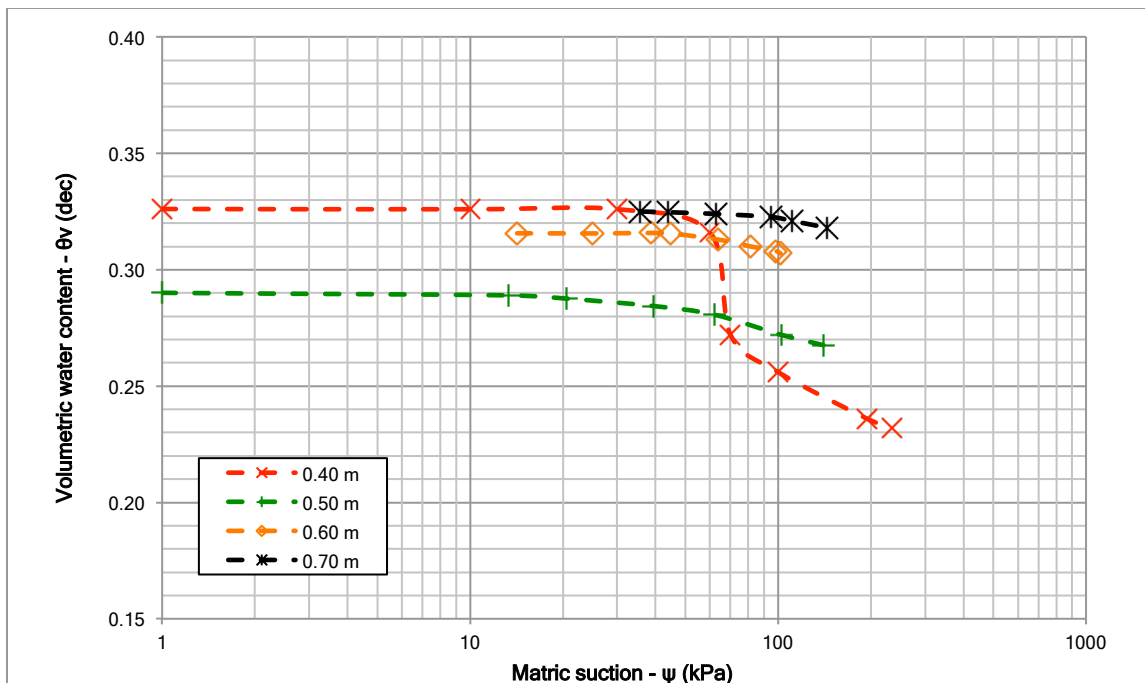


Figure 4-41: In-situ soil water characteristic curve for compacted clayey gravel till (lysimeter#1)

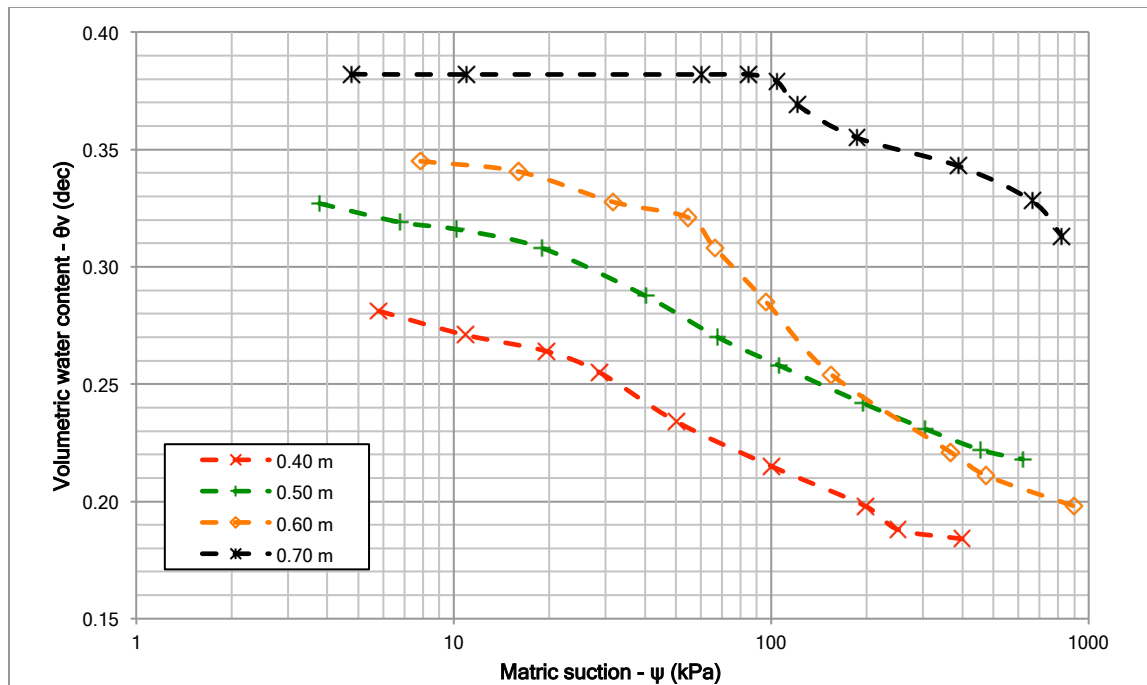


Figure 4-42: In-situ soil water characteristic curve for compacted silty till (lysimeter #5)

CHAPTER 5: PREDICTIVE NUMERICAL MODEL

Three numerical models in SoilCover (Unsaturated Soils Group, 2000) were created to have a better understanding of the different processes occurring in the cover systems at Antamina. These models are based on the initial base case model proposed by Urrutia (2012), but they were updated to include the findings from the geotechnical investigation campaigns, the data from the new instrumentation, and the meteorological records between 2011 and 2014. The numerical models were used to assess the performance of the different soil covers in terms of limiting water net percolation. For this purpose, the models were calibrated by comparing their results with the field experiment measurements. The calibrated model improved the reliability of the predictions, and allowed evaluating different scenarios and potential modifications to enhance the cover systems performance.

Lysimeters #1, #4, and #5 were the only ones modeled as part of this thesis. They were selected for their representation of the most and least effective alternatives in terms of limiting water percolation (lysimeters #4 and #5), for the reliability of their field records, and for their potential as oxygen barriers (lysimeters #1 and #5). Different sensitivity analyses were carried out with the objective of evaluating possible changes in both properties and thickness of the different elements of the cover systems. Furthermore, a tentative cover arrangement, based on the numerical model results and the field observations, is proposed. The following section presents the models' setup, and discusses the results of the sensitivity analysis.

5.1 Model Setup

As part of the initial assessment, Urrutia (2012) prepared a predictive numerical model for the soil cover in lysimeter #1. After four years, new information became available from the installed instrumentation, and the properties of the three cover materials were revised following the results of the field investigation program. As part of this thesis, the covers in lysimeter#1 (topsoil+compacted clayey gravel till), #4 (topsoil), and #5 (topsoil+compacted silty till) were modeled using SoilCover. The simulation period started in February 17, 2011 for lysimeter#1, and in March 24, 2011 for lysimeters #4 and #5. The analyzed period ended in December 30, 2014 for all lysimeters. These dates matched the ones selected

for the net percolation assessment (Chapter 4), and were also based on the availability of reliable percolation records for each lysimeter.

SoilCover is a one-dimensional fully coupled soil-atmosphere numerical predictive model. It is based on Darcy's, Fick's, and Fourier's Laws to characterize water and vapor flow, and to describe conductive heat flow in the soil below the soil/atmosphere boundary (Unsaturated Soils Group, 2000). Furthermore, evaporation fluxes in both unsaturated and saturated conditions can be predicted using the modified Penman formulation proposed by Wilson (1990, as cited in Wilson et al., 1994). For this purpose, SoilCover requires the atmospheric conditions, status of the vegetation, and soil properties during the evaluated period. The SoilCover version used during this research only allows the simulation of a 365 day period, and for this reason the predictions for the three covers were obtained on a yearly basis. The continuity and consistency of the predictions were achieved by using the results at the end of one simulation as the initial input conditions for the following one.

Although Urrutia (2012) defined the basic components of the numerical model, the revised version included new components, while other ones were updated. The components of the current assessment are as follows:

- Conceptual model,
- Finite element mesh,
- Initial Conditions,
- Material properties and meteorological data, and
- Base case model calibration.

5.1.1 Conceptual Model

The initial numerical model created by Urrutia (2012) for lysimeter #1 considered one single layer for each cover material (topsoil and compacted clayey gravel till). Field test results and instrumentation data collected during 2013 and 2014 showed that the geotechnical, hydrological, and unsaturated properties of the material were variable with depth. Although valid, the use of a single layer per material would not represent the conditions defined in-situ.

Figure 5-1 shows the profile of the conceptual model for the numerical simulations of lysimeters #1, #4, and #5.

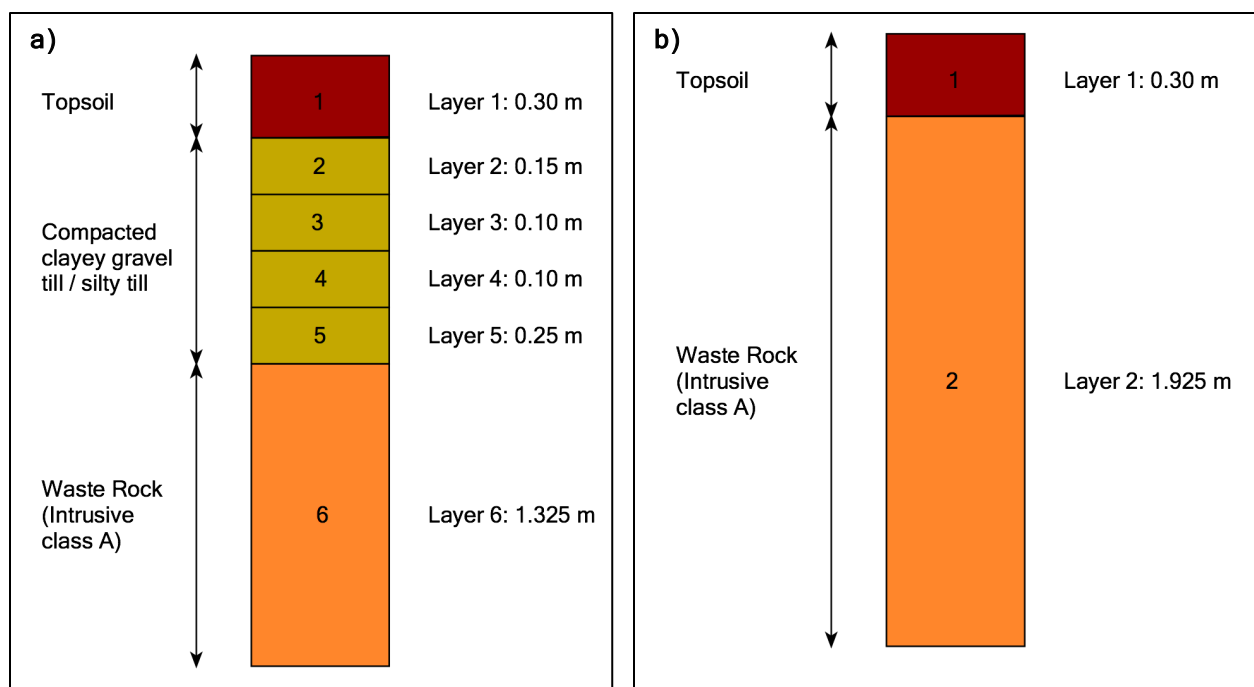


Figure 5-1: Conceptual model for a) lysimeters #1 and #5, and b) lysimeter #4

The conceptual models for lysimeters #1 and #5 have the same geometry, but have different material properties assigned to each layer. Both of them considered a 0.30 m layer of topsoil overlying four layers of either compacted clayey gravel till or silty till. The thicknesses of these four layers were defined based on the depths where the CS616 probes and CS229 sensors had been installed. Underlying the four layers is a single waste rock element of 1.325 m of thickness. The conceptual model for lysimeter #4 considers only a single 0.30 m thick topsoil layer overlying a 1.925 thick layer of waste rock. The purpose of dividing the barrier layer (clayey gravel till or silty till) in four elements was to reflect the changes in hydrological, geotechnical, and unsaturated properties with depth. Details of the values associated to each layer are discussed in Section 5.1.3.

5.1.2 Finite Element Mesh

The three models were developed following the cover system layout presented in Table 3-1, and the construction drawings prepared by Urrutia (2012). The models were intended to represent the covers and

waste rock profiles at the center of each lysimeter. The thickness of each layer was assigned following the guidelines in 5.1.1. and Figure 5-1.

The spacing of the mesh was selected with the purpose of maximizing the number of nodes in the cover materials. As percolation and evapotranspiration are the principal phenomena related to the covers' performance, having a high concentration of nodes in these areas improved the predictions. For the topsoil layer in lysimeters #1 and #5, a minimum and maximum spacing of 0.10 cm and 2.0 cm, respectively, with a 1.2 expansion factor were selected. The four elements of the barrier layers were modeled considering a minimum and maximum spacing of 1.0 and 2.0 cm, respectively, and an expansion factor of 1.5. For the underlying waste rock layer, the maximum and minimum spacing were 0.50 cm and 15 cm, respectively, with an expansion factor of 1.5. As the lysimeter #4 consisted of two layers, topsoil was modeled with a minimum and maximum spacing of 0.10 cm and 1.0 cm, respectively, and considering an expansion factor of 1.2. The underlying waste rock layer was modeled following the same criteria as for lysimeters #1 and #5. The resultant distribution of nodes for lysimeters #1 and #5 is shown in Figure 5-2, and the one for lysimeter #4 is presented in Figure 5-3.

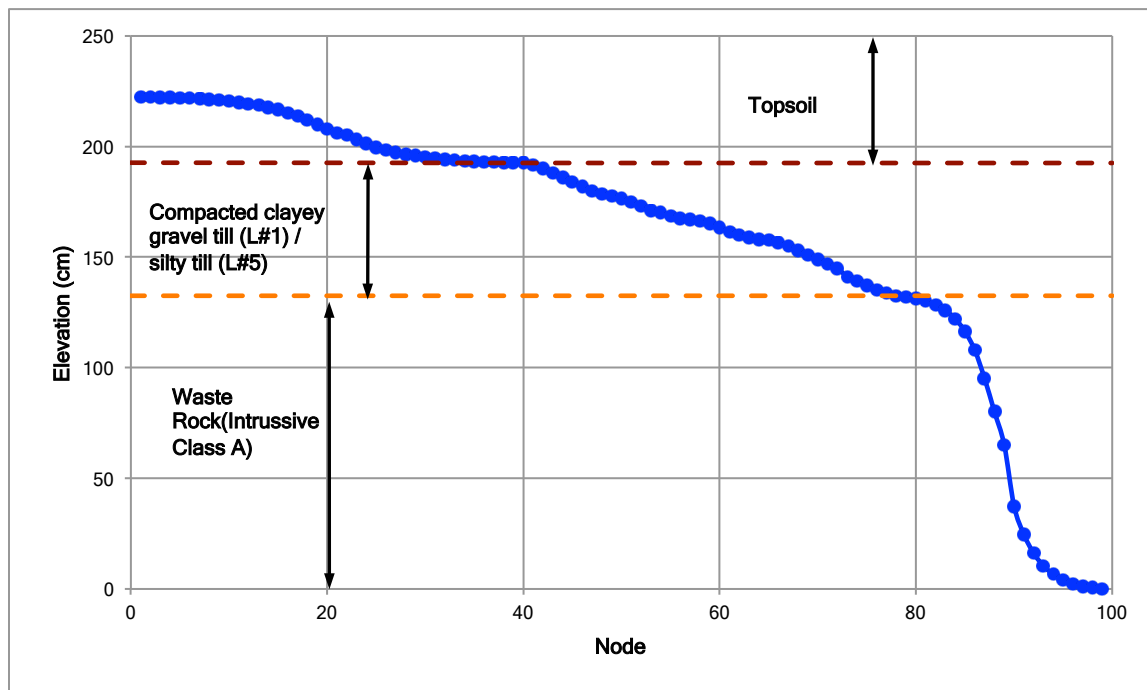


Figure 5-2: Distribution of nodes for lysimeters #1 (topsoil + compacted clayey gravel till) and #5 (topsoil + compacted silty till)

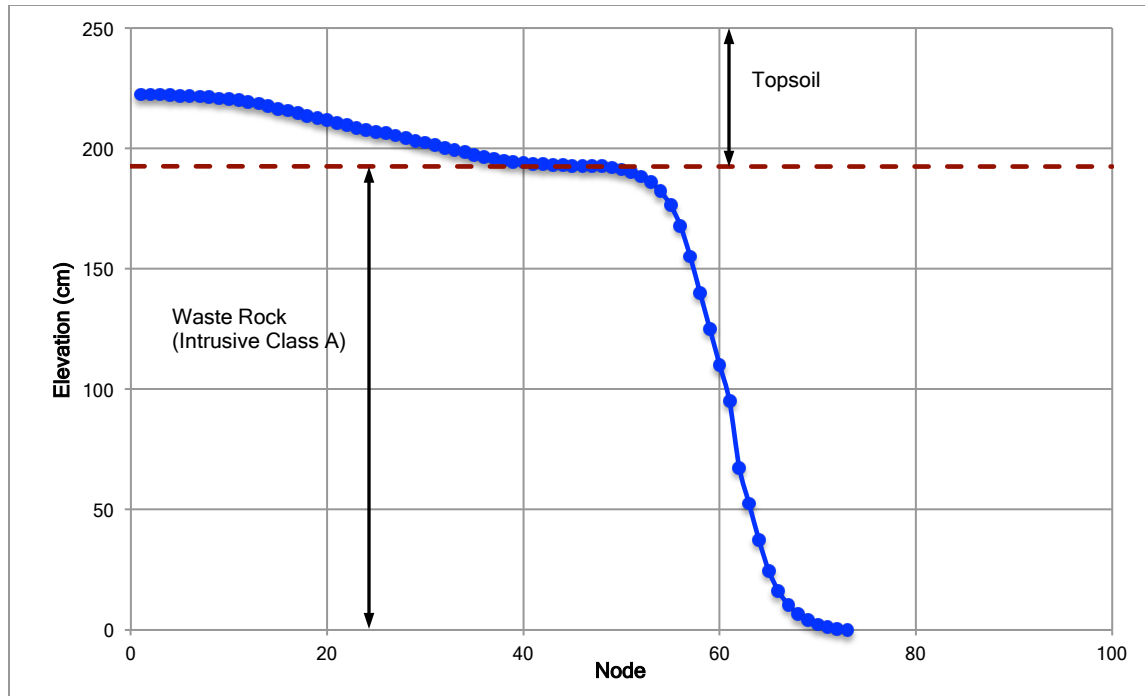


Figure 5-3: Distribution of nodes for lysimeter #4 (topsoil)

5.1.3 Material Properties and Meteorological Data

The geotechnical, hydrological, and unsaturated soil properties for each layer were defined following the results of the geotechnical investigations, and the instrumentation data collected between 2013 and 2014. A summary of the properties assigned to each layer for the three models is presented in Tables 5-1 to 5-3.

Table 5-1: Summary of parameters used in the SoilCover model for lysimeter #1

Material	Layer	Porosity (n)	Specific Gravity (G_s)	k_{SAT} (m/s)	Coefficient of volume change - m_v (1/kPa)	Quartz percentage - Q (%)	Mass Specific Heat - C_m (J/kg°C)
Topsoil	1	0.62	2.7	7.0×10^{-6}	2.6×10^{-3}	70	750
Compacted clayey gravel till	2	0.39	2.76	5.6×10^{-7}	1.3×10^{-5}	80	800
	3	0.35	2.76	6.2×10^{-6}	1.3×10^{-5}	80	800
	4	0.39	2.76	2.0×10^{-6}	1.3×10^{-5}	80	800
	5	0.35	2.76	2.0×10^{-6}	1.3×10^{-5}	80	800
Waste Rock	6	0.30	2.8	1.0×10^{-3}	1.0×10^{-5}	90	850

Table 5-2: Summary of parameters used in the SoilCover model for lysimeter #5

Material	Layer	Porosity (n)	Specific Gravity (G_s)	k_{SAT} (m/s)	Coefficient of volume change - m_v (1/kPa)	Quartz percentage - Q (%)	Mass Specific Heat - C_m (J/kg°C)
Topsoil	1	0.62	2.7	1.1×10^{-5}	2.6×10^{-3}	70	750
Compacted silty till	2	0.51	2.7	1.2×10^{-7}	1.3×10^{-5}	80	800
	3	0.43	2.7	1.2×10^{-7}	1.3×10^{-5}	80	800
	4	0.52	2.7	1.2×10^{-7}	1.3×10^{-5}	80	800
	5	0.45	2.7	1.2×10^{-7}	1.3×10^{-5}	80	800
Waste Rock	6	0.30	2.8	1.0×10^{-3}	1.0×10^{-5}	90	850

Table 5-3: Summary of parameters used in the SoilCover model for lysimeter #4

Material	Layer	Porosity (n)	Specific Gravity (G_s)	k_{SAT} (m/s)	Coefficient of volume change - m_v (1/kPa)	Quartz percentage - Q (%)	Mass Specific Heat - C_m (J/kg°C)
Topsoil	1	0.66	2.7	8.5×10^{-6}	2.6×10^{-3}	70	750
Waste Rock	2	0.30	2.8	1.0×10^{-3}	1.0×10^{-5}	90	850

The porosity (n) of the materials at different depths was calculated from the dry density measurements taken with the nuclear densometer. The specific gravity (G_s) was defined as part of the laboratory material characterization program conducted by Golder during the first stage of the project (Urrutia, 2012). The k_{SAT} used for topsoil was the geometric average of the test results obtained at the respective lysimeter. For the compacted clayey gravel till, the k_{SAT} selected for each layer was the geometric average of the results obtained at that depth. As no Guelph permeameter test was carried out at 0.70 m of depth, k_{SAT} at 0.60 m was assumed as constant for the bottom section of the barrier layer. The k_{SAT} selection for the compacted silty till followed a different approach, as using the k_{SAT} geometric average of the whole barrier material gave a better match during the calibration than the geometric average values per depth. The SWCCs for the topsoil and barrier materials in lysimeters #1 and #5 are those shown in Figure 4-43 to 4-45. For the compacted clayey gravel till (lysimeter #1), only the SWCCs at 0.40 m and 0.50 m were considered, as the ones at 0.60 m and 0.70 m were not fully determined during the monitoring period. As a result, the SWCC at 0.50 m was used to characterize layers 4 and 5. As CS616 and CS229 sensors

were not installed in lysimeter #4, the topsoil SWCC at lysimeter #1 (Figure 4-43) was selected for layer 1 in lysimeter #4 model. The coefficients of volume change (m_v) for topsoil, compacted clayey gravel till, and compacted silty till were selected from the suggested values in the SoilCover database for loose organic soil and over consolidated till.

Urrutia (2012) did not conduct any characterization test on waste rock, and the properties assigned to this material in the numerical model were based on tests conducted for Golden Sunlight that were included in the SoilCover database. The SWCC and k_{SAT} were maintained for the updated models, but the m_v value was replaced with the one defined experimentally by Wickland (2006). The SWCC for waste rock used for the updated models is shown in Figure 5-4.

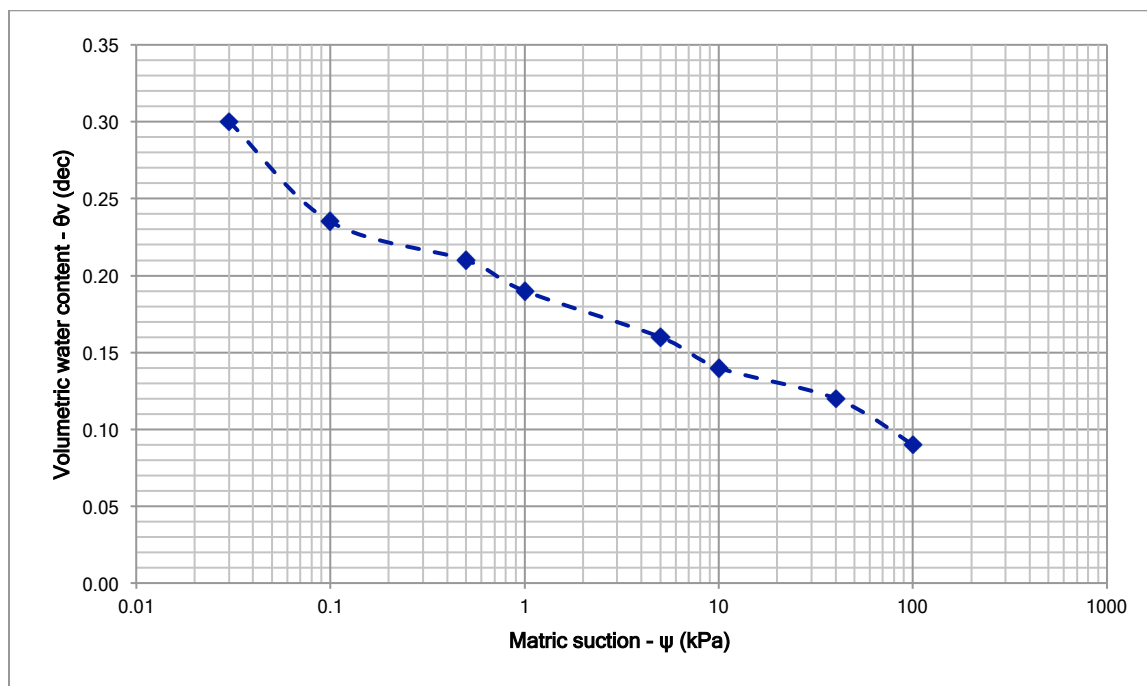


Figure 5-4: Soil water characteristic curve for Waste Rock (SoilCover database)

The meteorological data used for the numerical models came from Yanacancha and Punto B stations. As discussed in Chapter 4, records for air temperature, wind speed, net radiation, and relative humidity were available from both stations at different periods of time. Yanacancha station data was used from February 17, 2011 to April 29, 2014, while measurements at Punto B were available from April 30 to December 31, 2014. As discussed in Section 4.1.1.1.2, two sets of precipitation records were prepared to

assess the levels of percolation measured in the field-scale experiment. Both sets of precipitation were also used for the base case and the sensitivity analyses in SoilCover. The daily precipitation was assumed to have an average duration of 12 hours.

5.1.4 Initial Conditions

Matric suction, volumetric water content, and soil temperature can be used as initial conditions for the different simulated periods in SoilCover. As the SoilCover version used for this research only allowed a maximum simulation period of 365 days, the predictions for each lysimeter were obtained on a yearly basis. The conditions for the first year evaluation were supposed to be defined by the FTC-100 sensors readings installed at different depths. Due to the unreliability of the FTC-100 datalogger, Urrutia (2012) defined the initial conditions following an iterative process. In order to maintain consistency, the initial conditions set by Urrutia (2012) were maintained, but adjusted to fit the conceptual models adopted for this thesis. Matric suction at the bottom of the waste rock layer was set as 0 kPa, as this zone represents a draining zone, and it is assumed no water table is developed inside the lysimeters. Table 5-4 and Table 5-5 show the initial matric suction and temperature conditions adopted for the first year simulation in SoilCover.

Table 5-4: SoilCover initial matric suction and temperature conditions for lysimeters #1 and #5

Material	Layer	Top Suction (kPa)	Bottom Suction (kPa)	Top Temperature (°C)	Bottom Temperature (°C)
Topsoil	1	1	1	10	10
Compacted clayey (L#1) / silty (L#5) gravel till	2	1	1.5	10	10
	3	1.5	2	10	10
	4	2	2.5	10	10
	5	2.5	4	10	10
Waste Rock	6	4	0	10	5

Table 5-5: SoilCover initial matric suction and temperature conditions for lysimeter #4

Material	Layer	Top Suction (kPa)	Bottom Suction (kPa)	Top Temperature (°C)	Bottom Temperature (°C)
Topsoil	1	5	5	10	10
Waste Rock	2	5	0	10	5

The soil temperature and matric suction results from the first year simulation were used as initial conditions for the second year model (2012), and the same approach was followed for the third one (2013). As new instrumentation was installed in November 2013, soil temperature, volumetric water content, and matric suction records were available during 2014. This new information was used to simulate year four (2014) for lysimeters #1 and #5, assuming different initial conditions at the beginning of the run period. The outcomes of these alternatives models for year four were compared to the results obtained from the original model, where initial conditions were selected from the previous year predictions (2013). The difference between the original base case model, which calculated initial conditions and soil temperature, and the alternative ones was minimal in terms of the predicted net percolation. Therefore, the performance assessment between 2011 and 2014 was conducted deeming the original base case.

Vegetation root depth was considered to range from 0.01 to 0.30 m. These values were assumed for the initial model and were based on Antamina's experience with local species (Urrutia, 2012). This assumption was verified during the field investigations carried out in 2013 and 2014, as it was observed that root penetration did not exceed 0.30 m of depth. For this assessment, the vegetation parameters were updated to match the conditions observed in the lysimeters. A poor Leaf Area Index (LAI) was selected for the first year (2011), as the vegetation was in its early stages of growth (Urrutia, 2012). For the following years (2012 to 2014), an excellent LAI was adopted, as vegetation in all the covers had developed copiously.

As oxygen levels in the underlying waste rock at each lysimeters were measured at different times, an additional condition was assumed to evaluate oxygen diffusion through the cover materials. The oxygen content just beneath the contact between the barrier layer and waste rock was set equal to zero. The purpose of this assumption was to induce an oxygen content gradient between the atmosphere and the waste rock. This gradient would maximize oxygen diffusion through the cover material at any time during the simulation period.

5.2 Numerical Models First Run

The results of the first run of the three numerical models in SoilCover were compared with the percolation and runoff volumes measured in the field-scale experiment. The purpose of this comparison was to

evaluate the necessity of a calibration (change in the cover materials properties) to match the simulation results with field measurements. As the evaluated period was from 2011 to 2014, the simulation results were compared year by year and considered the two sets of precipitation defined in Section 4.1.1.2. The models for lysimeters #1 and #4 were found to match satisfactorily the field results, and no major changes or calibration were required. The match reflects the improvement achieved by the change of the conceptual model, and the update of the material properties. Some differences are observed in the percolation trend, and they may be associated to the daily rain distribution resultant from the different estimation methods.

Figure 5-5 shows the first run results for lysimeter #5 numerical model. The numerical model for lysimeter #5 needed a few adjustments to reflect the field-scale measurements; however, the adjustments were limited to the set of rainfall records used for the simulation. No runoff had been registered during the four years of monitoring, and the first run of the numerical model showed lower net percolation values in both a yearly and cumulative basis. Furthermore, the first run predicted runoff occurrence of up to 6% and 16% for cumulative and year-by-year analyses, respectively. SoilCover assumes that any precipitation that cannot infiltrate will become runoff, and this premise is applied to the surface node, and for every time step and iteration (Unsaturated Soils Group, 2000). This method produces a small error when there is a steep hydraulic gradient at the surface, which occurs when rainfall occurs after a dry period. It was observed that runoff was calculated at certain points in time when a precipitation event occurred after a short dry period. In order to minimize or eliminate runoff volume from the model, a single value of k_{SAT} was assigned to the compacted silty till instead of using different averages per layer. In addition, daily precipitation events leading to runoff occurrence were redistributed in the adjacent days for the same reason. The changes in k_{SAT} and daily precipitation values proved to be satisfactory, and although they did not eliminate runoff occurrence in the model, the volume was reduced up to less than 1% for the four-year analysis.

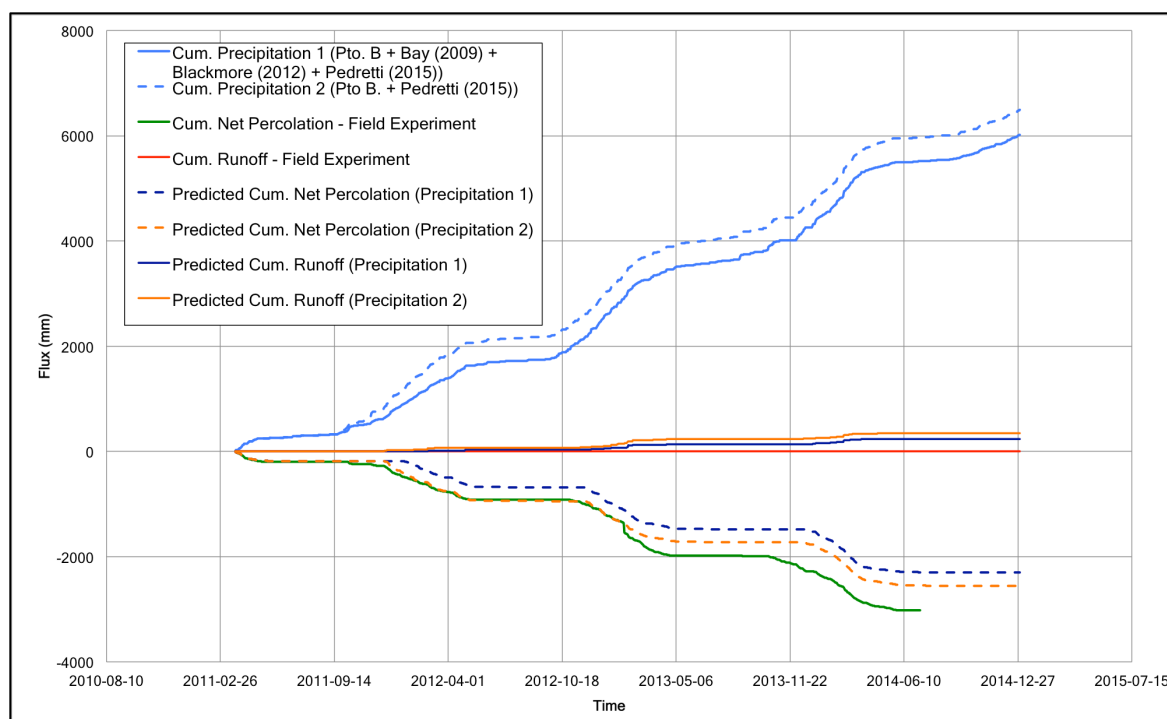


Figure 5-5: SoilCover first run results for lysimeter #5

5.3 Sensitivity Analysis

A sensitivity analysis was conducted for lysimeters #1 and #5 models. The purpose of the sensitivity analysis was to evaluate alternatives to improve the performance of the soil covers. The lysimeter #4 model was not included in the analysis due to the limited room for improvement associated to the cover material (topsoil).

Urrutia (2012) concluded that the performance of the cover system in lysimeter #1 might not be improved by the increase of vegetation. As the field investigation showed that the performance in terms of net percolation had been modified by a greater permeability of the barrier layer, the sensitivity analysis focused on the effects of changing the saturated hydraulic conductivity of the barrier layer and the thickness of the topsoil layer.

5.3.1 Thickness of the Topsoil Layer

The effect of reducing the thickness of the topsoil layer was evaluated by Urrutia (2012), and for that evaluation the parameters assigned to the base case model for lysimeter #1 were maintained. For this phase of the study, the updated base case models for lysimeters #1 and #5 were used for a sensitivity

analysis as detailed in Table 5-6. The root penetration depth was modified to match the variations in thickness of the topsoil layer, as no root penetration was observed during the field investigation.

Table 5-6: Sensitivity analyses for topsoil layer thickness - Lysimeters #1 and #5

Lysimeter	Case	Topsoil thickness (m)	Comments
1	Base case	0.30	Material parameters as in Table 5-1. Same topsoil porosity maintained for all the cases.
	1	0.10	
	2	0.15	
	3	0.20	
5	Base case	0.30	Material parameters as in Table 5-2. Same topsoil porosity maintained for all the cases.
	1	0.10	
	2	0.15	
	3	0.20	

5.3.2 Saturated Hydraulic Conductivity of the Barrier Layer

The base case model for lysimeter #1 considered the saturated hydraulic conductivity (k_{SAT}) profile defined by the field test results (Table 5-1). After calibration, the lysimeter #5 model did not include a k_{SAT} profile, but the geometric mean from the field results was selected as a single k_{SAT} for the whole barrier. As described in Chapter 2, the barrier materials characteristics, along with the moisture contents, energy and method of compaction during construction can modify both k_{SAT} and SWCC. Improving the quality control during the construction process might be able to reduce the permeability of the barrier layers, and hence reduce the net percolation volumes. For this reason, the sensitivity analysis for k_{SAT} contemplated a reduction of the base case values of up to two or three orders of magnitude. The details of the analyzed cases are shown in Table 5-7.

Table 5-7: Sensitivity analyses for saturated hydraulic conductivity (k_{SAT}) of the barrier layer - Lysimeters #1 and #5

Lysimeter	Case	Topsoil thickness (m)	k_{SAT} (m/s)	Comments
1	Base case	0.30	Table 5-1	Other material properties as in Table 5-1
	4		1×10^{-7}	k_{SAT} assumed constant for all the layers. Other material properties as in Table 5-1
	5		1×10^{-8}	
	6		1×10^{-9}	
5	Base case	0.30	Table 5-2	Other material properties as in Table 5-2
	4		1×10^{-8}	k_{SAT} assumed constant for all the layers. Other material properties as in Table 5-2
	5		1×10^{-9}	

5.4 Results

The results of the numerical simulations for the non-calibrated (lysimeters #1 and #4) and adjusted (lysimeter #5) base cases and the different sensitivity analyses are presented in the following sections. Net percolation and runoff predictions are initially presented, followed by degree of saturation and oxygen content.

5.4.1 Non-calibrated and Adjusted Base Cases

Figure 5-6 and Figure 5-7 present the cumulative net percolation, runoff, actual evaporation, actual transpiration, and actual evapotranspiration for lysimeter #1. Both figures include the two different cumulative precipitation records used for the simulations, and the cumulative net percolation measured in the field experiment. Fluxes entering (precipitation) and not entering (runoff) the cover system are presented as positive values, while negative values represent fluxes leaving the system (e.g. evaporation, net percolation, transpiration).

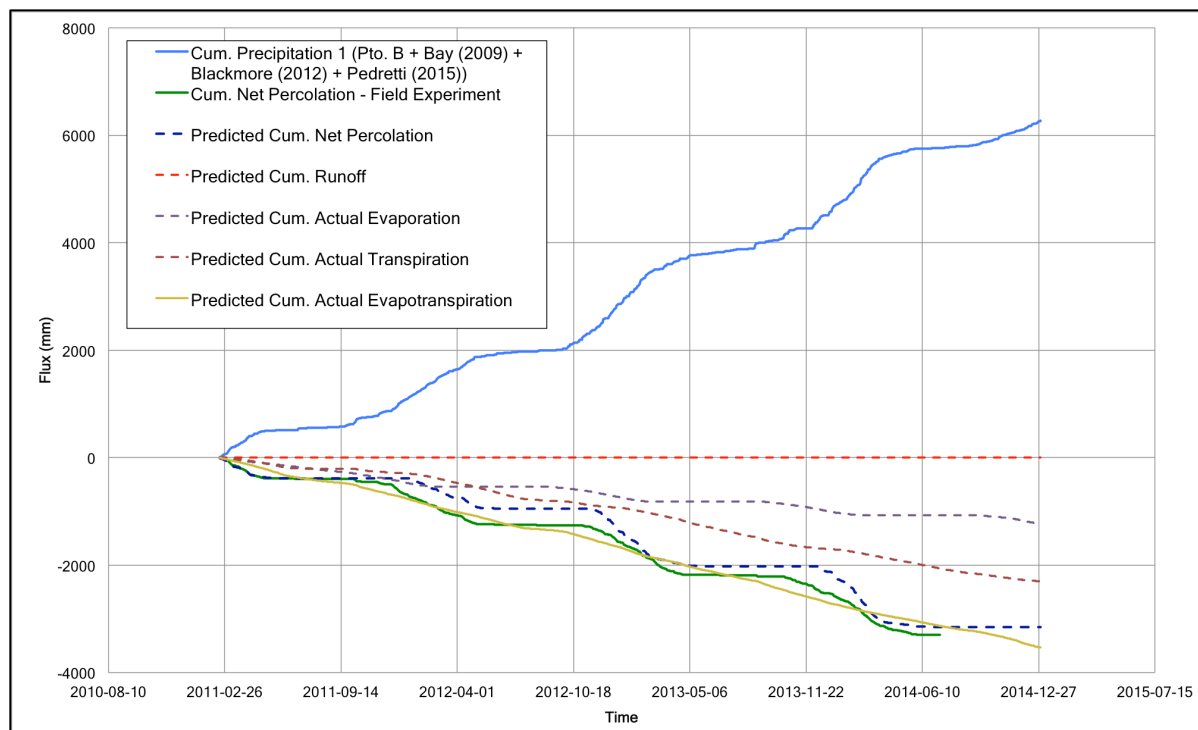


Figure 5-6: Non-calibrated base case cumulative water balance for lysimeter #1 - Precipitation 1

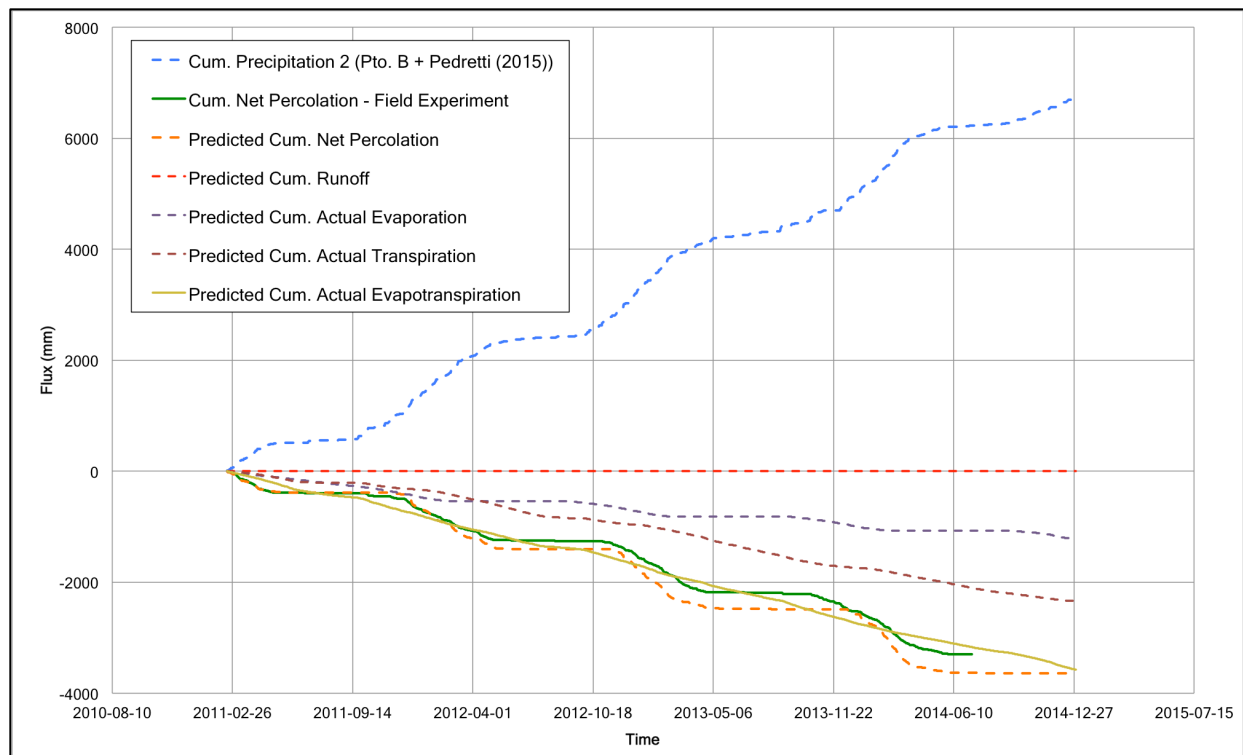


Figure 5-7: Non-calibrated base case cumulative water balance for lysimeter #1 - Precipitation 2

Figure 5-6 and Figure 5-7 show there is good agreement between the predictions and the field measurements. Predicted net percolation considering Precipitation 1 was underestimated between the end of 2011 and the beginning of 2012. This underestimation coincided with the period where the missing precipitation was estimated using Blackmore (2012) methodology. The difference impacted the cumulative net percolation prediction for the following years, as it set different initial conditions for the next simulations. As discussed in Section 4.1.1.1.1, the FP estimated precipitation has a 10% margin of error; for this reason, the cumulative percolation from Precipitation 1 moved closer to the field measurements at the end of the 2014, while the cumulative percolation for Precipitation 2 surpassed the field values. No runoff was predicted by any of the numerical models, which matched the field observations.

Figure 5-8 and Figure 5-9 present the predicted cumulative water balance for lysimeter #4, considering cumulative Precipitation1 and 2, respectively.

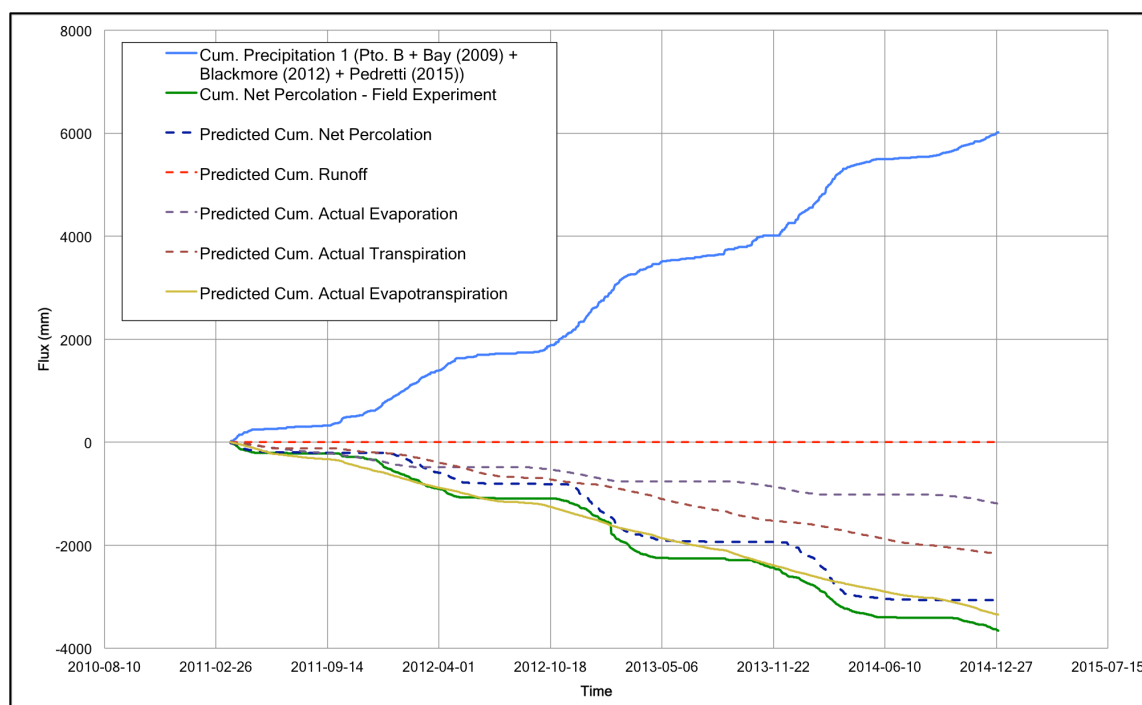


Figure 5-8: Non-calibrated base case cumulative water balance for lysimeter #4 - Precipitation 1

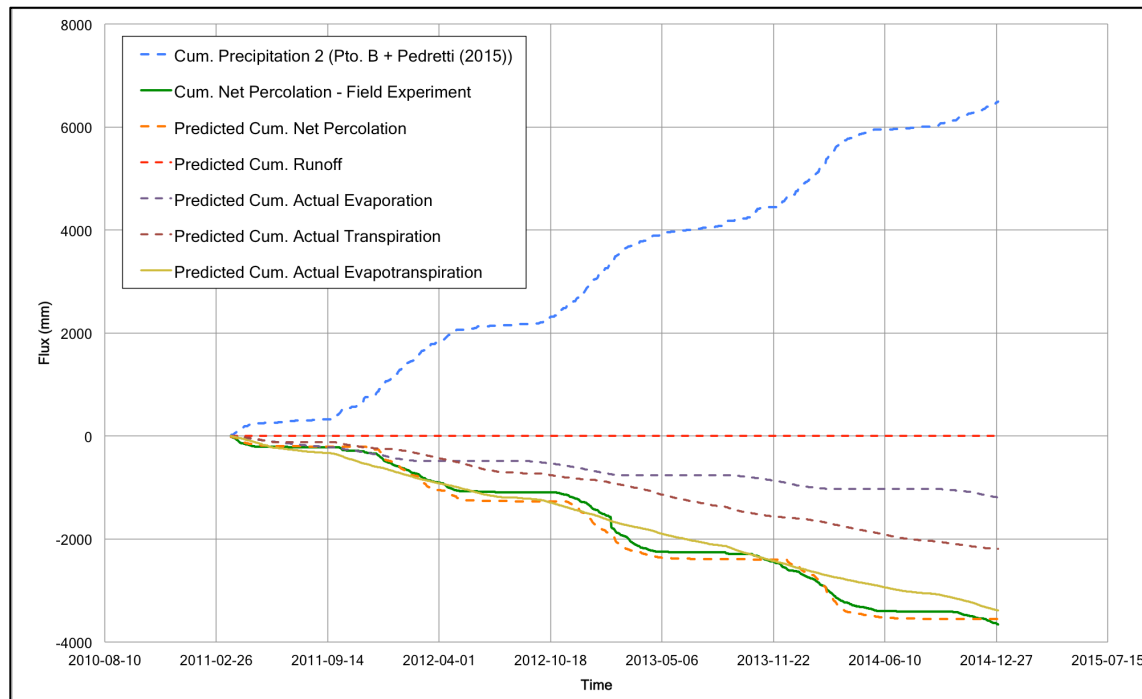


Figure 5-9: Non-calibrated base case cumulative water balance for lysimeter #4 - Precipitation 2

The model results for lysimeter #4 followed the same pattern as the results for lysimeter #1. The influence of the chosen precipitation set is evident, as predicted net percolation from Precipitation 1 is lower than the measured field values. On the other hand, predicted percolation from Precipitation 2 matched the field measurements. In the lysimeter #1 case, percolation from Precipitation 2 was slightly higher than field records. The difference between the predictions for both cases might be due to the level of characterization for each cover, and the source of the meteorological data. The soil cover in lysimeter #1 consists of two materials, and limited testing was carried out in the barrier layer. Topsoil was extensively tested in terms of permeability, and the lack of compaction might have reduced the degree of heterogeneity. In addition, it was noted in Section 4 that wind speed records from Punto B were lower than the ones registered at Yanacancha station. Furthermore, the lysimeters layout in Punto B may have an impact on the evaporation process, as air circulation in lysimeter #1 is different than in lysimeter #4 due to the proximity of lysimeter #1 to the adjacent slope face. As for lysimeter #1, no runoff was predicted by any of the models.

Figure 5-10 and Figure 5-11 show the base case model results for lysimeter #5 considering Precipitation 1 and 2, respectively.

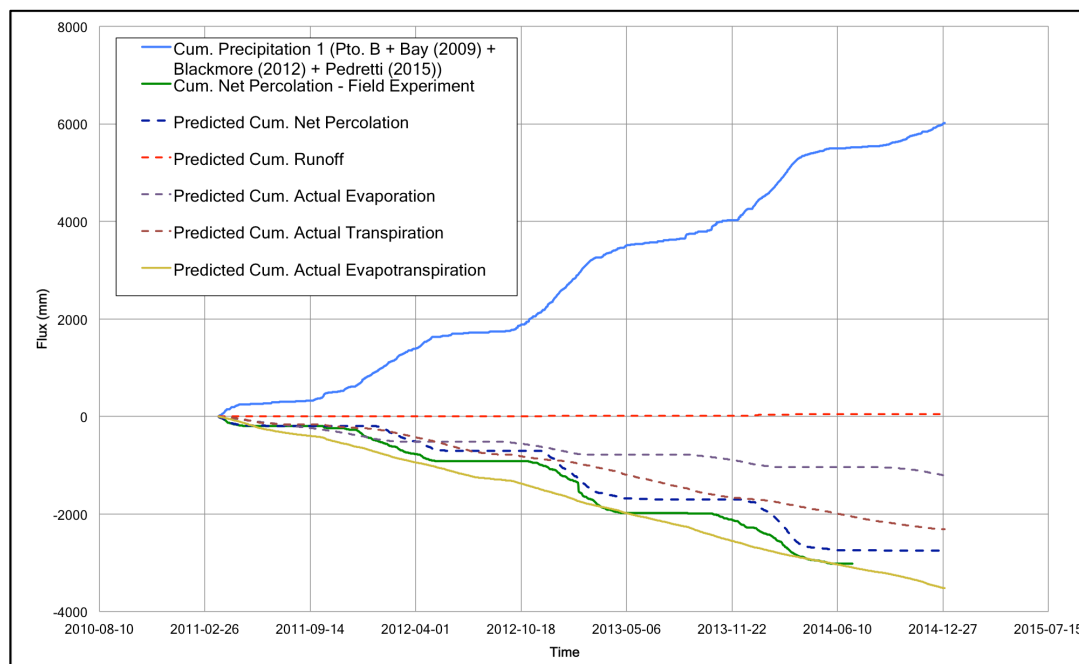


Figure 5-10: Adjusted base case cumulative water balance for lysimeter #5 - Precipitation 1

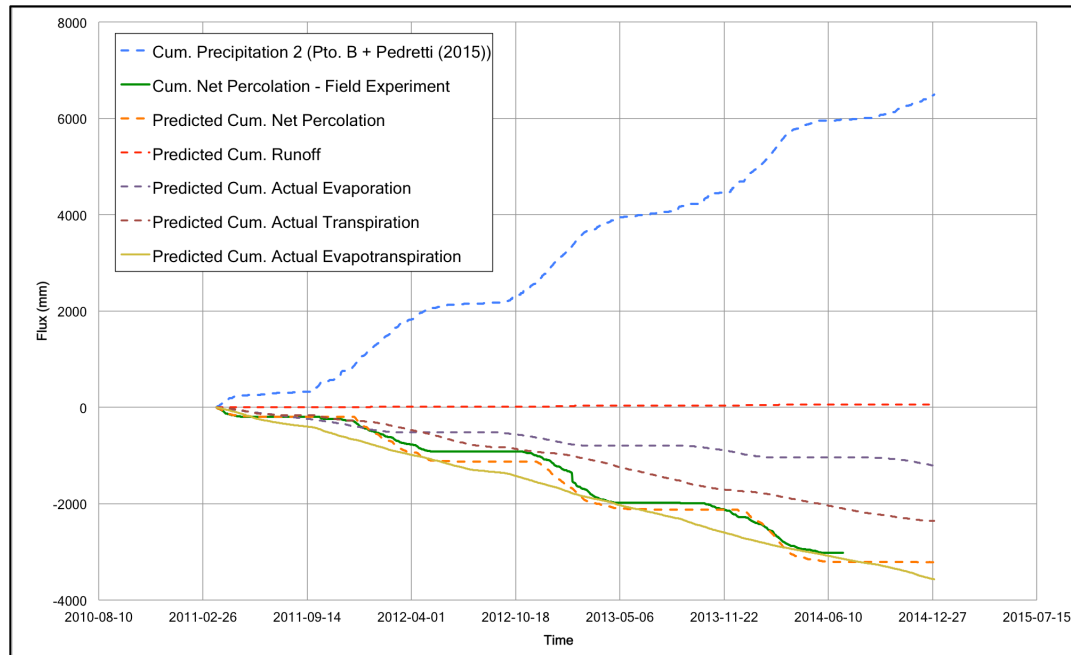


Figure 5-11: Adjusted base case cumulative water balance for lysimeter #5 - Precipitation 2

As for lysimeters #1 and #4, the calculations of the adjusted base case model for lysimeter #5 matched and followed the same trend as the field measurements. Once again, Precipitation 1 led to underestimated values when the FP calculated rainfalls were not used, while Precipitation 2 provided a good match when considering the entire evaluation period. As described in Section 5.2, the rainfall set was slightly adjusted to eliminate runoff occurrence due to high rain intensities after dry periods. The adjusted model predicted a greater volume of net percolation when compared to the first run results of the model showed in Figure 5-1. Although the adjusted model did not eliminate runoff completely, the predicted volume only occurred in one of the four evaluated years (2013), and it was less than 1% of the cumulative precipitation.

Figures 5-6 to 5-11 also included cumulative actual evaporation, actual transpiration, and actual evapotranspiration for lysimeters #1, #4, and #5. It was observed that for all the lysimeters, transpiration volumes were lower than evaporation ones during the first year, which was consistent as vegetation was still developing during that period. The details of the comparison between the field and predicted water balance are discussed in Section 5.5, but the predicted cumulative evapotranspiration for all the lysimeters was higher than the volume difference between precipitation and predicted net percolation.

This difference was also reported by Urrutia (2012) as part of the first year assessment, and it was suggested that water was being evapotranspired from the initial moisture of the cover. The difference might have also been induced by the changes in weather data, and the estimated precipitation records. The process was maintained during the following years, with evapotranspiration being the dominant mechanism during the dry season. The evapotranspiration volumes depend on the unsaturated properties of the cover material, with lysimeter #5 showing the highest evapotranspiration volumes.

5.4.2 Sensitivity Analysis

5.4.2.1 Thickness of the Topsoil Layer

Figure 5-12 and Figure 5-13 show the results of the sensitivity analysis conducted to evaluate the effect of variation in the thickness of the topsoil layer on lysimeter #1 performance. As for the base case models, the results are reported depending on the precipitation set used.

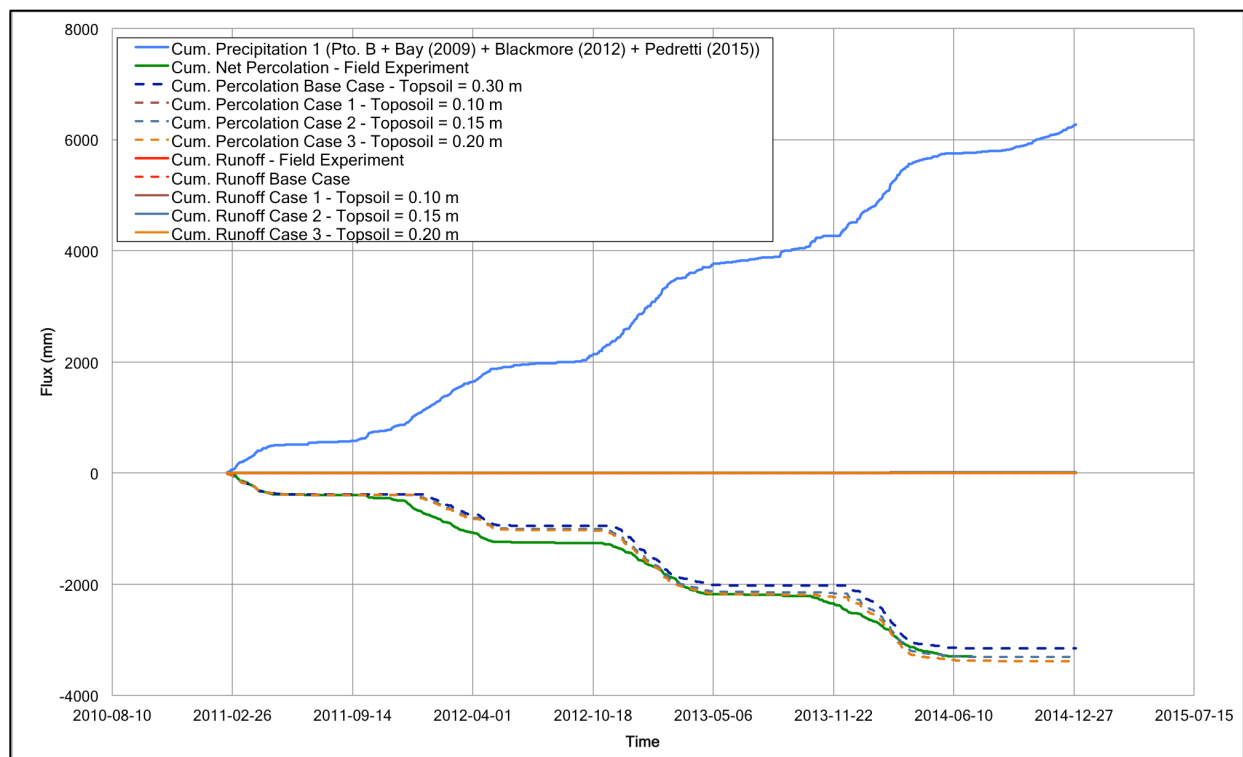


Figure 5-12: Net percolation sensitivity analysis results - Effect of topsoil layer thickness (Lysimeter #1, Precipitation 1)

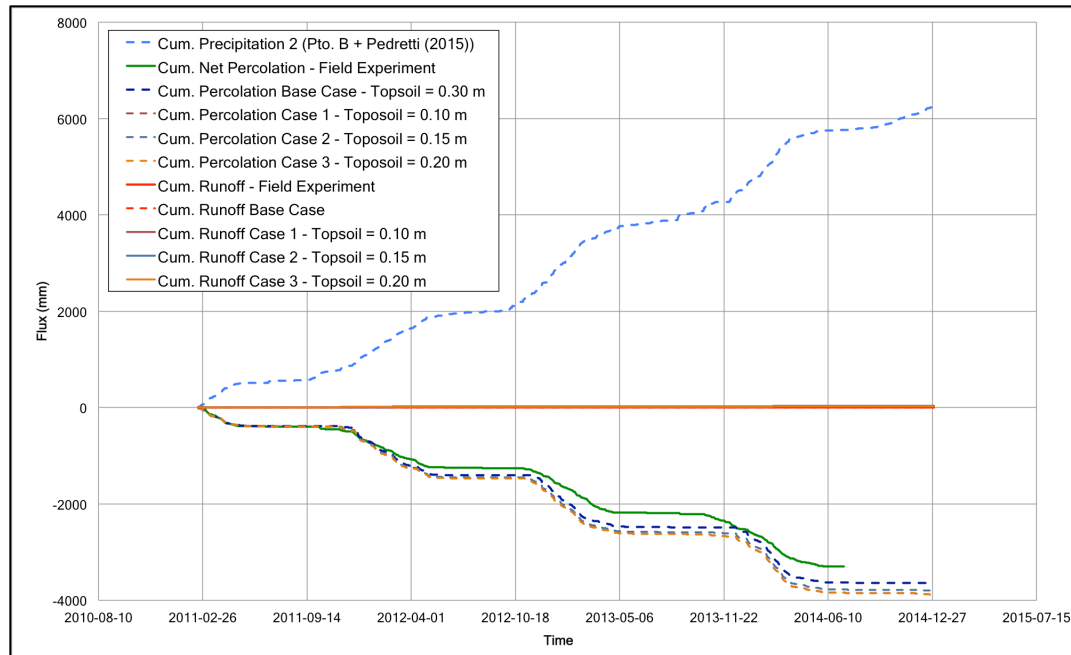


Figure 5-13: Net percolation sensitivity analysis results - Effect of topsoil layer thickness (Lysimeter #1, Precipitation 2)

The previous figures show the effect of reducing the topsoil thickness to 0.10 m (Case 1), 0.15 m (Case 2), and 0.20 m (Case 3). The amount of generated runoff would range between 7 (Case 3, Precipitation 1) and 37 mm (Case 1, Precipitation 2), representing less than 0.5 % of the total precipitation received. These results support the initial predictions obtained by Urrutia (2012) for lysimeter #1, where the runoff volume for a 0.10 m thick topsoil layer was equal to 3% (37 mm) of the total precipitation during the initial assessment. Net percolation values for the three analyzed cases are slightly below (Case 2, both sets of precipitation) or above (Cases 1 and 3, both sets of precipitation) the base case result (0.30 m thick topsoil layer), but the differences are smaller than 2% of the total precipitation. The change of thickness for the topsoil layer seems to have little or no effect on either reducing net percolation or generating runoff, given the level of accuracy of the field instrumentation, the missing precipitation method used for this thesis, and the cover materials current conditions.

The results of the sensitivity analysis using variable thickness of the topsoil layer for lysimeter #5 are shown in Figure 5-14 and Figure 5-15. The first one presents the results obtained considering Precipitation 1; outcomes from Precipitation 2 are shown in the second figure.

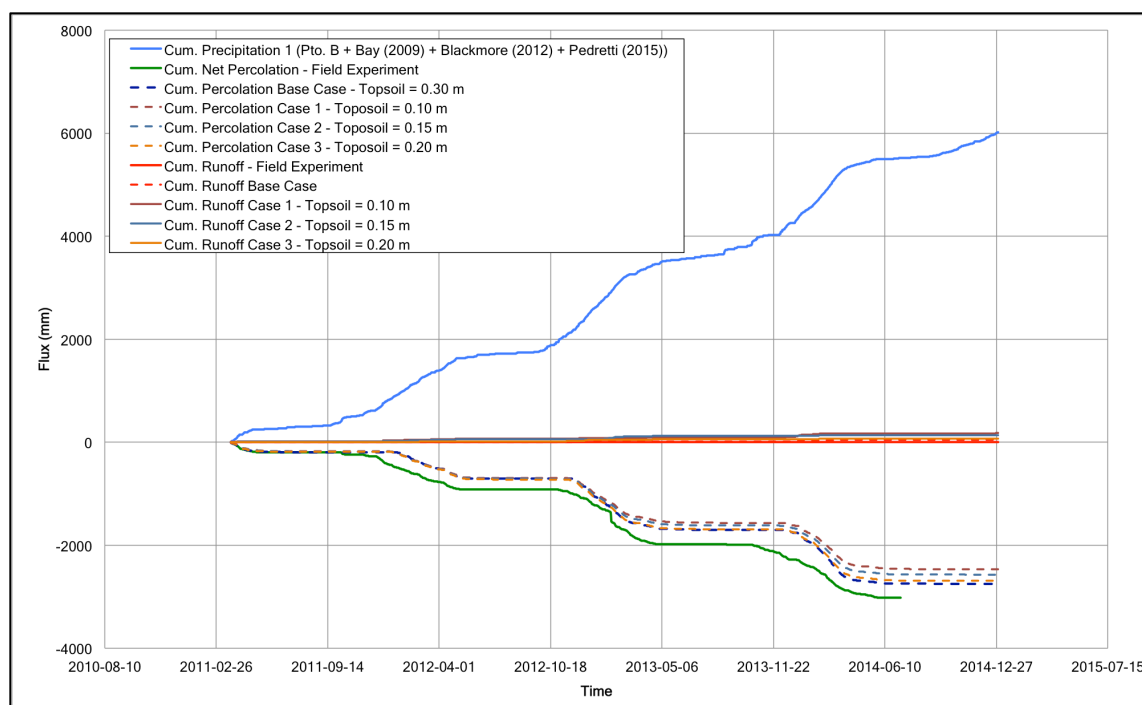


Figure 5-14: Net percolation sensitivity analysis results - Effect of topsoil layer thickness (Lysimeter #5, Precipitation 1)

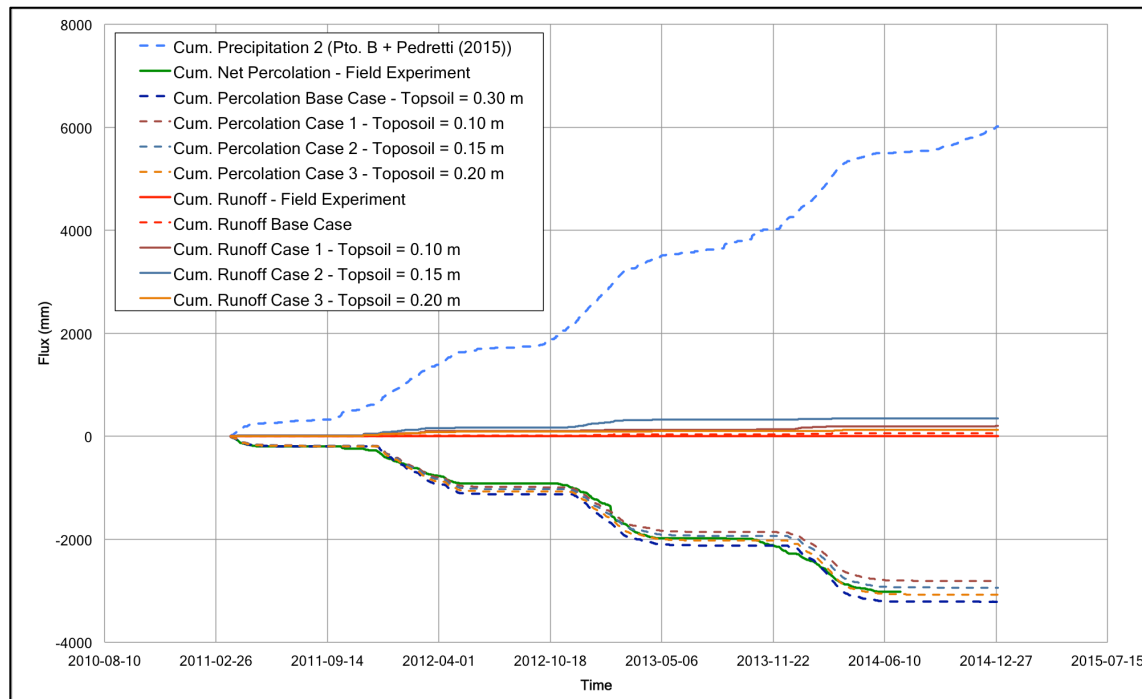


Figure 5-15: Net percolation sensitivity analysis results - Effect of topsoil layer thickness (Lysimeter #5, Precipitation 2)

The sensitivity analysis for lysimeter #5 showed that changing the thickness of the topsoil layer would not reduce net percolation significantly. Although some runoff was generated, the volume was not greater than 6% of the total precipitation (344 mm for Case 2, Precipitation 2). The predicted runoff volumes for lysimeter #5 were greater than the ones obtained for lysimeter #1, and this increased volume might be related to the difference in k_{SAT} between the barrier layer and topsoil. Topsoil in lysimeter #1 has a k_{SAT} in the order of 10^{-6} m/s, which is the same as that for the clayey gravel till. Thus, reducing the topsoil thickness would not have any effect as both materials have almost the same k_{SAT} . While k_{SA} for topsoil in lysimeter is in the 10^{-4} m/s order of magnitude, the silty till, has a lower k_{SAT} (10^{-7} m/s), and the difference allowed generating some runoff by exceeding the storage capacity of the topsoil layer. However, the volume is not significant when compared to the net percolation and, as stated by Urrutia (2012), constructing a cover with a layer as thin as 0.10 m would be difficult and impractical.

5.4.2.2 Saturated Hydraulic Conductivity of the Barrier Layer

Figure 5-16 and Figure 5-17 show the effect of changing the k_{SAT} of the clayey gravel till in the performance of lysimeter #1. The first figure shows the results obtained using Precipitation 1 and 2, respectively.

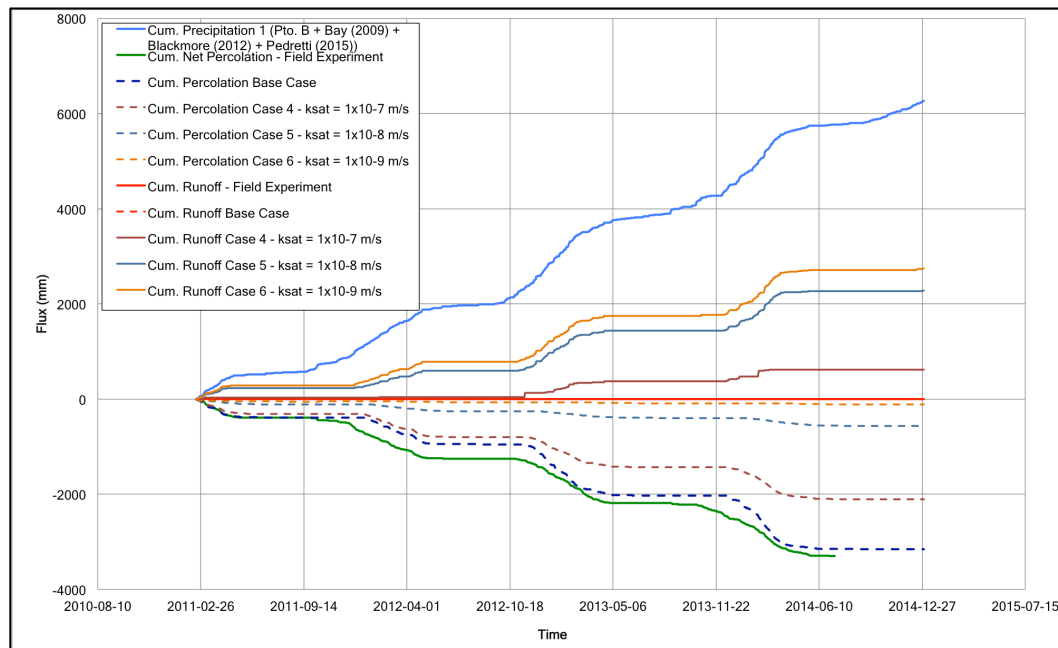


Figure 5-16: Net percolation sensitivity analysis results - Effect of barrier layer k_{SAT} (Lysimeter #1, Precipitation 1)

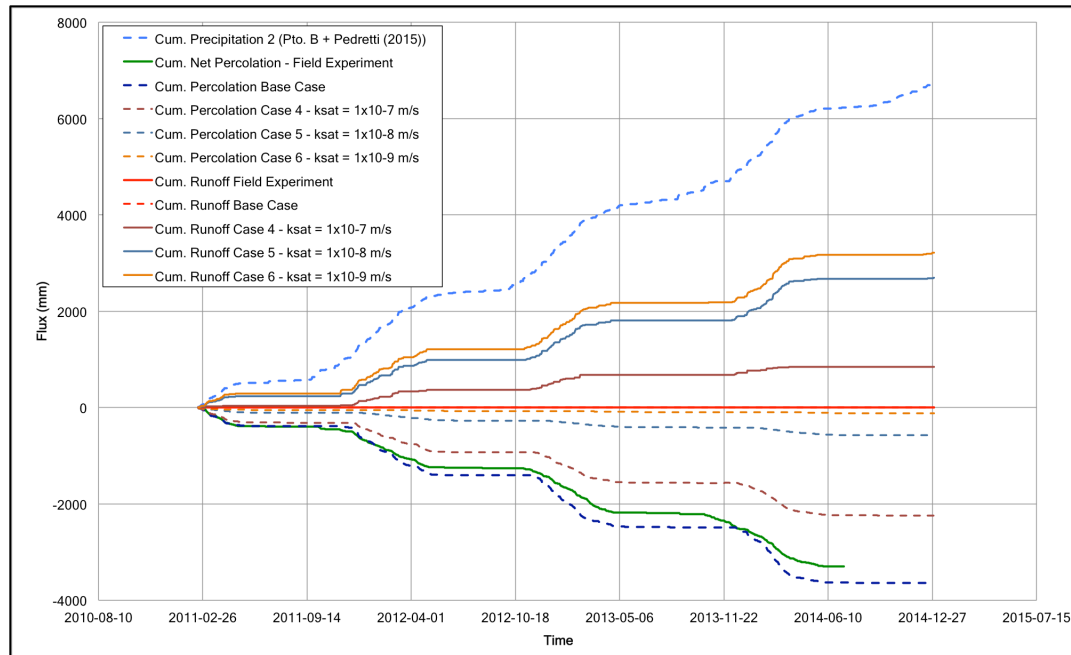


Figure 5-17: Net percolation sensitivity analysis results - Effect of barrier layer k_{SAT} (Lysimeter #1, Precipitation 2)

Reducing the k_{SAT} of the clayey gravel till has an evident impact on net percolation and runoff. The cumulative net percolation measured in the field experiment between 2011 and 2014 represents 57% and 53% of Precipitation 1 and Precipitation 2, respectively, while the predictions from the base case are equal to 55% and 58% for the same sets of rainfall records. By reducing k_{SAT} for the barrier layer by one order of magnitude (10^{-7} m/s), the net percolation was reduced to 36% of the total precipitation. The reduction in net percolation was a direct consequence of the occurrence of runoff, which was between 11% (Precipitation 1) and 14% (Precipitation 2). However, the reduced volume of net percolation was not only transferred to runoff. There was an 8% volume difference for both sets of precipitation that was accounted for as evapotranspiration. A reduced k_{SAT} changes the unsaturated flow regime, making more water available for evapotranspiration during the dry season. Case 6 considered a k_{SAT} of 10^{-9} m/s, which was the hydraulic conductivity defined by laboratory tests (Urrutia, 2012). Under these ideal conditions, net percolation was almost negligible (2% of the total precipitation), and runoff was the dominant mechanism by handling 47% and 51% of Precipitation 1 and 2, respectively. These outcomes represent what would have been the expected design performance of the soil cover.

The performance results after varying k_{SAT} for lysimeter #5 (topsoil and compacted silty till) are shown in Figure 5-18 and Figure 5-19.

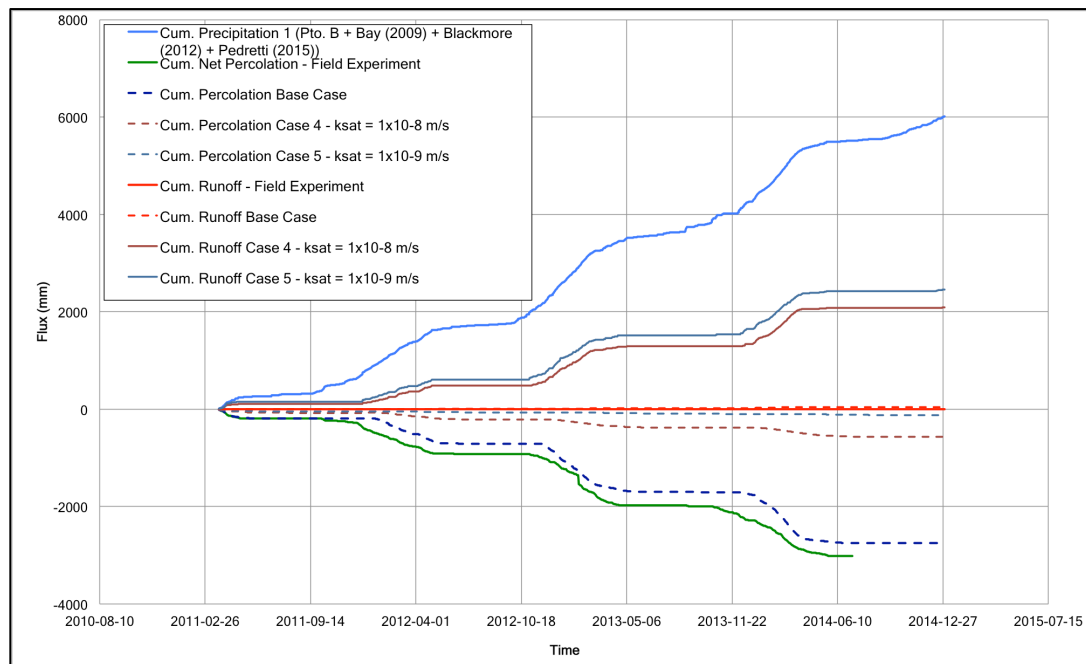


Figure 5-18: Net percolation sensitivity analysis results - Effect of barrier layer k_{SAT} (Lysimeter #5, Precipitation 1)

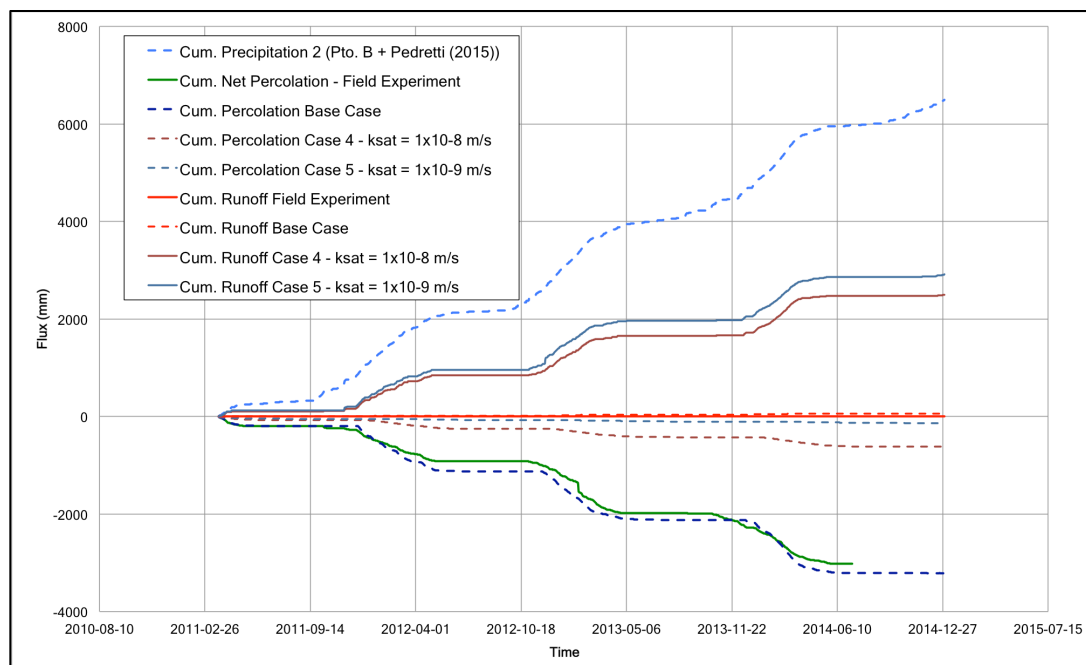


Figure 5-19: Net percolation sensitivity analysis results - Effect of barrier layer k_{SAT} (Lysimeter #5, Precipitation 2)

Field net percolation for lysimeter #5 is 55% and 51% of cumulative Precipitation 1 and 2, respectively. The net percolation for the base case model was 50% and 54% considering Precipitation 1 and 2, respectively, and these results were obtained assuming a constant k_{SAT} of 10^{-7} m/s for the silty till barrier. Reducing k_{SAT} for the silty till by one order of magnitude not only reduced percolation to 10% of the total precipitation, but also generated a runoff volume equal to 38% (Precipitation 1) and 41% (Precipitation 2) of the total rain received by the lysimeter. The decrease in percolation for lysimeter #5 is greater than the one achieved in lysimeter #1. As there was already a difference in k_{SAT} between the topsoil and barrier layer, reducing k_{SAT} for the latter by one order of magnitude overwhelmed the topsoil storage capacity easily and greater volumes of runoff were generated. As in lysimeter #1, the change in k_{SAT} also modified the unsaturated flow in the cover, increasing evapotranspiration in 2% and 3%. However, this increase is not as high as that reported for lysimeter #1 due to the low AEV of the in-situ SWCCs for the silty till.

5.4.3 Degree of Saturation and Oxygen Content

As the initial performance assessment of the different soil covers showed net percolation levels above the expected values, the effectiveness of the cover as an oxygen barrier became a subject of interest at this part of the research. Oxygen levels in the underlying waste were measured in 2013 and 2014 as part of the field investigation program, and the details of the procedure and measured values were described in Chapters 3 and 4. Although the time frame where oxygen measurements were recorded was limited, the results suggested only the cover in lysimeter #1 was capable of maintain a high degree of saturation, and hence of limiting oxygen diffusion. The numerical models in SoilCover were used to confirm the field outcomes, and to have a better understanding of the changes in oxygen content during a hydrological year.

Figure 5-20 shows the predicted degree of saturation (S_r) profiles for lysimeters #1 and #5. As the profiles obtained from Precipitation 1 and 2 showed minimum differences, Figure 5-20 only shows the profiles obtained from Precipitation 1. The dates for each profile were selected to match the ones used for the profiles calculated from the volumetric water contents measured by CS616 probes (Figure 4-34).

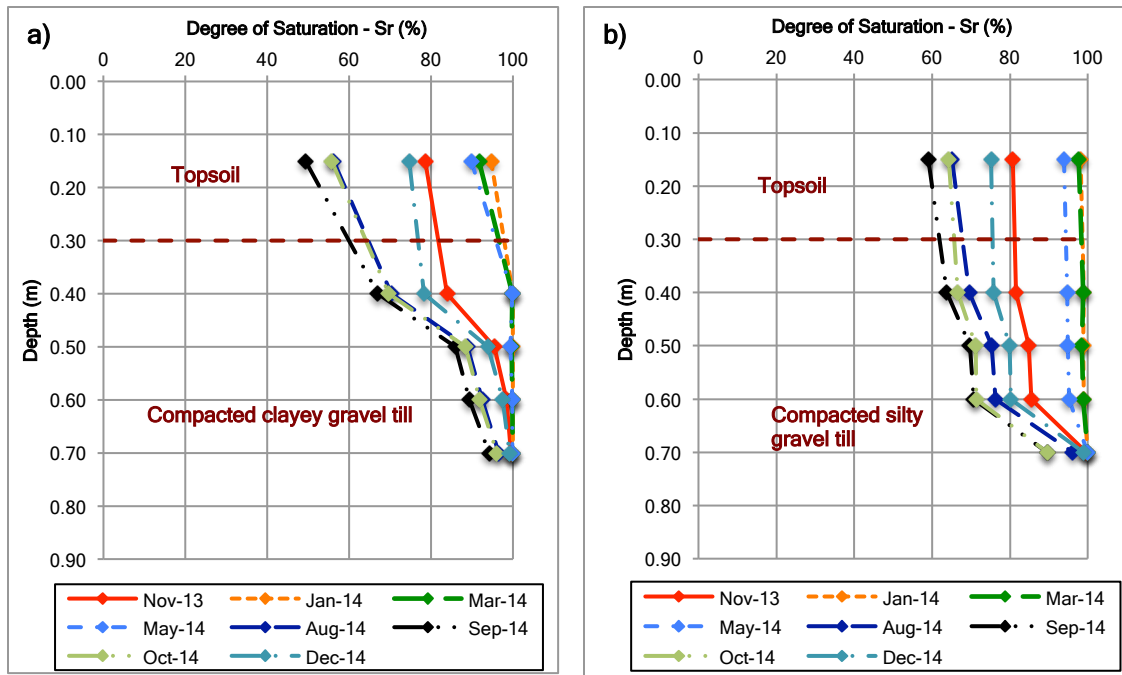


Figure 5-20: Predicted degree of saturation profiles from SoilCover models - a) Lysimeter #1, and b) lysimeter #5

The degree of saturation profiles showed in Figure 4-34 were calculated from the volumetric water content (θ_v) measured by the CS616 probes, and assuming both an average dry density and a constant specific gravity. The latter assumptions limited the accuracy of the calculation, but provided a realistic approach to the field conditions. On the other hand, profiles in Figure 5-20 are the result of a predictive numerical model. Although dry density and specific gravity used in the model followed the same criteria as for the computed profiles, the reliability of the predictions may be limited by other assumptions (e.g. a constant k_{SAT} , a simplified SWCC, material homogeneity).

Figure 5-20 a) shows the predicted degree of saturation profile for lysimeter #1. The similarities with Figure 4-34 a) are evident. The predicted profile showed S_r was higher than 80% below 0.50 m of depth during all the evaluated period, while S_r was as low as 75% in the computed profile at the end of the dry season. However, the difference is not very significant given the deemed assumptions. Therefore, a zone of the compacted clayey gravel till in lysimeter #1 seems to be able to sustain S_r greater than 80% during the whole hydrological year. The predicted profiles for lysimeter #5 (Figure 5-20 b)) did not match the calculated ones during the wet season (mid September to May), but they showed how S_r was reduced once the dry season started. There was a 20% reduction in S_r between 0.40 m and 0.60 m of depth at the

onset of the dry season, and a decrease of the same magnitude was observed in the computed profiles for the same range of depth. Only the bottom section of the compacted silty barrier (0.70 m) experienced a lower reduction in S_r (10%). The oxygen level measurements for lysimeter #5 at the onset of the dry season were as high as the oxygen level in fresh air (20.9% in volume). This quick recharge is consistent with the loss of saturation, as a drop of 20% in S_r can lead to an increase of at least one order of magnitude in the effective coefficient of diffusion (D_e) (Aubertin, 2005 as cited in INAP, 2014). Although the predicted profiles did not quantitatively match the computed ones, they provide enough evidences of the drastic lose of saturation experienced by the cover in lysimeter #5.

Figure 5-21 and Figure 5-22 present the oxygen level (% in volume) predictions for lysimeters #1 and #5, respectively. As with the degree of saturation predicted profiles, both figures show the results obtained from Precipitation 1 due to the minimal differences with the results from Precipitation 2. For effects of comparison with the field measurements, the period covered by the predictions is from November 21, 2013 to December 30, 2014. Predicted values are shown every five days, as this was the output frequency selected for the numerical models in SoilCover.

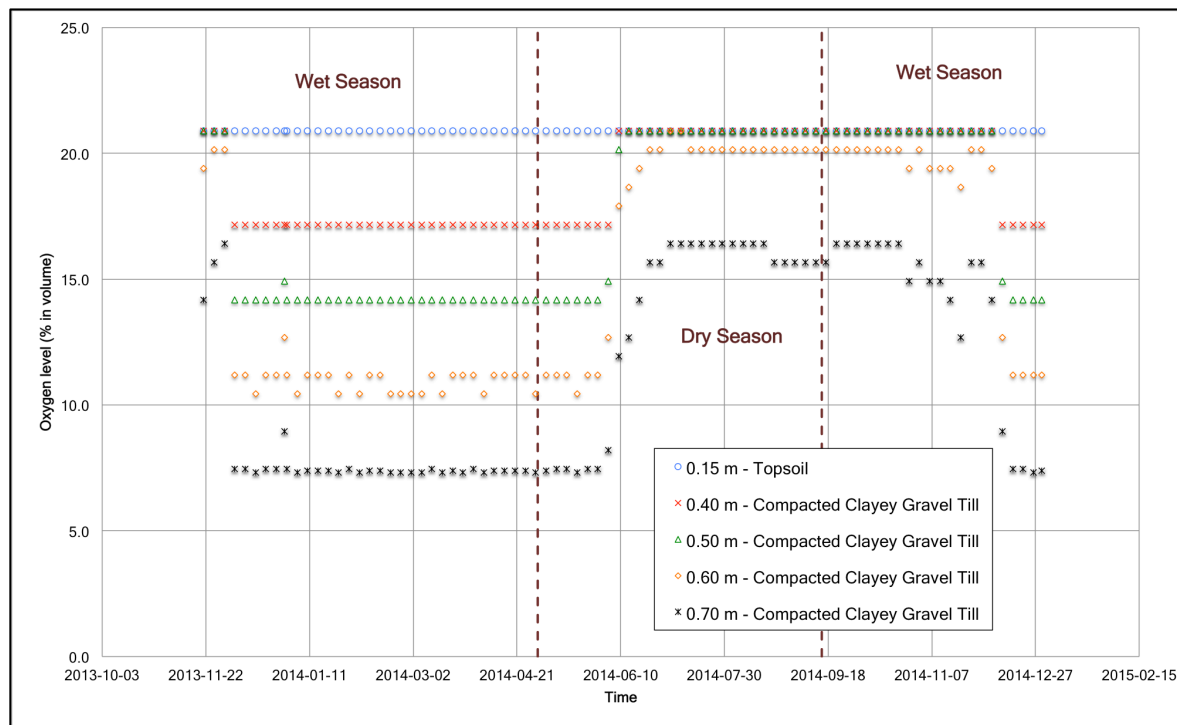


Figure 5-21: Predicted oxygen levels for lysimeter #1 (November 21, 2013 to December 30, 2014)

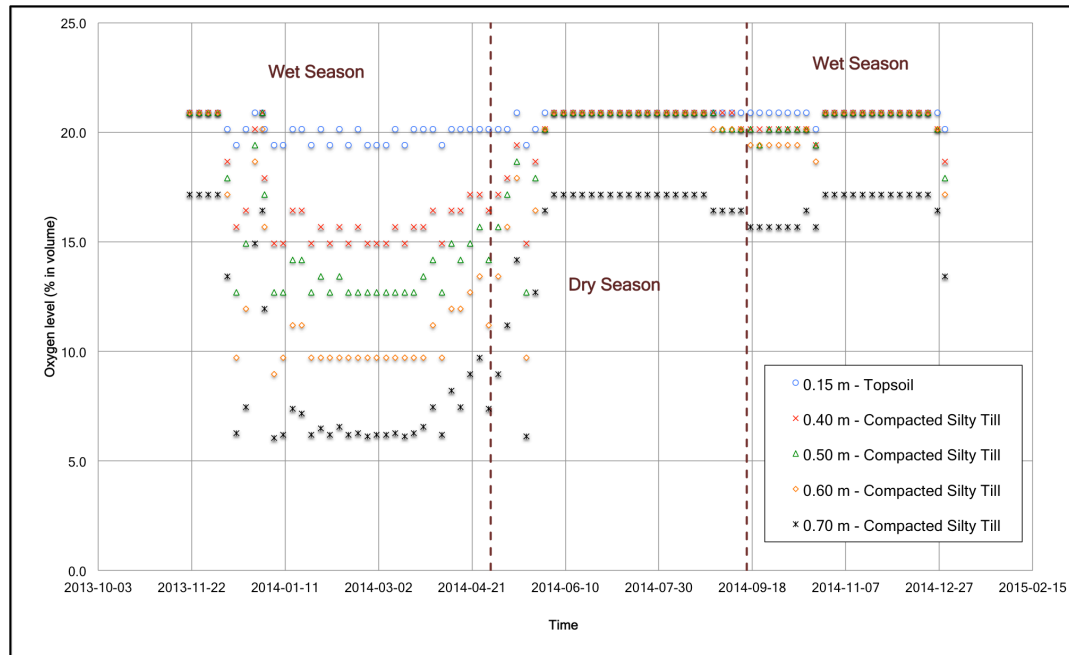


Figure 5-22: Predicted oxygen levels for lysimeter #5 (November 21, 2013 to December 30, 2014)

The previous figures show the predicted changes of oxygen level in the cover materials, not in waste rock. Furthermore, these results are limited by the assumptions made in the numerical model. In order to make oxygen flow through the cover during the simulation period, the oxygen level at the node beneath the contact between the barrier and waste rock was set as zero. Field measurements recorded during the onset of the 2014 dry season showed that oxygen levels in the underlying waste rock can be as high as the ones found in fresh air. Hence, the oxygen gradient is not constant in time as it was assumed for the numerical model. In addition, not only does oxygen diffusion depend on the existing gradient, but also in the effective coefficient of diffusion (D_e), which increases during the dry periods.

Based on the previous information, the results shown in Figure 5-21 for lysimeter #1 can only be considered as a good reference during the wet season. The oxygen level at the bottom of the barrier layer matched the average oxygen level recorded for lysimeter #1 during the onset of the wet season (5% in November 2013). In the case of lysimeter #5 (Figure 5-22), the oxygen levels for the top and mid sections of the barrier layer might be underestimated. As the predicted saturation profiles showed greater S_r than the calculated ones, D_e for the model is reduced, and lower oxygen diffusion is expected at the top and mid sections. Only the bottom section (0.70 m) of the cover in lysimeter #5 had S_r greater than 80% in

both computed and predicted S_r profiles. Therefore, the oxygen levels at this depth would be similar to the field values, as the oxygen gradient and D_e in the model would be close to the values of these parameters actually occurring in the field. The predicted oxygen level at 0.70 m in lysimeter #5 (6%) was close the average value measured in the field experiment in November 2013 (4%).

Oxygen levels predicted for the dry season may be overestimated due to the presence of a high oxygen gradient that might not be occurring in the field. Furthermore, D_e was underestimated in the model, as predicted S_r values were greater than the ones calculated from θ_v measurements. However, the predicted oxygen levels at the onset of the dry season provide an idea of how fast oxygen can be replenished. The oxygen level increased more rapidly in lysimeter #5 than in lysimeter #1, which is consistent with the field observations after considering the difference in S_r between both covers. If S_r in lysimeter #5 was actually as low as the values computed from θ_v records, D_e would be even higher and it would increase the oxygen flow rate and would lead to greater oxygen concentrations than the predicted values from the numerical model. The oxygen levels measured in lysimeter #5 in June 2014, which were on average equal to 20.9%, and thus support the previous statement.

5.5 Water Balance

The reliability of the SoilCover predictions depends on the cumulated water balance for all the time steps in a single run (Unsaturated Soils Group, 2000). The principal fluxes involved in a water balance (vapor, liquid water, and heat) are computed following Fick's, Darcy's, and Fourier's Laws, and the atmospheric coupling is achieved by using the modified Penman equation proposed by Wilson (1990, as cited in Wilson et al., 1994). The water balance is aimed to guarantee the equilibrium between fluxes entering, accumulating, and leaving the system during the simulation period. On the other hand, a water balance can be used to estimate one of the fluxes if the other ones are known. Therefore, actual evapotranspiration in lysimeters #1 and #5 was calculated after the following equation (Barbour et al., 2001 as cited in Strunk et al, 2009),

$$AET = PPT - R - DP - I - \Delta S$$

where AET is actual evapotranspiration, PPT is precipitation, R is runoff, DP is deep percolation, I accounts for interflow, and ΔS represents the change in water storage. The measurements recorded by

the different instruments installed in lysimeters #1 and #5 provided enough information to estimate actual evapotranspiration (*AET*) based on the other components of the water balance equation. Precipitation came from the direct measurements at Punto B and from FP estimations (Pedretti and Beckie, 2015). The tipping buckets installed as part of the field-scale experiment measured both runoff and net percolation. As the cover and underlying waste rock are analyzed as a single system, the net percolation volumes recorded by the tipping buckets can be considered as deep percolation. Runoff was not observed at any of the different lysimeters, and during any of the four years evaluated. Storage was calculated from the volumetric water content measured by the CS616 probes at different depths, and assuming a section of influence for each reading (Figure 5-1) (Strunk et al., 2009).

Figure 5-23 and Figure 5-24 present cumulative actual evapotranspiration (*AET*) for lysimeters #1 and #5. Both *AET* computed from the water balance equation and field measurements, and predicted from the numerical model in SoilCover are shown in both figures. Cumulative *AET* is presented only for year 2014, as CS616 probes were installed at the end of 2013.

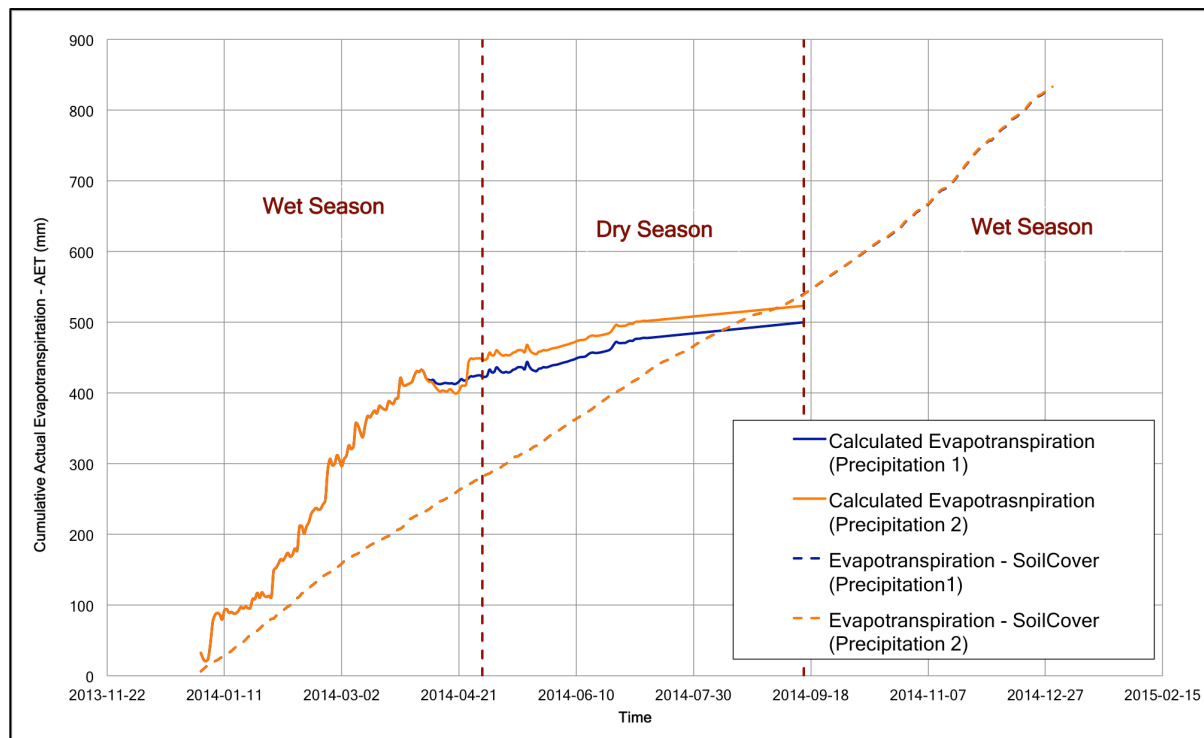


Figure 5-23: Calculated and predicted cumulative actual evapotranspiration (AET) - Lysimeter# #1

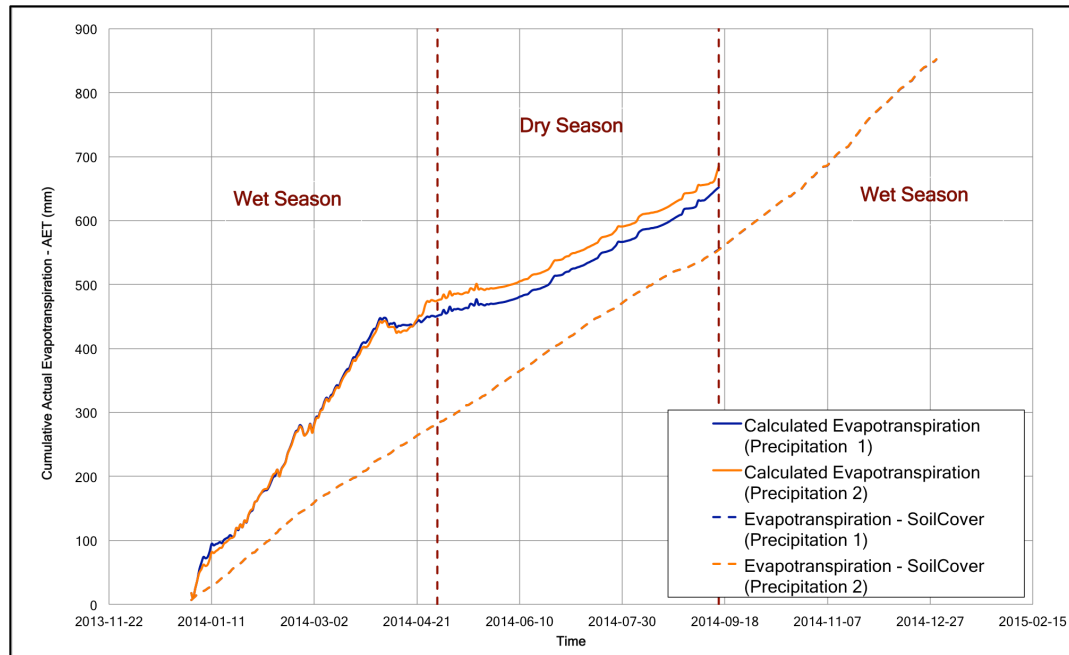


Figure 5-24: Calculated and predicted cumulative actual evapotranspiration (AET) - Lysimeter# #5

The water balance assessment was limited by the availability of net percolation records. Both lysimeters experienced data recording problems due to the corrosion of the magnetic reed switched. It is observed from both charts that computed *AET* volumes were greater than SoilCover predicted ones. The SoilCover predicted *AET* curves were the same independently of the set of rainfall used in the model (Precipitation 1 and 2). The computed cumulative *AET* volume during the wet season was almost the same for both lysimeters (approximately 450 mm), but *AET* rates were different during the dry season. The *AET* rate for lysimeter #1 was lower than the one for lysimeter #5, basically due to the high k_{SAT} and the SWCC shape (steep slope in the transition zone) of the compacted clayey gravel till. Although the compacted silty till in lysimeter #5 started drying quickly (low AEV) at the beginning of the dry season, a lower permeability and the characteristics of the SWCC made more water available to evapotranspire. By the end of the evaluated period (September 15, 2014), calculated *AET* in lysimeter #5 (Figure 5-24) was 15% (100 mm) greater than the *AET* calculated for lysimeter #1 (Figure 5-23).

The water balance results suggest that the SoilCover numerical models underestimate *AET*, and it is unable to replicate the seasonal variations in *AET*; however, the predictions are satisfactory enough considering the assumptions made for both calculations and predictions. The numerical model assumes

homogeneity in geotechnical, hydrological, and unsaturated properties for the cover materials. Although the conducted field investigation was intended to account for this variability in certain levels, limited testing constrained the accuracy of the field results. Furthermore, meteorological data for the field experiment zone was only available from April 30, 2014 onwards. Precipitation records from January to April 2014 were estimated using the FP method proposed by Pedretti and Beckie (2015). Other parameters (wind, speed, net radiation, relative humidity, and air temperature) came from the Yanacancha weather station. Although included in *AET* estimation, the change in water storage (ΔS) is negligible on a daily basis (less than 1% of the cumulative precipitation during the evaluated period); however, the volumetric water content readings showed both cover systems (topsoil+barrier layer) would have the same water storage capacity (approximately 300 mm). Furthermore, both covers released 50 mm (lysimeter #1) and 100 mm (lysimeter #5) during the dry season, and *AET* is the releasing mechanism as net percolation is small to null during the dry season.

5.6 Field results and Numerical Modeling Predictions Comparison

Figures 5-25 to 5-27 present both runoff and net percolation for lysimeters #1, #5, and #4. Measurements from the field experiment were compared to the results of the predictive numerical models for the non-calibrated and adjusted base cases and sensitivity analyses. Runoff and percolation were expressed as percentages of the cumulative precipitation (Precipitation 1 and 2) received by the lysimeters between February/March 2011 (lysimeter #1/lysimeter #4 and #5) and December 2014.

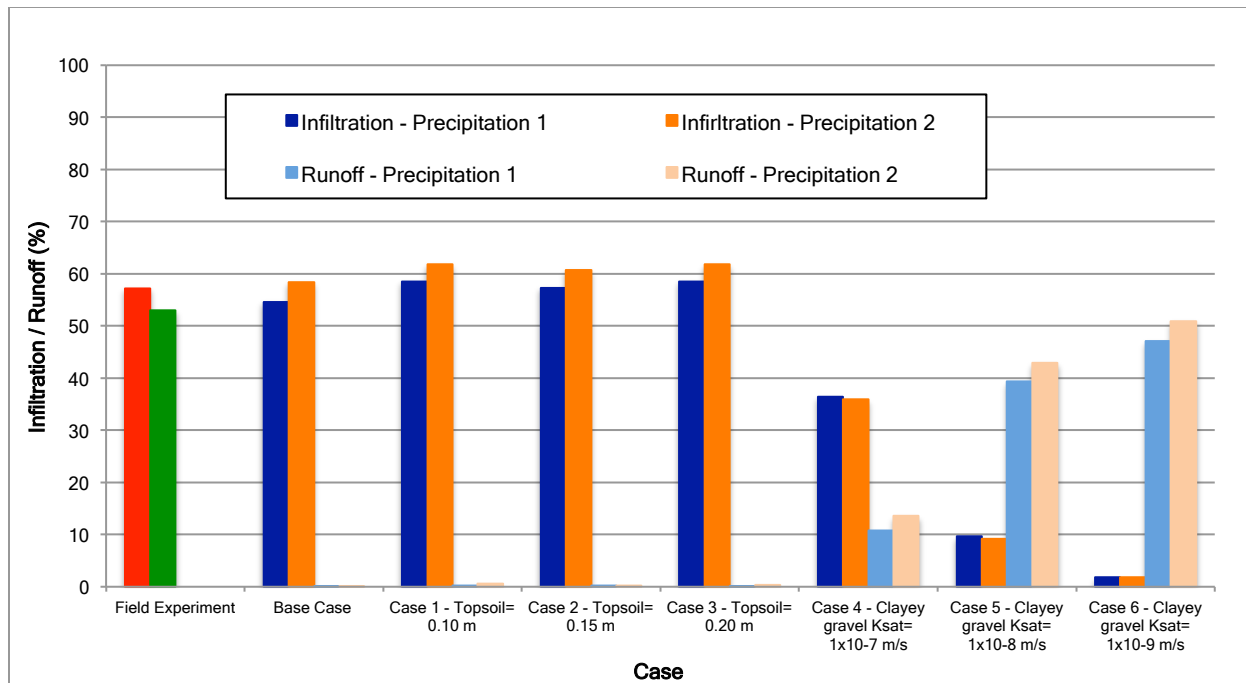


Figure 5-25: Runoff and net infiltration field measurements and predictions comparison - Lysimeter #1

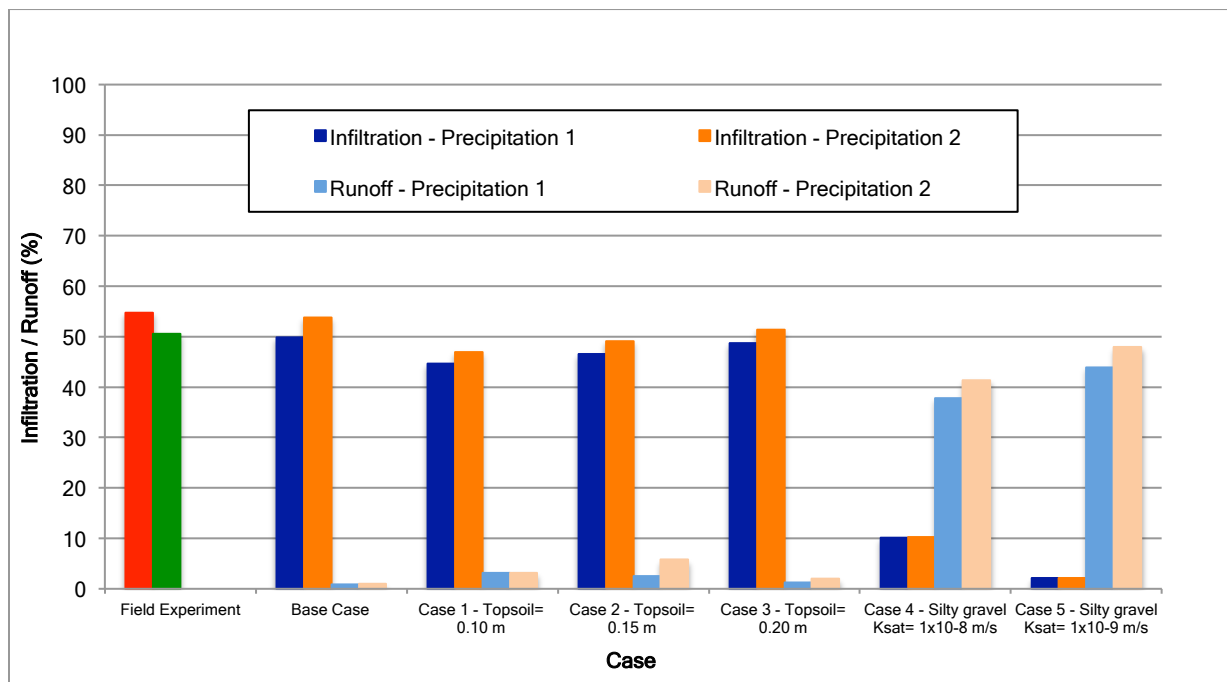


Figure 5-26: Runoff and net infiltration field measurements and predictions comparison - Lysimeter #5

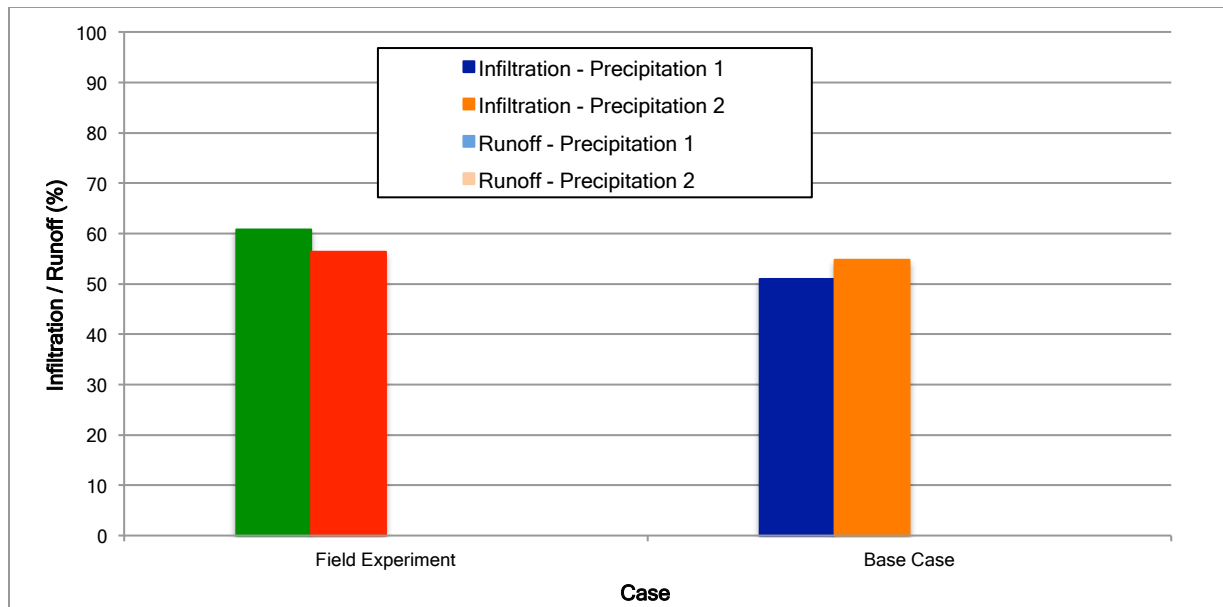


Figure 5-27: Runoff and net infiltration field measurements and predictions comparison - Lysimeter #4

The base case results for all the covers were affected by the type of precipitation set of data used, and by the use of meteorological data from Yanacancha station for three of the four evaluated years. However, the purpose of running every base case considering two different sets of precipitation was to define a range of possible outcomes. In general, net percolation predictions obtained from Precipitation 1 were lower than the values measured in the field experiment; on the other hand, predicted results from Precipitation 2 were higher or close the field experiment outcomes. The water balance (Section 5.5) showed that *AET* seems to be underestimated by the numerical model, and that lysimeters #1 and #5 had different *AET* rates during the dry season. The lower *AET* rate for lysimeter #1 during the dry season led to a match between predicted and computed values by the end of the dry season. As the change in the *AET* rate for lysimeter #5 was minimal during the dry season, the trend can be considered as constant and similar to one obtained from the numerical model.

Sensitivity analysis for both lysimeters showed the limited impact of reducing topsoil thickness on limiting net percolation. The reduction of net percolation and the generation of runoff in lysimeter #1 were negligible for all the different cases analyzed, while the results for lysimeter #5 did not represent an advantage considering how difficult it would be to construct a thinner topsoil layer. On the other hand, reducing the permeability of the barrier layer could decrease the net percolation in up to 55% for

lysimeter #1, and up to 45% for lysimeter #5. Therefore, the performance of the cover systems might be improved by reducing the saturated hydraulic conductivity (k_{SAT}) of the barrier layer. The improvement in performance would be reflected in a reduction of net percolation, and in the generation of runoff. The magnitude of the improvement would depend on how much k_{SAT} could be reduced, and the reduction is limited by the physical characteristics of the cover materials, and by the available construction equipment.

5.7 Potential Cover Alternatives

The result of the base case and sensitivity analyses for lysimeters #1 and #5 showed that net percolation could be limited if the permeability of the barrier layer is reduced. As described in Chapter 2, placing and compacting the barrier material on the dry side of the compaction curve can increase the permeability by two orders of magnitude (Watabe et al., 2009). Urrutia (2012) reported that the construction was impacted by the availability of materials and equipment, and as a result the materials were placed compacted on the dry side. Furthermore, Urrutia (2012) concluded that lowering the k_{SAT} of the barrier layer in one order of magnitude would reduce net percolation by 75%. Although this conclusion was limited to lysimeter #1 and was drawn by maintaining some laboratory properties in the model, the effect of lowering permeability in one order of magnitude differs depending on the material.

The sensitivity analyses in this thesis showed that percolation in lysimeter #1 could be reduced by 35% by lowering permeability in one order of magnitude (Figure 5-25). The net percolation in lysimeter #5 would be lowered by 80% if permeability were reduced in the same way (Figure 5-26). Although not part of the scope of this thesis, reducing permeability by one order of magnitude might be achievable with good quality control during the construction process. Therefore, the cover system in lysimeter #5 would represent the best alternative from the different options evaluated in terms of limiting percolation; however, the effects of compacting at moisture contents greater than the optimum would have to be evaluated since the silty fraction of the barrier material is sensitive to changes in water content. Furthermore, the oxygen levels in the underlying waste rock would not be reduced given the current unsaturated properties of the barrier layer. On the other hand, assuming the unsaturated properties measured on site could be maintained, and based on the field investigation and numerical prediction results, the cover in lysimeter #1 would represent the best option in terms of limiting oxygen flow.

Although reducing the thickness of the topsoil layer in lysimeter #1 proved to have no effect on reducing percolation or generating runoff (Figure 5-25), a combination of a barrier layer with lower permeability and reduced topsoil thickness might be able to improve the cover performance. A simulation between 2011 and 2014 for lysimeter #1 was run considering a k_{SAT} of 10^{-7} m/s for the compacted clayey gravel till, and a thickness of 0.20 m for the topsoil layer. The rest of the material properties were the same as the ones shown in Table 5-1. Both topsoil and compacted clayey gravel till maintained the soil water characteristic curves showed in Figure 4-43 and Figure 4-44. The initial conditions used for the base case were also used for this alternative run. As in all the previous simulations, this modified cover was analyzed considering two sets of precipitation records (Precipitation 1 and Precipitation 2).

Figure 5-28 and Figure 5-29 present the cumulative net percolation, runoff, actual evaporation, actual transpiration, and actual evapotranspiration for the modified cover system in lysimeter #1.

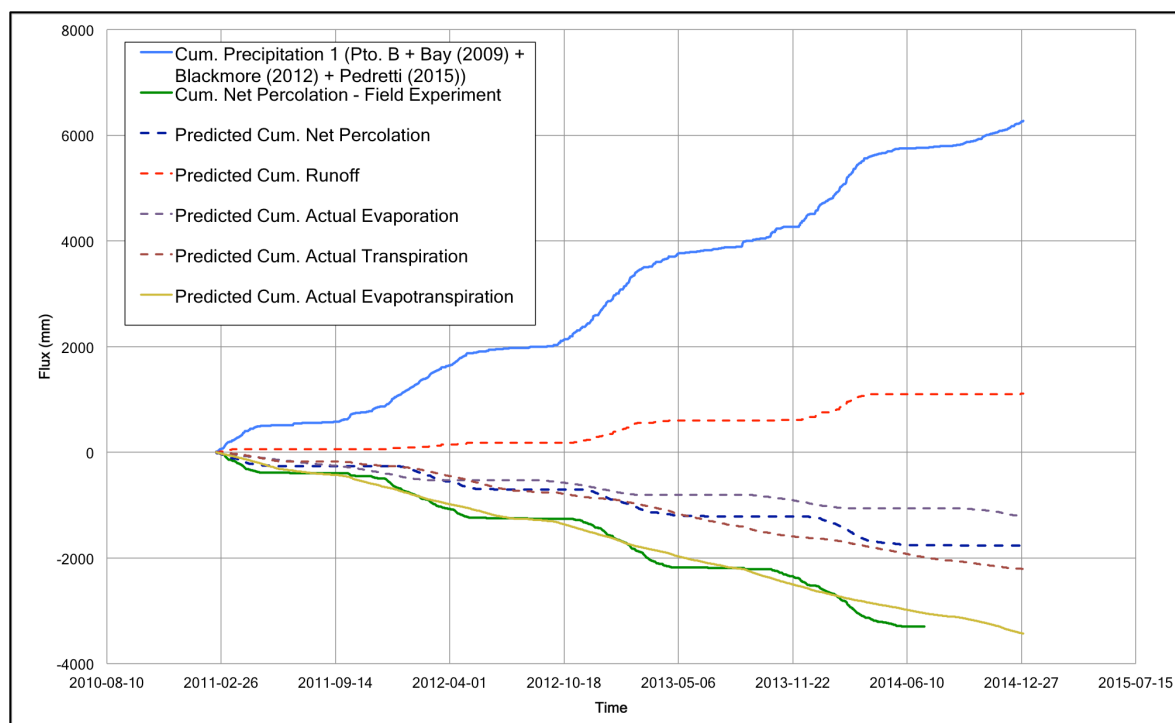


Figure 5-28: Cumulative water balance for modified cover system in lysimeter #1 - Precipitation 1

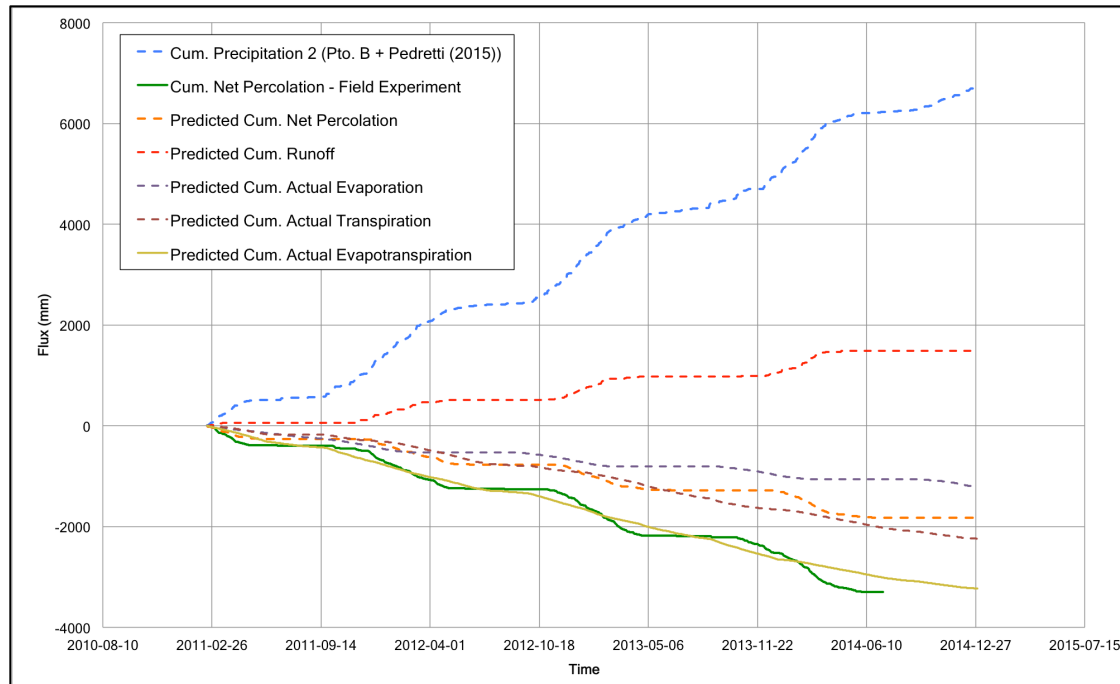


Figure 5-29: Cumulative water balance for modified cover system in lysimeter #1 - Precipitation 2

The modified cover reduced net percolation from 55% and 58% (base case) to 31% and 29% of the cumulative Precipitation 1 and 2 between 2011 and 2014. The reduced percolation was between 5% and 7% smaller than the values obtained from Case 4 in the sensitivity analysis, which considered a k_{SAT} of 10^{-7} m/s for the barrier layer and a topsoil layer 0.30 m thick. Although the net percolation was only slightly decreased, the reduction in k_{SAT} and a lower storage capacity of the topsoil layer led to greater runoff volumes. Runoff for the modified cover was 19% and 24% of cumulative Precipitation 1 and 2, respectively, but these percentages were approximately 50% higher than the ones obtained in Case 4. The cumulative water balance showed also that cumulative evapotranspiration for the modified cover was close to the evapotranspiration predicted from the base case model. The unsaturated properties (SWCC) of the cover materials were assumed as constant for the modified cover, and they control evapotranspiration along with the meteorological conditions. These conditions might not be able to be replicated on the field, as the compaction degree (porosity, dry density) and the SWCC (AEV, desaturation in the transition zone) will change depending on both water content and energy during compaction (Vanapalli et al., 1999; Benson and Daniel, 1990; Watabe et al., 2000; Prapaharan et

al., 1991). If compacted on the wet side and at the right degree of compaction, the properties considered for the alternative model might be improved, as a lower k_{SAT} is related to a lower porosity, and materials placed on the wet side tend to have a greater resistance to desaturation.

Figure 5-30 presents the oxygen level (% in volume) predictions for the modified cover in lysimeter #1. The numerical model considered the Precipitation 1 set of data.

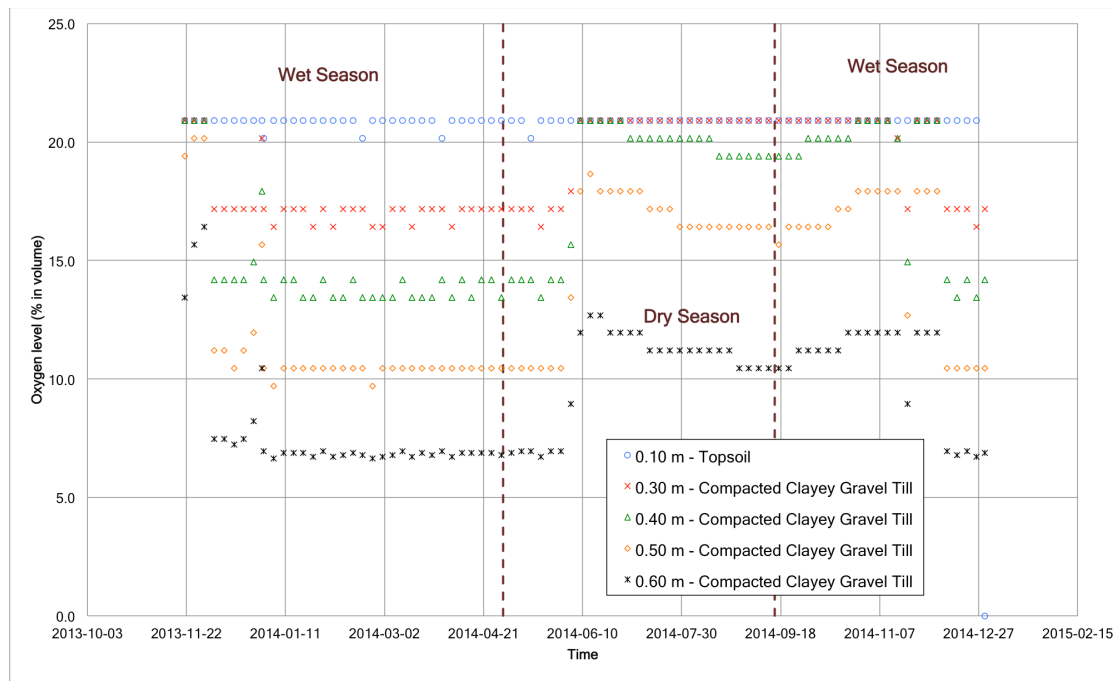


Figure 5-30: Predicted oxygen levels for the modified alternative cover in lysimeter #1 (November 21, 2013 to December 30, 2014)

Although the SWCC and porosity of the cover materials were maintained for the modified cover numerical model, the reduction in k_{SAT} had an immediate impact on oxygen levels in both the cover and underlying waste rock. The oxygen levels at the bottom of the barrier layer were close to the ones measured on the field, and predicted by the base case model during the wet season. The barrier performance during the dry season was improved as the computed oxygen levels were close to 10%. Given the assumptions made for the numerical model, the oxygen levels shown in Figure 5-30 might be considered as a conservative estimation. Reported oxygen levels are inside the cover, as the zone immediately underneath the contact point with the cover had a fixed oxygen level of 0 to induce an oxygen gradient. Furthermore, the change in hydraulic properties is accompanied by changes in both density and

unsaturated properties. Upon consideration of all the properties, it is concluded that the SWCC is very significant because it controls the desaturation and unsaturated water flux developed during the dry season; however, in general, k_{SAT} has the most significant impact in the covers' performance as it regulates the percolation volumes. As for the predictions from the other cases, the accuracy of the results is constrained by the intrinsic heterogeneity of the cover materials and by the changes induced during the construction process.

CHAPTER 6: SUMMARY AND CONCLUSIONS

6.1 Summary

Engineered soil covers are widely used as a reliable method for the closure and reclamation of mine waste management facilities around the world. The operational principle of soil covers consists on limiting water percolation and oxygen diffusion, and these characteristics make them a valuable tool for acid rock drainage (ARD) prevention and mitigation. As described in the literature review, the chosen cover materials, the slope of the cover, and the construction process can compromise the performance of a cover system. The purpose of this thesis was to evaluate the different factors affecting the performance of four different soil cover systems at the Antamina mine in Peru.

The soil cover experiment at Antamina consists of four cover systems installed over waste rock material placed in five lysimeters. These covers were designed to limit percolation by combining a store and release layer and a barrier layer. After one year of monitoring, measured percolation levels varied between 50% and 70% of the total precipitation received by the lysimeters (Urrutia, 2012). One of the objectives of this research was to evaluate the change in materials properties that might have compromised the hydraulic performance of the different covers. This goal was accomplished by conducting a field investigation to measure the in-situ geotechnical, hydrological, and unsaturated properties of the covers materials. Furthermore, additional instrumentation was installed to monitor the change of the unsaturated soil properties over time. The results of the field investigation and the instrumentation readings were used to update a predictive numerical model in SoilCover (Unsaturated Soils Group, 2000). This model was created to evaluate potential alternatives to improve the covers' performance.

The performance in terms of net percolation and runoff for the four cover systems is summarized in Table 6-1. Average oxygen levels (% in volume) in the underlying waste rock are also included as a reference of the effectiveness of the covers as oxygen barrier.

Table 6-1: Summary of Cover Systems Performance (2011 - 2014)

Lysimeter	Cover	Net percolation 2011-2014 (%)	Runoff 2011-2014 (%)	Average Oxygen Level - Nov 2013 (% in volume)	Average Oxygen Level - Jul 2014 (% in volume)
1	Compacted clayey gravel till+ topsoil	51 - 56	0	5.1	10 - 17
2	Non-compacted clayey gravel till + topsoil	20 - 21	0	17.8	20.9
3	No cover (Control)	55 - 65	0	Not measured	20.9
4	Topsoil	52 - 57	0	20	20.9
5	Compacted silty gravel till + topsoil	46 - 50	0	3.5	20.9

The control lysimeter (lysimeter #3, with no cover) reported the highest net percolation, with up to 65% of the total precipitation recorded as net percolation between April 2011 and December 2012. From the covered lysimeters, the cover installed on lysimeter #4 (topsoil) was the least effective in terms of limiting percolation, with up to 57% of the total precipitation reported as percolation between April 2011 and December 2014. On the other hand, the cover in lysimeter #5 (compacted silty gravel till+ topsoil) was the most effective arrangement with up to 50% of the total precipitation registered as percolation for the same period of time. The cover system on lysimeter #1 was classified as an intermediate case in terms of limiting percolation, with up to 56% of the total precipitation accounted as percolation. The performance of lysimeter #2 was not reliable due to the problems experienced by the tipping buckets measuring percolation volumes. As shown in Table 6-1, no runoff was registered at any of the five lysimeters. Furthermore, nor runoff or ponding was observed during the 2013 field investigation campaign.

The high percolation levels observed during the early stages of the field experiment, and maintained during the four years period of assessment, suggested the hydraulic properties of the cover might have been compromised. For this reason a field investigation program was conducted in 2013 in order to measure saturated hydraulic conductivity (k_{SAT}), dry density, soil matric suction, and water content in all the installed cover systems. Dry density tests showed the compacted barrier materials were placed at dry densities below those given in the construction specifications. The characteristics of the fine fraction of the barrier layer materials and the presence of gravel (30% on average), might have created micro and macro

pore structures reducing the density and increasing the permeability of the materials. No cracking or desiccation was observed during the field investigation, but the observations were constrained by the limited testing conducted that was intended to preserve the integrity of the cover. Furthermore, these materials were also placed and compacted during construction at moisture contents drier than optimum. Both the materials characteristics and the construction conditions impacted the saturated hydraulic conductivity of the barrier materials. In-situ measurements showed that the k_{SAT} of the clayey gravel till increased in up to four orders of magnitude. The difference between the field and laboratory values might have been caused by the coarse fraction of the barrier material, by the possible presence of macro pores and by the construction conditions. Samples used for laboratory testing did not include the coarse fraction, unlike the materials used for the barriers in lysimeters #1, #2, and #5. The difference was critical for lysimeters #1 and #2, as the barrier material had on average 30% of gravel. The barrier material in lysimeter #5 was the least affected by the presence of gravel, as grain size distribution tests showed the materials had up 70% of fine fraction in some cases.

The materials characteristics and the compaction conditions also modified the unsaturated soil properties. In-situ soil matric suction and moisture content measurements suggested the storage capacity, and soil water characteristic curves (SWCC) of both topsoil and barrier layer materials were also altered. These initial observations were confirmed by the instrumentation readings recorded between November 2013 and December 2014. The changes might have been caused by the presence of gravel (steep transition in the SWCC for clayey gravel till), by the placing of materials at moisture contents drier than the optimum one (lower air entry value for silty till), and by the energy of compaction (change in storage for all the materials due to the change in soil structure). In-situ matric suction and volumetric water content readings in lysimeters #1 and #5 defined five SWCCs at different depths. The in-situ SWCCs were significantly different from the ones defined by laboratory testing, and the difference affected how water content changed over time. The cover in lysimeter #5 behaved uniformly, and lost water during short dry periods, and hence it dried rapidly as soon the dry season started. The calculated degree of saturation (S_r) profiles showed that the cover in lysimeter #5 reduced its S_r in up to 35% during the dry season. A loss of water of that magnitude was able to increase the effective coefficient of diffusion in up to two orders of magnitude, enhancing the oxygen diffusive recharge. The oxygen measurements in the underlying waste rock

showed fresh air levels (20% in volume) during the dry season. Even though the barrier layer in lysimeter #1 had a greater k_{SAT} , the cover was able to maintain a high S_r for a longer period, and water was lost at a lower rate. The calculated degree of saturation profiles for the compacted clayey gravel till showed that half of the barrier layer was able to maintain S_r higher than 80%. The oxygen level measurements taken at the high of the dry season showed a slow diffusive recharge. The water content monitoring and oxygen levels measured suggested the cover in lysimeter #1 has the potential to limit or slow down oxygen diffusion from the atmosphere.

The results of the field investigation were used to improve the existing numerical model for lysimeter #1, and to create new models for lysimeters #4 and #5. The k_{SAT} and SWCCs measured or defined at different depths were used to account for the existing degree of heterogeneity in some extent. The change in soil properties proved to be very effective, as the percolation and runoff volumes predicted by the numerical model matched the field measurements without calibration. The non-calibrated model for lysimeter #1 and adjusted model for lysimeter #5 were used to conduct sensitivity analyses aimed to improve the performance of the cover systems. These sensitivity analyses evaluated the effect of changing the thickness of the topsoil layer, and of reducing the saturated hydraulic conductivity of the barrier layers. Changing the thickness of the topsoil layer proved to have no effect in reducing percolation or generating runoff in any of the cases, not only due to the material high permeability, but also due to the low rainfall intensities occurring in the zone. On the other hand, k_{SAT} is the factor controlling percolation. Reducing k_{SAT} by one order of magnitude would decrease percolation in 20% and 40% for lysimeters #1 and #5, respectively. The predictions from the numerical models also evidenced the potential the cover in lysimeter #1 has to limit oxygen diffusion. Although the model for lysimeter #5 was unable to replicate the S_r computed from volumetric water content measurements, it predicted the same loss of saturation (35%) calculated from field measurements. Such a reduction in S_r reduced the effectiveness of the cover as an oxygen barrier, as that loss of S_r increased the oxygen flow rate towards the underlying waste rock.

The reliability of the numerical model results was evaluated by comparing predicted actual evapotranspiration (AET) volumes with the ones from the measured field water balances. Predicted and computed on the basis of water balance AET accounted for approximately 50% of the total precipitation received by the cover, but the predicted values were smaller than the computed ones. On average,

calculated AET followed the same trend as the predicted values for lysimeter #1, with a change in the AET rate during the dry season compensating the higher volumes computed in the wet one. The seasonal change in the AET rate was also observed in lysimeter #5, but a greater AET rate in the dry season led to higher values at the end of the assessment period.

6.2 Conclusions

The following conclusions are drawn after four years of monitoring, two field investigation campaigns, and the consideration of both the instrumentation measurements and the predictions of numerical models in SoilCover:

- The soil covers installed in lysimeters #4 (topsoil) and #5 (topsoil and compacted silty till) represent the least and most effective alternatives in terms of limiting water percolation.
- Runoff was not generated or observed during any of the four years of the field experiment. Under the current conditions of the covers, rainfall intensities in the experiment zone are not high enough to overwhelm the storage capacity of the surficial layer (topsoil). Furthermore, the small contrasts in saturated hydraulic conductivity existing between the barrier layer and store and release layer does not contribute to runoff generation.
- The numerical model predictions showed that vegetation deals with approximately 30% of the total precipitation received in the form of actual transpiration (AT). Although AT contribution was limited during the first stage of the field experiment, it became a key element in the water balance once vegetation was fully developed in the four covers.
- Net percolation in the different soil covers is reduced by actual evapotranspiration (AET) in approximately 50%. Over half of the actual evapotranspiration volume predicted from the numerical models is handled as AT (30%), while the difference (20%) is accounted for as actual evaporation (AE).
- Compaction does not necessarily represent an advantage in terms of reducing saturated hydraulic conductivity (k_{SAT}) of the barrier layer material. The resultant saturated hydraulic conductivity will depend on the material characteristics, as well as the moisture content and energy applied during placement and construction, respectively. Limitations imposed by the

material fraction used for laboratory testing led to lower hydraulic conductivity values compared to those measured in the field. Furthermore, the characteristics of the glacial tills used as barrier layer materials might have created micro and macro pore structures that produced a more permeable material. The placing and compacting the glacial tills at moisture contents drier than the optimum also increased the permeability of the barriers. In summary the in-situ saturated hydraulic conductivity of the barrier layer in lysimeters #1 and #2 is two to four and one orders of magnitude greater than the laboratory values, respectively.

- In-situ water retention properties (SWCC) of the covers' materials differed from the ones determined by laboratory testing. The presence of coarser particles not included in laboratory testing changed the storage capacity and the behavior of the material in the field. Compaction energy and moisture at placement during construction also modified the barrier material structure, reducing storage capacity and making materials easy to desaturate.
- Although the cover systems were not designed to work as an oxygen diffusion barrier, the cover in lysimeter #1 (topsoil and compacted clayey gravel till) seems to be limiting oxygen diffusive flow from the atmosphere during the dry season. Field measurements showed 5% and 17% oxygen levels by volume at the onset and high of the wet and dry season, respectively. Nevertheless, the effects of both oxygen consumption and diffusive recharge in the oxidation and metal leaching of the underlying waste rock have not been evaluated yet.
- The updated numerical models for lysimeters #1, #4, and #5 produced reliable runoff and net percolation predictions. Predicted runoff and percolation volumes from the numerical models based on the updated in-situ properties showed good agreement with the field measurements. Although most of the meteorological data came from Yanacancha station, a comparison with the information collected at Punto B during 2014 showed minimal differences between almost all the parameters. The only exception was wind, as average values recorded in Yanacancha were 5 km/h greater than the ones measured in Punto B.
- The sensitivity analyses based in the non-calibrated and adjusted numerical models in SoilCover indicated that changing the thickness of the topsoil layer would not have any impact on either limiting percolation or generating runoff. Thinner topsoil layers would reduce net percolation in up

to 5%, but this does not represent a significant improvement considering the challenges related to the construction process.

- The performance in terms of limiting percolation is controlled by the saturated hydraulic conductivity of the barrier layer. The results of the sensitivity analyses denoted that a reduction of one order of magnitude in the saturated hydraulic conductivity would reduce net percolation in 20% and 40% for lysimeters #1 and #5, respectively.

Although the cover systems installed in lysimeters #1 and #5 had their hydraulic performance reduced, both of them have the potential to limit significantly water percolation. As the sensitivity analyses results showed, net percolation can be decreased in up to 40% just by reducing the saturated hydraulic conductivity of the barrier layer in one order of magnitude. It is important to note that the sensitivity analyses assumed the saturated hydraulic conductivity (k_{SAT}) can change without affecting other soil properties. A lower k_{SAT} might be associated with a higher dry density, and hence with a lower porosity; however, these changes are driven by characteristics of the materials. The clayey fraction of the barrier in lysimeter #1 is more susceptible to cracking and desiccation, and the low plasticity of this fraction might also limit the reduction of k_{SAT} (Benson & Trast, 1995). In the case of the silty till barrier layer in lysimeter #5, this material is sensitive to the changes in moisture content during compaction. As a result, placing a material at moisture contents higher or lower than the optimum would also change the resultant density, pore distribution and hence hydraulic properties..

As discussed in Chapter 2, placing and compacting the materials at moisture contents wetter than the optimum might lead to the desired reduction in k_{SAT} ; however, this possibility needs to be verified by conducting compaction trials using the barrier layer materials. Optimum quality control during construction is essential to obtaining a satisfactory level of performance and it is important to acknowledge that the improvement is controlled by the characteristics and heterogeneity of the barrier materials. The differences in compaction energy and in water content would also create a different soil structure, and hence different soil water characteristics curves; however, the resulting unsaturated behavior might have positive features, as materials compacted wetter than the optimum have a greater resistance to desaturation (high air entry value).

6.3 Further Steps and Closing Remarks

The conclusions presented in this thesis are based on four years of monitoring the field scale experiment, materials laboratory testing, field tests conducted as part of two field investigations, instrumentation readings, and numerical model results. Although extensive work has been conducted to evaluate the factors affecting the covers' performance, there is room for improvement.

As the meteorological conditions play a key role in the measurement and prediction of performance of the cover systems, an additional meteorological station should be installed at Punto B or at the experimental waste rock piles zone. The non-occurrence of runoff should be verified by conducting infiltration tests in the topsoil layer, and by maintaining a constant and reliable record of the rainfall intensities in the soil cover experiment zone. The numerical models should be updated using meteorological data collected at the experiment zone (Punto B). Furthermore, the unsaturated soil properties (SWCC) should be also updated or reviewed, including matric suction and volumetric water content data from the following years of monitoring. The purpose of this update is to evaluate any possible changes in the SWCCs over time. Additional instrumentation should be installed to validate the unsaturated properties determined for this thesis, and to account for materials' variability. Additional oxygen content measurements at the onset and high of both wet and dry season are recommended. The conclusions regarding the effectiveness of the covers as oxygen barrier were drawn from limited field measurements, and numerical model predictions, and hence the potential to limit oxygen diffusion from the atmosphere has to be verified.

The changes in oxygen levels impact the oxidation and metal leaching processes occurring in the underlying waste rock. This impact has not been quantified as part of this study, and it is suggested to monitor pH and metals concentrations in the percolated water. In order to make these measurements comparable, the same parameters measured in the water percolating through the adjacent experimental waste rock piles should be measured. Although percolated water follows different paths in those piles, the measurements would still represent a good reference as all the faces of the piles are bare, and oxygen supply is constant during the year.

The field investigation, continuous monitoring, and numerical modeling showed that two cover systems have the potential of limiting percolation and oxygen diffusion if certain conditions are achieved. Further works should be conducted to verify if those conditions can be implemented. Non-destructive geophysical

tests could be conducted to estimate density, porosity, and moisture content in the entire area and at different depths in the cover. Construction compaction trials should be executed using the barrier layer materials in lysimeters #1 and #5. The limitations imposed by the material characteristics and the effects of increasing water content at placement and of modifying the layer thickness would be evaluated directly. Dry density and in-situ permeability tests should be conducted to assess the effect of compaction and moisture content at placement in the resultant permeability.

The characteristics of the native soils and the meteorological conditions at the Antamina region represent a challenge for the implementation of a soil cover system. If the required compaction and hydraulic properties could not be achieved, the use of alternative materials should be evaluated. The suitability of these materials need to be assessed in terms of infiltration capacity and saturated hydraulic conductivity, as these properties control the volumes of percolation and runoff that would be generated.

The implementation of the field scale experiment proved to be the most valuable tool to evaluate the behavior of potential soil cover systems for the closure stage at Antamina. The observations and field-testing showed the limitations of a performance assessment only based only on laboratory results and numerical models. The soil cover study developed at the Antamina Mine highlights the importance of combining field observations, laboratory and field-testing, and numerical modeling.

REFERENCES

- Adu-Wusu, C., & Yanful, E. K. (2006). Performance of engineered test covers on acid-generating waste rock at Whistle mine, Ontario. *Canadian Geotechnical Journal*, 43(1), 1-18. <http://doi.org/10.1139/t05-088>
- Adu-Wusu, C., & Yanful, E. K. (2007). Post-closure investigation of engineered test covers on acid-generating waste rock at Whistle Mine, Ontario. *Canadian Geotechnical Journal*, 44(4), 496-506. <http://doi.org/10.1139/t06-132>
- ASTM Standard D2216, 2010, "Laboratory Determination of Water (Moisture) Content of Soil and Rock by Mass," ASTM International, West Conshohocken, PA, 2010, DOI: 10.1520/D2216-10, www.astm.org.
- ASTM Standard D6938, 2010, "In-Place Density and Water Content of Soil and Soil-Aggregate by Nuclear Methods (Shallow Depth)," ASTM International, West Conshohocken, PA, 2010, DOI: 10.1520/D6938-10, www.astm.org.
- Aubertin, M., Cifuentes, E., Apithy, S. A., Bussière, B., Molson, J., & Chapuis, R. P. (2009). Analyses of water diversion along inclined covers with capillary barrier effects. *Canadian Geotechnical Journal*, 46(10), 1146-1164. <http://doi.org/10.1139/T09-050>
- Barber, L., & Dobchuk, B., O'Kane Consultants Inc. (2013). *Standard Operating Procedure for Installing and Commissioning a Soil Moisture Station 3005-13/0*.
- Bay, D. (2009). Hydrological and hydrogeochemical characteristics of neutral drainage from waste rock test pile. (Master's thesis). Retrieved from <https://circle.ubc.ca/handle/2429/12473>
- Benson, C. H., & Daniel, D. E. (1990). Influence of clods on the hydraulic conductivity of compacted clay. *Journal of Geotechnical Engineering*, 116(8), 1231-1248. [http://doi.org/10.1061/\(asce\)0733-9410\(1990\)116:8\(1231\)](http://doi.org/10.1061/(asce)0733-9410(1990)116:8(1231))
- Benson, C. H., & Trast, J. M. (1995). Hydraulic Conductivity of Thirteen Compacted Clays. *Clays and Clay Minerals*, 43(6), 669-681. <http://doi.org/10.1346/ccmn.1995.0430603>
- Blackmore, S. (2012). *Methodology for Punto B precipitation data patching*. Unpublished manuscript.
- Blackmore, S., Javadi, M., Lorca, M., Laurenzi, L., Skierzkan, E., Mayer, U., Beckie, R., Blaskovich, R., St-Arnault, M., Urrutia, P., Klein, B., Perez, J., Wilson, W., Lindsay, M., (2013). *Antamina Waste Rock*

Study - 2012 Lessons Learned Report. University of British Columbia, University of Alberta, University of Saskatchewan.

Borghetti Soares, A., Ubaldo, M. de O., de Souza, V. P., Soares, P. S. M., Barbosa, M. C., & Mendonça, R. M. G. (2009). Design of a Dry Cover Pilot Test for Acid Mine Drainage Abatement in Southern Brazil. I: Materials Characterization and Numerical Modeling. *Mine Water and the Environment*, 28(3), 219-231. <http://doi.org/10.1007/s10230-009-0077-5>

Bussière, B., Aubertin, M., & Chapuis, R. P. (2003). The behavior of inclined covers used as oxygen barriers. *Canadian Geotechnical Journal*, 40(3), 512-535. <http://doi.org/10.1139/t03-001>

Bussière, B., Aubertin, M., Mbonimpa, M., Molson, J. W., & Chapuis, R. P. (2007). Field experimental cells to evaluate the hydrogeological behaviour of oxygen barriers made of silty materials. *Canadian Geotechnical Journal*, 44(3), 245-265. <http://doi.org/10.1139/t06-120>

Campbell Scientific, Inc. (2006). In Campbell Scientific, Logan, UT (Ed.). *Instruction Manual for NR-LITE Net Radiometer*.

Campbell Scientific, Inc. (2009). In Campbell Scientific, Logan, UT (Ed.). *Instruction Manual for LoggerNet*.

Campbell Scientific, Inc. (2009). In Campbell Scientific, Logan, UT (Ed.). *Instruction Manual for 229 Heat Dissipation Matrix Water Potential Sensor*.

Campbell Scientific, Inc. (2011). In Campbell Scientific, Logan, UT (Ed.). *Instruction Manual for CR1000 Measurement and Control System*.

Campbell Scientific, Inc. (2012). In Campbell Scientific, Logan, UT (Ed.). *Instruction Manual for CS616 and CS625 Water Content Reflectometers*.

Campbell Scientific, Inc. (2012). In Campbell Scientific, Logan, UT (Ed.). *Instruction Manual for Tripod Installation Manual Models CM110, CM115, CM120*.

Campbell Scientific, Inc. (2013). In Campbell Scientific, Logan, UT (Ed.). *Instruction Manual for AM16/32B Relay Multiplexer*.

Cash, A. E., Urrutia, P., Wilson, G. W., Robertson, J., Turgeon, M. H. (2012). A 2011 update for the single-layer desulphurised tailings cover completed in 1999 at Detour Gold. In A. Fourie & M. Tibbett (Eds.). *Mine Closure 2012 Proceedings*. Paper presented at the Seventh International Conference on Mine Closure, Brisbane, 25-27 September 2012 (pp. 149-162). Perth: Australian Centre for Geomechanics, 2012.

Cooper, H., Barber, L., Dobchuk, B., O'Kane Consultants Inc. (2013). *Standard Operating Procedure for Field Calibration of Water Content Sensors 3004-13*.

Flint, A. L., Campbell, G. S., Ellett, K. M., & Calissendorff, C. (2002). Calibration and Temperature Correction of Heat Dissipation Matric Potential Sensors. *Soil Science Society of America Journal*, 66(5), 1439. <http://doi.org/10.2136/sssaj2002.1439>

Fredlund, D. G., & Xing, A. (1994). Equations for the soil-water characteristic curve. *Canadian Geotechnical Journal*, 31(4), 521-532. <http://doi.org/10.1139/t94-061>

Fredlund, D.G., Rahardjo, H., & Fredlund, M.D. (2012). *Unsaturated Soil Mechanics in Engineering Practice*. Hoboken, New Jersey: John Wiley & Sons, Inc.

GCTS (2005). In Geotechnical Consulting & Testing Systems, Tempe, AZ (Ed.). User's Guide and Reference for SuctionData 1.13.

Gerke, H. H. (2006). Preferential flow descriptions for structured soils. *Journal of Plant Nutrition and Soil Science*, 169(3), 382-400. <http://doi.org/10.1002/jpln.200521955>

IntelligenceMine - Antamina. <http://www.infomine.com/intelligence/property/18474/antamina/>. Retrieved July 26, 2015.

Jubinvile, S. K. (2013). Prediction of rainfall runoff for soil cover modeling (Master's thesis). Retrieved from <http://hdl.handle.net/10402/era.29992>

MEND (2011). Volume 4: Prevention and Control. In G.A. Tremblay & C. M. Hogan (Eds.), *The MEND Manual*. Retrieved from http://mend-nedem.org/wp-content/uploads/5-4-2dVolume4_PreventionControlL.pdf

- Miller, C. J., Yesiller, N., Yaldo, K., & Merayyan, S. (2002). Impact of Soil Type and Compaction Conditions on Soil Water Characteristic. *Journal of Geotechnical and Geoenvironmental Engineering*, 128(9), 733-742. [http://doi.org/10.1061/\(asce\)1090-0241\(2002\)128:9\(733\)](http://doi.org/10.1061/(asce)1090-0241(2002)128:9(733))
- O'Kane, M., Wilson, G. W., & Barbour, S. L. (1998). Instrumentation and monitoring of an engineered soil cover system for mine waste rock. *Canadian Geotechnical Journal*, 35(5), 828-846. <http://doi.org/10.1021/ja01327a046>
- Pedretti, D., & Beckie, R. (2015). *Stochastic evaluation of simple pairing approaches to reconstruct incomplete rainfall time series*. Submitted for publication. University of British Columbia, Vancouver.
- Peterson, H.E. (2014). Unsaturated hydrology, evaporation, and geochemistry of neutral and acid rock drainage in highly heterogeneous mine waste rock at the Antamina Mine, Peru. (Doctoral dissertation). Retrieved from <https://circle.ubc.ca/handle/2429/46492>
- Prapaharan, S., White, D. M., & Altschaeffl, A. G. (1991). Fabric of Field and Laboratory Compacted Clay. *Journal of Geotechnical Engineering*, 117(12), 1934-1940. [http://doi.org/10.1061/\(asce\)0733-9410\(1991\)117:12\(1934\)](http://doi.org/10.1061/(asce)0733-9410(1991)117:12(1934))
- RAE Systems Inc. (2001). In Rae Systems, Sunnyvale, CA (Ed.). *Operation and Maintenance Manual for VRAE Multi Gas Monitor PGM-7800 & 7840*.
- Soil Moisture Equipment Corp. (2012). In Soil Moisture Equipment Corp., Santa Barbara, CA (Ed.). *Operating Instructions for 2800 Guelph Permeameter*.
- Soil Moisture Equipment Corp. (1997). In Soil Moisture Equipment Corp., Santa Barbara, CA (Ed.). *Operating Instructions for 2725 Jet Fill Tensiometer*.
- Strunk, R. L., Dobchuk, B. S., Barbour, S. L., Nieminen, G., & O'Kane, M. A. (2009). *SWANA's WASTECON 2009 Proceedings*. Paper presented at SWANA's WASTECON 2009 Conference, Long Beach, CA, 22-24 September 2009. Retrieved from http://www.okc-sk.com/wp-content/uploads/2012/02/Strunk-_Dobchuk_-Regina_landfill_paper.pdf

Swanson, D. A., Barbour, S. L., Wilson, G. W., & O'Kane, M. (2003). Soil-atmosphere modelling of an engineered soil cover for acid generating mine waste in a humid, alpine climate. *Canadian Geotechnical Journal*, 40(2), 276-292. <http://doi.org/10.1139/t02-116>

The International Network for Acid Prevention (INAP) (2014). *Global acid rock drainage guide (GARD guide)*. Retrieved from <http://www.gardguide.com/>

Unsaturated Soils Group (2000). In Unsaturated Soils Group, Department of Civil Engineering, University of Saskatchewan, Saskatoon, Canada (Ed.). *Soil Cover User's Manual*.

Urrutia, P., Wilson, W., Aranda, C., Peterson, H., Blackmore, S., Sifuentes, F., & Sanchez, M. (2011). Design and construction of field-scale lysimeters for the evaluation of cover systems at the Antamina Mine, Peru. *Tailings and Mine Waste 2011 Proceedings*. Paper presented at the 15th International Conference on Tailings and Mine Waste, Vancouver, 6-9 November 2011. Vancouver: Norman B. Keevil Institute of Mining Engineering, University of British Columbia. Retrieved from <https://circle.ubc.ca/handle/2429/38059>

Urrutia, P. (2012). Assessment of cover systems for waste rock in the Antamina Mine, Peru (Master's thesis). Retrieved from <http://circle.ubc.ca/handle/2429/43635>

Vanapalli, S. K., Fredlund, D. G., & Paufahl, D. E. (1999). Relationship between soil-water characteristic curves and the as-compacted water content versus soil suction for a clay till (pp. 991-998). *Proceedings*. Paper presented at the Eleventh Pan American Conference on Soil Mechanics and Geotechnical Engineering, Foz do Iguassu, 8-12 August 1999 (pp. 991-998). Associação Brasileira de Mecânica dos Solos e Engenharia Geotécnica, & International Society of Soil Mechanics and Geotechnical Engineering. Retrieved from <http://flash.lakeheadu.ca/~svanapal/papers/VFP4.pdf>

Wilson, G. W., Fredlund, D. G., & Barbour, S. L. (1994). Coupled soil-atmosphere modelling for soil evaporation. *Canadian Geotechnical Journal*, 31(2), 151-161. <http://doi.org/10.1139/t94-021>

Wilson, G. W., Fredlund, D. G., & Barbour, S. L. (1997). The effect of soil suction on evaporative fluxes from soil surfaces. *Canadian Geotechnical Journal*, 34(1), 145-155. <http://doi.org/10.1139/t96-078>

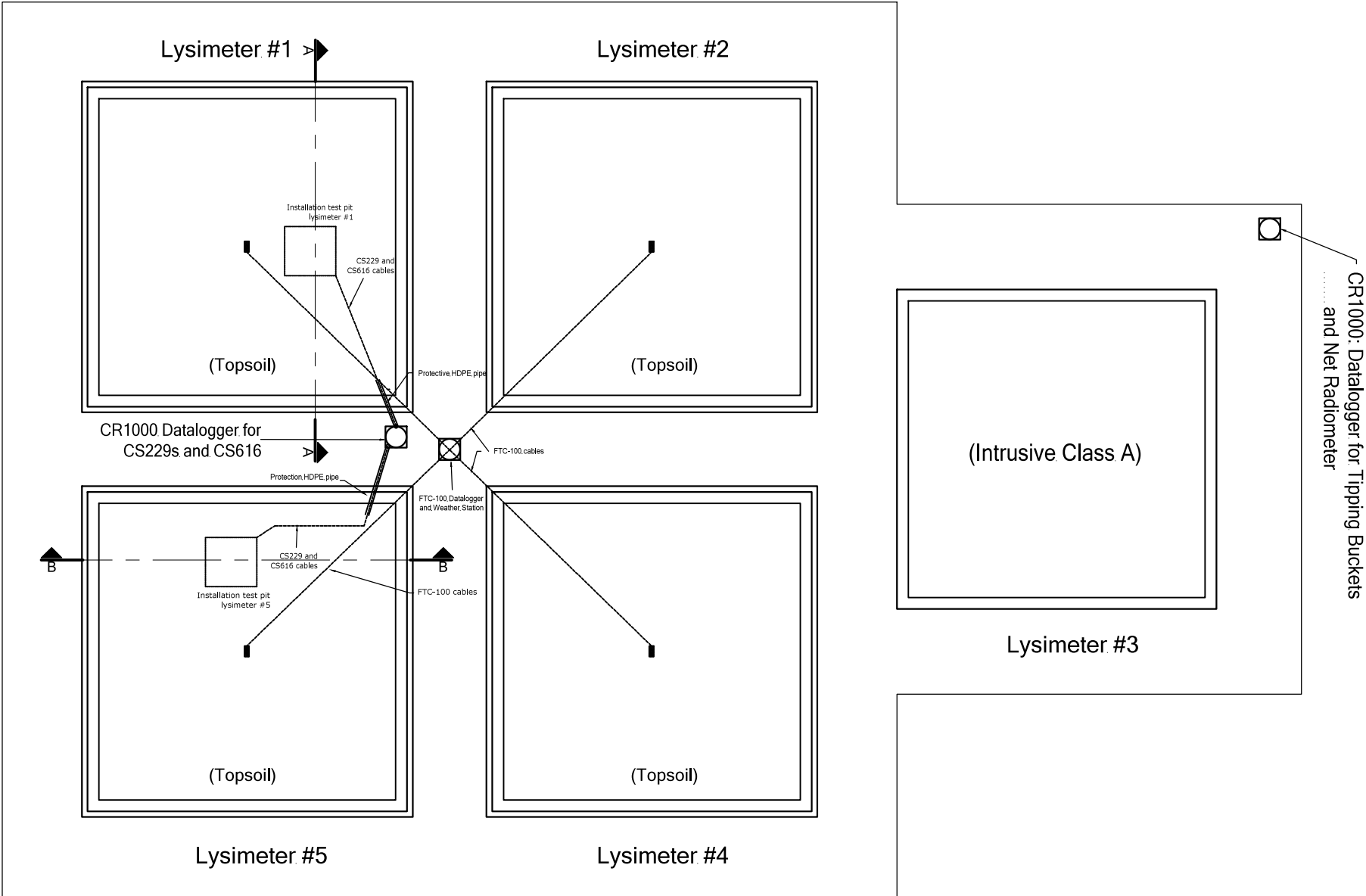
Watabe, Y., Leroueil, S., & Le Bihan, J. P. (2000). Influence of compaction conditions on pore-size distribution and saturated hydraulic conductivity of a glacial till. *Canadian Geotechnical Journal*, 37(6), 1184-1194. <http://doi.org/10.1139/t00-053>

Weeks, B. (2006). Three dimensional flux boundary conditions for soil covers (Doctoral dissertation). Retrieved from <https://circle.ubc.ca/handle/2429/18416>

Wickland, B. E. (2006). Volume change and permeability of mixtures of waste rock and fine tailings (Doctoral dissertation). Retrieved from <https://circle.ubc.ca/handle/2429/18412>

Zhou, J., & Yu, J.-L. (2005). Influences affecting the soil-water characteristic curve. *Journal of Zhejiang University SCIENCE*, 6A(8), 797-804. <http://doi.org/10.1631/jzus.2005.A0797>

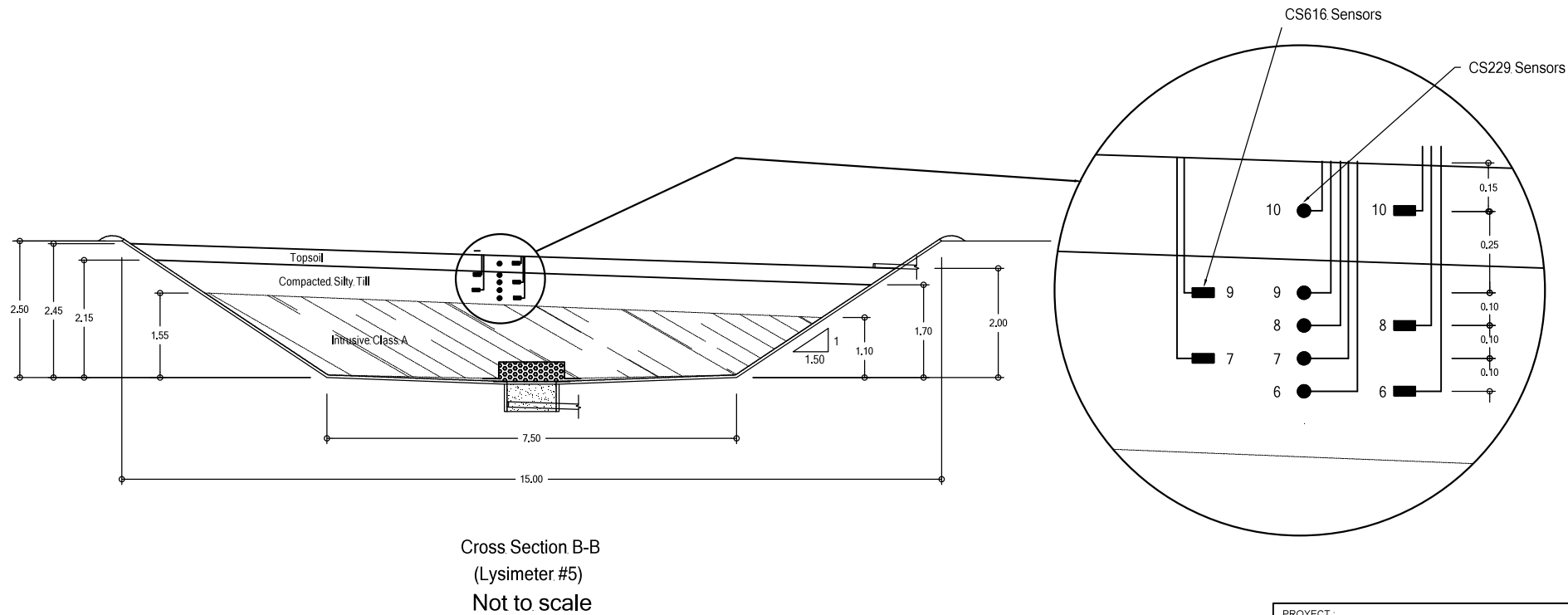
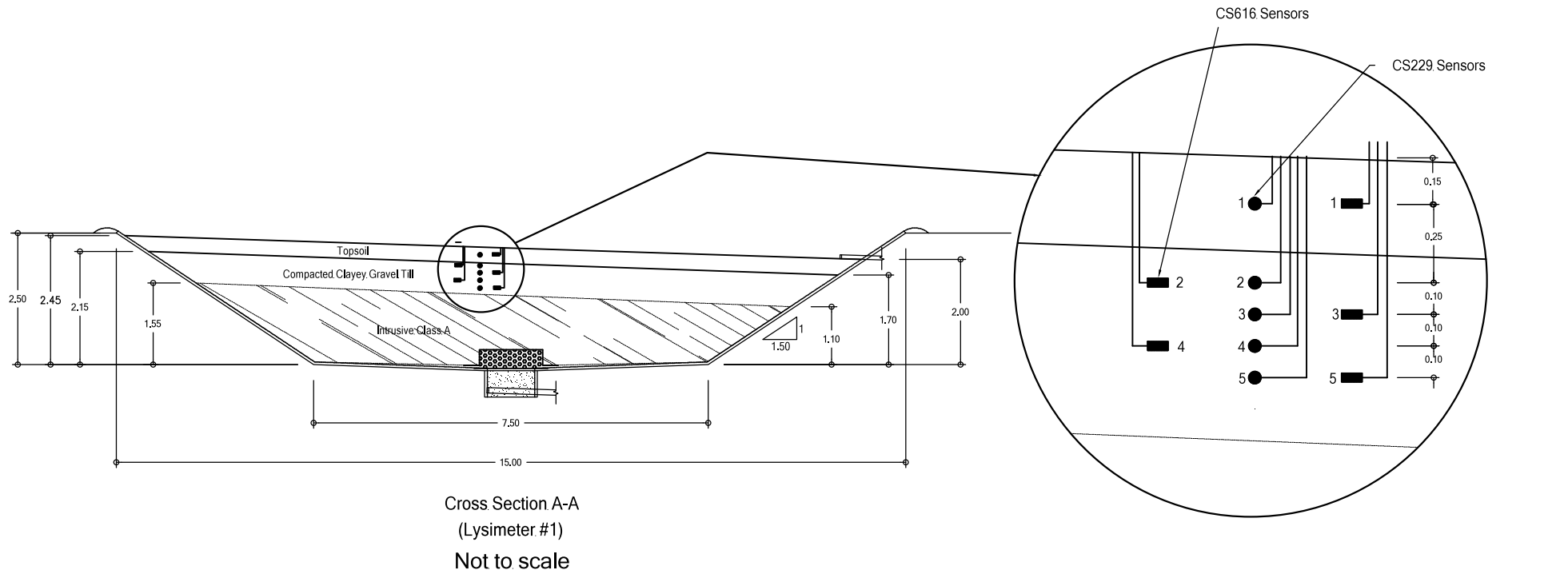
APPENDIX A: DRAWINGS



NOTE: Adapted from Urrutia (2012)

Not to scale

PROJECT : ASSESSMENT OF COVER SYSTEMS FOR WASTE ROCK AT ANTAMINA - 2013 FIELD INVESTIGATION			
2013 INSTRUMENTATION LAYOUT			
DRAWING:	UA.SC-01	DRAWN:	PU-JPL
DATE:	OCT-2015	PAGE:	164



NOTE: Adapted from Urrutia (2012)

PROJECT: ASSESSMENT OF COVER SYSTEMS FOR WASTE ROCK AT ANTAMINA - 2013 FIELD INVESTIGATION			
CROSS SECTIONS - 2013 INSTRUMENTATION DETAILS			
DRAWING: UA.SC-02	DRAWN: PU-JPL	DATE: OCT-2015	PAGE: 165

APPENDIX B: PHOTOS

2013 Field Investigation



Photo N° 1: View of lysimeter #1 (topsoil + compacted clayey gravel till) - October 2013.



Photo N° 2: View of lysimeter #2 (topsoil + non-compacted clayey gravel till) - October 2013.



Photo N° 3: View of lysimeter #3 (Control) - October 2013.



Photo N° 4: View of lysimeter #4 (topsoil) - October 2013.



Photo N° 5: View of lysimeter #5 (topsoil + compacted silty till) - October 2013.



Photo N° 6: View of the rain gauge and meteorological station installed in Punto B - October 2013.



Photo N° 7: Jet fill tensiometers saturation before testing.



Photo N° 8: Guelph permeameter installation at lysimeter #5 (topsoil + compacted silty till)



Photo N° 9: Jet fill tensiometers testing layout in lysimeter #1. Tensiometers out of the test pit measure matric suction in topsoil. Tensiometers in the test pit measure matric suction in the compacted silty till.



Photo N° 10: Jet fill tensiometers testing layout in lysimeter #4.



Photo N° 11: Permeability test with Guelph permeameter at lysimeter #1. The holes used to conduct the test at different depths are also observed.



Photo N° 12: VRAE PGM-7800 Multi Gas Monitor (RAE Systems Inc., 2001) calibration using a 0% oxygen cylinder.



Photo N° 13: Oxygen sampling tubes installed in lysimeter #2.



Photo N° 14: Oxygen level (percentage in volume) measurement in the underlying waste rock at lysimeter #1.



Photo N° 15: Detail of the expandable foam placed inside the HDPE pipe protecting the oxygen sampling tubes in lysimeter #5.



Photo N° 16: Plastic cap installed to protect the oxygen sampling tubes in lysimeter #4.

2014 Field Investigation



Photo N° 17: View of the soil cover experiment during the 2014 field investigation (June 2014)



Photo N° 18: View of lysimeter #4 (topsoil) in June 2014. The effects of the lack of precipitation and low temperatures registered during the dry season are observed.



Photo N° 19: Detail of the conditions of the topsoil layer in lysimeter #1 during the dry season (June 2014). Observed root penetration is less than 0.30 m.



Photo N° 20: Jet fill tensiometers testing layout in lysimeter #1 (June 2014). Tensiometers in the test pit measure matric suction in the compacted silty till at 0.40, 0.50, and 0.60 m of depth.



Photo N° 21: Jet fill tensiometer test in progress in lysimeter #4 (topsoil) - June 2014.



Photo N° 22: Jet fill tensiometers location for topsoil testing in lysimeter #1 - June 2014

Instruments



Photo N° 23: View of one of the Campbell Scientific 229 (CS229) Heat Dissipation Matric Water Potential sensors (November 2013).



Photo N° 24: View of the Campbell Scientific 616 (CS616) Water Content Reflectometers (November 2013).



Photo N° 25: Set up of the Campbell Scientific CR1000 datalogger, CE 4 Current Excitation Module, AM 16/32B Multiplexer, RF416 2.45 to 2.46 GHz Spread Spectrum Radio, and 12-V battery (November 2013).



Photo N° 26: View of the SX320J BP Solar Panel installed in the new monitoring station (November 2013).



Photo N° 27: Campbell Scientific 616 (CS616) Water Content Reflectometer calibration in topsoil (November 2013).



Photo N° 28: Campbell Scientific 616 (CS616) Water Content Reflectometer calibration in clayey gravel till (November 2013).



Photo N° 29: Campbell Scientific 616 (CS616) Water Content Reflectometer calibration in silty till (November 2013).



Photo N° 30: Installation of Campbell Scientific 229 and 616 sensors in the cover at lysimeter #1 (topsoil + compacted clayey gravel till, November 2013)



Photo N° 31: Backfilling and compaction with vibrating plate of the test pit excavated in lysimeter #1 (topsoil + compacted clayey gravel till, November 2013).



Photo N° 32: View of Campbell Scientific 616 (CS616) Water Content Reflectometer to be buried in the test pit in lysimeter #1 (topsoil + compacted clayey gravel till, November 2013).



Photo N° 33: Backfilled and compacted test pit in lysimeter #1 (topsoil + compacted clayey gravel till) for CS616s and CS229s installation. CS616 and CS229 in topsoil are observed (November 2013).



Photo N° 34: Campbell Scientific 616 (CS616) Water Content Reflectometer installation in lysimeter #5 (topsoil + compacted silty till). CS616 are installed staggered in the test pit sidewall, and buried at the required depth (November 2013).



Photo N° 35: Backfilled test pit in lysimeter #5 (topsoil + compacted silty till) for CS229s and CS616s (November 2013).



Photo N° 36: CS616 and CS229 sensors cables coming out through one of the corners of lysimeter #1 (topsoil + compacted clayey gravel till)



Photo N° 37: Tripod installed in Punto B to mount the new datalogger station. SX320J BP Solar Panel, Campbell Scientific L16755 2.4 GHz, 13 dBd Yagi Enclosed Directional Antenna, and lightning rod are mounted in the mast (November 2013).



Photo N° 38: Datalogger station for CS616s and CS229 installed at Punto B (November 2013)



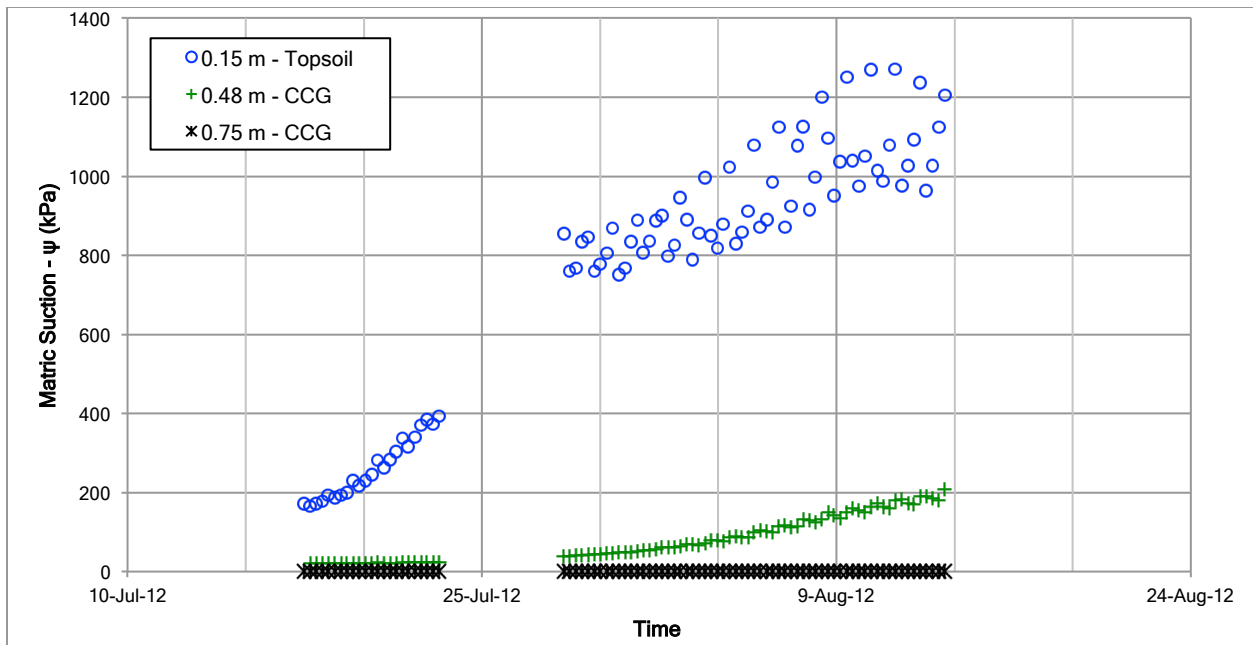
Photo N° 39: Artisanal protective cover to improve insulation of the FTC-100 sensors controller. Protective cover is made of insulating mat, cardboard, plastic wrap, and appliance epoxy paint (June 2014).



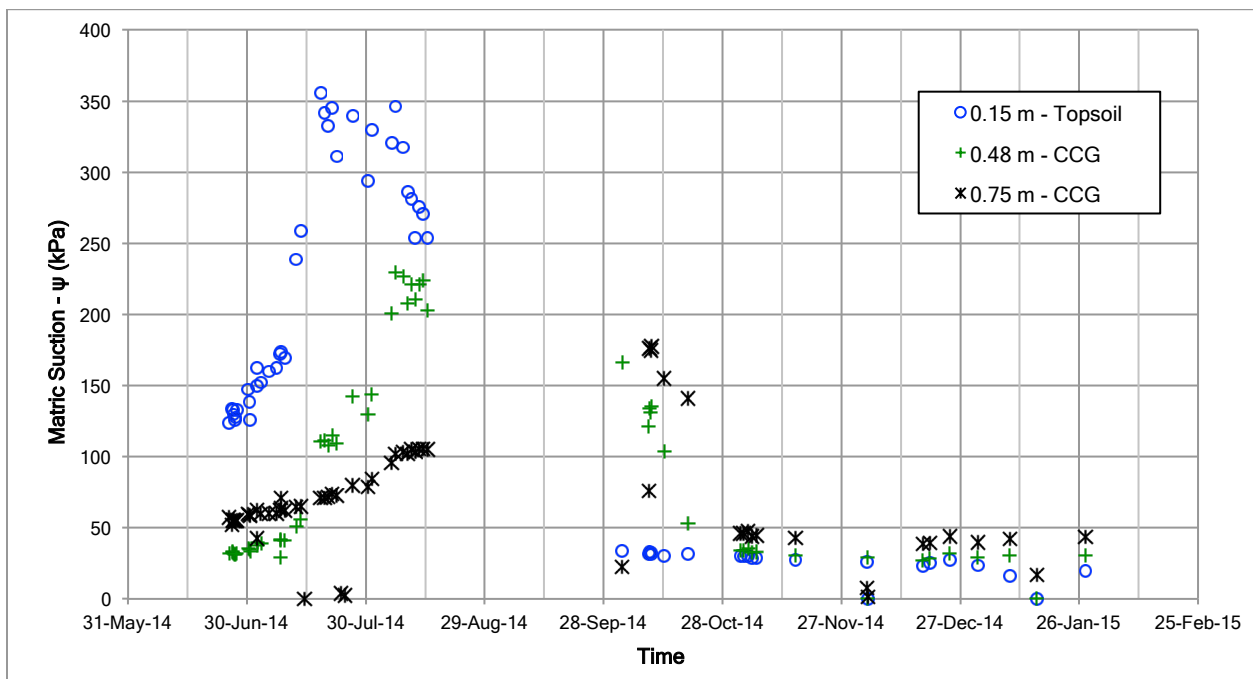
Photo N° 40: FTC-100 sensors controller reconnected and operative (July 2014).

APPENDIX C: FREDLUND THERMAL CONDUCTIVITY (FTC-100) SENSORS READINGS

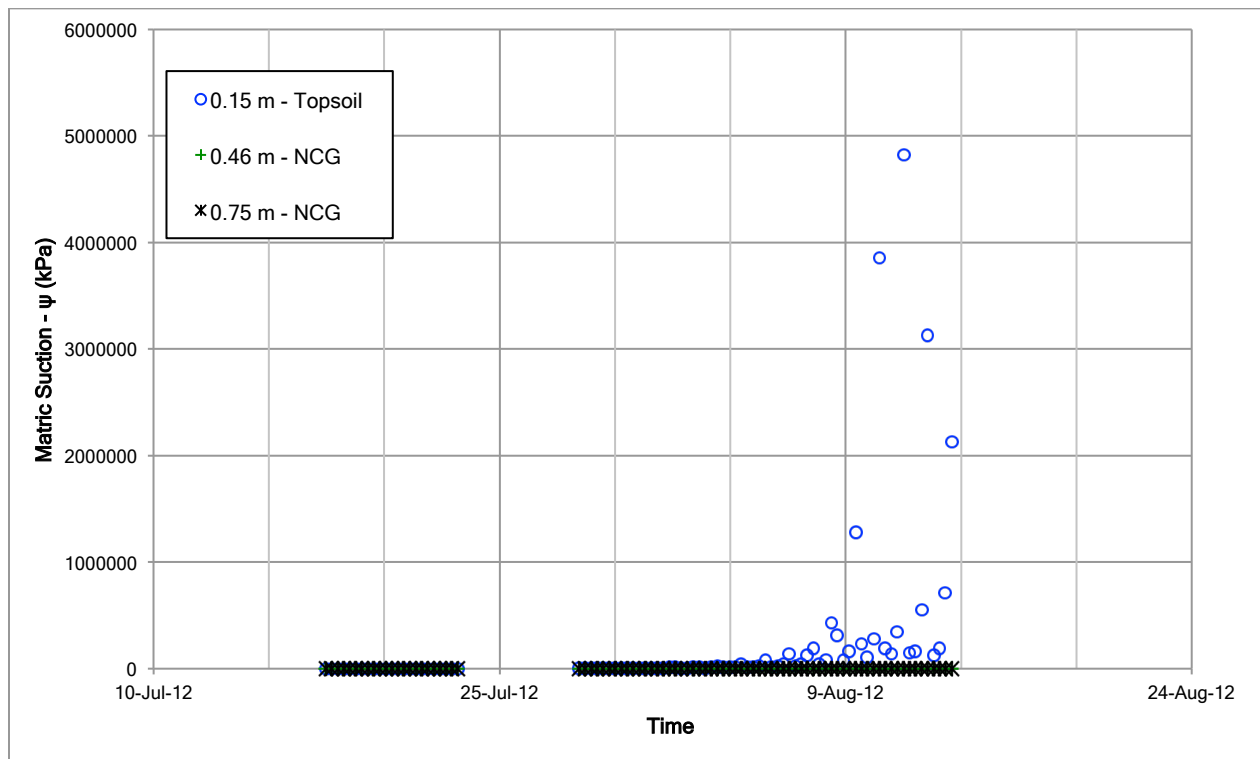
Cover 1: Topsoil + compacted clayey gravel till (July 17, 2012 to August 13, 2012)



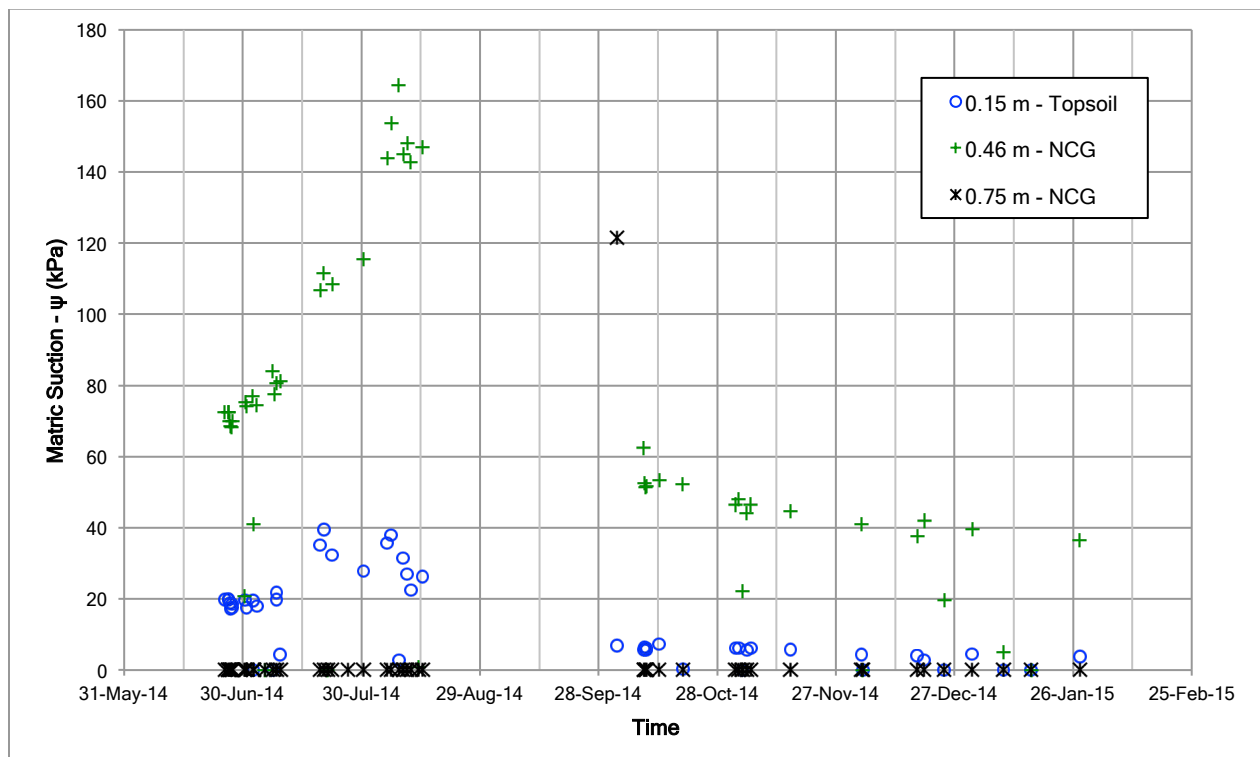
Cover 1: Topsoil + compacted clayey gravel till (June 25, 2014 to January 27, 2015)



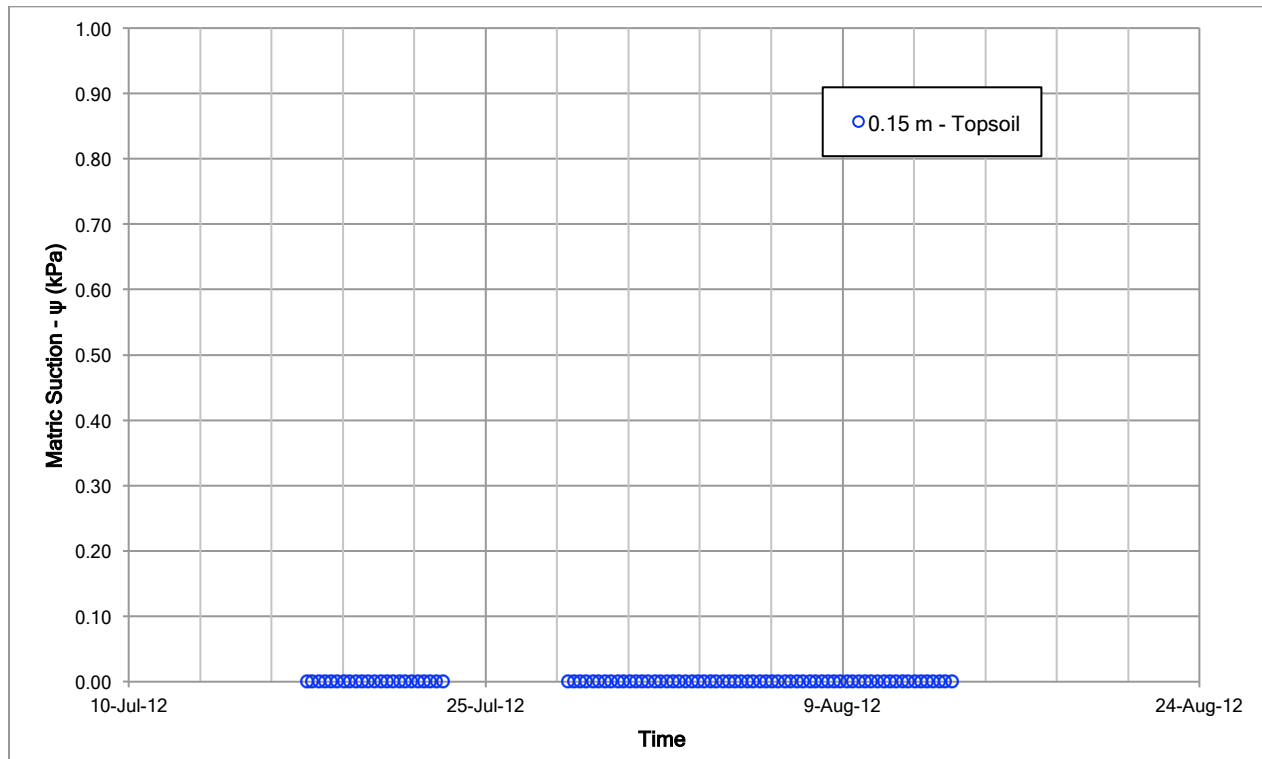
Cover 2: Topsoil + non-compacted clayey gravel till (July 17, 2012 to August 13, 2012)



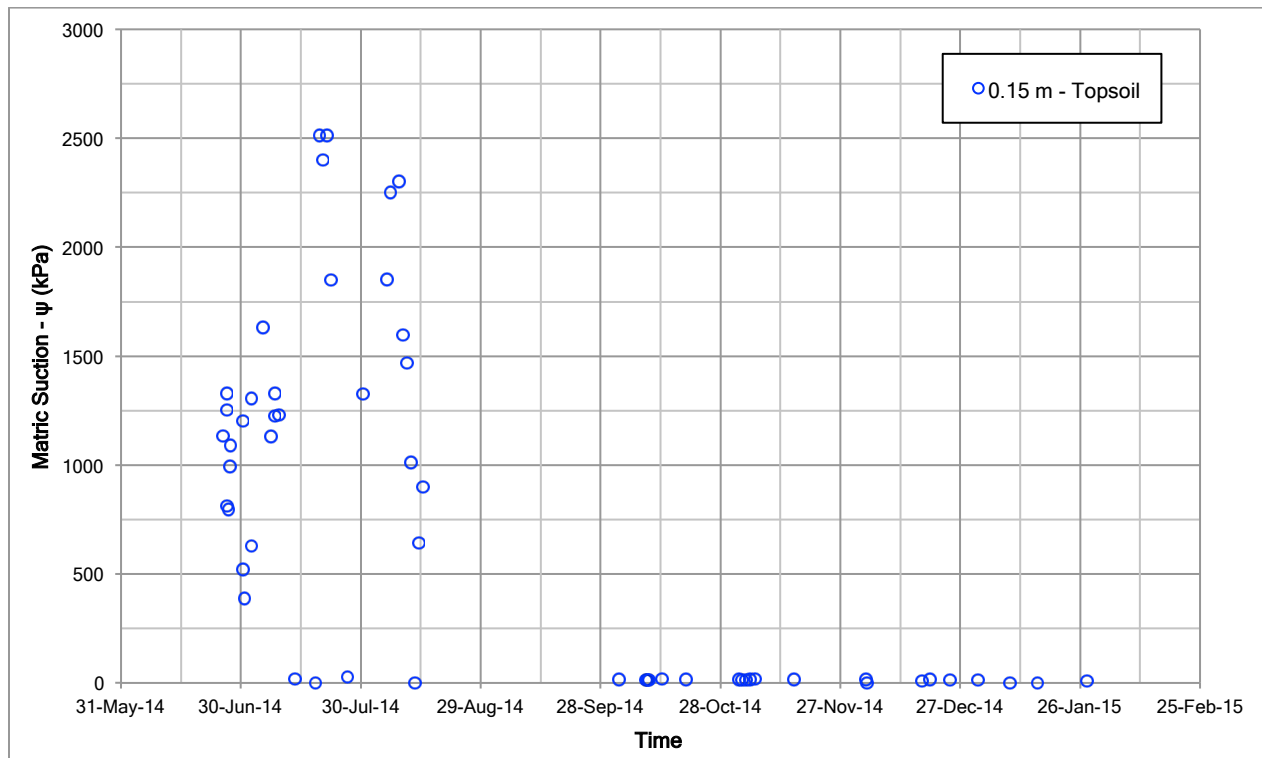
Cover 2: Topsoil + non-compacted clayey gravel till (June 25, 2014 to January 27, 2015)



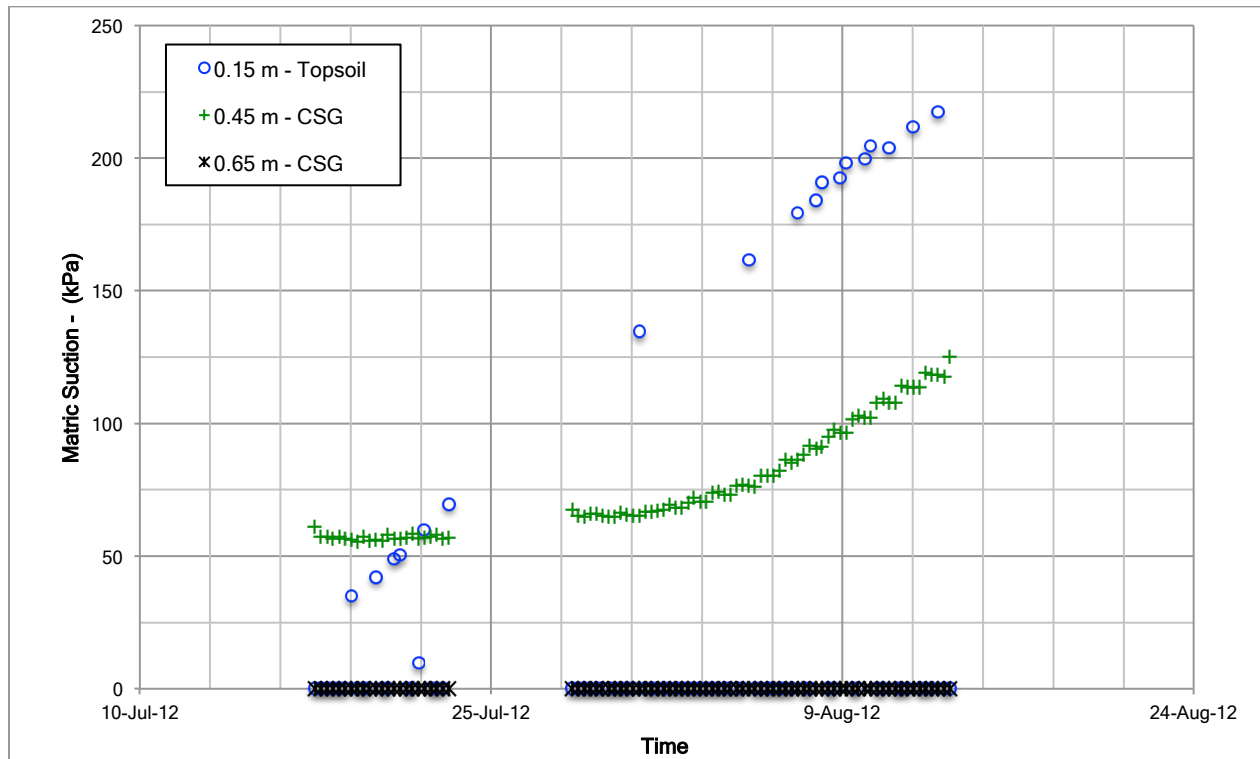
Cover 4: Topsoil (July 17, 2012 to August 13, 2012)



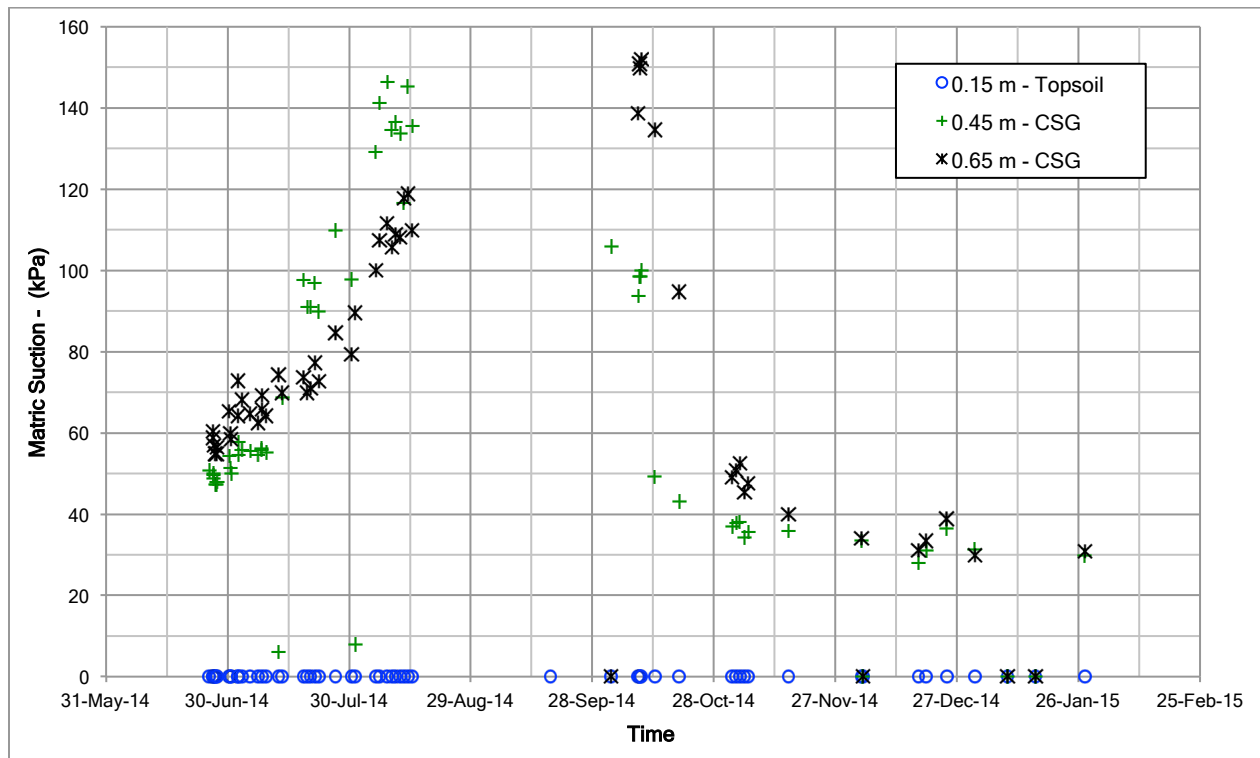
Cover 4: Topsoil (June 25, 2014 to January 27, 2015)



Cover 5: Topsoil + compacted silty till (July 17, 2012 to August 13, 2012)

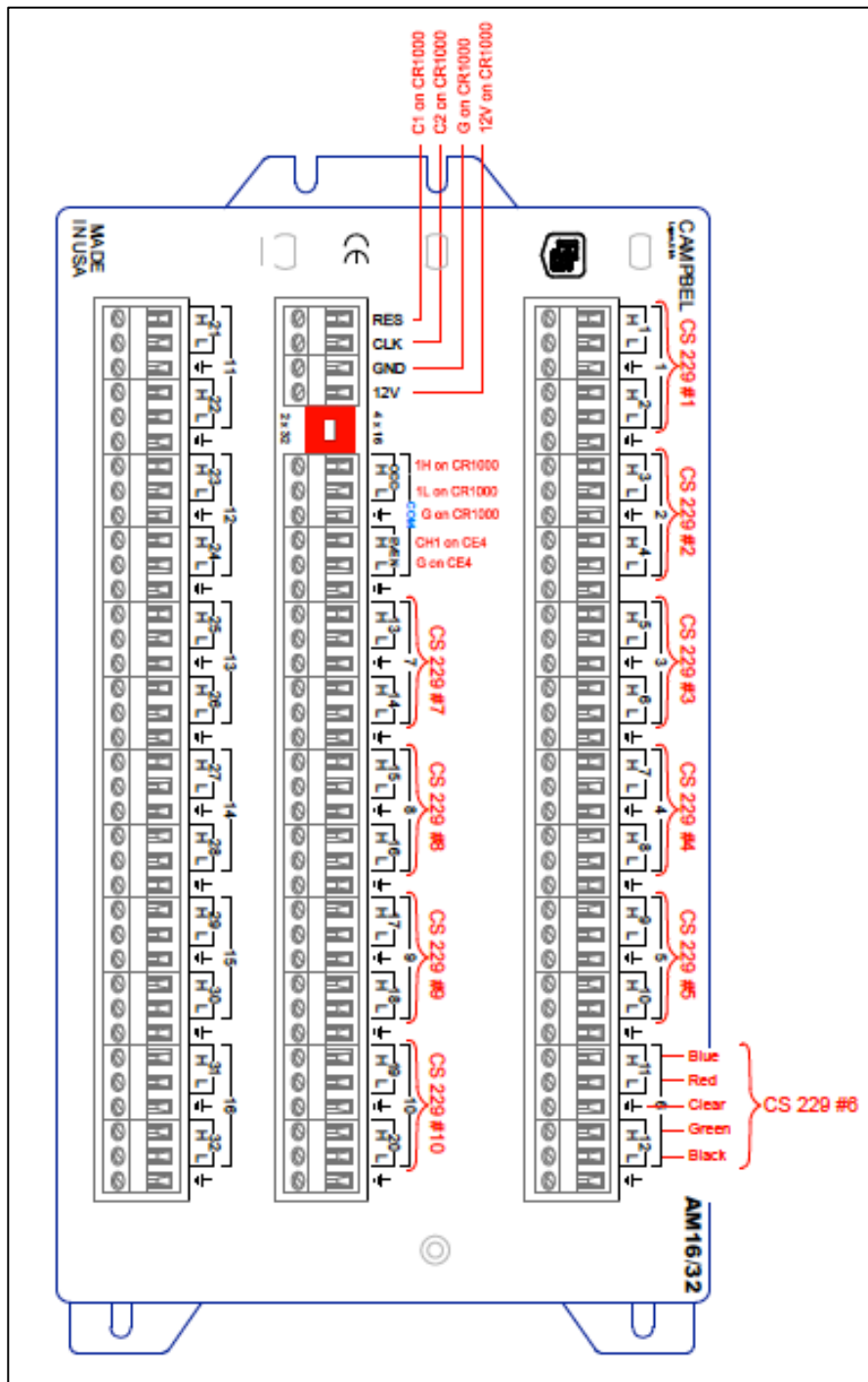


Cover 5: Topsoil + compacted silty till (June 25, 2014 to January 27, 2015)

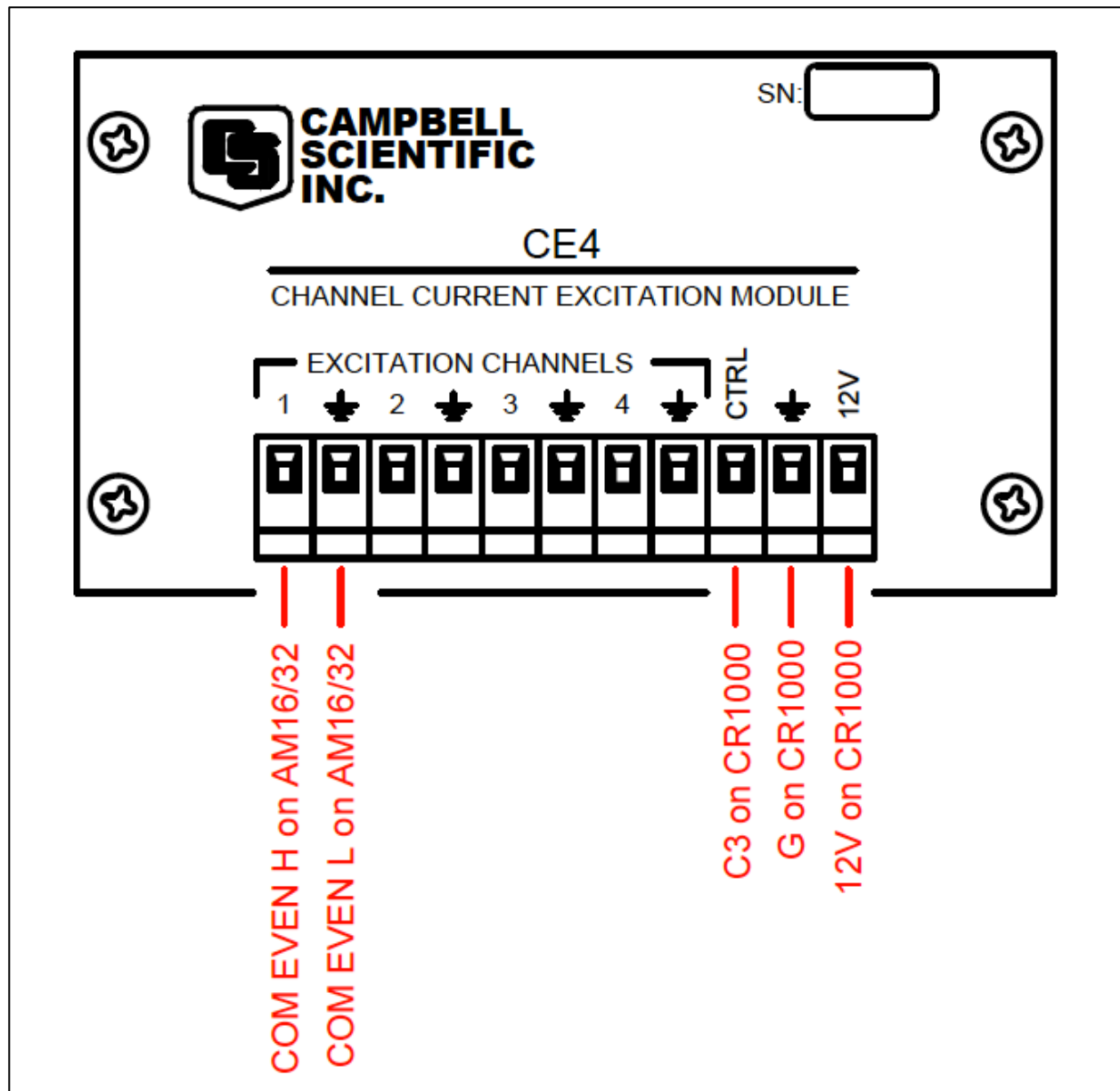


APPENDIX D: CAMPBELL SCIENTIFIC CR1000 DATALOGGER PROGRAM AND MONITORING STATION WIRING DIAGRAM

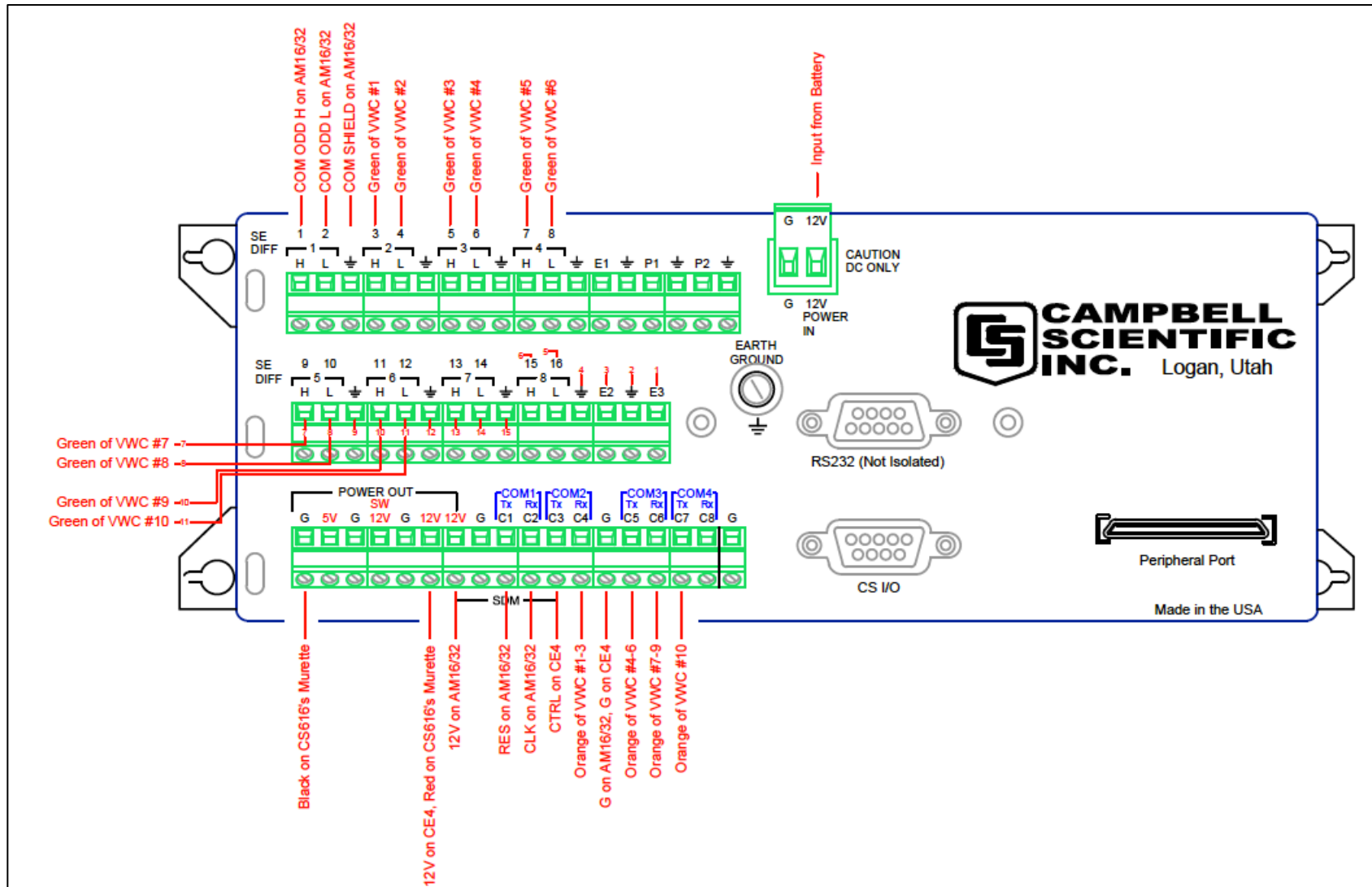
Campbell Scientific AM16/32B Multiplexer (Source: O’Kane Consultants Inc., 2013)



Campbell Scientific CE4 Current Excitation Module (Source: O’Kane Consultants Inc., 2013)



Campbell Scientific CR1000 Datalogger (Source: O’Kane Consultants Inc., 2013)



CS229s and CS616s CR1000 Monitoring Program (Source: O’Kane Consultants Inc., 2013)

'CR1000

'Created with CRBasic Editor

'Antamina Monitoring

'Version August 20, 2013

'Written by Larisa Barber of O’Kane Consultants Inc, Ph: 1-306-955-0719

'This program controls:

'10 Campbell Scientific Model 229 Matric Suction Sensors

'10 Campbell Scientific Model CS616 Volumetric Water Content Sensors

'10 Suction Sensors are connected to AM16/32 #1 multiplexer (RES to C1)

'10 Volumetric Water Content Sensors are connected directly to the datalogger

'The soil sensors are measured every four hours

'CR1000 Wiring:

'SG stands for 'Symbol Ground'

'1H = COM ODD H on AM16/32

'1L = COM ODD L on AM16/32

'SG = COM SHIELDS on AM16/32

'2H = green of VWC#1

'2L = green of VWC#2

'SG =

'3H = green of VWC#3

'3L = green of VWC#4

'SG =

'4H = green of VWC#5

'4L = green of VWC#6

'SG =

'5H = green of VWC#7

'5L = green of VWC#8

'SG =

'6H = green of VWC#9

'6L = green of VWC#10
 'SG =
 '7H =
 '7L =
 'SG =
 '8H =
 '8L =
 'SG =
 'EX1 =
 'SG =
 'EX2 =
 'SG =
 'EX3 =
 'P1 =
 'SG =
 'P2 =
 'SG =
 'C1 = RES on AM16/32
 'C2 = CLK on AM16/32
 'C3 = CTRL on CE4
 'C4 = Orange of VWC #1-3
 'G = G on AM16/32, G on CE4
 'C5 = Orange of VWC #4-6
 'C6 = Orange of VWC #7-9
 'C7 = Orange of VWC #10
 'C8 =
 'G = black on CS616s murette
 '5V =
 'G =
 'SW-12 =
 'G =
 '12V = 12v on CE4, red on CS616s murette
 '12V = 12V on AM16/32
 'G =

 'CE4 Wiring

 'CTRL = C3 on CR1000

'12V = 12V on CR1000

'G = G on CR1000

'CH1 = COM EVEN H on AM16/32

'G = COM EVEN L on AM16/32

'AM16/32 (229 Sensors) - 4x16 mode

'RES = C1 on CR1000

'CLK = C2 on CR1000

'12V = 12V on CR1000

'G = G on CR1000

'COM ODD H = 1H on CR1000

'COM ODD L = 1L on CR1000

'COM SH = SG on CR1000

'COM EVEN H = CH1 on CE4

'COM EVEN L = G on CE4

'CSCC Model 229 Matric Suction Sensor Wiring to AM16/32

'blue = ODD H

'red = ODD L

'green = EVEN H

'black = EVEN L

'clear = shield

'Declare Station Name to be stored in the Status Table

StationName (Antamina)

'Declare Public Variables, Dimensions and Units

'Declare variables that can be viewed in the Public Table

Public Batt_Volt

Public RefTemp_C

Public SoilTemp(10)

Public Temp_1sec_C(10)

Public Temp_30sec_C(10)

Public DelT(10)

Public Wat_Con(12)

Public Flag(1) As Boolean

'Declare Other Variables that remain hidden from the datalogger real-time tables

Dim K

'Declare unit labels to be displayed in header of the tables

Units Batt_Volt=Volts

Units RefTemp_C=Deg C

Units SoilTemp()=Deg C

Units DelT()=Deg C

Units Wat_Con()=raw count

'Declare Constants

Const high = true

Const low = false

'Define Data Tables

'Every day at midnight output minimum battery voltage and time Min. occurred.

'Note that the output time is actually 23:59 as CRBasic considers midnight as

'Day+1 0:00, without option for midnight as 24:00

DataTable(Daily,True,-1)

 DataInterval(1439,1440,Min,10)

 Minimum(1,Batt_Volt,FP2,False,True)

 Average (1,RefTemp_C,FP2,False)

EndTable

'Output data for CS229 and CS616 sensors every time measurements are taken

'(i.e. Flag 1 is high)

'Similarly the size of the table is determined from the frequency of readings.

'With readings every 4 hours, or 6 a day, 10000 records represent over 4 years of

'stored data

DataTable (SoilData,Flag(1)=True,10000)

 Sample (10,SoilTemp(),FP2)

 Sample (10,DelT(),FP2)

```

Sample (10,Wat_Con(),FP2)

EndTable

'Main Program
BeginProg

Scan(60,Sec,1,0)
'Default Datalogger Battery Voltage measurement Batt_Volt:
Battery(Batt_Volt)

'Measure reference temperature before starting 229 measurements
PanelTemp (RefTemp_C,_60Hz)

'Set flag 1 High every 4 hours
If IfTime (230,240,Min) Then Flag(1)=True

If Flag(1)=True Then

K=1

'Measure water content
'(Variable name,Reps=12, SEchannel=3,
CS616ControlPort=C4,RepsPerControlPort=3, Mult=1, Offset=0)
CS616 (Wat_Con(K),12,3,4,3,1.0,0)

'Initiate measurements for 229 sensors controlled by AM16/32
'Enable multiplexer (Set Reset port C1 high)
PortSet (1,1)

'Set Dim Variable K to equal 0 (initial state)
K=0
'Set sub scan loop counter for 10 sensors with 0 interval between
subscan

SubScan (0,Sec,10)
'Pulse port C2 for 20msec
'C2 is attached to the "Clock" channel on AM16/32
'This switches banks of channels

```

automatically prior
 'A second 20,000 microsecond delay is also included
 'to the measurement (built into the PulsePort instruction).
 PulsePort (2,20000)
 'Increment Dim Variable K
 'The Dim Variable K allows the program to keep track of
 which location to store
 'the measured value on each pass through the subscan
 K=K+1
 'Measure 229 starting temperature before heating
 TCDiff
 (SoilTemp(K),1,mV2_5C,1,TypeT,RefTemp_C,True,0,_60Hz,1.0,0)
 'Activate CE4 by setting port C3 high
 PortSet (3,1)
 'Heat CS229 sensor for 1 second
 Delay (0,1,Sec)
 'Measure INITIAL sensor temperature after 1 second of
 heating
 TCDiff
 (Temp_1sec_C(K),1,mV2_5C,1,TypeT,RefTemp_C,True,0,_60Hz,1.0,0)
 'Heat CS229 sensor for 29 more seconds
 Delay (0,29,Sec)
 'Measure FINAL sensor temperature after 30 seconds of
 heating
 TCDiff
 (Temp_30sec_C(K),1,mV2_5C,1,TypeT,RefTemp_C,True,0,_60Hz,1.0,0)
 'Deactivate CE4 by setting port C3 low
 PortSet (3,0)
 'Calculate temperature rise deltaT
 DelT(K)=Temp_30sec_C(K)-Temp_1sec_C(K)
 'End loop for temperature measurements
 NextSubScan
 'Disable multiplexer (Set port C1 low)
 PortSet (1,0)

'End conditional statement

EndIf

'Call data tables for soil sensors measurements and store data

CallTable SoilData

'Set Flag 1 low to end the measurements until the next correct interval

Flag(1)=False

'Call Data Tables

CallTable Daily

NextScan

EndProg